Official Journal of the
Malaysian Medical Association

The Medical Journal of Malaysia

PG Health Supplement

December 2025

Volume: 80

Supplement: 8

ISSN 0300-5283

MJM

Official Journal of the Malaysian Medical Association

Volume 80 Supplement 8 December 2025

EDITORIAL BOARD

ISSN 2948-3859

The Medical Journal of Malaysia is published six times a year.
MJM is published bimonthly ie. January, March, May, July, September and November.

Advertisement Rates:
Enquiries to be directed to the Secretariat.

Subscription Rates:
Price per copy is RM100.00 or RM360.00 per annum, for all subscribers.

Secretariat Address:
Malaysian Medical Association
4th Floor, MMA House, 124, Jalan Pahang, 53000 Kuala Lumpur.
Tel: (03) 4042 0617, 4041 8972, 4041 1375 Fax: (03) 4041 8187
E-mail: info@mma.org.my / mjm@mma.org.my
Website: www.mma.org.my

The Medical Journal of Malaysia

MJM

INSTRUCTION TO AUTHORS

The *Medical Journal of Malaysia* ***(MJM)*** welcomes articles of interest on all aspects of medicine in the form of original papers, review articles, short communications, continuing medical education, case reports, commentaries and letter to Editor. Articles are accepted for publication on condition that they are contributed solely to *The Medical Journal of Malaysia*.

NOTE: MJM is published bimonthly ie. January, March, May, July, September and November.

REQUIREMENTS FOR ALL MANUSCRIPTS
Please ensure that your submission to MJM conforms to the International Committee of Medical Journal Editors Recommendations for the Conduct, Reporting, Editing, and Publication of Scholarly Work in Medical Journals.

Neither the Editorial Board nor the Publishers accept responsibility for the views and statements of authors expressed in their contributions.

The Editorial Board further reserves the right to reject papers read before a society. To avoid delays in publication, authors are advised to adhere closely to the instructions given below.

MANUSCRIPTS
Manuscripts should be submitted in English (British English). Manuscripts should be submitted online through *MJM Editorial Manager*, http://www.editorialmanager.com/mjm.

Instructions for registration and submission are found on the website. Authors will be able to monitor the progress of their manuscript at all times via the *MJM Editorial Manager*. For authors and reviewers encountering problems with the system, an online Users' Guide and FAQs can be accessed via the "Help" option on the taskbar of the login screen.

MJM charges a one-time, non-refundable Article Processing Charge (APC) upon submission. Waiver of the APC applies only to members of the editorial board, and authors whose articles are invited by the editor. In addition, recipients of the MJM Reviewer Recognition Award from the previous year may enjoy a waiver of the APC for the next calendar year (e.g. recipients of MJM Reviewer Recognition Award 2022 will enjoy waiver of APC for articles submitted between January and December 2023).

The MJM processing fee is based on the categories stated below:
MJM
1. MMA Member - RM 400.00
2. Non-Member - RM 600.00
3. Overseas - USD 150.00

MJM Case Reports (effective 1st July 2022 up to further notice):
1. MMA Member - RM 200.00
2. Non-Member - RM 300.00
3. Overseas - USD 100.00

The MJM Article Processing Charge is a non-refundable administrative fee. Payment of the APC does not guarantee acceptance of the manuscript. Submitted articles will only be sent for reviews once the MJM APC has been successful completed.

All submissions must be accompanied by a completed **Copyright Assignment Form**, **Copyright Transfer Form and Conflict of Interest Form** duly signed by all authors. Forms can be download from MJM website at https://www.e-mjm.org/

Manuscript text should be submitted as **Microsoft Word** documents. Tables and flow-charts should be submitted as **Microsoft Word** documents. Images should be submitted as separate **JPEG files** (minimum resolution of 300 dpi).

PEER REVIEW PROCESS
All submissions must include at least two (2) names of individuals who are especially qualified to review the work. All manuscripts submitted will be reviewed by the Editor in-charge before they are send for peer review. Manuscripts that are submitted to MJM undergo a double-blinded peer review and are managed online. Proposed reviewers must not be involved in the work presented, nor affiliated with the same institution(s) as any of the authors or have any potential conflicts of interests in reviewing the manuscript. The selection of reviewers is the prerogative of the Editors of MJM.

ELIGIBILITY AS AN AUTHOR
MJM follows the recommendation of the International Committee of Medical Journal Editors (ICMJE) for eligibility to be consider as an author for submitted papers. The ICMJE recommends that authorship be based on the following four (4) criteria:
1 Substantial contributions to the conception or design of the work; or the acquisition, analysis, or interpretation of data for the work; AND
2 Drafting the work or revising it critically for important intellectual content; AND
3 Final approval of the version to be published; AND
4 Agreement to be accountable for all aspects of the work in ensuring that questions related to the accuracy or integrity of any part of the work are appropriately investigated and resolved.

TYPES OF PAPERS
Original Articles:
Original Articles are reports on findings from original unpublished research. Preference for publications will be given to high quality original research that make significant contribution to medicine. Original articles shall consist of a structured Abstract and the Main Text. The word count for the structured abstract should not exceed 500 words. The main text of the articles should not exceed 4000 words, tables/illustrations/figures/images up to five (5) and references up to 40. Manuscript describing original research should conform to the IMRAD format, more details are given below.

Original articles of cross-sectional and cohort design should follow the corresponding STROBE check-lists; clinical trials should follow the CONSORT check-list.

Review Articles:
Review Articles are solicited articles or systematic reviews. ***MJM*** solicits review articles from Malaysian experts to provide a clear, up-to-date account of a topic of interest to medical practice in Malaysia or on topics related to their area of expertise. Unsolicited reviews will also be considered, however, authors are encouraged to submit systematic reviews rather than narrative reviews. Review articles shall consist of a structured Abstract and the Main Text. The word count for the structured abstract should not exceed 500 words. Systematic Review are papers that presents exhaustive, critical assessments of the published literature on relevant topics in medicine. Systematic reviews should be prepared in strict compliance with MOOSE or PRISMA guidelines, or other relevant guidelines for systematic reviews.

Short Communications:
Shorts communication are short research articles of important preliminary observations, findings that extends previously published research, data that does not warrant publication as a full paper, small-scale clinical studies, and clinical audits. Short communications should not exceed 1,500 words and shall consist of a Summary and the Main Text. The summary should be limited to 100 words and provided immediately after the title page. The number of tables/illustrations/figures/images should be limited to three (3) and the number of references to ten (10).

Continuing Medical Education (CME) Articles:
A CME article is a critical analysis of a topic of current medical interest. The article should include the clinical question or issue and its importance for general medical practice, specialty practice, or public health. It shall consist of a Summary and the Main Text. The summary should be limited to 500 words and provided immediately after the title page Upon acceptance of selected articles, the authors will be requested to provide five multiple-choice questions, each with five true/false responses, based on the article. For guideline, please refer to: Sivalingam N, Rampal L. Writing Articles on Continuing Medical Education for Medical Journals. Med J Malaysia. 2021 Mar;76(2):119-124.

Case Reports:
Papers on case reports (one to five cases) must follow these rules: Case reports should not exceed 2,000 words; with a maximum of two (2) tables; three (3) photographs; and up to ten (10) references. It shall consist of a Summary and the Main Text. The summary should be limited to 250 words and provided immediately after the title page. Having a unique lesson in the diagnosis, pathology or management of the case is more valuable than mere finding of a rare entity. Being able to report the outcome and length of survival of a rare problem is more valuable than merely describing what treatment was rendered at the time of diagnosis. There should be no more than seven (7) authors.

Please note that all Case Reports will be published in the new MJM Case Reports Journal (www.mjmcasereports.org).

Commentaries:
Commentaries will usually be invited articles that comment on articles published in the same issue of the ***MJM***. However, unsolicited commentaries on issues relevant to medicine in Malaysia are welcomed. They should not exceed 2,000 words. They maybe unstructured but should be concise. When presenting a point of view, it should be supported with the relevant references where necessary.

Letters to Editor:
Letters to Editors are responses to items published in ***MJM*** or to communicate a very important message that is time sensitive and cannot wait for the full process of peer review. Letters that include statements of statistics, facts, research, or theories should include only up to three (3) references. Letters that are personal attacks on an author will not be considered for publication. Such correspondence must not exceed 1,500 words.

Editorials:
These are articles written by the editor or editorial team concerning the ***MJM*** or about issues relevant to the journal.

STRUCTURE OF PAPERS
Title Page:
The title page should state the brief title of the paper, full name(s) of the author(s) (with the surname or last name bolded), degrees (limited to one degree or diploma), affiliation(s), and corresponding author's address. All the authors' affiliations shall be provided after the authors' names. Indicate the affiliations with a superscript number at the end of the author's degrees and at the start of the name of the affiliation. If the author is affiliated to more than one (1) institution, a comma should be used to separate the number for the said affiliation.

Do provide preferred abbreviated author names for indexing purpose, e.g. L Rampal (for Lekhraj Rampal), BS Liew (for Liew Boon Seng), B Abdullah (for Baharudin Abdullah), Hoe VC (for Victor Hoe Chee Wai).

Please indicate the corresponding author and provide the affiliation, full postal address and email.

Articles describing Original Research should consist of the following sections (IMRAD format): Abstract, Introduction, Materials and Methods, Results, Discussion, Acknowledgment and References. Each section should begin on a fresh page.
Scientific names, foreign words and Greek symbols should be in italic.

Abstract and Key Words:
A structured abstract is required for Original and Review Articles. It should be limited to 500 words and provided immediately after the title page. Below the abstract provide and identify three (3) to 10 key words or short phrases that will assist indexers in cross-indexing your article. Use terms from the medical subject headings (MeSH) list from Index Medicus for the key words where possible. Key words are not required for Short Communications, CME articles, Case Reports, Commentaries and Letter to Editors.

Introduction:
Clearly state the purpose of the article. Summarise the rationale for the study or observation. Give only strictly pertinent references, and do not review the subject extensively.

Materials and Methods:
Describe your selection of the observational or experimental subjects (patients or experimental animals, including controls) clearly, identify the methods, apparatus (manufacturer's name and address in parenthesis), and procedures in sufficient detail to allow other workers to reproduce the results. Give references to established methods, including statistical methods; provide references and brief descriptions of methods that have been published but are not well-known; describe new or substantially modified methods, give reasons for using them and evaluate their limitations.

Identify precisely all drugs and chemicals used, including generic name(s), dosage(s) and route(s) of administration. Do not use patients' names, initials or hospital numbers. Include numbers of observation and the statistical significance of the findings when appropriate.

When appropriate, particularly in the case of clinical trials, state clearly that the experimental design has received the approval of the relevant ethical committee.

Results:
Present your results in logical sequence in the text, tables and illustrations. Do not repeat in the text all the data in the tables or illustrations, or both: emphasise or summarise only important observations in the text.

Discussion:
Emphasise the new and important aspects of the study and conclusions that follow from them. Do not repeat in detail data given in the Results section. Include in the Discussion the implications of the findings and their limitations and relate the observations to other relevant studies.

Conclusion:
Link the conclusions with the goals of the study but avoid unqualified statements and conclusions not completely supported by your data. Avoid claiming priority and alluding to work that has not been completed. State new hypotheses when warranted, but clearly label them as such. Recommendations, when appropriate, may be included.

Acknowledgements:
Acknowledgements of general support, grants, technical assistance, etc., should be indicated. Authors are responsible for obtaining the consent of those being acknowledged.

Referencing guide:
The Medical Journal of Malaysia, follows the Vancouver numbered referencing style. Citations to someone else's work in the text, should be indicated by the use of a number. In citing more than one article in the same sentence, you will need to include the citation number for each article. A hyphen should be used to link numbers which are inclusive, and a comma used where numbers are not consecutive. The following is an example where works 1.3,4,5.have been cited in the same place in the text.

Several effective drugs are available at fairly low cost for treating patients with hypertension and reducing the risk of its sequelae.[1,3-5]

The list of all of the references that are cited in the article should be presented in a list labelled as 'References'. This reference list appears at the end of the paper. Authors are responsible for the accuracy of cited references and these should be verified by the author(s) against the original documents before the manuscript is submitted. It is important that the author should never place in the list of references a document that he or she has not seen. The Journals names should be abbreviated according to the style used in the Index Medicus. All authors when six or less should be listed; when seven or more list only the first six and add et al.

If you are citingthe author's name in your text, you must insert the citation number as well. Jewell BL (8) underlined that as focus in the SARS-CoV-2 pandemic shifts to the emergence of new variants of concern (VOC), characterising the differences between new variants and non-VOC lineages will become increasingly important for surveillance and maintaining the effectiveness of both public health and vaccination programme. If you are citing more than one author's name in your text and you want to cite author names in your text, use 'et al.' after the first author. Example: Rampal et al. (9) highlighted that the. disregard of the manuscript guidelines and instruction to authors of the journal you submit, is one of the common reasons for 'Rejection' of the article.

Example references Journals:
Standard Journal Article
Rampal L and Liew BS. Coronavirus disease (COVID-19) pandemic. Med J Malaysia 2020; 75(2): 95-7.
Rampal L, Liew BS, Choolani M, Ganasegeran K, Pramanick A, Vallibhakara SA, et al. Battling COVID-19 pandemic waves in six South-East Asian countries: A real-time consensus review. Med J Malaysia 2020; 75(6): 613-25.

NCD Risk Factor Collaboration (NCD-RisC). Worldwide trends in hypertension prevalence and progress in treatment and control from 1990 to 2019: a pooled analysis of 1201 population-representative studies with 104 million participants. Lancet 2021; 11; 398(10304): 957-80.

Books and Other Monographs:
Personal Author(s)
Goodman NW, Edwards MB. 2014. Medical Writing: A Prescription for Clarity. 4 th Edition. Cambridge University Press.

Chapter in Book
McFarland D, Holland JC. Distress, adjustments, and anxiety disorders. In: Watson M, Kissane D, Editors. Management of clinical depression and anxiety. Oxford University Press; 2017: 1-22.

Corporate Author
World Health Organization, Geneva. 2019. WHO Study Group on Tobacco Product Regulation. Report on the scientific basis of tobacco product regulation: seventh report of a WHO study group. WHO Technical Report Series, No. 1015.

NCD Risk Factor Collaboration (NCD-RisC). Rising rural body-mass index is the main driver of the global obesity epidemic in adults. Nature 2019; 569: 260–64.

World Health Organization. Novel Coronavirus (2019-nCoV) Situation Report 85, April 14, 2020. [cited April 2020] Accessed from: https://www.who.int/docs/defaultsource/coronaviruse/situationreports/20200414-sitrep-85-covid-19.

Online articles
Webpage: Webpage are referenced with their URL and access date, and as much other information as is available. Cited date is important as webpage can be updated and URLs change. The "cited" should contain the month and year accessed.

Ministry of Health Malaysia. Press Release: Status of preparedness and response by the ministry of health in and event of outbreak of Ebola in Malaysia 2014 [cited Dec 2014]. Available from: http://www.moh.gov.my/english.php/database_stores/store_view_page/21/437.

Other Articles:
Newspaper Article
Panirchellvum V. 'No outdoor activities if weather too hot'. the Sun. 2016; March 18: 9(col. 1-3).

Magazine Article
Rampal L.World No Tobacco Day 2021 -Tobacco Control in Malaysia. Berita MMA. 2021; May: 21-22.

Tables:
All tables and figures should have a concise title and should not occupy more than one printed page. The title should concisely and clearly explain the content of the table or figure. They should be numbered consecutively with Roman numerals (e.g Table I) and figures with Arabic numerals (e.g. Figure 1), and placed after the sections of the manuscript which they reflect, particularly the results which they describe on separate pages. Cite tables in the text in consecutive order. Indicate table footnotes with lower-case letters in superscript font. Place the information for the footnote beneath the body of the table. If a table will be submitted as a separate document, the filename should contain the surname of the first author and match its label in the manuscript (e.g., SMITH Table 1).Vertical lines should not be used when constructing the tables. All tables and figures should also be sent in electronic format on submission of the manuscript as supplementary files through the journal management platform. Clinical Photographs should conceal the subject's identity. Tables and flow-charts should be submitted as Microsoft Word documents. Images should be submitted as separate JPEG files (minimum resolution of 300 dpi).

Photographs of Patients:
Proof of permission and/or consent from the patient or legal guardian must be submitted with the manuscript. A statement on this must be included as a footnote to the relevant photograph.

Colour reproduction:
Illustrations and diagrams are normally reproduced in black and white only. Colour reproductions can be included if so required and upon request by the authors. However, a nominal charge must be paid by the authors for this additional service; the charges to be determined as and when on a per article basis.

Abbreviations:
Use only standard abbreviations. The full-term for which an abbreviation stands should precede its first use in the abstract, article text, tables, and figures, unless it is a standard unit of measurement. Abbreviations shall not be used in the Title. Abbreviations should be kept to a minimum.

Formatting of text:
Numbers one to ten in the text are written out in words unless they are used as a unit of measurement, except in tables and figures. Use single hard-returns to separate paragraphs. Do not use tabs or indents to start a paragraph. Do not use the automated formatting of your software, such as hyphenation, endnotes, headers, or footers (especially for references). Submit the Manuscript in plain text only, removed all 'field codes' before submission. Do not include line numbers. Include only page number.

BEST PAPER AWARD
All original papers which are accepted for publication by the MJM, will be considered for the 'Best Paper Award' for the year of publication. No award will be made for any particular year if none of the submitted papers are judged to be of suitable quality.

CONTENTS Page

Original Articles

CONTENTS **Page**

Comparison of motor and haemodynamic profiles of epidural 0.5% Levobupivacaine with 0.75% Ropivacaine in patients undergoing elective below umbilical surgery

Ashok Kumar Balasubramanian, MD, Rathna Anbalagan, MD

Department of Anaesthesiology and Pain Management, Saveetha Medical College and Hospitals, Saveetha Institute of Medical and Technical Sciences, Chennai-602105, Tamil Nadu, India

ABSTRACT

Introduction: Our study focuses on comparing the motor and haemodynamic effects of levobupivacaine 0.5% and ropivacaine 0.75% when administered as epidural anaesthesia for surgeries below the umbilicus. This comparison is particularly important given that the racemic mixture of bupivacaine, which includes the dextro (D-(+)) and levo (L-(-)) isomers in equal proportion, is associated with significant cardiovascular and central nervous system complications, particularly due to the R-(+)-isomer. In contrast, the levorotatory isomers like our study drug levobupivacaine and ropivacaine are noted for their more reliable and stable pharmacological profiles.

Materials And Methods: Fifty-six patients with the American Society of Anaesthesiologists (ASA) classification 1 and 2 classifications were randomly assigned to one of two study groups.(17 ml of 0.5% levobupivacaine was given epidurally in Group L, while Group R received 17 ml of 0.75% ropivacaine).The prospective randomised double blinded study was carried out at Saveetha Medical College Hospital, S.I.M.A.T.S., from 2022 to 2024.

Results: The duration, onset, and regression of motor block were comparable in both groups. The motor block grade as per MBS in the two groups showed significant differences. (p<0.001) Group R achieved maximum motor blockage in 40.18 minutes, whereas group L achieved it in 17.86 minutes (p=0.043). In group R, the average duration of motor block was 146.25±48.58 minutes, while in group L it was 160.71±46.64 minutes (p>0.05). Heart rate (HR), mean arterial pressure (MAP), and oxygen saturation (SpO2) exhibited no significant differences between the two groups at various time intervals.

Discussion: Both levobupivacaine 0.5% and ropivacaine 0.75% effectively provide epidural anaesthesia for surgeries below the umbilicus. Levobupivacaine achieved maximum motor block more quickly than ropivacaine, but overall motor block duration was similar. Haemodynamic parameters were stable with no significant differences between the two groups.

KEYWORDS:
Epidural Anaesthesia, Levobupivacaine, Ropivacaine, Motor Profile, and Hemodynamic Profile. Isomers in Local anaesthesia drugs, Cardiotoxicity and Neurotoxicity in Local anaesthesia use

INTRODUCTION

Local anaesthetics work by blocking sodium channels on neural membranes, causing the interruption of neural conduction. The continuous pursuit of more advanced and secure anaesthetic drugs is vital to anaesthetics.[1] Isomerism is a crucial topic in this study since it refers to the phenomenon where compounds with the same chemical compositions exhibit distinct structures, leading to diverse behaviours. The local anaesthetic we use is usually a racemic mixture of dextro bupivacaine (D-(+) isomer) and levobupivacaine (L-(-) isomer), which is an equal amount of each thing.[2-4] Accidental intravascular injection has been associated with significant complications in the CVS and the CNS. The reactions are associated with the R-(+)-isomer of bupivacaine. Conversely, the levorotatory isomers demonstrate a pharmacological profile that is more reliable and stable. The equivalent dose of 0.5% levobupivacaine is 0.75% ropivacaine due to the decreased lipophilicity of ropivacaine.[1] The lipid solubility of levobupivacaine is 30, while the lipid solubility of ropivacaine is 2.8. The "up-down sequential allocation" technique was utilised to determine the minimum local anaesthetic concentration (MLAC) for pain management during childbirth. The findings indicate that bupivacaine has approximately 40% more potency compared to ropivacaine.[5,6] Our study looks at the differences and similarities in motor and hemodynamic effects between levobupivacaine 0.5% and 0.75% ropivacaine when given as epidural anaesthesia to people having surgery below the umbilicus.

MATERIALS AND METHODS

Ethical Approval and Consent

After obtaining approval from the Institutional IRB and IEC (clearance number: 009/06/2023/IEC/SMCH) and obtaining written consent from participants, 56 patients, who were scheduled for below-umbilical surgery with epidural anaesthesia, were included in our study. The prospective randomised double blinded study was carried out at Saveetha Medical College Hospital, S.I.M.A.T.S from 2022 to 2024.

Study Population

The study included patients aged between 15 and 65 years who were classified as the American Society of Anaesthesiologists (ASA) classification grades 1 and 2, with no history of allergic responses to amide local anaesthetics and no absolute or relative contraindications to regional

This article was accepted: 06 December 2024
Corresponding Author: Ashok Kumar Balasubramanian
Email: mbashok.2022@ gmail.com

anaesthesia. Exclusion criteria were patients younger than 15 years or older than 65 years, those with confirmed hypersensitivity reactions to amide local anaesthetics, individuals with a medical history and treatment of psychiatric disorders, patients classified as ASA grades 3, 4, or 5, and those with relative or absolute contraindications for regional anaesthesia.

Randomisation and Blinding
The participants were allocated into R and L groups, by computer-generated random numbers. The trial was done using a double-blind methodology which ensured that both the patients and the anaesthetic providers were unaware of the group assignments. Group R received a 17 ml dose of ropivacaine solution at a concentration of 0.75%, while Group L received a 17 ml dose of levobupivacaine solution at a concentration of 0.5%.

Preoperative Preparation
Prior to the procedure, each patient received a visit, and their consent was gained after being fully informed. The sequential development of events in the theatre was clarified. After confirming adequate fasting, patients were infused IV with 500 ml of Ringer Lactate solution. Upon entering the operating room, the patient's non-invasive blood pressure, their electrocardiogram (ECG), and their oxygen saturation using pulseoximetry were monitored. The aforementioned haemodynamic parameters were documented before the insertion of the epidural, at the commencement of the study, at 5-minute intervals until the 30-minute mark, and subsequently every 30 minutes thereafter. Group R was administered 17 millilitres of ropivacaine solution at a concentration of 0.75%, while Group L was administered 17 millilitres of levobupivacaine solution at a concentration of 0.5%.

Epidural Placement Procedure
The patients were positioned on their left lateral posture, and the L3-L4 interspinous area was located. 3 ml of 2% lignocaine was injected into the skin and subcutaneous tissue. The extradural space was located with an 18G Tuohy needle by employing the technique of loss of resistance to air. After verifying negative aspiration for blood or cerebrospinal fluid (CSF), 3 ml of 2% lidocaine with 1:200,000 adrenaline (test dose) was administered via extradural catheter. After ruling out the possibility of subarachnoid or intravascular injection, the double-blinded study drug was administered two minutes after the test dose.

In Group R, a total of 17 ml of 0.75% ropivacaine was given over a period of 5 minutes. After each dose of 6 ml, there was a 1-minute break, and after the second dose, there was another 1-minute break before providing the last dose of 5 ml and Group L was administered a total of 17 ml of 0.5% levobupivacaine over a period of 5 minutes, consistent with the prior statement.

Assessment of Motor and Sensory Blocks
The starting point for subsequent evaluations was the time of completion of the administration of the research drug. A 20-gauge catheter was placed 5 centimetres into the epidural space, and then the needle was removed. The patient was thereafter placed in a supine posture, lying on their back. Continuous monitoring was conducted on the patients' pulse rate (PR), blood pressure (BP), and oxygen saturation (SpO2). The administration of oxygen to all patients was done using a Hudson face mask at a flow rate of 4 L/min. The surgical operation commenced 30 minutes following the injection of the epidural drug. If the mean arterial pressure (MAP) decreased by more than 20%, it was addressed by administering a 6 mg dose of Ephedrine. If the heart rate (HR) fell below 50 beats per minute, it was administered a dosage of 0.6 mg of Atropine.

The sensory analgesia level was evaluated by doing a pin prick with the blunt end of a 25G needle. The commencement of surgical block was the block needed to attain the T10 dermatome level sensory block. If patients had inadequate sensory block after 30 minutes, an extra 7 ml of the experimental medication was administered. Following surgery, patients who desired pain medication were given an epidural administration of 100 mg of Tramadol mixed with 10 ml of distilled water, and the time of administration was documented.

The motor block onset was defined as the time taken to attain a Modified Bromage Score of 2, while the duration of the motor block refers to the time interval during which the score remained ≥2. The Modified Bromage Scale is as follows: Zero indicates a lack of paralysis with full flexion of hips, knees, and ankles; One indicates the ability to flex at the knee but an inability to raise the extended leg; Two indicates the ability to flex the ankle but an inability to flex the knee; and Three indicates total immobilisation of the lower extremity.
All patients received a sedative dose of 0.05 mg/kg of Midazolam throughout the surgery, and they were allowed to breathe spontaneously during the procedure. Patients who encountered dural puncture were supplemented with general anaesthesia and excluded from the study.

Statistical analysis
The most recent version of SPSS was used. The descriptive statistics were computed by the mean, standard deviation, range, and proportion. The inferential statistics used were the unpaired t-tests, and chi-square tests to determine significance. The p-value represents the probability, at a significance level of 0.05, for the given degree of freedom. ($p<0.05$ is considered statistically significant whereas $p<0.01$ are deemed highly significant).

RESULTS

The study compared the motor and hemodynamic effects of levobupivacaine 0.5% and ropivacaine 0.75% administered as epidural anaesthesia for surgeries below the umbilicus. The findings revealed that the duration, onset, and regression of motor block were comparable between the two groups. However, significant differences were observed in the motor block grade as per the Modified Bromage Scale (MBS) ($p<0.01$). Group R (ropivacaine) achieved maximum motor blockage in 40.18 minutes, whereas Group L (levobupivacaine) reached it in 17.86 minutes ($p=0.043$) (Tables I and II). The average duration of motor block was 146.25±48.58 minutes for Group R and 160.71±46.64

MOTOR PROFILE:

Table I: Motor block from 0 to 180 minutes

Time	R	L	p value
5	0.68±0.94	0.89±0.49	0
10	1.18±1.02	1.32±0.54	0.01
15	1.57±0.92	1.71±0.89	1
20	2.00±0.66	2.00±0.90	0.06
25	2.25±0.70	2.11±0.87	0.08
30	2.36±0.73	2.18±0.86	0.27
60	2.50±0.79	2.25±0.84	0.47
90	2.46±0.69	2.14±0.89	0.04
120	2.36±0.67	1.82±0.72	0.91
150	1.82±1.09	1.50±0.63	0.02
180	1.29±1.3	1.18±0.67	0

The Table I shows the motor block as per MBS from 0 to 180 minutes between Group R and L.

Table II: Motor Block Variables

Motor Block Variables	R	L	p value
MO	24.64	16.43	0.5
MR	170.54	177.14	0.84
TTMBS≥2	146.25	160.71	0.53
Maximum MBS	2.86	2.21	0
Time taken for maximum MBS	40.18	17.86	0.004

Table II shows the time for motor onset (as defined by Modified Bromage Scale ≥2 (MO), time for motor reversal <2 (MR), time to reach MBS ≥2 (TTMBS2), maximum MBS reached, and time taken to reach maximum MBS between Group R and L.

HAEMODYNAMIC PROFILE:

Table III: Heart rate from 0 to 180 minutes

Time	R	L	p value
Pre procedure	86.68±19.22	83.54±17.31	0.39
0	88.54±19.11	84.61±17.05	0.33
5	88.64±24.43	83.93±17.68	0.19
10	85.54±16.69	81.18±19.39	0.26
15	79.25±16.73	79.43±18.77	0.45
20	77.79±14.04	106.21±154.71	0.93
25	78.75±15.63	78.21±16.66	0.84
30	77.04±14.77	79.46±16.34	0.59
60	74.11±14.05	79.11±15.28	0.62
90	70.29±13.47	77.43±15.43	0.27
120	72.75±14.06	78.11±16.25	0.31
150	74.36±14.02	78.50±14.18	0.85
180	76.64±15.37	78.32±13.19	0.6

Table: III display heart rate between 0 to 180 minutes between Group R and L.

Table IV: Mean Arterial Pressure (MAP) from 0 TO 180 minutes

Time	R	L	p value
Pre procedure	98.40±15.71	93.97±10.62	0.05
0	98.80±15.65	89.16±10.28	0.01
5	87.090±14.70	86.68±10.62	0.05
10	83.68±15.68	83.64±10.83	0.08
15	81.47±17.18	82.52±12.56	0.24
20	79.40±10.71	81.81±12.76	0.53
25	81.27±15.46	82.48±12.82	0.9
30	83.00±17.75	83.37±12.51	0.42
60	81.29±20.84	82.98±9.51	0.06
90	79.66±15.74	84.05±8.97	0.02
120	85.34±20.80	84.85±10.98	0.01
150	85.00±14.71	84.65±11.42	0.23
180	84.71±13.29	85.79±11.74	0.93

Table IV display MAP between 0 and180 minutes for Group R and L.

Table V: Arterial oxygen saturation from 0 to 180 minutes

Time	R	L	p value
Pre procedure	99.14±2.52	98.86±2.17	0.91
5	98.93±1.08	99±2.43	0.1
10	98.93±1.18	99.07±1.94	0.17
15	99.07±1.05	98.93±2.38	0.03
20	98.82±1.61	99.39±1.54	0.26
25	99±1.36	99.36±1.22	0.25
30	99.14±1.22	99.61±1.13	0.1
60	99.18±1.56	99.46±1.20	0.29
90	99.75±0.79	99.64±1.54	0.42
120	99.86±0.44	99.75±1.32	0.35
150	99.71±0.85	99.68±1.36	0.68
180	99.79±0.56	99.64±1.89	0.35

Table V show oxygen saturation between 0 and 180 minutes forGroup R and L.

minutes for Group L, with no significant difference (p>0.05) (Table II). Haemodynamic parameters such as heart rate (HR), mean arterial pressure (MAP), and oxygen saturation (SpO2) showed no significant differences between the two groups at various time intervals (Tables III, IV and V). These results suggest that while the onset of motor block was faster with levobupivacaine, the overall duration of motor block was similar for both anaesthetics. Additionally, both maintained stable hemodynamic profiles throughout the observation period.

DISCUSSION

The demographic profile and type of surgeries between the two groups were similar. In our study, the motor onset (MO) was 24.64 min in group R and 16.43 min in group L, (p=0.502), findings consistent with other studies.[4,7,8] Saha et al. found that the mean onset of motor block in group I (L) was 28.07±4.01 min and that of group II (R) was 23.07±2.77. (p<0.001)9Maheshwari et al. observed that the mean time for MO was significantly shorter in group II (R) (23.14±2.73 min) compared to group I (L) (31.43±2.59min) (p<0.05).[10] A study by Gandhi et al., compared the effects of epidural levobupivacaine 0.5% (group A) and ropivacaine 0.75% with fentanyl 100 mcg (group B) in patients undergoing orthopaedic surgeries and found that the MO and motor duration were comparable in both groups.[11]

Motor regression (MR) in our study was 170.54 min in group R and 177.14 min in group L, (p-value of 0.84). Our study suggests that the motor regression was faster in the R group, implying that this drug may be suitable for surgeries requiring early ambulation, postoperative analgesia, and obstetric analgesia. Olofsen Erik et al., recorded in their study that ropivacaine had a slower onset and offset than levobupivacaine.[12]

In the present study, the duration of motor block in group R was 146.25±48.58 min, while in group L it was 160.71±46.64 min. Brockway et al. demonstrated that the MO in ropivacaine group was slower and its duration of motor blockade was shorter than that of levobupivacaine.[13] Casati et al., compared epidural 0.5% of levobupivacaine and ropivacaine and found both groups had similar motor profiles.[8] Saha et al., found that the mean duration of Motor Block in group I (L) was 143.51±5.69 min and that of group II (R) patients was 141.78±3.35 min. (p=0.082).[9]

The mean motor block grade between the two groups (mean 2.86±0.35 in group R vs. 2.21±0.87 in group L) significantly differed, with a p<0.001. The time taken to reach maximum motor blockade was 40.18 minutes in group R and 17.86 minutes in group L (p=0.004). Additionally, 71.4% of patients achieved MBS 3 in motor block in group R, compared to 50% in group L, indicating a lower grade motor block in group L. Peduto et al. compared the effects of epidural administration of levobupivacaine 0.5% and ropivacaine 0.75% for lower limb procedures and observed that both drugs have similar clinical profiles.[2] This observation was also supported by Katz J A et al.[14] and Casati et al.[8] In our study the MO was shorter and duration of motor block lasted longer in group L compared to R. The time taken to obtain maximum motor grade was longer but denser in R group.

The intraoperative haemodynamic profiles of both groups were similar showing no significant statistical significance. Senard et al., observed similar efficacy with use of equal doses of levobupivacaine and ropivacaine postoperatively via PCEA, with the only difference being that patients receiving ropivacaine were able to ambulate earlier.[15] There were no significant differences in the total amount of intravenous fluids infused and ephedrine usage (4 instances in each group).

CONCLUSION

Our study demonstrates that both levobupivacaine 0.5% and ropivacaine 0.75% are effective and well-tolerated for providing epidural anaesthesia in patients undergoing surgeries below the umbilicus. The motor block characteristics, including the duration, onset, and regression, were comparable between the two groups. However, significant differences were noted in the motor block grade and the time to achieve maximum motor blockage, with ropivacaine taking longer (40.18 minutes) compared to levobupivacaine (17.86 minutes). Despite these differences, the overall duration of the motor block was similar between the two groups. Haemodynamic parameters such as heart rate, mean arterial pressure, and oxygen saturation remained stable and showed no significant differences

throughout the study. Therefore, both levobupivacaine and ropivacaine can be considered reliable options for epidural anaesthesia in lower abdominal surgeries.

FUNDING ACKNOWLEDGEMENTS
No funding received for this study.

ETHICAL STATEMENTS
The study was approved by the ethical committee of Saveetha institute of medical and technological science (S.I.M.A.T.S) with number: 009/06/2023/IEC/SMCH.

ACKNOWLEDGEMENTS:
I would like to thank my Guide Dr. A. Rathna, Professor, Department of Anaesthesiology and Pain Management, Saveetha Medical College and Hospital, S.I.M.A.T.S., Chennai for her constant encouragement and motivation for my study.

CONFLICT OF INTEREST
None

REFERENCES
1. Khan A, Nanda HS, Chandra R. Levobupivacaine versus Ropivacaine: A Comparative Study of the Analgesic and Hemodynamic Spectrum. Int J Sci Stud 2016; 4(1): 190-5.
2. Peduto VA, Baroncini S, Montanini S, Proietti R, Rosignoli L, Tufano R, et al. A prospective, randomized, double blind comparison of epidural levobupivacaine 0.5% with epidural ropivacaine 0.75% for lower limb procedures. Eur J Anaesthesiol 2003; 20: 979-83.
3. Koch T, Fichtner A, Schwemmer U, Standl T, Volk T, Engelhard K, et al. Levobupivacaine for epidural anaesthesia and postoperative analgesia in hip surgery: A multi-center efficacy and safety equivalence study with bupivacaine and ropivacaine. Anaesthesist 2008; 57: 475-82.
4. Yang CW, Jung SM, Kwan HU, Kung PS, Ryu SH. Comparison of epidural anesthesiology with 0.5% levobupivacaine and 0.5% ropivacaine for cesarean section. Korean J Anesthesiol 2007; 52: 284-90.
5. Capogna G, Celleno D, Fusco P, Lyons G, Columb M. Relative potencies of bupivacaine and ropivacaine for analgesia in labour. Br J Anaesth1999; 82: 371-3
6. Polley LS, Columb MO, Naughton NN, Wagner DS, vandeVen CJ. Relative Analgesic potencies of ropivacaine and bupivacaine for epidural analgesia in labor:implications for therapeutic indexes. Anesthesiology1999; 90: 944-50
7. Casati A, Putzu M. Bupivacaine, levobupivacaine and Ropivacaine:are they clinically different? Best Pract Res Clin Anaesthesiol 2005; 19: 247-68.
8. Kumar GS, Kanth L, Srinath M. A Comparative Study between Bupivacaine 0.5% and Ropivacaine 0.75% in Epidural Analgesia in Patients Undergoing Elective Lower Abdominal and Lower Limb Surgeries. Int J Sci Stud 2018; 6(5): 126-34
9. Gunjan S, Bipul D, Kammauj S, Sonowal K. Comparative study of Epidural Levobupivacaine 0.5% and Ropivacaine 0.75% on lower limb Orthopaedic surgeries. International Journal of Science and Research (IJSR) 2023; 12(3): 325-8.
10. Maheshwari V, Rasheed MA, Singh RB, Choubey S, Sarkar A. Comparison of ropivacaine with levobupivacaine under epidural anaesthesia in the lower limb orthopaedic surgeries: A randomized study. Anesth Essays Res 2016; 10(3): 624-30.
11. Gandhi GS, Bindra TK, Kumar P, Kaushal B. Comparative evaluation of levobupivacaine - fentanyl and ropivacaine - fentanyl in epidural anaesthesia in lower limb orthopaedic surgeries in elderly patients. Indian Journal of Clinical Anaesthesia 2020; 7(2): 324-8.
12. Olofsen E, Burm AG, Simon MJ, Veering BT, van Kleef JW, Dahan A. Population pharmacokinetic-pharmacodynamic modeling of epidural anesthesia. Anesthesiology 2008; 109(4): 664-74.
13. Brockway MS, Bannister J, McClure JH, McKeown D, Wildsmith JA. Comparison of extradural ropivacaine and bupivacaine. Br J Anaesth 1991; 66: 31–7.
14. Katz JA, Jefferey AK, Donna K. A double blind comparison of 0.5% Bupivacaine and 0.75% ropivacaine administered epidurally in humans. Reg Anesth 1990; 15: 250-2.
15. Senard M,Kaba A,Jacquemin MJ, Maquoi LM, Geortay MN, Honoré PD, et al. Epidural levobupivacaine 0.1% or ropivacaine0.1% combined with morphine provides comparable analgesia after abdominal surgery. Anesth Analg 2004; 98:389-94.

Haematological indices as screening tool in distinguishing beta thalassemia trait and iron deficiency anaemia: Insights from a tertiary hospital study

Yogalakshmi E, DCP, Vimal Chander R, MD, Sulochana Sonti, MD, Kavitha K, MD

Department of Pathology, Saveetha Medical College and Hospital, Saveetha Institute of Medical and Technical Sciences, Chennai

ABSTRACT

Introduction: Beta thalassemia trait (BTT) or heterozygous, is an inherited haematological disease characterised by more than 100 different mutations that lead to reduced beta chain formation. Distinguishing BTT from Iron deficiency anaemia (IDA) is challenging since both conditions are characterised by microcytic anaemia, have distinct underlying causes, and thus require different approaches in treating the condition. The aim of our study is to determine the utility of haematological indices as a screening marker in detecting cases of beta thalassemia carriers and differentiating it from IDA in our tertiary care hospital.

Materials and Methods: A retrospective analysis of the data at the Department of Pathology from January 2020 to December 2023 (4 years duration) was conducted. The analysis included a comparison of haematological parameters and RBC (Red Blood Cell) indices between the 78 cases of BTT and the 60 cases of IDA. Complete blood count (CBC) samples were collected in 2 ml of K2 EDTA (Di potassium Ethylene Diamine Tetra Acetic acid) vacutainer tube and processed in the automated haematology analyser, Sysmex XN 1000. Haematological parameters were analysed, and RBC indices were calculated. HPLC (High Performance Liquid Chromatography) analysis was done to detect HbA2/F levels. HbA2 levels more than 4% were diagnosed as BTT in our study. Various discriminating formulas, such as Srivastav index(SI), Red blood cell Distribution Width Index (RDWI), Shine and Lal index (SLI), Ricera index (RI), Green and King index (GKI), Mentzer index (MI), Sirdah Index (SI), Mean density of Haemoglobin/litre of blood (MDHL), England and Fraser index (EFI), Mean Cell Haemoglobin Density (MCHD), and Ehsani Index (EI), were applied to differentiate BTT cases from IDA Cases.

Results: The mean haemoglobin in BTT was 10.8 g/dl, while in IDA, the mean Hb was 7.4 g/dl. The mean RBC count in BTT was 5.6 million/mm3, while in IDA it was 3.8 million/mm3. The values of haemoglobin (HB), Red blood cell Distribution Width – Coefficient of Variation (RDW-CV), Mean Corpuscular Haemoglobin Concentration (MCHC) and Mean Corpuscular Volume (MCV), between BTT cases and IDA cases showed statistical significance of p<0.05. Among the 11 discriminator formulas applied in our study, maximum accuracy was observed with the Ehsani index (84.06%), followed by the MI (82.61%). Maximum sensitivity was observed with RDWI (97.44%), followed by SLI (96.15%), EI (83.3%), and MI (79.45%). Youdens' score was highest in Ehsani index (68.33%), followed by MI (66.16 %), and the Green and King index (59.87%).

Discussion: Among the various discriminator formulas applied, two indices, such as EI and MI showed the highest accuracy, and maximum score in Youdens' formula. Hence, in mass screening or in cases suspected to have IDA, either MI <13 or Ehsani index <17 with normal serum ferritin levels can be subjected to HPLC evaluation for the diagnosis of beta thalassemia carrier cases.

KEYWORDS:
BTT, Mentzer index, Microcytic hypochromic anaemia, High performance liquid chromatography

INTRODUCTION

Beta thalassemia trait (BTT), or heterozygous, is an inherited haematological disease characterised by more than 100 different mutations that leads to reduced beta chain.[1] BTT is indeed often clinically asymptomatic or presents with minimal symptoms.[2] Distinguishing between BTT and Iron deficiency anaemia (IDA) are challenging, since both conditions are characterised by microcytic anaemia, have distinct underlying causes and thus require different approaches in treating the condition.[3] BTT generally doesn't require iron supplementation unless there is a co-existing iron deficiency.[4] Unnecessary iron supplementation in individuals with BTT can lead to iron overload.[5] BTT carries groups, implications, if both the parents are carriers of the BTT.[6] Several formulas and Red blood cell indices (RBCI) are formulated to differentiate between IDA and BTT.[7] RBC parameters such as mean corpuscular volume(MCV) and mean corpuscular haemoglobin concentration (MCH) are lower in cases of BTT as well as in IDA while the RBC count is often normal or even elevated in the cases of BTT and lower in IDA.[8,9] discriminating formulas such as Srivastav index(SI),Red cell distribution width index (RDWI), Mentzer index (MI), Ricera index(RI), Shine and Lal index(SLI), Green and King index(GKI), Sirdah Index(SI), Mean density of Haemoglobin/litre of blood (MDHL), England and Fraser index(EFI), Mean Cell Haemoglobin Density(MCHD) and Ehsani Index (EI) are nowadays utilised as a screening method in distinguishing BTT cases from IDA.[10-13] Hence proper differentiation of BTT with RBC indices and Discriminating formula allows appropriate genetic

This article was accepted: 12 December 2024
Corresponding Author: Kavitha K
Email: drkavithasmch@gmail.com; doctorkavithalink@gmail.com

counselling for affected individuals and their families, informing them about the risks and implications for their children. The aim of our study is to determine the utility of haematological indices, as a screening marker in detecting cases of Beta thalassemia carrier and in differentiating it from IDA in our tertiary care hospital.

MATERIALS AND METHODS

Study design:
A retrospective study was conducted in our institution, in the Department of Pathology, for a duration of four years (January 2020- December 2023). This study received clearance from the institutional ethics committee with an IEC Reference number 008/12/2022/IEC/SMCH.

Inclusion criteria:
The study included a comparison of haematological parameters and RBC indices between the two groups BTT (78 cases) and IDA (60 cases). Cases with HbA2 more than 4% in HPLC study were considered BTT. Cases of IDA were diagnosed based on the iron studies that were included for comparison.

Exclusion criteria:
Cases with a history of blood transfusion less than three months and other haemoglobinopathies were excluded from the study.

Study methodology:
Complete blood count was analysed using Sysmex automated haematology analyser XN1000. Haematological parameters such as HB, RDW, Haematocrit, RBC, MCV, MCHC and Mean corpuscular haemoglobin (MCH) were observed. The following Indices as SRI, RDWI, MI, RI, SLI, GKI, SI, MDHL, EFI, MCHD and EI were calculated and statistically analysed using SPSS statistical package version 23 and JASP version 0.18.3. Chi-square test and Anova test were used to compare between the two groups BTT with IDA. A $p<0.05$ was generally considered to be statistically significant. Receiver operating characteristic (ROC) curve analysis was completed using the same software to elicit the area under the curve (AUC) for the red cell indices and discriminator formula. The point of the curve where sensitivity and specificity were almost equal was considered as the optimal cut off for the red cell parameters.

RESULTS

Age and gender distribution among BTT and IDA cases:
This study included 78 cases of BTT and 60 cases of IDA. The age group included among BTT cases were between 1 year and 56 years, and the age group of the IDA cases were between 1 year - 49 years. The mean age in BTT was 26 years and the mean age in IDA was 24 years. The male to female ratio in BTT was 1.29:1 and in IDA was 7.5:1. Majority of IDA cases were found to be females, whereas most of BTT cases were found to be males.

Analysis of haematological parameters in BTT and IDA cases:
The mean haemoglobin in BTT includes 10.8 g/dl with a range of 4.8g/dl to 17 g/dl. While in IDA mean Hb was 7.4 g/dl with a range of Hb 3.6 g/dl to 10.3 g/dl. Mean RBC count in BTT was 5.6 million/mm3 while in IDA was 3.8 million/mm3. Mean MCV, MCH, MCHC and RDW-CV values in BTT were 63.5 fl, 19.6 pg, 30.7g/dl and 18.2% retrospectively. While in IDA, mean values of MCV, MCH, MCHC and were as 69.6 fl, 19.3 pg, 27.6g/dl and 19.9% retrospectively. The values of HB, MCV, MCHC and RDW-CV between BTT and IDA show statistical significance with p value <0.05, tabulated in Table I.

Various formulas used to differentiate BTT and IDA cases:
Table II showed the various discriminating indices in differentiating BTT from IDA. Statistical significance of $p<0.05$ was seen in indices such as MI, EFI, GKI, SRI, RI, SI, EI, RDWI and MDHL.

Statistical analysis of various index in BTT cases:
In this study accuracy, sensitivity, specificity, positive predictive value (PPV), negative predictive value (NPV) and Youden's index were calculated for the following haematological indices such as MI, GKI, SRI, RIC, MCHD, RDWI, SLI, EFI, SI, EI and MDHL

The formula used for accuracy, sensitivity, specificity, positive predictive value (PPV), negative predictive value (NPV) and Youden's index are as follows:
Accuracy = (True positive +True negative) (True positive +True negative +False positive +False negative)] × 100

sensitivity=True positive /True positive + False negative × 100

specificity=True negative/True negative + False positive × 100
positive predictive value (PPV)=True positive /True positive + False positive × 100

negative predictive value (NPV) =True negative/True negative + False negative × 100
Youden's formula = (Sensitivity + Specificity) – 100

The maximum accuracy was observed in, EI (84.06%) followed by the MI (82.61%). The maximum sensitivity was observed in RDWI (97.44%), SLI (96.15%), EI (83.3%) and MI (79.45%) retrospectively. Youdens' score was best in EI 68.33%, followed by MI 66.16 % and GKI 59.87% retrospectively.

Receiver operating characteristic (ROC) curve for Mentzer index:
The diagnostic efficacy of MI for predicting thalassemia cases was assessed using the ROC curve as shown in figure 1. ROC plots displayed sensitivity versus 1-specificity, such that area under the curve generated was 0.89, indicating increased discriminating ability.

DISCUSSION

The most common cause of anaemia in developing countries is IDA. Microcytic picture is seen in both cases of IDA and BTT cases hence diagnosis of BTT is often missed, all microcytic anaemia is managed with iron treatment. There is a chance of 25 % risk of having thalassemia major baby in each pregnancy if both the parents are of beta thalassemia carrier. Many formulas and indices are used as a screening tool to

Table I: Characteristics of haematological parameters in BTT vs. IDA

Parameters	MCV (fl)	MCH (pg)	MCHC (g/dl)	RDW-CV (%)	HB g%	RBC in millions
			BTT			
Mean	63.5	19.6	30.7	18.2	10.8	5.6
SD	7.2	2.6	1.6	3.0	2.2	1.1
Minimum	52.4	14.6	25.6	13.5	4.8	1.49
Maximum	98	32.2	34	30.2	17	7.69
			IDA			
Mean	69.6	19.3	27.6	19.9	7.4	3.8
SD (Standard Deviation)	9.9	4.6	2.9	4.1	1.7	0.63
Minimum	53	9.2	21.1	13.2	3.6	2.6
Maximum	90	29.4	33.1	30.0	10.3	5.3
p-value Significance between BTT & IDA group	<0.001	0.646	<0.001	0.006	<0.001	<0.001

Table II: Discriminating formula in differentiating cases of BTT vs. IDA

INDEX	FORMULA	CUT OFF	NO OF CASES	BTT	IDA	p value
MI	MCV / RBC	13	< 13	62	8	<0.001*
			>13	16	52	
GKI	(MCV × MCV × RDW) / (Hb × 100)	65	<65	48	1	<0.001*
			>65	30	59	
EFI	MCV – (5 × Hb) – RBC – 3.4	0	<0	45	0	<0.001*
			>0	33	60	
MCHD	MCH/MCV	0.35	>0.35	0	1	0.33
			<0.35	78	59	
SRI	MCH / RBC	3.8	<3.8	57	13	0.001*
			>3.8	21	47	
RI	RDW / RBC	4.4	>4.4	7	45	<0.001*
			<4.4	71	15	
SI	MCV – RBC – (3 × Hb)	27	27	50	0	<0.001*
			>27	28	60	
EI	MCV – (10 × RBC)	17	<17	65	9	<0.001*
			>17	13	51	
MDHL	(MCH/MCV) × RBC	1.67	>1.67	45	0	<0.001*
			<1.67	33	60	
SLI	(MCV)2× MCH/100	1530	<1530	75	50	0.190
			>1530	3	10	
RDWI	MCV × RDW/RBC	220	<220	76	60	0.0318*
			>220	2	0	
RBC in million/mm^3		5.5	>5.5	45	0	<0.001*
			<5.5	33	68	

*Statistically significant MI- Mentzer index, RDWI- Red blood cell Distribution Width Index, SLI- Shine and Lal index, RI- Ricera index, GKI- Green and King index, SI- Sirdah Index, MDHL- Mean density of Haemoglobin/litre of blood, EFI- England and Fraser index, MCHD- Mean Cell Haemoglobin Density, EI- Eshani Index.

Table III: Accuracy /Sensitivity /specificity /PPV/NPV/Youdens' indices in BTT cases

INDEX	Sensitivity (%)	Specificity (%)	Accuracy	PPV (%)	NPV (%)	Youdens'
MI	79.49	86.67	82.61	85.57	76.47	66.16
SLI	96.15	16.67	61.59	60	76.92	12.82
EFI	57.69	100	76.09	100	64.52	57.69
GKI	61.54	98.33	77.54	97.96	66.29	59.87
SRI	73.08	78.3	75.36	81.43	69.12	51.41
RI	8.97	25	15.94	13.46	17.44	66.03
SI	64.1	100	79.71	100	68.18	64.1
EI	83.3	85	84.06	87.84	79.69	68.33
MDHL	57.69	100	76.09	100	64.52	57.69
MCHD	0	98.33	42.75	0	43.07	-1.67
RDWI	97.44	0	55.07	55.88	0	-2.56
RBC	57.69	100	76.09	100	64.52	57.69

MI- Mentzer index, RDWI- Red blood cell Distribution Width Index, SLI- Shine and Lal index, RI- Ricera index, GKI- Green and King index, SI- Sirdah Index, MDHL- Mean density of Haemoglobin/litre of blood, EFI- England and Fraser index, MCHD- Mean Cell Haemoglobin Density, EI- Ehsani Index.

Table IV: comparison of sensitivity among the various discriminator formula between our study and other study

STUDY	Present study	Bhargava et al., study
RDWI	97.4	70.4
SLI	96.1	100
EI	83.3	80.6
MZ	79.4	80.6
SRI	73	34.6
SI	64.1	77.5
GKI	61.5	78.5
EFI	57.6	77.5
MDHL	57.69	62.24
RI	8.9	100
MCHD	0	40.82
RBC	57.6	63.2

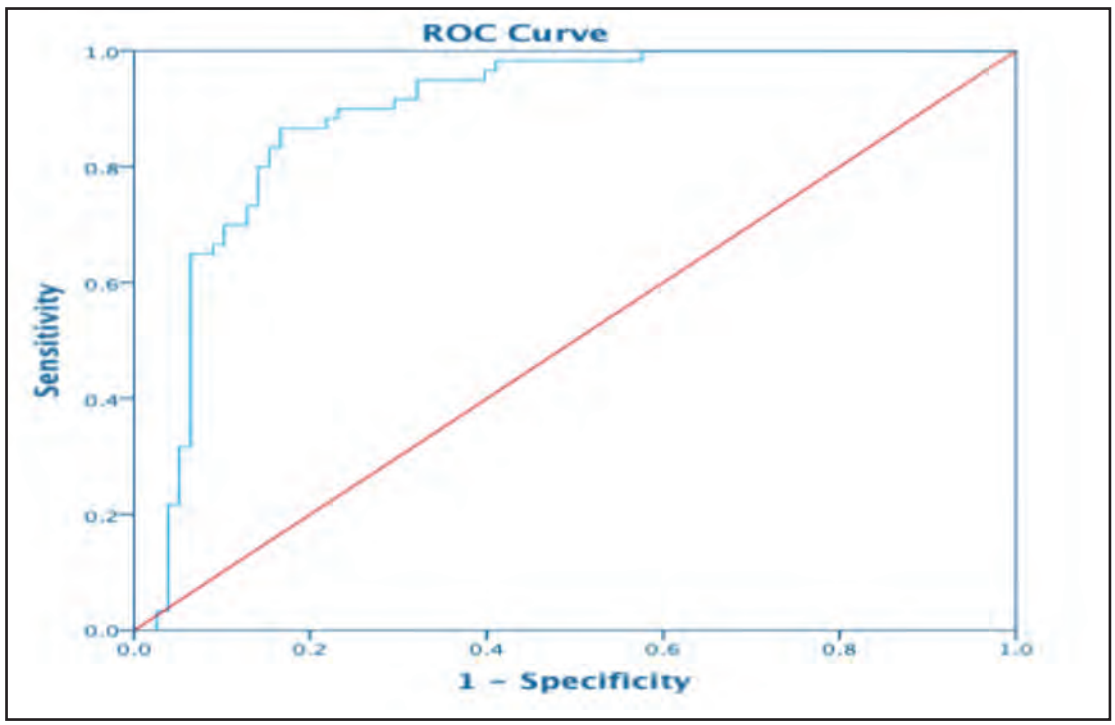

Fig. 1: ROC Curve - Mentzer index

differentiate BTT from IDA. These indices are helpful in mass screening. According to (TIF) the International Thalassemia Federation guidelines, MCH <27 pg, MCV <78 fl, and with microcytic, hypochromic picture findings in blood smear were suspected as carriers.[14] Our study showed that mean MCV as 63.5 fl and Mean MCH as 19.6pg. Mean RBC count in BTT is 5.6 million/cu.mm compared to the IDA of 3.8 millions.cu.mm which is the distinguishing finding in differentiating BTT. The values of HB, MCV, MCHC and RDW-CV compared between BTT and IDA show statistical significance of $p<0.05$ while the MCH does not show statistical significance.

The maximum sensitivity observed in our study was RDWI (97.44%) which was in concordance with the Jameel et al., study showed that 94% sensitivity for BTT cases[8] followed by RDWI index, SLI showed 96.15% sensitivity in present study similar to Bhargava M et al study showed 100% sensitivity. A study by Bordhar et al., showed 87.6% sensitivity for the cases of BTT.10,15 (Table IV)

In our research, Youden's highest score was observed in the EI at 68.33%, with the MI following closely behind at 66.16%, and the GKI at 59.87%. Conversely, in the study conducted by Bhargava et al, the highest Youden score was identified in the EFI at 89.92%, with the RIC index following closely behind at 87.39%.

In our research, the EI achieved the highest accuracy at 84%, succeeded by the MI at 82.6% and the SI index at 79.71%. Comparatively, when aligning our results with the Bhargava et al study, the GKI index exhibited the highest accuracy at 97.5%, with the RBC index closely trailing at 96.56%.

CONCLUSION

The difference between IDA and BTT requires careful interpretation of red cell indices. Mentzer index is also helpful to distinguish IDA and BTT cases. In our study, among the various discriminator formulas applied, two indices, such as EI and MI, had shown highest accuracy and maximum score in the Youdens' formula. Hence in mass screening or in cases of suspected IDA, either MI <13 or EI <17 with normal serum ferritin levels should be subjected to HPLC study for the diagnosis of BTT cases. And also, antenatal women with microcytic hypochromic anaemia with normal iron profile should undergo HPLC screening.

CONFLICT OF INTEREST

All co-authors had read and agreed the manuscript and there is no conflict of interest in this study.

REFERENCES

1. Jaing TH, Chang TY, Chen SH, Lin CW, Wen YC, Chiu CC. Molecular genetics of β-thalassemia: A narrative review. Medicine (Baltimore) 2021; 100(45): e27522.
2. Origa R. β-Thalassemia. Genet Med 2017; 19(6): 609-19.
3. Kabootarizadeh L, Jamshidnezhad A, Koohmareh Z. Differential diagnosis of iron-deficiency anemia from β-thalassemia trait using an intelligent model in comparison with discriminant indexes. Acta Inform Med 2019; 27(2): 78-84.
4. Verma S, Gupta R, Kudesia M, Mathur A, Krishan G, Singh S. Coexisting iron deficiency anemia and Beta thalassemia trait: effect of iron therapy on red cell parameters and hemoglobin subtypes. ISRN Hematol 2014; 2014: 293216
5. Basu S, Rahaman M, Dolai TK, Shukla PC, Chakravorty N. Understanding the Intricacies of Iron Overload Associated with β-Thalassemia: A Comprehensive Review. Thalassemia Reports. 2023; 13(3): 179-94.
6. Noor FA, Sultana N, Bhuyan GS, Islam MT, Hossain M, Sarker SK, et al. Nationwide carrier detection and molecular characterization of β-thalassemia and hemoglobin E variants in Bangladeshi population. Orphanet J Rare Dis 2020; 15(1): 15.
7. Shuang X, Zhenming W, Zhu M, Si S, Zuo L. New logarithm-based discrimination formula for differentiating thalassemia trait from iron deficiency anemia in pregnancy. BMC Pregnancy Childbirth 2023; 23(1): 100.
8. Jameel T, Baig M, Ahmed I, Hussain MB, Alkhamaly MBD. Differentiation of beta thalassemia trait from iron deficiency anemia by hematological indices. Pak J Med Sci 2017; 33(3): 665-9.
9. Wickramaratne KA, Wijewickrama DC. Screening for beta-thalassemia trait; applicability of red cell indices and parameters -A study in Sri Lanka. Int J Health Sci (Qassim) 2021; 15(1): 29-34.
10. Bhargava M, Kumar V, Pandey H, Singh V, Misra V, Gupta P. Role of hematological indices as a screening tool of beta thalassemia trait in Eastern Uttar Pradesh: an institutional study. Indian J Hematol and Blood Transfus 2020; 36(4): 719-24.
11. Kumar A, Saha D, Kini J, Murali N, Chakraborti S, Adiga D. The role of discriminant functions in screening beta thalassemia trait and iron deficiency anemia among laboratory samples. J Lab Physicians 2017; 9(03): 195-201.
12. Ebrahimpour Sadagheyani H, Sharafkhani R, Sakhaei S, Jafaralilou H, Shahmirzalou P. The evaluation of results of twenty common equations for differentiation of beta thalassemia trait from iron deficiency anemia: A cross-sectional study. Iran J Public Health 2022; 51(4): 929-38.
13. Jain AKK, Sharma P, Saleh S, Dolai TKK, Saha SCC, Bagga R, et al. Multi-criteria decision making to validate performance of RBC-based formulae to screen β-thalassemia trait in heterogeneous haemoglobinopathies. BMC Med Inform Decis Mak 2024; 24(1): 5.
14. Sari DP, Wahidiyat PA, Setianingsih I, Timan IS, Gatot D, Kekalih A. Hematological parameters in individuals with Beta thalassemia Trait in South Sumatra, Indonesia. Anemia 2022; 2022: 3572986.
15. Bordbar E, Taghipour M, Zucconi BE. Reliability of Different RBC indices and Formulas in Discriminating between β-thalassemia minor and other microcytic hypochromic cases. Mediterr J Hematol Infect Dis 2015; 7(1): e2015022.

Insights into necrotising fasciitis: A prospective pilot study in a Tertiary Care Hospital

Touzeen Hussain, Mudduluru Vishnu Priya

Department of General Surgery, Saveetha Institute of Medical and Technical Sciences

ABSTRACT

Introduction: Necrotising fasciitis, commonly referred to as "flesh-eating disease," is a rapidly spreading soft tissue infection characterised by extensive necrosis of the skin, subcutaneous tissue, and fascia while sparing the underlying muscle. Despite its low overall incidence, it is a significant soft tissue infection due to its rapid spread and associated high mortality risk.

Materials and Methods: This prospective pilot study aims to analyse 25 consecutive cases of necrotising fasciitis to assess various aspects, including age and sex incidence, microbial flora, role of co-morbidities in prognosis, and overall outcome. We conducted a descriptive study involving 25 patients aged 18-84 years diagnosed with necrotising fasciitis over a 6-month period (January 2022 to June 2022) at Saveetha Medical College.

Results: Of the 25 patients treated, 21 (84%) were male and 4 (21%) were female, resulting in a male-to-female ratio of 5.25. The age ranged from 18 to 84 years (Mean age: 50.24 ± Standard deviation, SD=14.175). Trauma was identified as the main precipitating factor in approximately 40% of cases, while Diabetes Mellitus (40%) emerged as the most common co-morbidity. Lower limb involvement was predominant in both male and female patients. The infection was mono-microbial in 32% of cases (Enterococci 16% + Bacteroides 16%) and poly-microbial in 68% with Streptococcus pyogenes + Escherichia coli being the most common organism combination. Wound debridement followed by split skin graft was the most common treatment modality (84%), with the number of debridement sessions varying based on infection severity (corresponding with higher LRINEC scores). Prolonged hospital stay was the most common complication, observed in 52% of cases.

Discussion: Our analysis revealed that necrotising fasciitis is more prevalent in individuals aged over 50 years with a male predominance. Streptococcus pyogenes with Escherichia coli was the predominant microflora, and Diabetes Mellitus emerged as the most common co-morbidity. Early recognition, prompt control of diabetes mellitus, aggressive surgical treatment, and supportive therapy are essential steps in managing necrotising fasciitis.

KEYWORDS:
Necrotising fasciitis, LRINEC score, Wound debridement

INTRODUCTION

Necrotising fasciitis (NF) is a rapidly spreading soft tissue infection characterised by extensive necrosis of the skin, subcutaneous tissue, and fascia while sparing the underlying muscle. It is often referred to as "suppurative fasciitis" or "flesh-eating disease." Despite its low overall incidence, NF is a significant soft tissue infection due to its rapid spread and associated high mortality risk. While the exact aetiology of NF remains unclear, it can develop following traumatic events or skin infections. It may also occur in patients following childbirth or those with burns. Factors predisposing individuals to NF include immunosuppression, chronic systemic diseases, and intravenous drug abuse. The Panton-Valentine leucocidin (PVL) toxin, produced by MRSA, has been implicated in its pathogenesis.

NF is classified into two types based on microbiological growth: Type 1 (Polymicrobial) infections involving a combination of aerobic and anaerobic organisms, and Type 2 (Monomicrobial) infections. A third type is reserved for myonecrosis caused by Clostridial infections. Diagnosis of NF relies on clinical and laboratory findings. Clinical presentation typically includes oedema and prominent signs of inflammation. The Laboratory Risk Indicator for Necrotising Fasciitis (LRINEC) score is increasingly used to assess the likelihood of NF, with a score of ≥6 indicating high suspicion. The primary approach to managing NF is surgical, with prompt wound debridement being the cornerstone of treatment. Microbial culture of debrided specimens guides specific antimicrobial coverage. Emerging modalities such as vacuum-assisted closure have shown promise in treatment. Our study aims to comprehensively assess the clinical features, laboratory parameters, prognostic factors, and treatment strategies employed in managing NF in a tertiary care hospital.

MATERIALS AND METHODS

The study was conducted after obtaining approval from the Institutional Ethics Committee (IEC) of Saveetha Medical College and Hospital, a tertiary care hospital in Chennai, Tamil Nadu, India, and aimed to comprehensively assess the clinical features, laboratory parameters, prognostic factors, and treatment strategies employed in managing NF. The LRINEC score, a validated tool, is calculated based on factors such as white blood cell count, haemoglobin, creatinine, sodium, and glucose levels, each of which can indicate systemic inflammation, anaemia, kidney dysfunction, electrolyte imbalance, or impaired immune function. A score

This article was accepted: 14 December 2024
Corresponding Author: Mudduluru Vishnu Priya
Email: vishnu.mudduluru96@gmail.com

Table I: Demographics and characteristics of the participants

S.NO	VARIABLES	Correlation coefficient	p-value
Age	<60 yr	20	80
	≥60 yr	5	20
Gender	Male	21	84
	Female	4	16
Co-morbid illness	Diabetes Mellitus	10	40
	Peripheral Vascular Disease	2	8
	Systemic Hypertension	1	4
	Chronic Kidney Disease	1	4
	Malignancy	1	4
Clinical stage at time of presentation	Stage 1	2	8
	Stage 2	6	24
	Stage 3	17	68
Microbial culture	Streptococcus pyogenes+ Escherichia coli	5	20
	Bacteroides	4	16
	Enterococcus	4	16
	MRSA	3	12
	Pseudomonas	2	8
	Streptococcus pyogenes+ Clostridium Perfingens	2	8
	Staphylococcus+ Proteus mirabilis	2	8
	Klebsiella Pneumonia+ Moraxella morganii	2	8
	Streptococcus pyogenes + Klebsiella pneumoniae	1	4
Lab parameters	**Component**	**Lab value mean**	**LRINEC component score mean**
	Haemoglobin	10.166	1.6±0.577
	TLC	16.376	0.68±0.476
	CRP	140.92	0.72±0.458
	Serum sodium	130.92	1.68±0.748
	Serum creatinine	1.14	0.64±0.952
	Blood glucose	125.4	0.68±0.476
	LRINEC	N/A	8.12±1.691

TLC- Total leucocyte count, CRP- C- reactive protein.

Table II: Correlation between clinical staging and Demographic variables

S.NO	VARIABLES	Correlation coefficient	p-value
1.	AGE#	0.017	0.934
2.	GENDER	-0.343	0.09
3.	COMORBID	-0.256	0.216
4.	MICROBIAL CULTURE	0.095	0.652
5.	ICU ADMISSION	-0.336	0.100
6.	MORTALITY	-0.219	0.293
7.	LIRENC SCORE#	0.710	<0.001*

#Continuous variable- The test used Pearson Correlation; Others- categorical variable- test used- Point Biserial Correlation; *p<0.01- Statistically significant

Table III: Correlation between LIRENC Score and demographic variable

S.NO	VARIABLES	Correlation coefficient	p-value
1.	AGE#	-0.099	0.639
2.	GENDER	-0.304	0.140
3.	COMORBID	-0.172	0.410
4.	MICROBIAL CULTURE	-0.080	0.704
5.	ICU ADMISSION	-0.316	0.124
6.	MORTALITY	-0.547	0.005*

#Continuous variable- The test used Pearson Correlation; Others- categorical variable- test used- Point Biserial Correlation; *p<0.01- Statistically significant

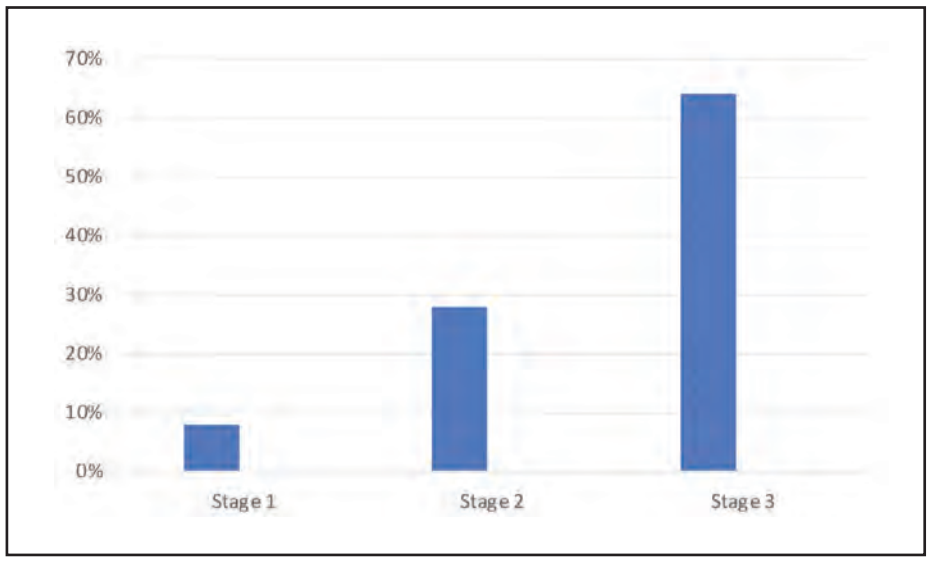

Fig. 1: Distribution of clinical staging of necrotising fasciitis at presentation

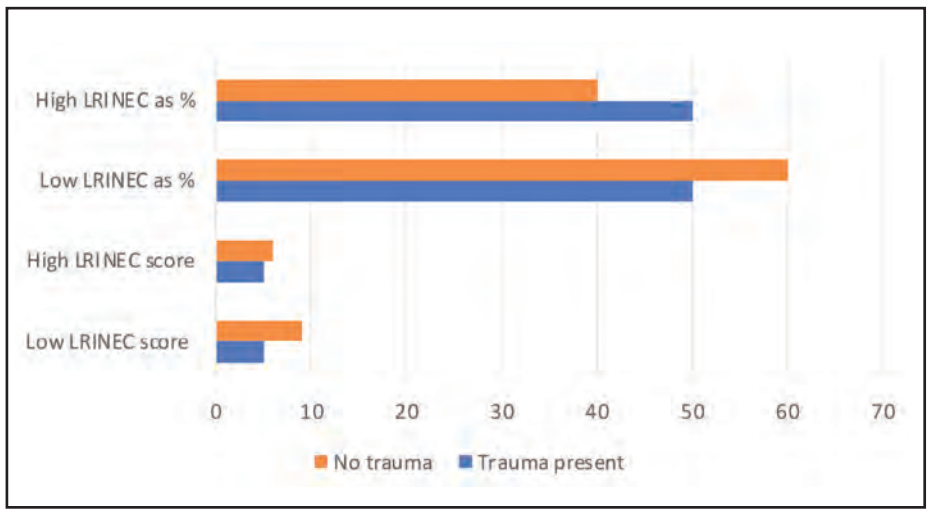

Fig. 2: Association of trauma with LRINEC score

of ≥6 is considered indicative of a high risk of necrotising fasciitis. This cross-sectional study included patients clinically diagnosed with necrotising fasciitis using convenience sampling, aged above 18 years old. A total of 25 adult patients of both sexes admitted to the Department of General Surgery at Saveetha Medical College and Hospital with a clinical diagnosis of necrotising fasciitis over a study period of 6 months were enrolled. Patients with diabetic foot ulcers, burn ulcers, skin malignancies, or cellulitis (after LRINEC score confirmation <6, along with the absence of a characteristic clinical course observed in necrotising fasciitis) were excluded from the study.

A comprehensive history was obtained, documenting the patient's age, sex, and presenting complaints along with the duration of symptoms. Specific inquiries were made regarding any preceding trauma, such as insect bites, acupuncture needle insertion, skin infections, or intravenous drug injections. Additionally, the history included chronic systemic diseases like diabetes, hypertension, peripheral vascular disease, malignancy, chronic kidney disease, and chronic alcohol intake. Any history of organ transplantation, use of immunosuppressant drugs, or corticosteroids was also noted.

A thorough general examination and assessment of vital signs were conducted to identify any undiagnosed chronic systemic diseases or signs suggestive of immunosuppression, such as oral candidiasis. The infection site was carefully examined for signs of inflammation, including erythema, swelling, warmth, and tenderness. Patients were categorised into clinical stages of necrotising fasciitis based on the extent of tissue involvement. Upon admission, laboratory assessments were performed, including haemoglobin levels, total leukocyte count, C-reactive protein, serum creatinine, serum sodium, and blood glucose levels. The LRINEC score was calculated for each patient to stratify the severity of the disease into low or high risk based on the score range.

Clinical risk factors for necrotising fasciitis are based on the patient's clinical presentation, such as trauma history and underlying medical conditions. Laboratory risk factors are based on laboratory test results, such as elevated white blood cell count and abnormal renal function tests. The LRINEC score is a tool to quantify laboratory risk, with scores ≥6 indicating high risk. Data analysis involved descriptive statistics and appropriate statistical tests. To minimise bias related to age and sex, the study population was representative of the general population of patients with necrotising fasciitis, and statistical methods were used to adjust for these factors.

Surgical treatment modalities included debridement of necrotic tissue, fasciotomy, disarticulation of digits, or vacuum-assisted closure. Repeat sessions of surgical debridement were conducted until complete removal of infected tissue was achieved. Empirical antimicrobial therapy was initiated promptly and adjusted based on microbial culture and sensitivity reports. Patients were closely monitored on a daily basis to track disease progression and response to treatment. The overall outcome, including cure, hospital stay, admission to intensive care, or mortality, was documented for each patient. Data collected were tabulated using MS Excel and analysed using SPSS 20.0 for statistical analysis.

RESULTS

After eliminating bias regarding age and sex by noting consecutive fitting of the inclusion criteria, it was found that the mean age of patients presenting with necrotising fasciitis was 50.24 years. Among the study population, 80% were aged <60 years, while 20% were aged ≥60 years. Male patients constituted the majority, accounting for 84% of the cases diagnosed with necrotising fasciitis, whereas females comprised 16%.

The mean clinical staging at admission was 2.56±0.651, reflecting the severity of the condition upon presentation. Diabetes emerged as the most prevalent comorbidity, affecting 40% of the patient cohort, followed by peripheral vascular disease (8%). A notable 40% of patients had a history of trauma preceding the development of necrotising fasciitis, shown in Table I, with males being disproportionately affected (80% male vs. 20% female).
Culture analysis revealed polymicrobial infections in 48% of cases, with the most common combination being Streptococcus + Escherichia coli (20%). Streptococcus emerged as the predominant organism overall, accounting for 32% of cases, emphasising its role in the pathogenesis of necrotising fasciitis.

Upon admission, patients exhibited abnormal laboratory findings indicative of systemic inflammation and organ dysfunction. The mean haemoglobin level was 10.166 g/dL, suggesting varying degrees of anaemia. Elevated levels of total leukocyte count (TLC) at 16.376 cells/mm3 and C-reactive protein (CRP) at 140.92 mg/L indicated an active inflammatory process. Serum sodium levels averaged 130.92 mEq/L, while serum creatinine and blood glucose levels were within normal limits at 1.14 mg/dL and 125.4 mg/dL, respectively Table I. The mean LRINEC score, a validated tool for predicting necrotising fasciitis, was 8.12±1.691, highlighting the severity of the disease in the study cohort.

Table II displays the correlation between clinical staging and various demographic variables. The Pearson correlation test was used for continuous variables, while the Point Biserial correlation test was used for categorical variables. Notably, the LIRENC score showed a statistically significant correlation ($r=0.710$, $p<0.001$) with clinical staging.

Figure 2 illustrates the association between trauma history and LRINEC scores in patients diagnosed with necrotising fasciitis. Among patients with a history of trauma, an equal number (50%) presented with low and high LRINEC scores, indicating a balanced distribution of disease severity. Conversely, among patients without a history of trauma, a higher percentage (60%) exhibited low LRINEC scores compared to those with high LRINEC scores (40%). This suggests a potential correlation between trauma history and LRINEC scores, with trauma possibly influencing the severity of necrotising fasciitis.

Table III presents the correlation between the LIRENC score and various demographic variables. Among the variables analysed, mortality showed a statistically significant negative correlation with the LIRENC score ($r=-0.547$, $p=0.005$), indicating that higher LIRENC scores are associated with lower mortality rates. Other demographic variables, including age, gender, comorbid conditions, microbial culture results, and ICU admission, did not show statistically significant correlations with the LIRENC.

DISCUSSION

Necrotising fasciitis (NF) presents a formidable challenge in both diagnosis and management, characterised by rapid tissue necrosis and potentially fatal outcomes. Its aetiology encompasses a spectrum of traumatic events,[1] from minor injuries to major surgical interventions, underscoring the diverse array of precipitating factors. Contributing to this complexity are predisposing conditions such as diabetes mellitus, immunosuppression, peripheral vascular disease,[2] and intravenous drug abuse,[3] each serving to heighten susceptibility to NF. This intricate interplay of risk factors underscores the multifaceted nature of the disease and emphasises the importance of comprehensive risk assessment in clinical practice.

The clinical manifestation of NF typically unfolds in distinct stages, beginning with local signs of inflammation and progressing to more severe manifestations characterised by bullae formation and extensive tissue necrosis. Despite advances in medical technology, early diagnosis remains challenging due to the absence of specific clinical markers, leading to delays in treatment initiation and potentially adverse outcomes. However, adjunctive diagnostic tools, such as frozen section biopsy, offer promise in enhancing diagnostic accuracy and guiding timely surgical intervention, thereby improving patient prognosis and outcomes. The timing of treatment initiation following admission emerges as a critical prognostic factor in NF management,

highlighting the urgency of prompt recognition and intervention. Delayed surgical intervention beyond 24 hours is associated with unfavourable outcomes, underscoring the imperative of expedited therapeutic measures.[4] Central to NF management is aggressive wound debridement, aimed at removing necrotic tissue and controlling microbial proliferation. This cornerstone approach, coupled with meticulous monitoring and supportive care, forms the backbone of NF treatment strategies.

Microbiological analysis reveals a predominance of polymicrobial infections in NF cases,[5] implicating a diverse array of bacterial species in disease pathogenesis. The most common organisms implicated in necrotising fasciitis are Bacteroides, aerobic streptococci, staphylococci, Enterococci, Clostridium and gram-negative rods.[2] There are two types of necrotising fasciitis, classified on the basis of microbiological growth: Type 1 infections (Polymicrobial) with a combination of aerobic and anaerobic organisms and Type 2 infections (Monomicrobial).[6] A third type is reserved for myonecrosis caused by Clostridial infections. The LRINEC scoring system serves as a valuable tool in identifying disease severity and guiding therapeutic interventions.[7] However, its application must be tempered with clinical judgment, considering its inherent limitations and the dynamic nature of NF progression. Emerging modalities, including advanced imaging techniques (MRI, CT), and innovative wound care approaches (negative pressure wound therapy, tissue engineering), offer promising avenues for enhancing diagnostic accuracy and optimising therapeutic outcomes in NF.8 Additionally, multidisciplinary rehabilitation programs play a pivotal role in addressing long-term sequelae and improving overall patient quality of life post-NF.

Our study findings corroborate the significant impact of comorbidities, advanced age, and gender on NF outcomes.[9] Diabetes mellitus emerged as the most prevalent comorbidity, associated with adverse outcomes and prolonged hospital stays. Similarly, advanced age and male gender were identified as risk factors for NF, aligning with previous research findings.[10] These observations underscore the importance of tailored management approaches that account for individual patient characteristics and underlying health conditions.

CONCLUSION

A comprehensive understanding of the multifaceted nature of NF is paramount for effective management and improved patient outcomes. Early recognition, prompt intervention, and multidisciplinary collaboration are essential components of successful NF management strategies, aimed at mitigating morbidity and mortality associated with this life-threatening condition. Necrotising fasciitis, although rare, poses a significant threat due to its potential for rapid deterioration and systemic toxaemia. Our study highlights the critical importance of early diagnosis and aggressive management strategies in mitigating patient morbidity and mortality associated with this devastating condition.

Our findings underscore several key epidemiological and clinical observations. Specifically, we observed a higher incidence of necrotising fasciitis in individuals aged over 50 years, with a notable male predominance. Furthermore, our microbiological analysis revealed Streptococcus pyogenes and Escherichia coli as the predominant pathogens implicated in the disease process. Importantly, we identified diabetes mellitus as the most common comorbidity associated with necrotising fasciitis, emphasising the significance of prompt control of this condition in NF management protocols. Based on our findings, we advocate for a multidisciplinary approach that prioritises early recognition, aggressive surgical intervention, and supportive therapy as essential components of effective NF management strategies.

Further research into novel diagnostic modalities and therapeutic interventions is warranted to enhance our understanding and management of this challenging condition. By implementing proactive measures and adopting a comprehensive approach to patient care, we can strive to improve outcomes and reduce the burden of necrotising fasciitis on affected individuals and healthcare systems alike.

CONFLICT OF INTEREST

The authors declare that there is no conflict of interests that would prejudice the impartially of this scientific work.

ACKNOWLEDGEMENTS

Authors would like to express gratitude to Saveetha Medical College and Hospital.

REFERENCES

1. Misiakos EP, Bagias G, Papadopoulos I, Danias N, Patapis P, Machairas N, et al. Early diagnosis and surgical treatment for necrotizing fasciitis: A multicenter study. Front Surg 2017; 4: 5.
2. Liu TJ, Tai HC, Chien KL, Cheng NC. Predisposing factors of necrotizing fasciitis with comparison to cellulitis in Taiwan: A nationwide population-based case-control study. J Formos Med Assoc 2020; 119(1 Pt 1): 18-25.
3. Chen JL, Fullerton KE, Flynn NM. Necrotizing fasciitis associated with injection drug use. Clin Infect Dis 2001; 33(1): 6-15.
4. McHenry CR, Piotrowski JJ, Petrinic D, Malangoni MA. Determinants of mortality for necrotizing soft-tissue infections. Ann Surg 1995; 221(5): 558-65.
5. Elliott D, Kufera JA, Myers RA. The microbiology of necrotizing soft tissue infections. Am J Surg 2000; 179(5): 361-6.
6. Levine EG, Manders SM. Life-threatening necrotizing fasciitis. Clin Dermatol 2005; 23(2): 144-7.
7. Wong CH, Khin LW, Heng KS, Tan KC, Low CO. The LRINEC (Laboratory Risk Indicator for Necrotizing Fasciitis) score: A tool for distinguishing necrotizing fasciitis from other soft tissue infections. Crit Care Med 2004; 32(7): 1535-41.
8. Simonart T. Group A beta-haemolytic streptococcal necrotizing fasciitis: Early diagnosis and clinical features. Dermatology 2004; 208(1): 5-9.
9. Swain RA, Hatcher JC, Azadian BS, Soni N, De Souza B. A five-year review of necrotizing fasciitis in a tertiary referral unit. Ann R Coll Surg Engl 2013; 95(1): 57-60.
10. Wong CH, Chang HC, Pasupathy S, Khin LW, Tan JL, Low CO. Necrotizing fasciitis: Clinical presentation, microbiology, and determinants of mortality. J Bone Joint Surg Am 2003; 85(8): 1454-60.

ORIGINAL ARTICLE

Evaluation of embryonic toxicology, antimicrobial, anti-inflammatory, and antioxidant activity of the *Equisetum arvense* mediated Magnesium oxide nanoparticles

Sulochana Govindhraj, MSc, Rajeshkumar Shanmugam, PhD

Nanobiomedicine Lab, Centre for Global Health Research, Saveetha Medical College and Hospital, Saveetha Institute of Medical and Technical Sciences, Chennai-602 105.

ABSTRACT

Introduction: Preparing and stabilising various types of nanoparticles using herbal extract has proven to be an intriguing prospective environmentally beneficial technology. Magnesium oxide nanoparticles (MgONPs) are finding a broad range of applications in the environmental and medical sciences due to their impressive antioxidant, anticancer, and antibacterial activity. The traditional uses of *Equisetum arvense* included wound and ulcer healing, renal issues, tuberculosis treatment, and bleeding control. This work intended to synthesise magnesium oxide nanoparticles in an environmentally friendly manner utilising E. arvense, with potential uses in biomedicine.

Materials And Methods: Using a green fabrication technique, E. arvense extract was used to create magnesium oxide nanoparticles (MgONPs). The antibacterial activity of the resulting MgO NPs against wound infections was evaluated. The ABTS, Nitric Oxide, DPPH, FRAP, and H_2O_2 assays were used to measure antioxidant activity. Utilising zebrafish survivability during MgONPs treatment, cytotoxicity was evaluated.

Results: The green-produced MgONPs showed good antibacterial activities against wound infectious microbes, compared to the E. arvense control. It also demonstrated outstanding biocompatibility and antioxidant activity.

Discussion: The potential application of plants mediated NPs as antibacterial, and an antioxidant agent is the primary conclusion of the research.

KEYWORDS:
Green synthesis, antioxidant, anti-inflammatory, antimicrobial, eco-friendly, biocompatibility

INTRODUCTION

In recent years, the nanoparticles have been synthesised by using the green synthesis process. It is also known as the biosynthesis process; the biosynthesis process was done by using the plant-mediated nanoparticles. The green synthesis process efficacy of applications of natural reducing agents, without using chemicals and with less toxicity, is a perfect and stabilising agent.[1] Magnesium oxide nanoparticles are one of the metal ion-based nanoparticles, a lot of research is going into the metal-based nanoparticles by using plant-based. The metal-based nanoparticles are used to synthesise the green synthesised method and it has maintained the bioefficacy.[2] The *Equisetum arvense* is a perennial herb and native to the plant northern Himalayas. The local name of the plant is Field horsetail or Horsetail, genus *Equisetum*, and the species *arvense*.[3] Horsetail is one of the best treatments for skin disease, to treat pimples and dermatitis, it has present the excellent wound-healing activity of the skin conditions.[4] It has been used for cosmetics like moisturising agents, body shampoos, soaps, cosmetic cleaners, and skin conditioning agents.[5] *E. arvense* contains sterols, a rich source of vitamin C, phenolic acid, and flavonoids.[6] It has also shown efficacy against fungi species.[7] In pharmaceutical studies, *E. arvense* has an additional medicinal therapy, and excellent antioxidant and anti-inflammatory properties.[8]

The plant-based nanoparticles are used, and they reduce toxicity and are eco-friendly. The magnesium oxide nanoparticles have both metal and metal oxide based, they have different biomedical and biochemical applications catalysis, tissue regeneration, and antimicrobial and anticancer agents.[9] Magnesium oxide has excellent stability, bioavailability, and antiviral and antipathogenic activity.[10] The green method is used to develop the magnesium oxide nanoparticle synthesis using cost-reduction, energy efficiency, removal of environmental pollution, and biocompatibility.[11] The green synthesised magnesium oxide nanoparticles are used in biomedical therapy for cancer, inflammation, oxidation, and diabetes.[12] The concept of the research work has been to evaluate the preparation of nanoparticles, antimicrobial activity against wound pathogens, time-kill curve assay, antioxidant, anti-inflammatory activity, thrombolytic activity, cytotoxic effect against brine shrimp lethality assay, and the embryonic toxicology using zebrafish embryos.

MATERIALS AND METHODS

Preparation of plant extract

At an Ayurvedic store in Poonamalli, Chennai, the dried E. arvense was bought. A 150 ml of distilled water were combined with three grams of *E. arvense*. A 150 ml of *E. arvense* extract were thoroughly agitated and then heated to 60°C for 15-20 minutes in the heating mantle. After it was boiled and filtered through muslin material, the extract was

This article was accepted: 11 February 2025
Corresponding Author: Rajeshkumar Shanmugam
Email: rajeshkumars.smc@saveetha.com

prepared and used for the manufacture of nanoparticles and additional study.[13]

Preparation of MgO nanoparticles

The magnesium oxide nanoparticles were prepared using 50 mm of magnesium chloride (MgCl), which was precursor to the magnesium oxide nanoparticle. To prepare the magnesium chloride solution, 50 ml of distilled water and 50 mm of MgCl were combined. The 50 mL magnesium chloride solution was combined with the 50 ml *E. arvense* extract. Colour changes were noticed in the solution after it was stirred for 48 hours at 600 rpm using a magnetic stirrer. Up to 250–650 nm, the first stage of UV–visible spectroscopic characterization was seen. After centrifuging the nanoparticle solution for ten minutes at 8000 rpm, the pellets were separated and distributed in various sterile containers.[14]

Antimicrobial activity

E. arvense was used to perform the antibacterial activity for the green process of magnesium oxide nanoparticles utilising the agar well technique. Mueller Hinton Agar medium was added to the sterile Petri plate. Sterile micro tips (9mm) are used to help prepare the agar well diffusion technique in sterile petri plates. Fresh microbiological cultures, including *E. coli, S. aureus, Pseudomonas sp.*, and Candida albicans, were used to generate the various microbial stains using Muller-Hinson broth. In the sterile swab in the agar plates, the microbial broth culture was distributed uniformly. Following the addition of magnesium oxide nanoparticles at three distinct concentrations (25, 50, and 100 µg/mL), the agar plates were allowed to incubate for a full day at room temperature. The inhibitory zones were measured in diameter on the plates after an incubation period. A pure aqueous extract of *E. arvense* was utilised as the control in each microbiological culture.[15]

Time kill curve assay

To create a standardised vaccine, the isolated microbial broth was cultured. Nanoparticle solutions were put into 96-well plates at different concentrations (25, 50, and 100 µg/ml). Additionally, pure aqueous extract of *E. arvense* was used as the positive control, antibiotics as the standard, and simply microbial culture was added as the negative control. At room temperature, the plate was incubated, at regular intervals of 0, 2, 4, 6, 8, and 24 hours, observations for microbial cultures have been collected. It was able to determine the killing rate by plotting the total number of living cells as $\log_{10}$ (CFU/mL) against time.[16]

Anti-inflammatory activity

Bovine serum albumin denaturation assay

Anti-inflammatory efficacy of green production of magnesium oxide nanoparticles using *E. arvense*, the prevention of albumin denaturation approach—which was previously investigated by Mizushima et al., has been somewhat modified. Five different concentrations (10-50 µg/ml) were added to the nanoparticles. Adding a 1% aqueous solution of the fractional representation of bovine albumin together with test extracts to the reaction mixture. To modify the pH of the reaction mixture, a very small amount of 1N HCl was added. The sample extracts were chilled, and the turbidity was measured at 660 nm after 20 minutes of incubation at 37°C and 20 minutes of heating at 51°C.

Egg albumin denaturation assay

A 0.2 ml of egg albumin, PBS (2.8 ml of Phosphate Buffer Saline, keeping a pH range of 6.4), and the five different concentrations of nanoparticle solutions (10-50 µg/ml) were added to the 5 mL reaction mixture. Double-distilled water in an equivalent volume is used as a control. In addition to determining the absorbance of standard values, standard medications like diclofenac sodium were employed. After 15 minutes of incubation at room temperature, the mixed solutions were heated to 50°C for five minutes to bring the water to a boil. Measure the absorbance at 660 nm after the liquids have cooled. The formula was used to determine the percentage of inhibition of protein denaturation.

Membrane stabilization assay

Preparation of Red Blood cell (RBC) suspension.

A euthanized human volunteer was selected based on health, and blood was drawn into centrifuge tubes only after the donor had abstained from NSAID use for two weeks before the experiment. The tubes underwent three rounds of sterilisation using the same volume of regular saline after being centrifuged for ten minutes at 3000 rpm. Following that, using a standard saline solution, the volume of the blood was measured and reconstituted at a 10% v/v concentration.

Heat-induced method

One millilitre of 10 % RBC suspension and one millilitre of magnesium oxide nanoparticles made with *E. arvense* at different concentrations (10-50 µg/ml) made up the reaction mixture (2 ml). Ordinary saline was added to the control test tube in place of magnesium oxide nanoparticles made with *E. arvense*. A popular standard was vitamin C. Each centrifuge tube holding the reaction mixture was incubated for 30 minutes at 56°C in a water bath. Following the incubation time, the tubes were cooled using running tap water. The absorbance of the supernatants was measured at 560 nm after the reaction mixture was centrifuged for five minutes at 2500 rpm. The experiment was performed in duplicate for each test sample.[17]

Antioxidant activity

DPPH assay

A solution of 10 ml methanol and 0.1 mm DPPH was prepared. Five varying amounts of nanoparticle solutions (10-50µg/ml) were combined with 1 mL of DPPH methanol solutions. Following that, the mixed solutions were allowed to sit at room temperature for 30 minutes in a dark incubator. Ascorbic acid served as the standard, while DPPH solution served as the control. A UV-visible spectrophotometer was used to detect the absorbance at 517 nm following the completion of the incubation. The greater activity of scavenging free radicals is indicated by the lower absorbance. Using the DPPH assay, the percentage of inhibition was calculated for each concentration of nanoparticles based on the percentage of antioxidant activity.

H_2O_2 assay
The Halliwell technique[18] has brought about a few changes to the assay's completion. All of the solutions were made from the beginning. In 1.0 ml, the following ingredients make up the reaction's solution: A mixture of 100 µl of 28 mm 2-deoxy-2-ribose (dissolved in phosphate buffer, pH 7.4), 500 µl of various nanoparticle concentration solutions (10-50 µg/ml), 200µl of 1.04 mm EDTA and 200 mM Fecl3, 100µl of H2O2 (1.0 mm), and 100µl of ascorbic acid (1.0 mm) were used. A 60-minute incubation period at 37°C allowed for the determination of the degree of deoxyribose breakdown using the TBA reaction. The absorbance is measured by comparing it to the blank solution at 532 nm. The vitamin E was used as a positive control.

FRAP (Ferric Reducing Antioxidant Power) assay:
This technique works by decreasing the ability of Fe3+ to Fe2+ ions in the sample. Ferric-tripyridyltriazine complex to decrease the ferrous form in the presence of low pH, TPTZ (2,4,6-Tri(2-pyridyl)-s-triazine), and the formulations indicated the blue colour has been absorbed in the UV-Visible spectrophotometer at 593 nm. Aqueous extract (0.7 ml) and 2.3 ml of the FRAP formulation reagents were combined with five different doses of nanoparticle solutions (10-50 µg/ml). The mixed solutions were then left to incubate for 30 minutes at room temperature in the dark. The ascorbic acid used in the standard was substituted with double-distillation water for the control. A UV-visible spectrophotometer was used to detect the absorbance at 593 nm following the incubation period. To demonstrate the increase in the reduction capabilities, the absorbance value was improved.

ABTS Assay
The chemical compound ABTS (2, 2-azinobis (3-ethylbenzothiazoline-6-sulphonic acid)). To create the stock solution, 7 mm of ABTS was combined with distilled water, and 2.45 mM of potassium per sulphate was combined with an equivalent volume of aqueous solution. After the mixed solutions were incubated for 12 to 16 hours at room temperature in the dark and used. The working solution and the measuring absorbance at 734 nm were made by diluting the stock solution in methanol. A working ABTS solution of 2 ml was combined with five different concentrations of nanoparticle solutions (10-50 µg/ml), and the mixture was left to incubate for 10 minutes at room temperature in the dark. Following that, a volume of ABTS working solution equal to one millilitre was added as the control. The standard was butylated hydroxytoluene or BHT. At 734 nm, the absorbance was measured with a spectrophotometer. The percent of inhibition was determined as the percentage of antioxidant activity in each concentration of the nanoparticles on the DPPH assay.

Nitric acid assay
Griess reagent (0.5 ml; 1% sulfanilamide, 2% H_3PO_4, and 0.1% N-(1-naphthyl) ethylenediamine dihydrochloride) was added) is used to measure nitrite ions, which are produced when sodium nitroprusside spontaneously releases nitric oxide in physiological pH aqueous solution. The creation of nitrite ions is inhibited by nitrite scavengers, which compete with oxygen. Sodium nitroprusside (10 mm) was mixed with different concentrations of dissolved nanoparticle solutions (10-50 µg/ml) in phosphate-buffered saline, and the combination was then allowed to sit at room temperature for 2.30 hours. After that, a control experiment with an identical volume of double-distilled water was conducted. It was determined that the absorbance was 546 nm. Instead of quercetin, a positive control was employed.[19]

Thrombolytic activity
Using a sterile glass slide, one drop of blood was taken and incubated at the ideal temperature for 45 minutes. Add the 20 µg/ml solution of magnesium oxide nanoparticles after the blood has clotted. Afterward, without adding any solution, compare with the control. The ideal temperature for the glass slide was maintained for 90 minutes, and the incubation hours were recorded to track the lysis of the clot. Blood was removed and then re-infused ten times following the incubations.[20]

Cytotoxic effect
Brine shrimp lethality assay
The test organism for the cytotoxic test was *Artemia salina* (nauplii), and the lethality assay of brine shrimp was employed in its execution. Thirty milligrams of *Artemia salina* (brine shrimp egg) were introduced to the saltwater in a sealed black container. The black container with aeration was used to aid in the hatching of the nauplii eggs. *Artemia salina* eggs hatch and transform into larvae after 24 hours. Following that, five distinct doses of nanoparticles were injected into each of the six-well plates that held ten individuals Artemia salina hatchings (5, 10, 20, 40, and 80 µg/mL). The control was added solely to the saltwater and the six well plates were incubated for a full day at room temperature. The number of nauplii in the 6-well plate was counted when the incubation concluded.[21]

Embryonic toxicology
The fish tank had been preserved under excellent environmental conditions, the pH was preserved in the range of 6.8 to 8.4, and the zebrafish were bought from neighbourhood merchants in Tamil Nadu. Fish foods like blood worms or ideal meals, which are both commercially accessible, were fed to the fish twice a day. Where the breading tanks were filled with three male and one female zebrafish. The eggs were carefully removed without causing any damage to the viable embryos that were formed. Three times, the eggs were cleaned in an E3 medium that was devoid of methylene blue. With 10 embryos in 2 ml of solution per well, the eggs were put into three different well plates, measuring 6, 12, and 24. In this experiment, the E3 medium that was diluted from the stock using sterilised water was utilised. Once that was established, the pH was kept between 7.2 and 7.3. In a study conducted 24 to 96 hours after conception, embryos in good health were exposed to different concentrations of nanoparticle solutions (5, 10, 20, 40, and 80 µg/ml). Nanoparticles and the E3 medium solution were combined before the embryos were used. The embryos were counted, and the dead ones were taken out after the incubation period. All the experimental plates were kept at 28°C and covered with foil sheets to avoid light interference.

Evaluation of Zebrafish Embryos
Using a stereo microscope, the developmental stages of the fertilised zebrafish embryos were examined. Following a 24-

78-hour post-fertilization period, the embryos were introduced to different concentrations of nanoparticle solutions (5, 10, 20, 40, and 80 µg/ml). The study's endpoint is the proportion of embryos that die and hatch within the time frame. Under the microscope, any deformity or anomaly was detected for both the treatment group and the control group.[22]

RESULTS

Preparation of Magnesium oxide nanoparticles

The colours of the nanoparticles' solution at the beginning and end stages of the green synthesis of *E. arvense*-mediated magnesium oxide nanoparticles were pale brown and dark brown, respectively. This demonstrates magnesium oxide nanoparticles are present and formed. The most popular method for examining the optical characteristics of nanoparticles is UV-visible spectroscopy. Bio reduction kinetics of the reaction between an aqueous extract of *E. arvense* at varied time intervals and concentrations between 250 and 650 nm. Because surface plasmon vibrations were excited, a maximum absorbance peak was seen at 380 nm for the synthesising of magnesium oxide nanoparticles (Fig.1). Figure 1(B, C, & D) displayed the SEM (Scanning Electron Micrographs comparing the morphology of E. arvense mediated Magnesium oxide nanoparticles. Fig. 1B), shows that the Magnesium oxide nanoparticles had exhibited with more spherical shapes, Similarly Fig. 1C, revealed the morphology of MgO NPs had spherical shape and mild agglomeration, and Fig. 1D while the MgONPs had irregular shapes and more agglomeration.

Antimicrobial activity

Antimicrobial activity against wound infections was demonstrated by the magnesium oxide nanoparticles. Fig. 2 shows the zone of inhibition for magnesium oxide nanoparticles against wound pathogens at varying doses (25, 50, and 100 µg/mL). In 16 mm, *Pseudomonas sp* exhibited the largest zone of inhibition at the higher level (100 µg/mL) and the lowest level (25 µg/mL) in 12 mm. Similarly, *C. albicans* and *S. aureus* observed the inhibitory zone in 14 mm at the higher level (100 µg/mL) and 11 mm at the lower level (25 µg/mL). The *E. coli* was then detected in Fig. 2 at the lowest concentration (25 µg/mL) in 9 mm and at the highest level (100 µg/mL) in 14 mm, respectively. The control observed the same level of zone of inhibition (9 mm) in clinical pathogens.

Time kill curve assay

The time-kill curve assay findings show that the produced MgONPs reduced the number of live cells for the assessed wound pathogens. The time kill curve evaluation graphs in Fig. 2F, 2G, 2H, and 2I, show that the *E. arvense*-mediated MgONPs had a significant bactericidal activity against *Pseudomonas sp.* The produced nanoparticles exhibit ideal bactericidal and fungal activities against *S. aureus* and *C. albicans*. Similarly, the modest bactericidal and bacteriostatic action of MgONPs was observed in *E. coli*. According to the results, the microbial and micro static activities of the E. arvense-mediated MgONPs develop gradually over time. Significantly, as compared to the standard (fungi – fluconazole, and bacteria – amoxyrite) resistance of the assessed organism, the resulting nanoparticles exhibit maximum microbiological activity at a concentration of 100 µg/mL, respectively. MgO NPs mediated by *E. arvense*, work. Metal ions harm the microbial cell wall and can infiltrate it. The microorganism caused mortality and reduced growth. By comparing the results with the control group, it is possible to see how much MgONPs have helped lower bacterial counts and how promising they are as an antibacterial agent for clinical management. It was measured at 600 nm using the ELISA reader. Because the control sample included entirely bacteria, it proliferated at a greater rate. Similar to the standard values, a greater growth reduction was observed in the fourth hour at the higher dose (100 µg/ml). The microbial growth in the fourth hour was also lowered by the lower concentration (25 µg/ml), respectively.

Thrombolytic activity

The clotted drop of blood was added to the 20 µg/ml of magnesium oxide nanoparticles, which have a thrombolytic property. After mixing the clotted blood with the nanoparticle solution for 20 minutes, the clotted blood liquefied once more, as represented in Fig. 3D & E, where Fig 3D as before adding the MgONPs and E) After adding the

MgONPs.*Anti-inflammatory activity*

Bovine serum albumin denaturation assay

The magnesium oxide nanoparticles were found to be effective at all concentrations (10-50 µg/ml) in the anti-inflammatory activity assessments conducted using the bovine serum albumin denaturation assay Fig. 3A. The 50 µg/ml showed the highest percentage of inhibition (78.4%), which was followed by the 40 µg/mL at 72.9 %, 30 µg/ml at 67.7 %, 20 µg/ml at 54.3 %, and 10 µg/ml at 44.6 %. In comparison to typical values, it was shown that magnesium oxide nanoparticles may have an anti-inflammatory effect.

EA assay

Using the egg albumin denaturation assay, Figure 3(B) magnesium oxide nanoparticles were evaluated for their anti-inflammatory action and shown to be effective at all concentrations (10-50 µg/ml). The 50 µg/ml showed the highest percentage of inhibition (78.6%), which was followed by the 40 µg/mL (68.4%), 30 µg/mL (64.1 %), 20 µg/ml (59.3%), and 10 µg/ml (53.7%). When compared to conventional values shown that magnesium oxide nanoparticles may have an anti-inflammatory effect.

MSA assay

Magnesium oxide nanoparticles were found to be effective at all concentrations (10-50 µg/ml) in the anti-inflammatory activity assessments conducted using the membrane stabilization assay. The samples with the highest percentage of inhibition were those containing 50 µg/ml (84.8%), 40 µg/mL (78.7%), 30 µg/mL (73.3%), 20 µg/ml (65.4%), and 10 µg/ml (54.5%). Fig. 3C shows that when compared to typical values, magnesium oxide nanoparticles may have an anti-inflammatory effect.

Antioxidant activity

DPPH assay

Magnesium oxide nanoparticles were found to be effective at all concentrations (10-50 µg/ml) when their antioxidant activity was evaluated using the DPPH test. The 50 µg/ml

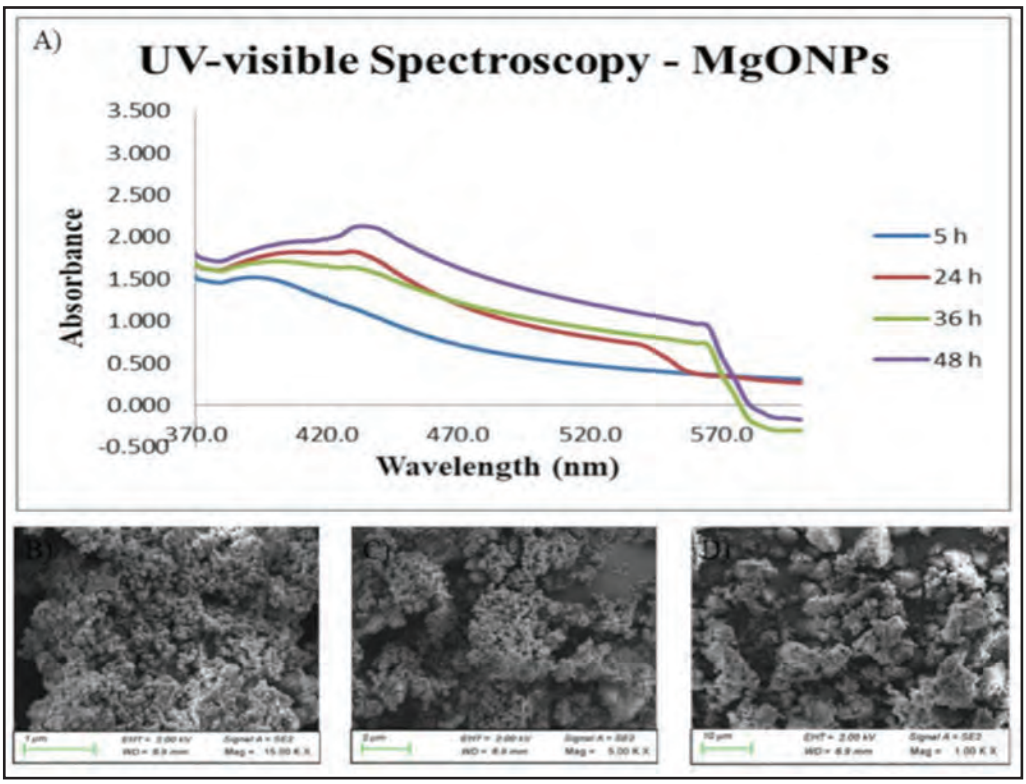

Fig. 1: A) UV-visible absorption spectra of magnesium oxide nanoparticles after bioreduction kinetics of the reaction of E. arvense aqueous extract in the concentration range of 250 - 650 nm with different time intervals. The SEM image of green synthesised magnesium oxide nanoparticles using E. arvense at different micrometre B) 1 µm, C) 2 µm, and D) 10 µm.

showed the largest percentage of inhibition, 89.57%; the 40 µg/mL showed 84.12%; the 30 µg/ml showed 81.09%; the 20 µg/ml showed 74.76%; and the 10 µg/ml showed 62.44%. In comparison to conventional values, Fig. 4A shows that magnesium oxide nanoparticles may have an antioxidant effect.

H_2O_2 assay

The H_2O_2 assay, which measures antioxidant activity, demonstrated the effectiveness of magnesium oxide nanoparticles at all concentrations (10-50 µg/ml). The samples with the highest percentage of inhibition were those with 50 µg/ml (86.9 %), 40 µg/ml (73.16 %), 30 µg/ml (63.5 %), 20 µg/ml (53.7 %), and 10 µg/ml (48.6 %). When compared to conventional values, Fig. 4B shows the possibility antioxidant effect of magnesium oxide nanoparticles.

FRAP assay

The efficacy of magnesium oxide nanoparticles was demonstrated in all concentrations (10-50 µg/ml) by the FRAP assay, which was used to assess antioxidant activity. Following the 50 µg/ml at 86.32%, 40 µg/mL at 80.94%, 30 µg/ml at 77.51%, 20 µg/ml at 73.14%, and 10 µg/ml at 67.86%, the highest percentage of inhibition was documented in this sample. When magnesium oxide nanoparticles are compared to conventional values, Fig. 4C shows that they may have an antioxidant effect.

ABTS assay

The assessment of antioxidant activity using ABTS assay showed the efficacy of magnesium oxide nanoparticles in all various concentrations where (10-50 µg/ml). The highest percentage of inhibition was noted in the 50 µg/ml at 87.58%, followed by the 40 µg/ml at 80.95%, 30 µg/ml at 78.72%, 20 µg/ml at 70.64%, and 10 µg/ml at 65.81%. Fig. 4D, illustrates that magnesium oxide nanoparticles have an antioxidant potential effect compared with standard values.

Nitric oxide assay

Magnesium oxide nanoparticles were found to be effective at all concentrations (10-50 µg/ml) when their antioxidant activity was evaluated utilising a nitric oxide analysis. Eighty-eight percent inhibitions were seen at 50 µg/mL, the maximum percentage of inhibition was found at 40 µg/ml (79.15%), 30 µg/ml (78.01%), 20 µg/ml (72.83%), and 10 µg/ml (67.45 %). When magnesium oxide nanoparticles are compared to conventional values, Fig. 4E shows the antioxidant effect against Nitric oxide assay.

Toxicology studies

Brine shrimp lethality assay

Magnesium oxide nanoparticles' cytotoxic effect is depicted in Fig. 5F, where it is noted that the particles' toxicity was reduced. 80% of live nauplius was found to have the highest concentration (40 & 80 µg/ml), while 100% of live nauplii was found to have the lowest concentration (5 & 10 µg/ml). A reduced percentage of living nauplii has been seen with increasing nanoparticle concentration. It was found that at increasing concentrations, magnesium oxide nanoparticles were less harmful.

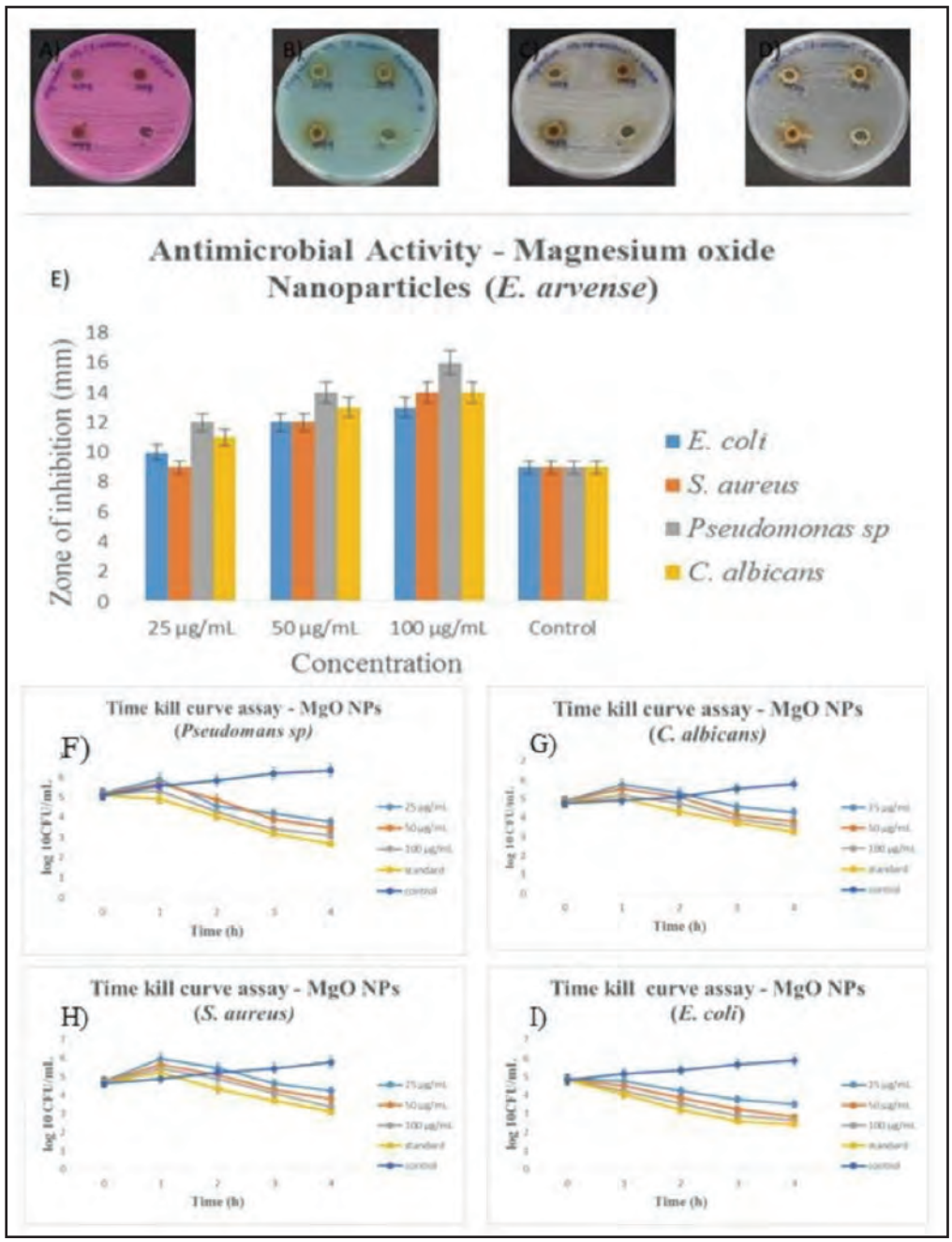

Fig. 2: Image representing Inhibition zone and time-kill curve assay of magnesium oxide nanoparticles against treated Clinical pathogens especially A) *C. albicans* B) *Pseudomonas sp.* C) *S. aureus*, D) *E. coli*, E) graphical representation of antimicrobial activity, F) Time kill curve assay of MgONPs against *Pseudomonas sp.*, G) Time kill curve assay of MgONPs against *C. albicans*, H) Time kill curve assay of MgONPs against *S. aureus*, and I) Time kill curve assay of MgONPs against *E. coli*.

Embryonic toxicology

The hatching rate of zebrafish embryos after being treated with the magnesium oxide nanoparticles.

A range of quantities, including 5, 10, 20, 40, and 80 µg/ml, were introduced to the magnesium oxide nanoparticles mediated by *E. arvense*. The different levels were administered to the zebrafish embryos, which were then examined under a microscope for a duration of 0 to 24 hours. The hatching rate of zebrafish embryos treated with magnesium oxide nanoparticles is depicted in Fig. 5A. 100 % of the zebrafish eggs hatched out at the lowest concentrations (5, 10 & 20 µg/ml). The zebrafish embryos that hatched at a rate of 80% had the highest concentration of nanoparticles. The zebrafish embryos did not hatch later than expected, and the magnesium oxide nanoparticles exhibited reduced toxicity.

The viability rate of zebrafish embryos after being treated the magnesium oxide nanoparticles

A range of quantities, including 5, 10, 20, 40, and 80 µg/ml, has been applied to the magnesium oxide nanoparticles mediated by *E. arvense*. After applying the different levels to the zebrafish embryos, the embryos were examined under a

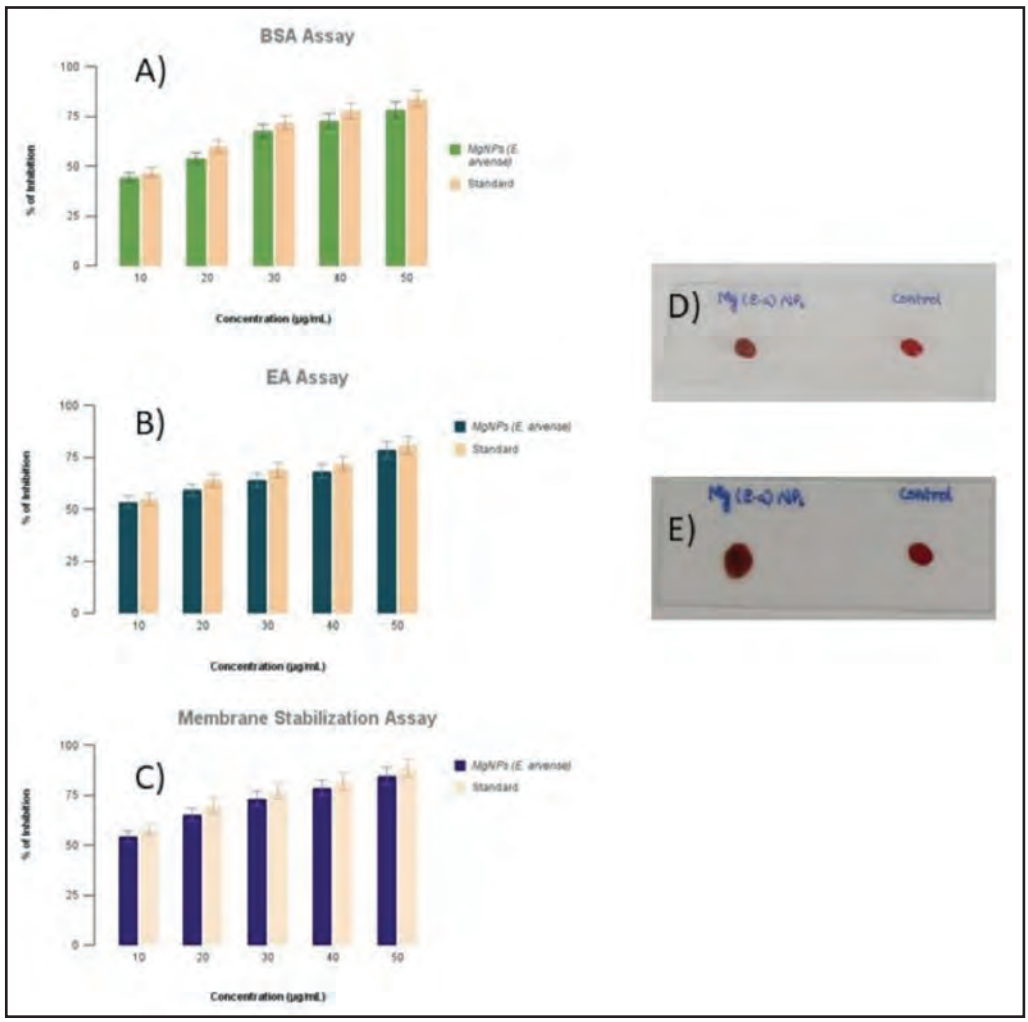

Fig. 3: Image representing the anti-inflammatory activity of Magnesium oxide nanoparticles using A) BSA assay, B) EA assay, C) MSA assay, D) the thrombolytic activity of MgO NPs before adding the sample, and E) after adding the MgO NPs.

microscope for a duration of 0 to 76 hours. Following treatment with magnesium oxide nanoparticles, Fig. 5B displays the viability rate of the zebrafish embryos. The zebrafish embryos exhibit a 100 % survivability rate when seen through the lens of the lowest concentrations (5 & 10 µg/ml). Eighty percent of the zebrafish eggs hatched at nanoparticle doses of 20 and 40 µg/ml. A 60% viability rate has been observed at the highest concentration of magnesium oxide nanoparticles. The zebrafish larvae's delayed growth and the treated embryos' deformity were not seen showed in Fig. 5(C - E), despite the toxicity of the magnesium oxide nanoparticles.

DISCUSSION

The green synthesis of magnesium oxide nanoparticles using E. arvense to produce the biological applications and the synthesis process. The *E. arvense* aqueous extract with the magnesium chloride solution was treated. The magnesium chloride was reacted with water and the plant-based bioreducing compound to release the metal ion. It was reduced to magnesium ions, the magnesium ion reacted with the bioactive of *E. arvense* to make the magnesium oxide nanoparticles. In previous research, the magnesium chloride (MgCl2). H_2O_2 was reacted with the *Moringa oleifera, Vernonia amygadaina, and Occimum gratissimun* extract. Both solutions were placed in the shaker and the 24 hrs magnesium chloride was broken into magnesium ions using the M*oringa oleifera, Vernonia amygadaina, and Occimum gratissimun* bio-reducing agent. The magnesium ion was bonded to the bioactive compound of *Moringa oleifera, Vernonia amygadaina, and Occimum gratissimun* to form the magnesium oxide nanoparticles.[23] The synthesis of magnesium oxide nanoparticles observed the changing of colour from pale brown to dark brownish. Similarly, The phytochemical constituents that appear in the *A. precatorius* bark were identified as a useful substance for obtaining MgO NPs. The aqueous magnesium ions were treated with *A. precatorius* extract and were reduced, and magnesium oxide nanoparticles formed. the *A. precatorius-mediated* magnesium oxide nanoparticles showed a colour change from a brownish colour to a dark brownish colour. The magnesium oxide nanoparticles were observed at the peak of 272 nm using UV characterisation.[24] In similar work, The production of MgO-NPs was confirmed by measuring the maximum surface plasmon resonance (SPR) by UV-Vis spectroscopy. UV-Vis spectroscopy of myco-synthesised MgO-NPs showed maximum SPR at 280 nm.[25]

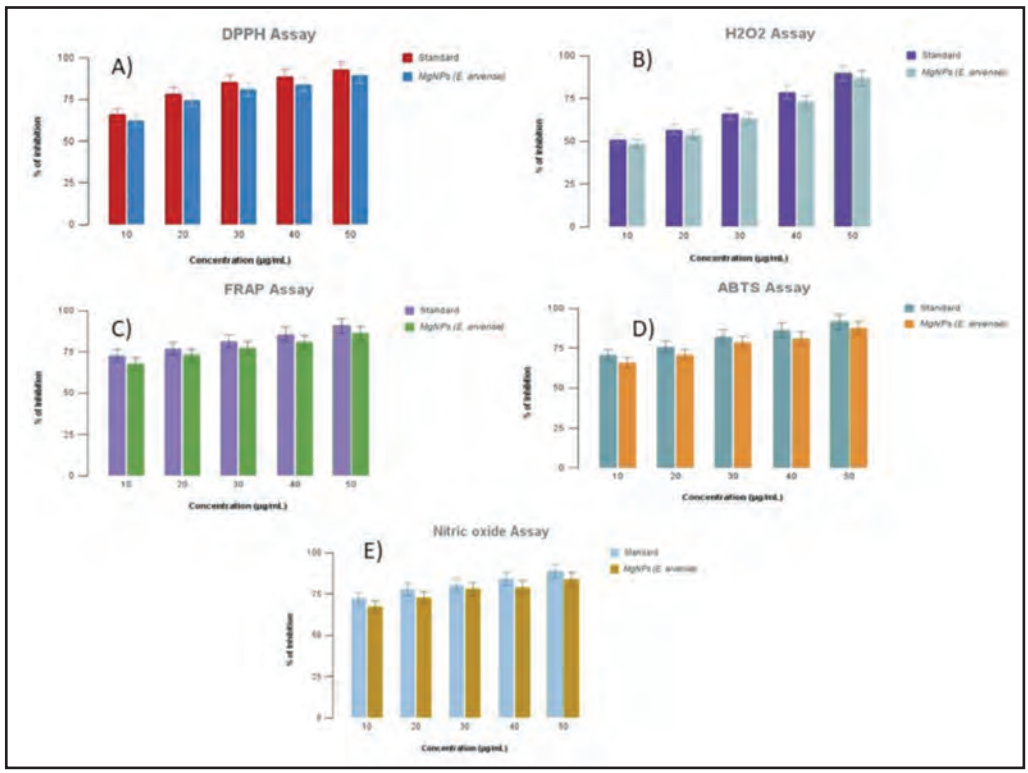

Fig. 4: Image representing the antioxidant activity of Magnesium oxide nanoparticles using A) DPPH assay, B) H2O2 assay, C) FRAP assay, D) ABTS assay, and E) Nitric oxide assay

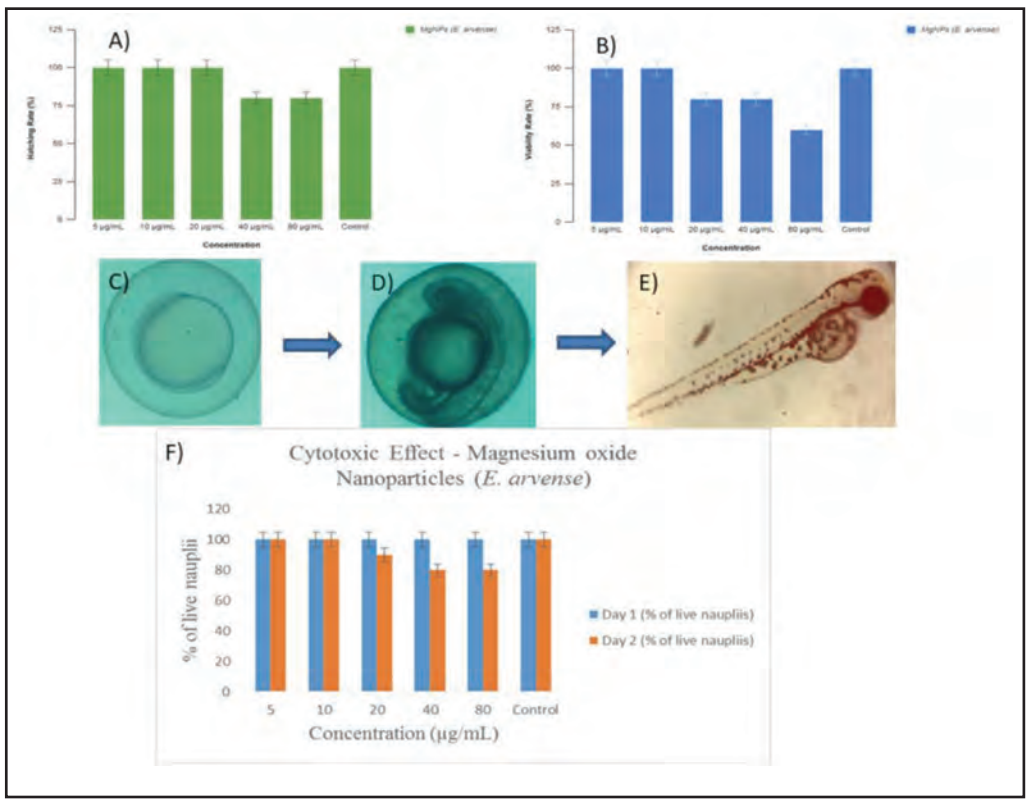

Fig. 5: The graph represents the cytotoxic effect A) Hatching rate of the embryos, B) Viability rate of the embryos, C) Day 1 of embryos, D) Day 2 stage, E) Day 3 stage, and F) Brine shrimp lethality assay

On the previous research study, the magnesium oxide nanoparticles based on rubber leaf shown the more spherical shape and lesser agglomeration.[26] In similar study, the Green synthesis of magnesium oxide nanoparticles using *Hyphaene thebaica* extract showed the SEM micrograph has confirmed the formation of quasi-spherical shape with agglomeration.[27] *Rhizopus oryzae*-Mediated Green Synthesis of Magnesium Oxide Nanoparticles, SEM image showed well-dispersed spherical MgO-NPs without any aggregation.[28] In present research work has shown very good antimicrobial activity against wound pathogens. In similarly, the *Dalbergia sissoo* extract mediated magnesium oxide nanoparticles showed antibacterial efficacy against *E. coli* at 11 mm in 3 mg/ml (higher concentration). The processes of lipid peroxidation and generation of reactive oxidative species in the container were responsible for the antibacterial potential of MgO-NPs.[29]

The previous work, *Plicosepalus curviflorus* extract and green synthesised PC-MgONPs were tested for their antibacterial efficacy against *C. albicans, MRSA, S. aureus, E. coli, and P. aeruginosa*. PC-MgONPs were shown to have a zone of inhibition of 17 mm for *E. coli* and 16 mm for *Candida albicans,* respectively.[30] Similarly, magnesium oxide nanoparticles' potential antibacterial mechanism. However, magnesium oxide nanoparticles have the ability to increase reactive oxygen species (ROS) in bacteria. This process, which results in inflammation, has seriously harmed their proteins, nucleic acids, and membrane lipids.[31] Some of the hazardous radicals that produce ROS in comparatively small amounts are hydrogen peroxide (H_2O_2), a mild oxidising agent, reactive hydroxyl radical (•OH), and superoxide anion radical (O_2^-). H2O2 is produced when the superoxide anion radical ($•O_2^-$) combines with hydrogen ions to form the $•HO_2^-$ radical. It can interact with proteins, DNA, and cell membranes, ultimately leading to microbial death.[32] In the anti-inflammatory activity, naturally, the *E. arvense-mediated* magnesium oxide nanoparticles have excellent anti-inflammatory properties. In other research work, Green-synthesised MnO2 NPs were tested for their anti-inflammatory activity by Bovine Serum Albumin (BSA) method and Egg Albumin (EA) method. Inflammation is the tissue or organ injurious causes characteristic pain, swelling, temperature, and redness. In the BSA method, the *M. annua* plant extract and MnO2 NPs showed a percentage inhibition of denaturation at 100 µg/mL is 75.42% and 77.49%. In the EA method, showed 59.88% and 71.73% of inhibition denaturation. In the extract showed lesser inhibitory potential compared to MnO2 NPs.[33] Naturally, the *E. arvense-mediated* magnesium oxide nanoparticles have excellent antioxidant properties. Antioxidants are substances that prevent some types of oxidative damage, and plant extracts are numerous in bioactive components with a high antioxidant concentration.[34] In another work, *E. arvense* methanolic extract demonstrated a higher per centage of inhibition was shown in ABTS and FRAP, and the DPPH assay showed the per centage of inhibition. DPPH is a deep purple chemical compound with an odd electron that absorbs light at 517 nm. DPPHH, a yellow material that absorbs at lower wavelengths, is the result of its degradation by antioxidants and free radical scavengers (biomolecules).[35]

The magnesium oxide nanoparticles have a thrombolytic property. Previous research work, the thrombolytic activity was evaluated by measuring the ability of the extracts to lyse blood clots and represented by percent clot lysis (%). The extracts, the highest thrombolytic activity (35.5%) was found for Delonix regia at its 10 mg/ml concentration which was followed by 32.2% thrombolytic activity of *Cassia fistula* at its 10 mg/mL concentration.[36] In which the cytotoxic effect, brine shrimp lethality assay was done. It showed less toxicity of the magnesium oxide nanoparticles. Normally, the brine shrimp cytotoxicity bioassay test can be utilised as an initial assessment for research into the potential for pesticide and anticancer effects.[37] Similarly, Cytotoxicity test was used to measure the degree of toxicity on certain cells. The brine shrimps lethality bioassay was employed here in order to predict its suitability for pharmaceutical applications, magnesium oxide nanoparticles using *Phyllanthus emblica* had the least cytotoxic effects observed in the higher concentrations (80 µl) as only 10% of mortality rate.[38]

In previous research, metal nanoparticles based on the cytotoxic effect using brine shrimp lethality assay. The brine shrimp lethality assay results for AgNPs indicate that, at the concentrations tested, there is no significant cytotoxic effect observed on Day-1. The percentage of live nauplii in all AgNP treatment groups and the control group was 100%. AgNPs, there is a reduction in the percentage of live nauplii compared to the control group, indicating increasing cytotoxicity. This effect becomes more pronounced as the concentration of AgNP increases, with the highest concentration of 80 µg resulting in a noticeable decrease in survival, as reflected by a reduction to 70% live nauplii on Day-2.[39] In the present research work was done by embryonic toxicology using zebrafish embryos, Zebrafish embryo viability was determined to be 50% at 80 µg/ml of *C. bonplandianum* ethanolic extract concentrations, 70% at 40 µg/ml, 80% at 20 µg/ml, 90% at 10 µg/ml, and 100% at 5 µg/ml. the presence of fully developed viable embryos within the egg on the second day, and the emergence of healthy zebrafish on the third day. No somatic malformations, such as a bent tail and bent spine, were observed, and there was no indication of edema.[40] In comparison to the control group, the results exhibited an increasing viability rate at all tested concentrations (100-1000 µg/mL), suggesting minimal liability. At all the concentrations, no abnormalities in development were identified, and the mortality concentration of silver nanoparticles was found to be 750 µg/ml.[41]

LIMITATION

An In-vitro study was assessed on the *E. arvense-mediated* magnesium oxide nanoparticles. In future studies develop characterizations such as TEM, FTIR, XRD, and EDX. The magnesium oxide nanoparticles will develop the gel form, and the gel will be used for the wound healing activity.

CONCLUSION

The current research work was done by using the green synthesis of *E. arvense-mediated* magnesium oxide nanoparticles. The analysis of in-vitro study UV spectroscopy, SEM, antioxidant, anti-inflammatory, antimicrobial, time-

kill curve assay, and the toxicology study whereas embryonic toxicology using zebrafish, and brine shrimp lethality assay was also estimated by the *E. arvense* mediated magnesium oxide nanoparticles. In which future studies to develop the characterization and the biomedical applications in in-vivo studies.

CONFLICT OF INTEREST

The authors declare that no conflict of interest would prejudice the impartiality of this scientific work.

ACKNOWLEDGEMENTS

The authors would like to thank Saveetha Medical College and Hospital for supporting this research.

REFERENCES

1. Hussain I, Singh NB, Singh A, Singh H, Singh SC. Green synthesis of nanoparticles and its potential application. Biotechnol Lett 2016; 38: 545-60.
2. Bordiwala RV. Green synthesis and applications of metal nanoparticles-A review article. Results Chem 2023; 5: 100832.
3. Barkley TM, editor. Flora of the great plains. University Press of Kansas; 1986.
4. Kuriyama K, Watanabe Y, Hotta H, Takisada M, Senoo M, Kameyama K. Anti-acne and anti-dandruff compositions containing lignan glycosides and antisebum/antibacterial agents. Jpn Kokai Tokkyo Koho 1998; 13.
5. Yamamoto Y, Takei M. Skin-moisturizing and-conditioning preparations containing plant extracts and lipids. Jpn Kokai Tokkyo Koho 2001; 22.
6. Mimica-Dukic N, Simin N, Cvejic J, Jovin E, Orcic D, Bozin B. Phenolic compounds in field horsetail (Equisetum arvense L.) as natural antioxidants. Molecules 2008; 13(7): 1455-64.
7. Garcia D, Ramos AJ, Sanchis V, Marín S. Equisetum arvense hydro-alcoholic extract: phenolic composition and antifungal and antimycotoxigenic effect against Aspergillus flavus and Fusarium verticillioides in stored maize. J Sci Food Agric 2013; 93(9): 2248-53.
8. Jeong SY, Yu HS, Ra MJ, Jung SM, Yu JN, Kim JC, et al. Phytochemical Investigation of Equisetum arvense and Evaluation of Their Anti-Inflammatory Potential in TNFα/INFγ-Stimulated Keratinocytes. Pharmaceuticals. 2023; 16(10): 1478.
9. Rabiee N, Ahmadi S, Akhavan O, Luque R. Silver and gold nanoparticles for antimicrobial purposes against multi-drug resistance bacteria. Materials 2022; 15(5): 1799.
10. Bhoi H, Tiwari S, Lal G, Jani KK, Modi SK, Seal P, et al. Green synthesis and characterization of Mg0. 93Na0. 07O nanoparticles for antimicrobial activity, cytotoxicity and magnetic hyperthermia. Ceram Int 2022; 48(19): 28355-73.
11. Nguyen NT, Nguyen LM, Nguyen TT, Tran UP, Nguyen DT, Van Tran T. A critical review on the bio-mediated green synthesis and multiple applications of magnesium oxide nanoparticles. Chemosphere 2023; 312: 137301.
12. Velsankar K, Aravinth K, Cláudia PS, Wang Y, Ameen F, Sudhahar S. Bio-derived synthesis of MgO nanoparticles and their anticancer and hemolytic bioactivities. Biocatal Agric Biotechnol 2023; 53: 102870.
13. Anandan J, Shanmugam R, Jayasree A. Antioxidant, Anti-inflammatory, and Antimicrobial Activity of the Kalanchoe pinnata and Piper longum Formulation Against Oral Pathogens. Cureus 2024; 16(4): e58063.
14. Amrulloh H, Fatiqin A, Simanjuntak W, Afriyani H, Annissa A. Antioxidant and antibacterial activities of magnesium oxide nanoparticles prepared using aqueous extract of Moringa oleifera bark as green agents. J Multidiscip Appl Nat Sci 2021; 1(1): 44-53.
15. Chandran N, Ramesh S, Shanmugam R, Jayalakshmi S. A Comparative Evaluation of Antimicrobial and Cytotoxic Efficacy of Biosynthesized Silver Nanoparticles and Chemically Synthesized Silver Nanoparticles Against Enterococcus faecalis: An In Vitro Study. Cureus 2024; 16(4): e58428..
16. Haran P, Shanmugam R, Deenadayalan P. Free Radical Scavenging, Anti-inflammatory and Antibacterial Activity of Acorus calamus Leaves Extract Against Pseudomonas aeruginosa and Staphylococcus aureus. Cureus 2024; 16(3): e56978.
17. Rukmani PA, Shanmugam R, Manigandan P. Anti-Inflammatory Effect of Herbal Mouthwash Prepared Using Andrographis Paniculata and Rosa Formulation. J Pharm Bioallied Sci 2024; 16(Suppl 2): S1345-9.
18. Halliwell B, Gutteridge JM, Aruoma OI. The deoxyribose method: a simple "test-tube" assay for determination of rate constants for reactions of hydroxyl radicals. Anal Biochem 1987; 165(1): 215-9.
19. Anandan J, Shanmugam R, Jayasree A. Antioxidant, Anti-inflammatory, and Antimicrobial Activity of the Kalanchoe pinnata and Piper longum Formulation Against Oral Pathogens. Cureus 2024;16(4): e58063.
20. Siddique MA, Khan MA, Bokhari SA, Ismail M, Ahmad K, Haseeb HA, et al. Ascorbic acid-mediated selenium nanoparticles as potential antihyperuricemic, antioxidant, anticoagulant, and thrombolytic agents. Green Process Synth 2024; 13(1): 20230158.
21. Shanmugam R, Govindharaj S, Arunkumar P, Sanjana GS, Manigandan P, Sulochana G, et al. Preparation of a Herbal Mouthwash With Lemongrass and Mint-Mediated Zinc Oxide Nanoparticles and Evaluation of Its Antimicrobial and Cytotoxic Properties. Cureus 2024; 16(2): e55223.
22. Aardra BS, Sundar S, Shanmugam R, Ramadoss R, Panneerselvam S, Ramani P, et al. Camellia sinensis Assisted Synthesis of Copper Oxide Nanoparticles (CuONPs) and Assessment of Its Antioxidant Activity and Zebrafish Embryonic Toxicology Evaluation. Cureus 2023; 15(12): e49595.
23. Shittu HO, Igiehon E, Eremwanarue AO, Oijagbe RE, Momoh MO, Agbontian MA. Optimization of phytosynthesis of magnesium oxide and magnesium chloride nanoparticles. Nigerian Journal of Biotechnology 2020; 37(2): 74-83.
24. Ali S, Sudha KG, Thirumalaivasan N, Ahamed M, Pandiaraj S, Rajeswari VD, et al. Green synthesis of magnesium oxide nanoparticles by using abrus precatorius bark extract and their photocatalytic, antioxidant, antibacterial, and cytotoxicity activities. Bioengineering 2023; 10(3): 302.
25. Saied E, Eid AM, Hassan SE, Salem SS, Radwan AA, Halawa M, et al. The catalytic activity of biosynthesized magnesium oxide nanoparticles (MgO-NPs) for inhibiting the growth of pathogenic microbes, tanning effluent treatment, and chromium ion removal. Catalysts 2021; 11(7): 821.
26. Ikhuoria EU, Uwidia IE, Otabor GO, Ifijen IH. Comparative analysis of magnesium oxide nanoparticles biosynthesized from rubber seed shell and rubber leaf extracts. Biomed Mater Devices 2024; 2(2): 1078-88.
27. Muhaymin A, Mohamed HE, Hkiri K, Safdar A, Azizi S, Maaza M. Green synthesis of magnesium oxide nanoparticles using Hyphaene thebaica extract and their photocatalytic activities. Sci Rep 2024; 14(1): 20135.
28. Hassan SE, Fouda A, Saied E, Farag MM, Eid AM, Barghoth MG, et al. Rhizopus Oryzae-mediated green synthesis of magnesium oxide nanoparticles (MgO-NPs): A promising tool for antimicrobial, mosquitocidal action, and tanning effluent treatment. J Fungi 2021; 7(5): 372.
29. Khan MI, Akhtar MN, Ashraf N, Najeeb J, Munir H, Awan TI, et al. Green synthesis of magnesium oxide nanoparticles using Dalbergia sissoo extract for photocatalytic activity and antibacterial efficacy. Appl Nanosci 2020; 10: 2351-64.
30. Alrashoudi RH, Abudawood M, Mateen A, Tabassum H, Alghumlas NI, Fatima S, et al. Characterization and antimicrobial, antioxidant, and anti-proliferative activities of green synthesized magnesium oxide nanoparticles with shoot

extracts of Plicosepalus curviflorus. Asian Pac J Trop Biomed 2023; 13(7): 315-24.
31. Cai L, Chen J, Liu Z, Wang H, Yang H, Ding W. Magnesium oxide nanoparticles: Effective agricultural antibacterial agent against Ralstonia solanacearum. Front Microbiol 2018; 9: 790.
32. Nejati M, Rostami M, Mirzaei H, Rahimi-Nasrabadi M, Vosoughifar M, Sobhani Nasab A, et al. Green methods for the preparation of MgO nanomaterials and their drug delivery, anti-cancer and anti-bacterial potentials: A review. Inorg Chem Commun 2022; 136: 109107.
33. Thangapushbam V, Rama P, Sivakami S, Jothika M, Muthu K, Almansour AI, et al. Potential in-vitro antioxidant and anti-inflammatory activity of Martynia annua extract mediated Phytosynthesis of MnO2 nanoparticles. Heliyon 2024; 10(8): e26933.
34. Kuunal S, Rauwel P, Rauwel E. Plant extract mediated synthesis of nanoparticles. In: Makhlouf ASH, Barhoum A, editors. Emerging Applications of Nanoparticles and Architecture Nanostructures. Amsterdam: Elsevier; 2018. p. 411-46.
35. Liang N, Kitts DD. Antioxidant property of coffee components: assessment of methods that define mechanisms of action. Molecules 2014; 19(11): 19180-208.
36. Rahman FB, Ahmed S, Noor P, Rahman MM, Huq SA, Akib MT, et al. A comprehensive multi-directional exploration of phytochemicals and bioactivities of flower extracts from Delonix regia (Bojer ex Hook.) Raf., Cassia fistula L. and Lagerstroemia speciosa L. Biochem Biophys Rep 2020; 24: 100805.
37. Yue J, Feliciano TJ, Li W, Lee A, Odom TW. Gold nanoparticle size and shape effects on cellular uptake and intracellular distribution of siRNA nanoconstructs. Bioconjug Chem 2017; 28(6): 1791-800.
38. Behera K, Nasim I, Rajesh Kumar S. Evaluation of Cytotoxicity of Magnesium Oxide Nanoparticles-An In vitro Study. Int J Dent Oral Sci 2021; 8(5): 2905-9.
39. Varghese RM, Kumar A, Shanmugam R. Cytotoxicity and characterization of zinc oxide and silver nanoparticles synthesized using Ocimum tenuiflorum and Ocimum gratissimum herbal formulation. Cureus 2024; 16(2): e55223.
40. Shanmugam R, Deenadayalan P, Manigandan P. Anticariogenic, antidiabetic, and toxicology evaluation of the ethanolic extract of Croton bonplandianum: an in vitro study. Cureus 2024;16(7): e63813.
41. Tharani M, Rajeshkumar S, Al-Ghanim KA, Nicoletti M, Sachivkina N, Govindarajan M, et al. Terminalia chebula-assisted silver nanoparticles: biological potential, synthesis, characterization, and ecotoxicity. Biomedicines 2023;11(5): 1472.

A prospective study comparing the efficacy of Budesonide nasal douching vs. Fluticasone nasal spray in Post FESS patients

Shravanthi Mantra Prithviraj, N Raadhika Shree, Subagar Anbarasan, Haritha S

Department of Otolaryngology and Head & Neck Surgery, Saveetha medical college and hospital, SIMATS, Chennai, Tamil Nadu, India

ABSTRACT

Introduction: The study assessed and compared the efficacy of Budesonide steroid nasal douching versus Fluticasone nasal spray in preventing recurrence of symptoms and nasal polyps post-FESS.

Materials And Methods: A prospective cohort study conducted in the Department of ENT, Saveetha Medical College and Hospital, Thandalam from June 2022 to June 2023 involving 60 patients diagnosed as Chronic sinusitis with polyposis were scheduled for FESS. Inclusion criteria included adults aged 18 and above with a confirmed diagnosis based on clinical symptoms, endoscopic findings, and radiological imaging. The severity of CRS was evaluated with SNOT22 score and Lund-Kennedy Endoscopic grading system. Patients were randomly assigned to two groups: Group A which was started on Budesonide nasal irrigation twice a day, and Group B, which received Fluticasone nasal spray.

Results: The average age of participants were 33.23 years, with an even distribution between females and males. Preoperative SNOT-22 and Lund-Kennedy scores were similar between both groups. One month postoperatively, both the groups had similar SNOT22 scores, but the Budesonide group had significantly lower Lund-Kennedy scores. At three months, no significant differences were observed. However, at six months, the Budesonide group had significantly lower SNOT22 and Lund-Kennedy scores when compared to the patients receiving Fluticasone.

Discussion: While Budesonide and Fluticasone are both effective post-FESS treatments, Budesonide nasal irrigation may offer better long-term symptom control and endoscopic outcomes. The broader nasal coverage achieved through nasal douching could contribute to its enhanced therapeutic effect.

KEYWORDS:
FESS, Budesonide, Sinusitis, Steroid nasal spray, Nasal Polyp

INTRODUCTION

Functional endoscopic sinus surgery is performed on patients diagnosed with chronic sinusitis and nasal polyps that are unresponsive to medical and conservative treatments to restore airflow and function of the paranasal sinuses.[1] Patients who undergo FESS have a good response in terms of their symptoms, with around 80-90% of them having a positive prognosis.[2,3] Postoperative therapy for FESS includes both topical and systemic medications. Topical treatments comprise antibiotics, steroids, and nasal irrigation, which can be saline or saline mixed with steroids such as budesonide, fluticasone, or mometasone. Topical antibiotics are also part of this category.[4-6]

The primary medications used in clinical therapy for sinusitis following FESS include normal saline, commercially available nasal douching solutions, and topical steroid nasal sprays. Studies have shown that budesonide, in different forms like powder form, in the aqueous form, or as respules of budesonide in normal saline, is more effective when used with high-volume, high-pressure irrigation devices.[7,8]

Combining the aqueous version of Budesonide with nasal saline is the standard procedure that is currently being used. A nasal irrigation is performed with the combination that was produced to assist in the reduction of local inflammation, to facilitate the early healing of wounds, and to improve the patient's overall outcomes in terms of symptom relief outcomes. The management of the patient after surgery is essential for maximising the results and minimising the likelihood of a recurrence. There is a dearth of direct comparative data evaluating the efficacy of Budesonide nasal douching and Fluticasone nasal spray in this patient population, even though both of these treatments are frequently used as post-FESS treatments to reduce inflammation and prevent recurrence. Both budesonide and fluticasone are classified as corticosteroids; but, because to differences in their pharmacokinetics, tissue penetration, and receptor affinities, they may have differing effects on the body.[9,10] To customise treatment regimens, it is crucial to have a solid understanding of how these variations translate into clinical results after FESS. The identification of the postoperative treatment option that appears to be the most effective can result in improved symptom control, enhanced quality of life, and decreased consumption of healthcare services for patients who have undergone FESS.

The aim of the study is to evaluate the efficacy of Budesonide nasal douching in enhancing post-operative outcomes following functional endoscopic sinus surgery (FESS), compare its effectiveness with Fluticasone nasal spray in reducing post-operative symptoms such as nasal obstruction,

This article was accepted: 24 February 2025
Corresponding Author: Subagar Anbarasan
Email: subagaranbarasan@gmail.com

discharge, and inflammation, and assess the safety profile and incidence of side effects for both treatment modalities in post-FESS patients.

MATERIALS AND METHODS

Study design: A prospective cohort study was performed in the Department of ENT, Saveetha Medical College and Hospital from June 2022 to June 2023, on 60 patients diagnosed as CRS with polyposis planned for Endoscopic Sinus Surgery.

The study included patients who were over 18 years of age with a confirmed diagnosis of chronic rhinosinusitis (CRS) with polyposis. The diagnosis was based on clinical symptoms, endoscopic findings, and radiological imaging. The severity of CRS in these patients was assessed using the SNOT-22 score and the Lund-Kennedy Endoscopic Grading System.

Exclusion criteria included the presence of other significant upper respiratory tract conditions, a diagnosis of chronic rhinosinusitis without polyposis, any known allergy to anaesthesia or contraindications to undergoing Functional Endoscopic Sinus Surgery (FESS), and uncontrolled systemic conditions that could potentially impact surgical outcomes.
Preoperative Assessment involved a detailed clinical history including the duration and severity of CRS, assessment of the symptoms using validated CRS scoring systems SNOT-22, comprehensive endoscopic evaluation of nasal anatomy, assessed by Lund Kennedy endoscopic scoring system and Imaging studies (computed-tomography (CT) scans) to determine the extension of the disease into the sinuses and identify potential anatomical variations.

Intervention (FESS)- All Patients underwent Functional Endoscopic Sinus Surgery performed by experienced otolaryngologists. The surgical procedure focussed on addressing sinus pathologies, optimising sinus ventilation, and alleviating any mechanical obstruction contributing to CRS. Pack removal was done for all patients on postoperative Day-1 or Day-2 depending on intraoperative bleeding, followed by nasal decongestants and saline nasal drops on the day of removal. Postoperatively, all patients were treated with oral antibiotics and proton pump inhibitors for five days, and analgesics as per requirement.

Sixty patients were divided into two groups: A and B, each group containing 30 post-FESS patients. Patients in the Group A received a solution of 1 mg Budesonide in 200 ml saline, administered as a nasal irrigation twice daily. This high-volume irrigation was designed to maximise mucosal coverage and drug distribution throughout the sinonasal cavity. In Group B patients received 50 µg of Fluticasone per puff, with two puffs applied to each nostril twice daily. These specific concentrations and volumes will facilitate replication in future studies and clinical practice, allowing for more consistent application of these treatment regimens.

Postoperative Follow-up included regular postoperative visits at specified frequencies (e.g., 1-month, 3-month, 6-month), assessment of symptom improvement using validated CRS scoring systems SNOT-22, endoscopic examinations to monitor sinus health postoperatively, which are assessed using the Lund-Kennedy scoring system. Patient-reported outcomes regarding quality of life, symptom resolution, and satisfaction with the intervention.

Ethical clearance for this study was obtained from the Institutional Ethics Committee of Saveetha Medical College and Hospital. The study was conducted in accordance with ethical guidelines for research involving human participants, ensuring patient confidentiality and informed consent. All participants provided written informed consent before enrolment in the study.

Statistics Analysis: Descriptive statistics were reported as mean (Standard Deviation, SD) for continuous variables and as frequencies (percentages) for categorical variables. An independent t-test was used to assess the relationship between the continuous variables of the two groups. A repeated measures ANOVA was employed to assess significance within the same group across time. The data analysis was conducted using IBM SPSS Statistics for Windows, Version 26.0 (IBM Corp., Chicago, IL).

RESULTS

SNOT-22: Sino-Nasal Outcome Test-22 LK score: Lund-Kennedy Endoscopic Grading System

The average age of the participants in the study was 33.23 years with a standard deviation of 7.96 years. The study included an approximately equal number of male and female participants. Prior to surgery, the mean SNOT-22 score was 74.97 (±10.84) in the budesonide nasal douching group and 75.07 (±9.85) in the fluticasone nasal spray group, with no statistically significant difference observed between the two groups (p=0.97). Similarly, the mean preoperative Lund-Kennedy (LK) score was 7.00 (±0.98) in the budesonide nasal douching group and 7.13 (±0.90) in the fluticasone nasal spray group, with no significant difference noted (p=0.59).

One month postoperatively, the mean SNOT-22 score was 27.87 (±6.42) in the budesonide nasal douching group and 27.30 (±6.43) in the fluticasone nasal spray group, showing no significant difference (p=0.73). However, the postoperative LK score at one month was significantly reduced in the budesonide nasal douching group, mean 1.20(±0.93) compared to the fluticasone nasal spray group, mean 1.70(±0.65) with a p=0.01.

At three months postoperatively, the mean SNOT-22 scores were 31.77 (±8.56) and 32.30 (±8.28) in the budesonide nasal douching and fluticasone nasal spray groups, respectively, showing no significant difference (p=0.81). The mean LK scores at three months were 1.33 (±0.77) in the budesonide nasal douching group and 1.63 (±0.97) in the fluticasone nasal spray group, with no significant difference observed (p=0.18).

At six-months postoperatively, the mean SNOT-22 score was 30.23 (±7.38) in the budesonide nasal douching group and 41.27 (±8.62) in the fluticasone nasal spray group, showing a

Table I: At six months postoperatively, the Budesonide group had significantly lower SNOT22 and LK scores compared to the participants receiving Fluticasone. Black line with arrow indicates Budesonide nasal douching and the orange line indicates Fluticasone nasal spray

Sl. no	Variable	Budesonide nasal douching	Fluticasone nasal spray	p
1	Age	32.17±8.53	34.30 ± 7.33	0.31
2	Pre op SNOT 22	74.97±10.84	75.07±9.85	0.97
3	Pre op LK score	7.00±0.98	7.13±0.90	0.59
4	Post op SNOT 22 (1 month)	27.87±6.42	27.30±6.43	0.73
5	Post op LK score (1 month)	1.20±0.93	1.70±0.65	0.01
6	Post op SNOT 22 (3 months)	31.77±8.56	32.30±8.28	0.81
7	Post op LK score (3 months)	1.33±0.77	1.63±0.97	0.18
8	Post op SNOT 22 (6 months)	30.23±7.38	41.27±8.62	<0.001
9	Post op LK score (6 months)	1.36±1.01	2.70±0.92	<0.001

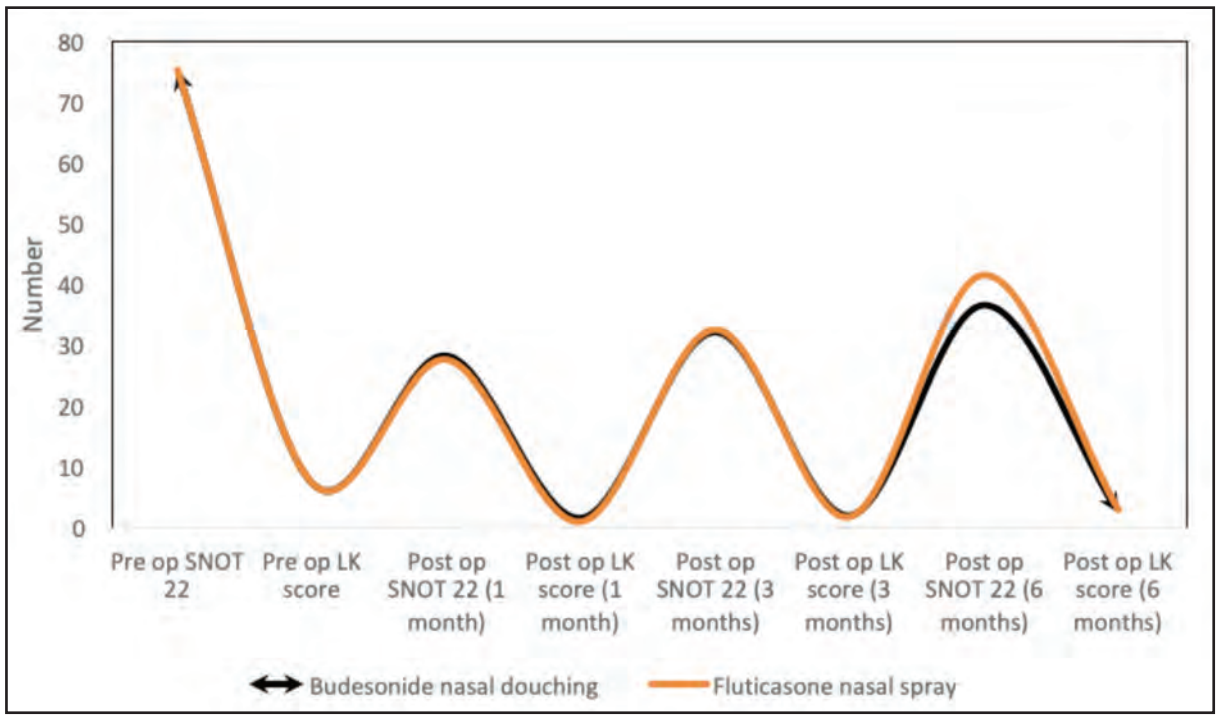

Fig. 1: At six months postoperatively, the Budesonide group had significantly lower SNOT22 and LK scores compared to the participants receiving Fluticasone. Black line with arrow indicates Budesonide nasal douching and the orange line indicates Fluticasone nasal spray

significant difference (p<0.001). Likewise, the mean LK scores at six months were significantly different between the two groups, with values of 1.36 (±1.01) and 2.70 (±0.92) in the budesonide nasal douching and fluticasone nasal spray groups, respectively (p<0.001). (As per Figure 1)

SNOT-22: Sino-Nasal Outcome Test-22 LK score: Lund-Kennedy Endoscopic Grading System

In the Budesonide nasal douching group, the mean preoperative SNOT-22 score was 74.97, which significantly decreased to 27.87 at one month postoperatively (p<0.001). This reduction remained statistically significant at three months (mean=31.77) and six months (mean=30.23), demonstrating a progressive increase in the score over time, with each interval showing statistical significance (p<0.001). Similarly, the mean preoperative Lund-Kennedy (LK) score in this group was 7.00, significantly decreasing to 1.20 at one month postoperatively (p<0.001). This reduction was maintained at three months (mean=1.33) and six months (mean=1.36), with each interval exhibiting statistical significance (p<0.001).

In the group receiving fluticasone nasal spray, the mean preoperative SNOT-22 score was 75.07, which significantly decreased to 27.30 at one month postoperatively (p<0.001). This reduction remained statistically significant at three months (mean = 32.30) and six months (mean=41.27), with each time point showing a progressive increase in the score and statistical significance (p<0.001). Similarly, the mean preoperative Lund-Kennedy (LK) score in this group was 7.13, significantly decreasing to 1.70 at one month postoperatively (p<0.001). This reduction was maintained at three months (mean=1.63) and six months (mean=2.70), with each interval exhibiting statistical significance (p<0.001).

DISCUSSION

The demographic characteristics of the study participants indicates an average age of 33.23 years with a standard deviation of 7.96 years. The study included a balanced representation of both male and female participants, ensuring a diverse sample. Prior to surgery, comparable baseline scores were observed between the Budesonide nasal douching and Fluticasone nasal spray groups for both the SNOT22 and Lund-Kennedy (LK) scores, indicating similarity in the severity of symptoms and endoscopic findings.

One month postoperatively, both treatment groups exhibited significant improvements in their SNOT-22 scores compared to baseline, with no significant difference noted between both groups. However, the Fluticasone nasal spray group showed a significantly lower LK score at one month compared to the Budesonide nasal douching group, suggesting a more favourable endoscopic outcome with Fluticasone nasal spray during the early postoperative period.

At three months postoperatively, no significant differences were found between the two treatment groups in terms of SNOT-22 and LK scores, indicating similar levels of symptom improvement and endoscopic outcomes. However, at six months postoperatively, significant differences emerged between the two groups in both SNOT-22 and LK scores. The Budesonide nasal douching group maintained lower scores compared to the Fluticasone nasal spray group, indicating better long-term symptom control and endoscopic outcomes with Budesonide nasal douching.

Steinke et al. in 2009 observed that Budesonide nasal douching showed a better response to symptoms and patient's CT imaging and endoscopic scores. However, the study did not specify the volume, dosage, or frequency of the irrigation.[11] Similarly, a retrospective study by Nader et al., from 2010, advocated for Budesonide douching thrice daily post-FESS, reporting a 61% resolution rate of symptoms. This study also did not provide details on the volume or dosage of Budesonide used.[12]

Snidvongs et al., in 2012 published a study where patients post FESS received Budesonide steroid irrigation (1 mg in 240ml, four time daily). The study found that 95% of patients showed improvement, with those having high tissue eosinophilia experiencing greater benefits when compared to those with decreased eosinophils. Participants with ASA sensitivity, polyps, and asthma showed a good response to those without these conditions.[13]

Our findings align with prior studies that emphasise the benefits of corticosteroid nasal douching post-FESS. Bourhis et al., demonstrated that Budesonide nasal douching after surgery led to enhanced distribution across the sinonasal mucosa, resulting in better symptom control and reduced recurrence of polyps.[14] Shipman et al., quantified the retention of Budesonide in the sinonasal cavity following high-volume saline irrigation, highlighting the increased sinonasal coverage achievable with douching. This improved coverage and retention may underlie the observed long-term benefits of Budesonide in our study, as enhanced mucosal exposure likely facilitates a more robust and sustained anti-inflammatory response.[15]

Calvo-Henriquez et al., supported these findings in a systematic review, concluding that corticosteroid irrigations are highly effective in chronic rhinosinusitis management, especially in post-FESS patients. The review noted that corticosteroid douching enhances mucociliary clearance, contributing to improved long-term symptom control. These mechanisms are consistent with our observation that Budesonide nasal douching provided better symptom control than Fluticasone spray at six months, suggesting that the broader nasal surface coverage achieved by douching plays a significant role in its sustained efficacy.[16]

Senior et al., investigated the exhalation delivery system with Fluticasone, finding it effective in patients unresponsive to standard sprays. Although beneficial, their study noted that the spray's distribution was limited compared to irrigations, which may partially explain the lesser long-term efficacy of Fluticasone spray observed in our study.[17]

The study's design minimised bias by blinding evaluators to treatment groups, although patient blinding was not feasible due to the differences between nasal douching and spray application. This lack of blinding among patients may introduce subjective bias, particularly in patient-reported outcomes such as symptom severity. Future studies could consider a double-blind design with a placebo control to further mitigate potential bias. The specific concentrations and volumes used in this study will facilitate replication in future studies and clinical practice, allowing for more consistent application of these treatment regimens.

In summary, although both Budesonide and Fluticasone showed comparable effectiveness, our findings imply a potential benefit for steroid nasal irrigation. The broader coverage of nasal surfaces achieved through nasal douching might contribute to a more thorough therapeutic impact in individuals post-FESS. These findings suggest in our study that while both Budesonide nasal douching, and Fluticasone nasal spray are effective in improving symptoms and endoscopic outcomes post-FESS, Budesonide nasal douching may offer superior long-term benefits in terms of symptom control and endoscopic outcomes. Further research, including larger randomised controlled trials, is warranted to confirm these findings and elucidate the underlying mechanisms contributing to the observed differences in efficacy among the two treatments given.

CONCLUSION

Budesonide steroid douching versus Fluticasone nasal spray in patients post FESS suggest that while both treatments are effective in the short term, Budesonide nasal douching may offer superior long-term benefits, potentially reducing recurrence in CRS with polyposis patients post-FESS. Further research, including larger randomised controlled trials, is necessary to validate these findings and elucidate the underlying mechanisms driving the observed differences in efficacy between the two treatment modalities.

REFERENCES

1. Slack R, Bates G. Functional endoscopic sinus surgery. Am Fam Physician 1998; 58(3): 707-18.
2. Smith TL, Kern R, Palmer JN, Schlosser R, Chandra RK, Chiu AG, et al. Medical therapy vs surgery for chronic rhinosinusitis: a prospective, multi-institutional study with 1-year follow-up. Int Forum Allergy Rhinol 2013; 3(1): 4-9.
3. Stammberger H, Posawetz W. Functional endoscopic sinus surgery: concept, indications and results of the Messerklinger technique. Eur Arch Otorhinolaryngol 1990; 247(2): 63-76.
4. Levine HL. Functional endoscopic sinus surgery: evaluation, surgery, and follow-up of 250 patients. Laryngoscope 1990; 100(1): 79-84.
5. Lund VJ, MacKay IS. Outcome assessment of endoscopic sinus surgery. J R Soc Med 1994; 87(2): 70-2.
6. Lund VJ, Scadding GK. Objective assessment of endoscopic sinus surgery in the management of chronic rhinosinusitis: an update. J Laryngol Otol 1994; 108(9): 749-53.
7. Venkatraman G, Likosky DS, Zhou W, Finlayson SRG, Goodman DC. Trends in endoscopic sinus surgery rates in the Medicare population. Arch Otolaryngol Head Neck Surg 2010; 136(5): 426-30.
8. Suh JD, Kennedy DW. Treatment options for chronic rhinosinusitis. Proc Am Thorac Soc 2011; 8(1): 132-40.
9. Harvey RJ, Psaltis A, Schlosser RJ, Witterick IJ. Current concepts in topical therapy for chronic sinonasal disease. J Otolaryngol Head Neck Surg 2010; 39(3): 217-31.
10. Rotenberg BW, Zhang I, Arra I, Payton KB. Postoperative care for Samter's triad patients undergoing endoscopic sinus surgery: a double-blinded, randomized controlled trial. Laryngoscope 2011; 121(12): 2702-5.
11. Steinke JW, Payne SC, Tessier ME, Borish LO, Han JK, Borish LC. Pilot study of budesonide inhalant suspension irrigations for chronic eosinophilic sinusitis. J Allergy Clin Immunol 2009; 124(6): 1352-4.e7.
12. Nader ME, et al. Using response to a standardized treatment to identify phenotypes for genetic studies of chronic rhinosinusitis. J Otolaryngol Head Neck Surg 2010; 39(1): 69-75.
13. Nader ME, Abou-Jaoude P, Cabaluna M, Desrosiers M. Using response to a standardized treatment to identify phenotypes for genetic studies of chronic rhinosinusitis. J Otolaryngol Head Neck Surg 2010; 39(1): 69-75.
14. Bourhis T, Mouawad F, Szymanski C, Mortuaire G. Budesonide transnasal pulsating nebulization after surgery in chronic rhinosinusitis with nasal polyps. Drug Deliv Transl Res 2022; 12(4): 925-30.
15. Shipman PA, Yathavan B, Gill AS, Pollard CE, Yellepeddi V, Ghandehari H. Quantification of Budesonide Retained in the Sinonasal Cavity After High-Volume Saline Irrigation in Post-Operative Chronic Rhinosinusitis. Am J Rhinol Allergy 2024; 38(3): 169-77.
16. Calvo-Henriquez C, Viera-Artiles J, Rodriguez-Iglesias M, et al. The Role of Corticosteroid Nasal Irrigations in the Management of Chronic Rhinosinusitis: A State-of-the-Art Systematic Review. J Clin Med 2023; 12(10): 3605.
17. Senior BA, Schlosser RJ, Bosso J, Soler ZM. Efficacy of the exhalation delivery system with fluticasone in patients who remain symptomatic on standard nasal steroid sprays. Int Forum Allergy Rhinol 2021; 11(5): 837-45.

ORIGINAL ARTICLE

Multi-target prediction to Detect the Anti-cancerous Potential of Sida cordifolia in Treating Breast Cancer

Aswathi K Biju, MSc[1], Nisha B, MD[2], Rajeshkumar Shanmugam, PhD[1]

[1]Nanobiomedicine Lab, Centre for Global Health Research, Saveetha Medical College and Hospital, Saveetha Institute of Medical and Technical Sciences, Thandalam, Chennai, Tamil Nadu, India, [2]Department of Community Medicine, Saveetha Medical College and Hospital, Saveetha Institute of Medical and Technical Sciences, Chennai, India

ABSTRACT

Introduction: Breast cancer arises from the uncontrolled proliferation of breast cells, leading to tumour. Sida cordifolia, commonly known as Bala, an herbaceous plant widely used in traditional medicine, particularly in Ayurveda, due to its numerous medicinal properties. This study investigates the multi-target therapeutic mechanisms of S. cordifolia against breast cancer using network pharmacology.

Materials and Methods: Phytochemicals of S. cordifolia were extracted from the IMPPAT database, and their ADME (Absorption, Distribution, Metabolism, and Excretion) properties were evaluated using SwissADME database. The web tool SwissTargetPrediction identified phytochemical targets, and breast cancer targets were retrieved from the database Open Targets Platform. Shared targets were identified using the web tool Venny 2.1.0, and a PPI (Protein-Protein Interaction) network was generated via STRING database. Hub genes were analysed in Cytoscape 3.10.2 software, with KEGG (Kyoto Encyclopaedia of Genes and Genomes) and GO (Gene Ontology) was performed using the tool ShinyGO 0.80.

Results: The KEGG pathway analysis revealed five genes: Epidermal growth factor receptor (EGFR), Estrogen receptor 1 (ESR1), mammalian target of rapamycin (mTOR), Progesterone receptor (PGR), and tumour protein p53 (TP53) that directly participate in the breast cancer pathway. These genes were identified as core targets and are targeted by the phytochemicals present in S. cordifolia, including quinazoline, abietaic acid, malvalic acid, linoleic acid, and 20-hydroxyecdysone.

Discussion: This study highlights S. cordifolia's potential as a multi-target therapeutic agent against breast cancer, with key phytochemicals targeting critical genes involved in cancer progression. These findings suggest that S. cordifolia could be a valuable candidate for further research in breast cancer treatment.

KEYWORDS:
breast cancer, medicinal plants, phytochemicals, S. cordifolia, targeted genes

INTRODUCTION

Breast cancer is the main cancer-related mortality cause for women globally. Changes to breast cells can occasionally result in breast cancer.[1] Breast cancer typically begins in the cells lining the ducts, or the tubes that carry milk from the glands to the nipple.[2] Developed nations make up almost half of the cases worldwide. This tendency is mostly the result of Western lifestyle, which has been associated to low physical activity, bad food, diabetes, and excessive stress.[3] Usually, breast cancer starts out silently and only becomes apparent when a lump develops in the region of the breast or the disease spreads. Although newly developed lumps are frequently indicative of malignancy, most of them are not. Breast tumours that are firm, painless, and have uneven margins have an increased chance of becoming malignant. A skin modification such as a redness, dimpling, or rash can also happen, as well as changes in shape, texture, and size. There might be redness or itching near the nipples. Less frequent symptoms include breast soreness, fluid leakage from the nipples, and inflammatory breast carcinoma, which produces pain, redness, and inflammation.[4] Alternative treatment options are necessary since the therapies, such as hormone therapy and chemotherapy, can lead to side effects and resistance.[5] The effectiveness and safety of natural products especially, those derived from medicinal plants in cancer therapy have drawn attention.

S. cordifolia, often known as bala (family: Malvaceae), is a highly esteemed medicinal herb utilised in Ayurveda as well as other traditional medical systems in India and other countries. Bala is classified as a bulk-promoting herb (brahmhaniya), a tonic (balya), and a reproductive aid (prajasthapana) by the famous Ayurvedic physician Charaka. Bala is also considered by Charaka to be rejuvenating (rasayana) for the muscular system and muscle tissue.[6] *S. cordifolia* utilised as an antirheumatic, analgesic, antipyretic, laxative, diuretic, hypoglycaemic, nasal anti-congestant, aphrodisiac, anti-asthmatic, and hepatoprotective in Ayurveda medicine.[7] It has been studied for its anti-inflammatory properties in the treatment of cancer and in promoting liver regeneration.[8] However, a contemporary scientific viewpoint on the medicinal potential of this traditional herb is still unclear.

Network pharmacology, an emerging field that integrates multiple scientific disciplines, explores the interactions

This article was accepted:
Corresponding Author: S Rajeshkumar
Email: rajeshkumars.smc@saveetha.com

between diverse compounds and various biological targets and pathways.[9] Using a network pharmacology approach, this study methodically uncovered multiple targets and pathways by which *S. cordifolia* offers its anti-cancerous properties. This study reveals the plant's regulatory function in pathways associated to breast cancer by identifying significant phytochemicals and their core targets. The findings validate the use of *S. cordifolia* as an intricate and effective treatment for breast cancer and provide a thorough understanding of the possible therapeutic advantages of the plant.

MATERIALS AND METHODS

Identification of S. cordifolia's phytochemicals

The phytochemical-based IMPPAT database (IMPPAT - accessed on 25 June 2024)[10,11] was utilised to retrieve the phytochemicals present in *S. cordifolia*. The Simplified Molecular Input Line Entry System (SMILES) is the standard way for depicting the chemical structures of phytochemicals. It was acquired using PubChem to identify possible target molecules (PubChem - accessed on 25 June 2024).

Absorption, Distribution, Metabolism, and Excretion (ADME) prediction

The ADME of the phytochemicals was estimated using the web tool SwissADME (SwissADME - accessed on 25 June 2024).[12] According to their high gastrointestinal (GI) absorption and 0.3 or higher oral bioavailability threshold, the phytochemicals of *S. cordifolia* were selected.

Target identification of S. cordifolia

SwissTargetPrediction (SwissTargetPrediction – accessed on 25 June 2024) is an online tool that forecasts the targets of phytochemicals. It has been updated with the canonical SMLES of ADME-qualified phytochemicals.[13] The targets were selected based on a probability score of 0.1 or higher, and the resulting targets were designated for further investigation.

Breast cancer associated target identification

Open Targets Platform, which was accessed on 25 June 2024, contains information on predicted and annotated targets related to human illnesses.[14] This database has been used to get molecular targets associated with breast cancer. A global score of 0.3 or above was used to filter the targets of breast cancer. The Venn diagram drawing tool, Venny 2.1.0 (Venny 2.1.0 - accessed on 25 June 2024),[15] was utilised to identify the overlapping targets in order to acquire the common targets of *S. cordifolia's* phytochemicals and breast cancer-related targets. Cytoscape 3.10.2 was utilised to create a plant-phytochemicals-target-disease network.

Construction of Protein-Protein Interaction network and HUB genes

The PPI network was created once the screened common targets were loaded into the protein-protein association networks analyser tool, STRING 12.0 (STRING – accessed on June 25 2024).[16] The species was specified as "*Homo sapiens*," 0.400 was chosen as medium confidence level and all other parameters were left unchanged. In order to get core targets for network analysis, the collected PPI results were imported into Cytoscape 3.10.2 (Cytoscape - accessed on 19 May 2024). It facilitates the visualisation of complex networks and attribute data integration. Using the CytoHubba plugin's MCC (Maximum Clique Centrality) topological analysis technique, the hub genes inside the intricate PPI network were identified.

Functional enrichment analysis

On the hub genes, the KEGG pathway enrichment analysis and GO studies were performed using Shiny GO 0.80, a graphical enrichment analysis tool (ShinyGO 0.80 - accessed on June 25 2024).[17] The results have been shown using a bar plot. The only species accepted was "*Homo sapiens*." The output of enriched GO terms for molecular function (MF), biological process (BP), cellular component (CC) was displayed using bar plot. Using 0.05 as False Discovery Rate (FDR) limit, bar plots representing the distribution of genes linked to each process were produced based on these data. The -log10FDR, fold enrichment, and gene counts for the GO analysis were displayed in the bar plot. Depending on the total number of genes associated with each pathway, the KEGG pathway analysis found pathways relevant to the targets.

RESULTS

Target identification

From Twenty phytochemicals were identified for *S. cordifolia* from the IMPPAT database and fifteen phytochemicals meet the requirements for ADME screening. Those fifteen phytochemicals' canonical SMILES were submitted for target prediction using the Swiss Target Prediction online tool. A total of 211 targets have been found to have a probability score of 0.1 or greater. 1107 targets related to breast cancer were retrieved from the Open Targets Platform based on a global score of 0.3 or higher. To find the overlapping genes, the Venny 2.1.0 database was integrated with the disease-targeted genes of breast cancer and the phytochemical-targeted genes of *S. cordifolia*. From the Venn diagram, fifty-three common targets were identified and used for further investigation (Fig. 1). The complex data was better understood by using Cytoscape 3.10.2 to produce a degree-sorted circular arrangement for a systematic depiction of the plant-phytochemical-target-disease network (Fig. 2).

Protein-Protein Interaction network construction and Hub gene screening

A PPI network was created for the fifty-three shared targets of *S. cordifolia* and breast cancer by employing the STRING database, with <-1.0e-16 as the enrichment p-value. The network consists of 399 edges (interaction) and 53 nodes (gene) with an average node degree of 15.1 (Fig. 3a). Edge thickness in the PPI network indicates the strength of the data support. The PPI network was analysed using the CytoHubba plugin to identify the top 10 most important genes, and the MCC method was used (Fig. 3b). Hub genes have a greater degree of interaction significance, suggesting a significant impact on the condition of the disease. The topmost ten hub genes are TP53, EGFR, BCL2, ESR1, BCL2L1, mTOR, MDM2, AR, PGR, and CCNA2.

Functional enrichment analysis

GO and KEGG analyses are performed on the ten hub genes

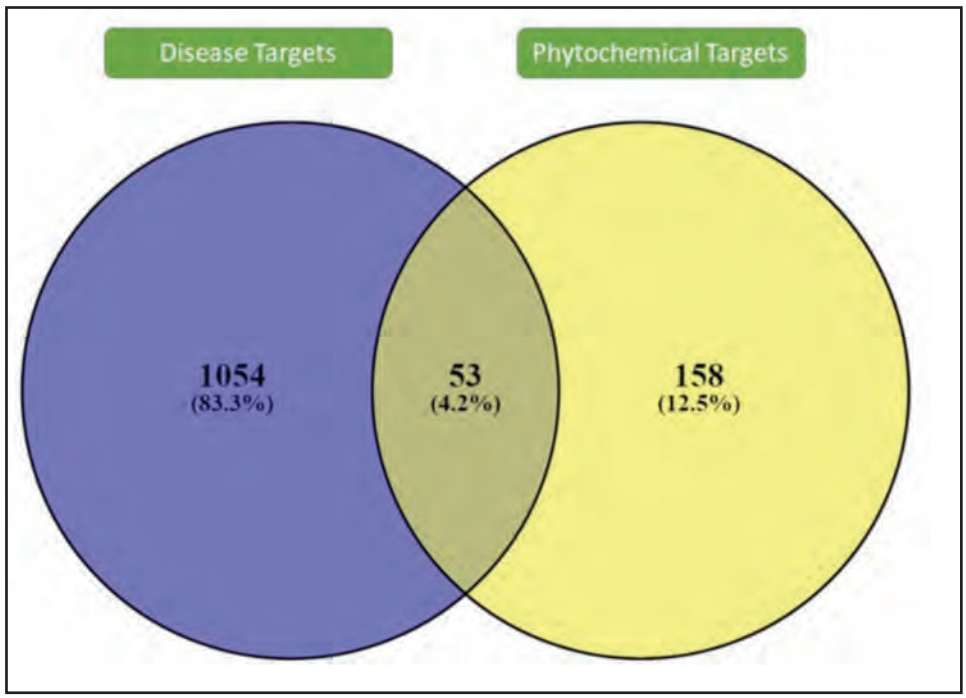

Fig. 1: Venn diagram illustrating the overlap between disease targets and phytochemical targets. The blue circle represents the 1,054 disease-targets, while the yellow circle represents the 158 phytochemical-targets. The intersection of the two circles shows 53 shared targets

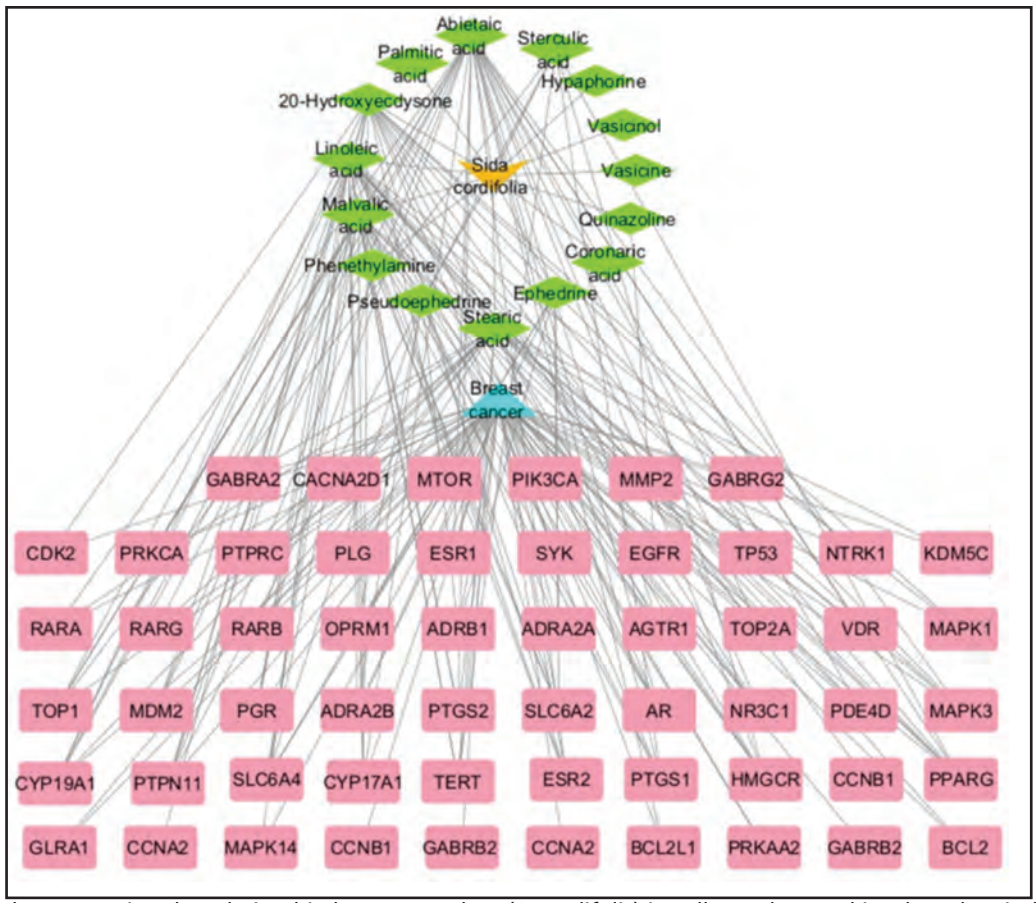

Fig. 2: A network representing the relationship between a plant (*S. cordifolia*) in yellow colour and its phytochemicals (green nodes), common targets for both phytochemicals and disease (peach nodes), and the disease (blue nodes) is depicted

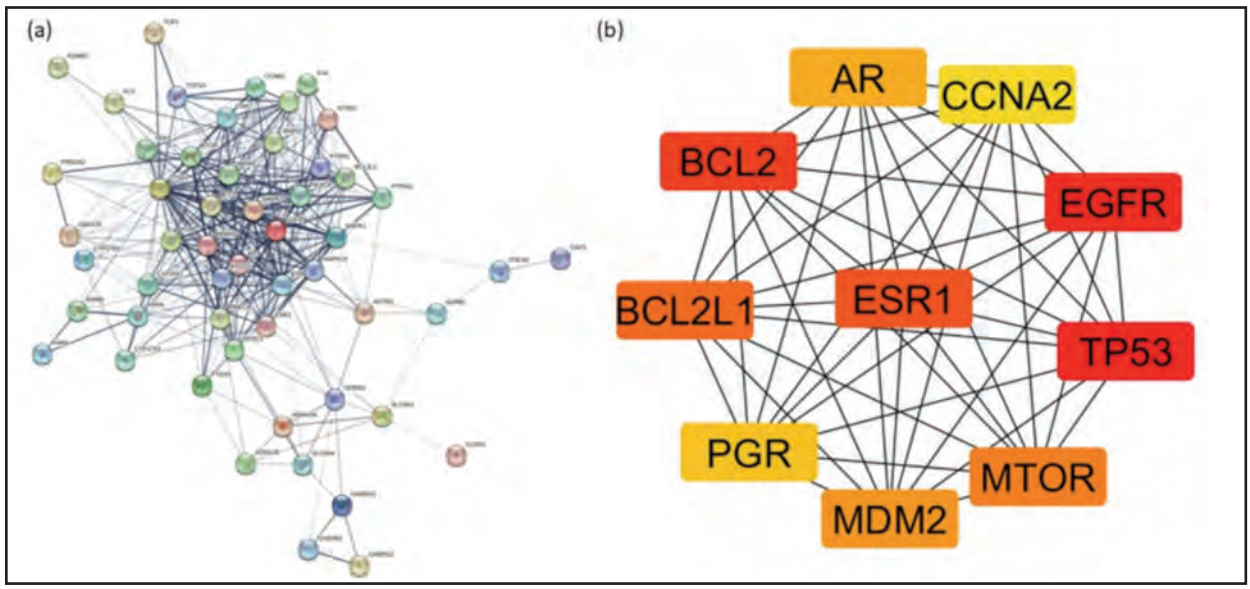

Fig. 3: (a) Protein-Protein Interaction network of the shared genes in *S. cordifolia* and breast cancer. (b) The top 10 hub genes obtained from the shared targets

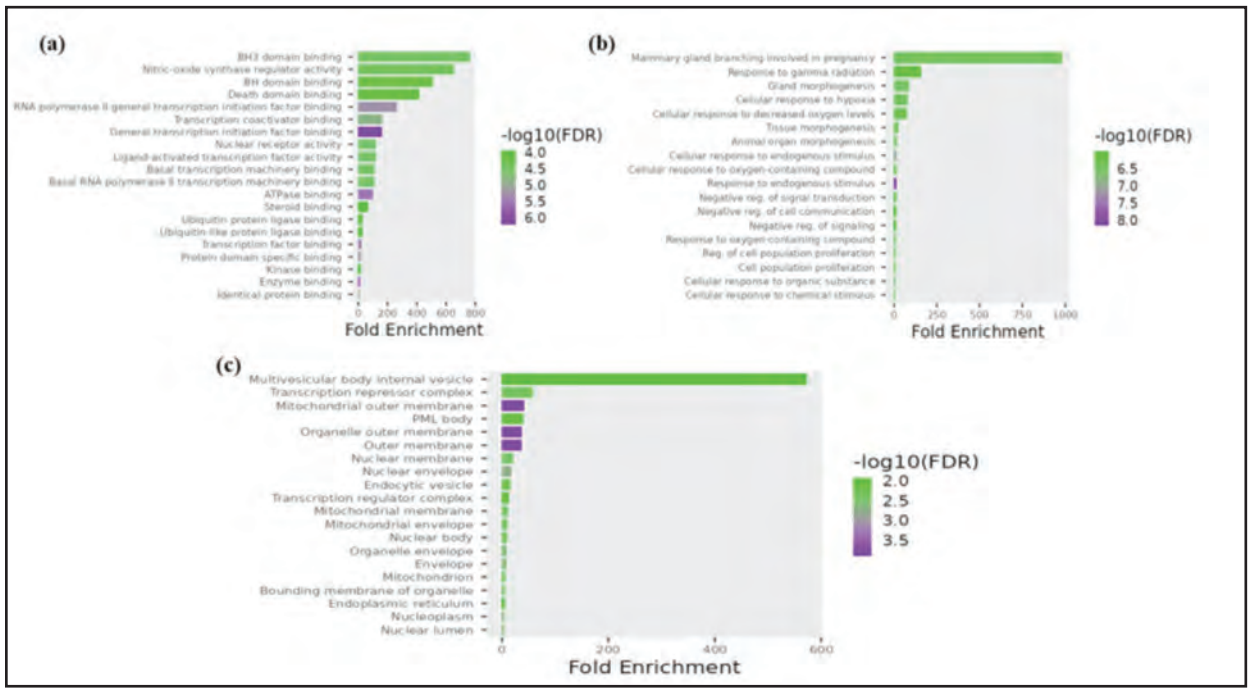

Fig. 4: Bar plot depicting the gene ontology of the predicted targets were utilized. These plots showcase the molecular function (a), biological process (b), and cellular component (c) are the segment terms from gene ontology analysis

in order to provide more insight into their functions. A bar plot has been created to show the targeted protein's GO (molecular function, biological process, and cellular component,) (Fig. 4). On the X-axis, the fold enrichment is shown. The Y-axis displays the process names and each bar's size, and colour correspond to the -log10FDR and gene count. The targeted gene's biological process found to be mostly engaged in the mammary gland branching involved in pregnancy and response to gamma radiation. The targeted gene's cellular component indicated their involvement in the multivesicular body internal vesicle. The targeted genes play a role in BH3 domain binding, nitric-oxide synthase regulator activity, and BH domain binding according to their molecular function. KEGG pathway enrichment analysis, with an FDR cut-off criterion of 0.05, has been used to identify the topmost 20 biological pathways network for the core targeted genes. The hub genes are actively participating in cancer pathway, endocrine resistance, and breast cancer pathway were selected as the pathways with the highest significant gene count. The total number of genes involved in a pathway is represented by the size of the pathway node in the pathway network. The number of overlapping genes is

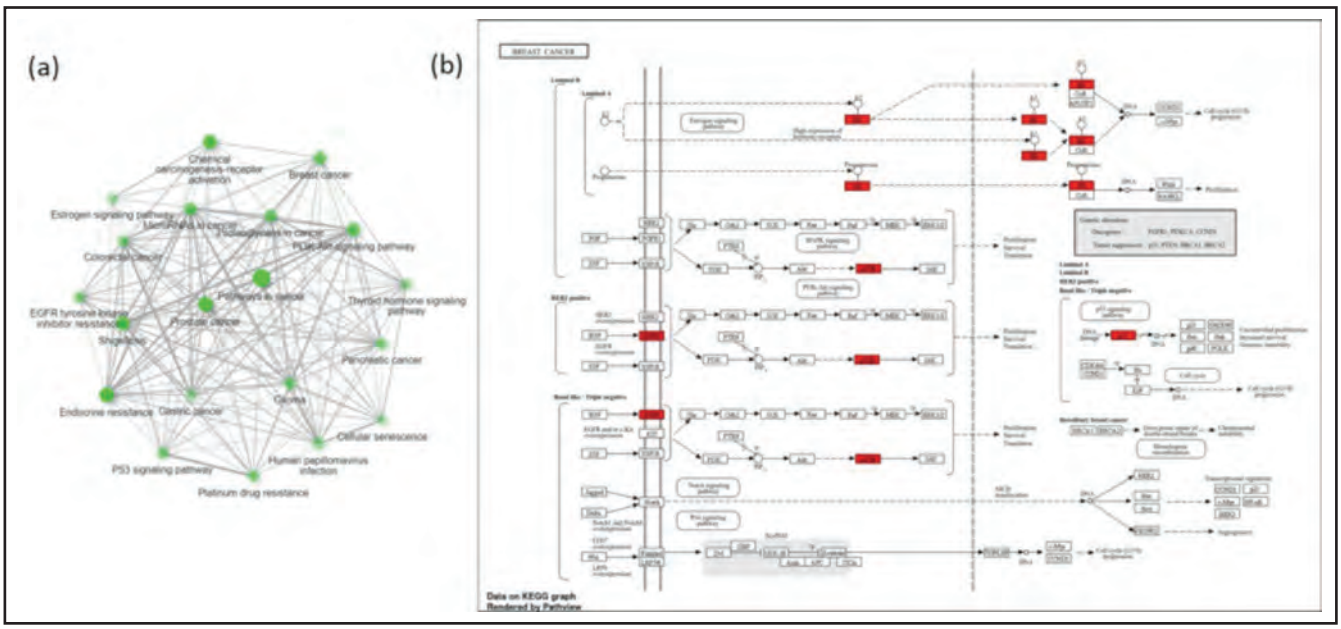

Fig. 5: (a) Top 20 KEGG pathway network of the targeted genes. (b) Breast cancer pathway, displays the core targets in red colour was created using the web tool ShinyGO.0.80

shown by the thickness of the edges (Fig.5a). In the breast cancer pathway five gene such as EGFR, ESR1, mTOR, PGR, and TP53 are directly involved were considered as the core targets. The core targeted genes were highlighted as red colour in the breast cancer pathway (Fig. 5b). Five phytochemicals found in *S. cordifolia* target the five core targeted genes: EGFR by Quinazoline, ESR1 by Abietaic acid, mTOR by 20-Hydroxyecdysone, Malvalic acid, Linoleic acid and 20-Hydroxyecdysone by PGR, and TP53 by Abietaic acid.

DISCUSSION

The multitargeted therapeutic effect of *S. cordifolia* on breast cancer has been clarified, exposing the complex nature of its therapeutic processes, through utilising the technique of network pharmacology. Using this method, five core targeted genes were identified according to their direct involvement in breast cancer pathway.[18] These genes are EGFR, ESR1, mTOR, PGR, and TP53. Epidermal growth factor receptor (EGFR) is abundantly shown in breast cancer, particularly triple-negative breast cancer (TNBC). It is a key player in controlling and maintaining the biological traits of breast cancer, including stemness, proliferation, invasion, and metastasis.[19] Patients with oestrogen receptor-positive (ER-positive) breast carcinoma are much more likely to benefit from endocrine therapy and typically have a reduced early-stage risk of recurrence than those with ER-negative breast cancer. Patients who test positive for ER are specifically between 7 and 8 times more probable to benefit from such therapy. On the other hand, mutations within the Estrogen receptor 1 (ESR1) ligand-binding region in metastatic breast carcinoma (MBC) may result in resistance to endocrine treatment. The overall survival statistics of ER-positive patients are negatively impacted by the 20% of individuals who may have ER expression loss in their metastases. As a result, resistance in ER-positive cancer of the breast persists despite the use of ovarian suppression medications and aromatase inhibitors in premenopausal women, who attempt to deprive the malignancy of its ligands. Consequently, in order to stop the course of the disease and develop efficient treatment plans, early identification, and precise evaluation of ESR1 level are essential.[20] The mammalian target of rapamycin (mTOR) is often implicated in breast cancer; preclinical research has demonstrated that it may be inhibited, and there are currently several Phase I to III clinical trials evaluating the effectiveness of mTOR inhibitors in both solid tumours and breast cancer.[21] The crucial function of mTOR in breast cancer is highlighted by the reported reduction in mTOR activity in the MCF7 breast carcinoma cell line after treatment with lactoferrin (Lf). In breast cancer, mTOR, a crucial regulator of cell metabolism and growth, is usually hyperactive, which promotes tumour development and therapy resistance. Since mTOR expression is downregulated in response to Lf, it is possible that Lf affects mTOR signalling and hence inhibits mTOR activity, which might hinder the development and proliferation of cancer cells. This outcome emphasises how effective it may be to target mTOR pathway in breast cancer therapy plans.[22] Progesterone receptor (PGR) promoters A and B is frequently expressed weakly in invasive breast cancer, and DNA methylation at these promoters is closely linked to lower protein production of ERα and PR.[23] Compared to the oestrogen receptor (ER), the progesterone receptor may provide a more accurate indicator of endocrine responsiveness. PR is becoming more widely acknowledged as a critical marker in breast cancer. Approximately forty percent of ER-positive tumours are resistant to endocrine therapy, even though ER positivity is correlated with a favourable response to such therapies. While ER is a better predictor of the likelihood of recurrence in primary breast cancer, PR, the by-product of oestrogen action, may offer a more accurate indicator of therapy success. Thus, assessing PR in addition to ER may improve patient outcomes and allow for more customised treatment strategies.[24]

Approximately 20-40% of breast cancer patients encompass mutations in the tumour protein p53 (TP53) gene, which are thought to be crucial early stages of the condition and are affected by the size and stage of the tumour.[25] The network pharmacology study incorporated herbal applications that are widely used in biomedical practices.[26-28]

CONCLUSION

The pharmacological action of S. cordifolia as a multitarget therapeutic drug for breast cancer is well understood through this study. The combination of ADME prediction, identifications of core targets, functional enrichment analysis provides an extensive basis to comprehend the medicinal properties of *S. cordifolia*. The phytochemicals satisfy ADME requirements demonstrate their potential efficacy for oral administration. The relationship between these phytochemicals and breast cancer were demonstrated by GO and KEGG pathway analysis. The results of the research indicate that *S. cordifolia* is a versatile breast cancer treatment option. Further, experimental study is required to conform the curative prospective, safety, and efficacy of this medicinal plant.

CONFLICT OF INTEREST

The authors declare that no conflict of interest would prejudice the impartiality of this scientific work.

ACKNOWLEDGEMENTS

The authors would like to thank Saveetha Medical College and Hospital for supporting this research.

REFERENCES

1. Waks AG, Winer EP. Breast cancer treatment: a review. JAMA 2019; 321(3): 288-300.
2. Obeagu EI, Obeagu GU. Breast cancer: A review of risk factors and diagnosis. Medicine (Baltimore) 2024;103(3): e36905.
3. Smolarz B, Nowak AZ, Romanowicz H. Breast cancer—epidemiology, classification, pathogenesis and treatment (review of literature). Cancers (Basel) 2022; 14(10): 2569.
4. Ali AS, Nazar ME, Mustafa RM, Hussein S, Qurbani K, Ahmed SK. Impact of heavy metals on breast cancer. World Acad Sci J 2024; 6(1): 4.
5. Burguin A, Diorio C, Durocher F. Breast cancer treatments: updates and new challenges. J Pers Med 2021; 11(8): 808.
6. Dhalwal K, Deshpande YS, Purohit AP, Kadam SS. Evaluation of the Antioxidant Activity of Sida cordifolia. Pharm Biol 2005; 43(9): 754-61.
7. Srinivasan N, Murali R, Sivakrishnan S. Sida cordifolia-an update on its traditional use, phytochemistry, and pharmacological importance. Int J Pharm Res Allied Sci 2022; 11(1): 74-86.
8. Khurana N, Sharma N, Patil SH, Gajbhiye AS. Phyto-pharmacological properties of Sida cordifolia: a review of folklore use and pharmacological activities. Asian J Pharm Clin Res 2016; 9(Suppl 2): 52-8.
9. Hopkins AL. Network pharmacology: the next paradigm in drug discovery. Nat. Chem. Biol 2008; 4(11): 682-90.
10. Vivek-Ananth RP, Mohanraj K, Sahoo AK, Samal A. IMPPAT 2.0: An enhanced and expanded phytochemical atlas of Indian medicinal plants. ACS Omega 2023; 8(9): 8827-45.
11. Mohanraj K, Karthikeyan BS, Vivek-Ananth RP, Chand RB, Aparna SR, Mangalapandi P, et al. IMPPAT: A curated database of Indian Medicinal Plants, Phytochemistry and Therapeutics. Sci Rep 2018; 8(1): 4329.
12. Daina A, Michielin O, Zoete V. SwissADME: a free web tool to evaluate pharmacokinetics, drug-likeness and medicinal chemistry friendliness of small molecules. Sci Rep 2017; 7(1): 42717.
13. Daina A, Michielin O, Zoete V. SwissTargetPrediction: updated data and new features for efficient prediction of protein targets of small molecules. Nucleic Acids Res 2019; 47(W1): W357-64.
14. Ochoa D, Hercules A, Carmona M, Suveges D, Baker J, Malangone C, et al. The next-generation Open Targets Platform: reimagined, redesigned, rebuilt. Nucleic Acids Res 2023; 51(D1): D1353-9.
15. 15.Oliveros JC. VENNY. An interactive tool for comparing lists with Venn Diagrams. 2007. [Accessed on 25 June 2024] Available from: http://bioinfogp.cnb.csic.es/tools/venny/index.html
16. Szklarczyk D, Kirsch R, Koutrouli M, Nastou K, Mehryary F, Hachilif R, et al. The STRING database in 2023: protein–protein association networks and functional enrichment analyses for any sequenced genome of interest. Nucleic Acids Res 2023;51(D1): D638-46.
17. Ge SX, Jung D, Yao R. ShinyGO: a graphical gene-set enrichment tool for animals and plants. Bioinformatics 2020; 36(8): 2628-9.
18. Zhang P, Zhang D, Zhou W, Wang L, Wang B, Zhang T, et al. Network pharmacology: towards the artificial intelligence-based precision traditional Chinese medicine. Brief. Bioinform 2024; 25(1): bbad518.
19. Li X, Zhao L, Chen C, Nie J, Jiao B. Can EGFR be a therapeutic target in breast cancer? Biochim Biophys Acta Rev 2022; 1877(5): 188789.
20. Raei M, Heydari K, Tabarestani M, Razavi A, Mirshafiei F, Esmaeily F, et al. Diagnostic accuracy of ESR1 mutation detection by cell-free DNA in breast cancer: a systematic review and meta-analysis of diagnostic test accuracy. BMC cancer 2024; 24(1): 908.
21. Lee JJ, Loh K, Yap YS. PI3K/Akt/mTOR inhibitors in breast cancer. Cancer Biol Med 2015; 12(4): 342.
22. Gaudet MM, Campan M, Figueroa JD, Yang XR, Lissowska J, Peplonska B, et al. DNA hypermethylation of ESR1 and PGR in breast cancer: pathologic and epidemiologic associations. Cancer Epidemiol Biomarkers Prev 2009; 18(11): 3036-43.
23. Kholerdi AM, Moradian F, Mehralitabar H. In vitro study of the expression of autophagy genes ATG101, mTOR and AMPK in breast cancer with treatment of lactoferrin and in silico study of their communication networks and protein interactions. Prog Biophys Mol 2024; 190: 19-27.
24. Clark GM, McGuire WL. Progesterone receptors and human breast cancer. Breast Cancer Res Treat 1983; 3: 157-63.
25. Børresen-Dale AL. TP53 and breast cancer. Hum Mutat 2003; 21(3): 292-300.
26. Ramarajyam G, Murugan R, Rajendiran S. Network pharmacology and bioinformatics illuminates punicalagin's pharmacological mechanisms countering drug resistance in hepatocellular carcinoma. Hum Genet 2024; 42: 201328.
27. Kumar RR, Kannan B, Pandi C, Pandi A, Jayaseelan VP, Arumugam P. Dysregulation of a novel m6A regulator YWHAG is correlated with metastasis and poor prognosis in oral squamous cell carcinoma–a cross-sectional study. Arch Oral Biol 2024; 169: 106090.
28. Biju AK, Nisha B, Shanmugam R, Nisha B. A Thorough Examination of Peltophorum pterocarpum Phytochemicals in Network Pharmacology-Based Management of Acne Vulgaris. Cureus 2024; 16(8): e68159.

ORIGINAL ARTICLE

Alkaline phosphatase as an adjunct for Appendicitis Inflammatory Response score

Abidah Tanweer Abdul Malik, MS[1], Rahul Raj Chennam Lakshmikumar, MS[1], Evelyn Elizabeth Ebenezer, MD[2], Khalilur Rahman, MS[1], Dakshay A Chordia, MS[1], Manish Babbu UG, MBBS[1]

[1]Department of General Surgery, Saveetha Medical College and Hospital, Saveetha Institute of Medical and Technical Sciences, Saveetha Nagar, Thandalam, Chennai Bengaluru, Chennai, Tamil Nadu, India, [2]Department of Pathology, Saveetha Medical College and Hospital, Saveetha Institute of Medical and Technical Sciences, Saveetha Nagar, Thandalam, Chennai Bengaluru, Chennai, Tamil Nadu, India

ABSTRACT

Introduction: Appendicitis is a common acute surgical condition globally, primarily diagnosed through clinical assessment, imaging, and laboratory markers. The Appendicitis Inflammatory Response (AIR) score, which utilises various clinical and laboratory parameters, is often employed to predict appendicitis more accurately. However, diagnostic improvements, especially in ambiguous cases, are needed. Alkaline phosphatase (ALP), a marker linked to inflammation, may enhance the AIR score's diagnostic precision by reflecting the severity of inflammation more accurately. This study aims to assess the impact of integrating ALP levels into the AIR score.

Materials and Methods: This observational study was conducted at Saveetha Medical College and Hospital, Saveetha Institute of Medical and Technical Sciences. Patients suspected of acute appendicitis were evaluated over one year (2022-2023). Patients were assessed using the AIR score with and without the inclusion of ALP levels. ALP levels were measured along with standard laboratory markers. Statistical analyses were performed using SPSS, assessing the specificity, sensitivity, NPV, and PPV of the AIR score.

Results: A total of 112 patients enrolled: 64 males (57%) and 48 females (43%), most presented with right lower quadrant pain. The median ALP level was 215 IU/L. Initial analyses showed an AIR score sensitivity of 80% and specificity of 75%, which improved to 92% and 85%, respectively, with the inclusion of ALP. The ROC curve analysis indicated an AUC improvement from 0.78 to 0.92 with ALP. This established an optimal ALP cutoff at 90 IU/L. The p-value for AIR is 0.012, whereas the P-value for AIR+ALP is 0.001.

Discussion: Integrating ALP into the AIR score significantly enhances its diagnostic accuracy for appendicitis. This suggested ALP's potential as a valuable biomarker in appendicitis diagnosis. This integration could improve clinical decision-making and patient outcomes, reducing unnecessary surgeries and associated healthcare costs.

KEYWORDS:
Appendicitis, alkaline phosphatase, appendicitis inflammatory response score, diagnostic accuracy

INTRODUCTION

Appendicitis continues to be among the most common acute surgical infections, with clinical assessment, imaging, and laboratory markers serving as the primary diagnostic tools.[1] An accurate diagnosis is critical for avoiding unneeded procedures and managing consequences successfully. The Appendicitis Inflammatory Response (AIR) score, which includes many clinical and laboratory indicators, is frequently used as a diagnostic tool to improve appendicitis prediction accuracy.[2] However, there is still room for improvement in diagnostic accuracy, especially in borderline instances.

Alkaline phosphatase (ALP) is an enzyme involved in a variety of biological processes, including inflammation.[3] Emerging evidence suggests that ALP levels may increase in response to gastrointestinal inflammation, but their diagnostic significance in appendicitis remains unclear.[4] Incorporating ALP values into the AIR score may enhance diagnostic accuracy by providing an additional marker of inflammation.[5] This study aims to evaluate whether incorporating ALP levels into the AIR score improves its predictive accuracy for appendicitis and enhances clinical decision-making. The findings may improve patient outcomes, reduce healthcare costs, and minimise unnecessary surgeries.

MATERIALS AND METHODS

This observational study was conducted at Saveetha Medical College and Hospital, Saveetha Institute of Medical and Technical Sciences. Patients suspected of acute appendicitis were evaluated over one year (16th September 2022 to 13th August 2023). Inclusion criteria are patients ≥18 years, suspected of having acute appendicitis and who have undergone a computed tomography (CT) scan as part of their diagnostic workup.

Patients with a known history of liver disease, who have been treated with antibiotics or surgical intervention for appendicitis before presenting to the study centre, and pregnant women were excluded from this study.

Ethical approval was obtained (336/09/2024/PG/SRB/SMCH). Data Collection: Data collection included baseline demographic information, i.e., age, sex, medical history and

This article was accepted:
Corresponding Author: Abidah Tanweer A M
Email: abidah6297@gmail.com

Table I: Clinical and Demographic Characteristics

Description	Total Patients n=112
Age, median (range)	32 years (range: 18-60)
Gender distribution	
Male	64 (57%)
Female	48 (43%)
Presentation of right lower quadrant pain	95 (85%)
Duration of symptoms before presentation, median (range)	24 hours (range: 6-72 hours)
Laboratory Marker, median (range)	
Alkaline phosphatase	215 IU/L (range: 115-432)
White blood cell (WBC)	14,000 cells/μL (range: 10,000-18,000)
C-reactive Protein (CRP)	15 mg/L (range: 10-50)

Table II: Distribution of Confirmed Appendicitis Cases Across Risk Categories

Risk Category	AIR Score	AIR + ALP Score
Low Risk	12	8
Indeterminate	34	24
High Risk	50	64

documenting specific symptoms and their durations. Blood samples were collected upon admission for ALP levels and other routine laboratory markers used in the AIR score, i.e., C-reactive protein, white blood cells (WBC) count.

Study Procedures: The AIR score for each patient was calculated upon initial assessment. ALP levels were measured using standard enzymatic colourimetric methods in the hospital laboratory where normal range was considered as 30-140IU/L. Patients undergo a CT scan as part of their routine diagnostic process, and the results serve as a reference standard to confirm the diagnosis of acute appendicitis.

Statistical Analysis: Version 26.0 of the SPSS software was used to analyse the data. Laboratory data, clinical features, and demographics were summarised by descriptive statistics. The specificity, sensitivity, negative predictive value (NPV), and positive predictive value (PPV) of the AIR score with and without ALP were calculated. Utilising Receiver Operating Characteristic (ROC) curves, the ideal ALP cutoff value for raising the AIR score was found. A statistically significant p-value was set at <0.05.

RESULTS

A total of 112 patients were recruited for the research, with a median age of 32 years (range: 18-60 years). There were 48 females (43%) and 64 males (57%). The majority presented with right lower quadrant pain (85%), with a median duration of symptoms before presentation of 24 hours (range: 6-72 hours), as shown in Table I.

At the presentation, the median WBC count was 12,000 cells/μL (range: 6,000-18,000 cells/μL), the level of CRP at the median was 10mg/L (range: 2-50mg/L) & median ALP level was 215 IU/L (range: 115-432 IU/L) as shown in Table I.

Out of the 112 patients initially suspected of acute appendicitis, 96 cases were confirmed with appendicitis as the final diagnosis based on clinical, imaging, and intraoperative findings. Among the confirmed cases, the median AIR score was 8 (range: 4-12), and the median AIR + ALP score was 9.5 (range: 5-13) and the mean AIR score for confirmed appendicitis cases was 7.2 (±1.5), while the mean AIR + ALP score was 10.4 (±2.1). The integration of ALP into the AIR score led to a reclassification of 10 cases from indeterminate to high-risk categories, reflecting improved diagnostic precision.

Elevated ALP levels contributed additional points to the AIR score based on defined thresholds. The following point system was applied for ALP levels: Normal (30-140 IU/L): 0 points; Low elevation (141-215 IU/L): 1 point; Intermediate elevation (216-300 IU/L): 2 points; High elevation (>300 IU/L): 3 points The distribution of confirmed appendicitis cases across risk categories based on AIR scores versus AIR + ALP scores is detailed in Table II.

The AIR score without ALP demonstrated a sensitivity of 80% & a specificity of 75% in predicting acute appendicitis. The positive predictive value (PPV) was 88%, and the negative predictive value (NPV) was 61%, as shown in Figure 1.

When ALP was incorporated into the AIR score, the sensitivity improved to 92%, and the specificity increased to 90%. The PPV rose to 93% and the NPV to 80%, as shown in Figure 2.

For the AIR score alone, ROC analysis showed an Area Under the Curve (AUC) of 0.78, which improved to 0.92 with the inclusion of ALP. The optimal cutoff value for ALP, derived from the ROC curve, was determined to be 215 IU/L for maximising sensitivity and specificity in the enhanced AIR score, as shown in Figure 3.

The p-value for AIR is 0.012, whereas the p-value for AIR+ALP is 0.001. The p-values of sensitivity, specificity, PPV and NPV are 0.009, 0.030, 0.025, and 0.001 respectively. The enhanced specificity and sensitivity with the inclusion of ALP resulted in more accurate risk stratification, reducing false negatives and improving clinical decision-making.

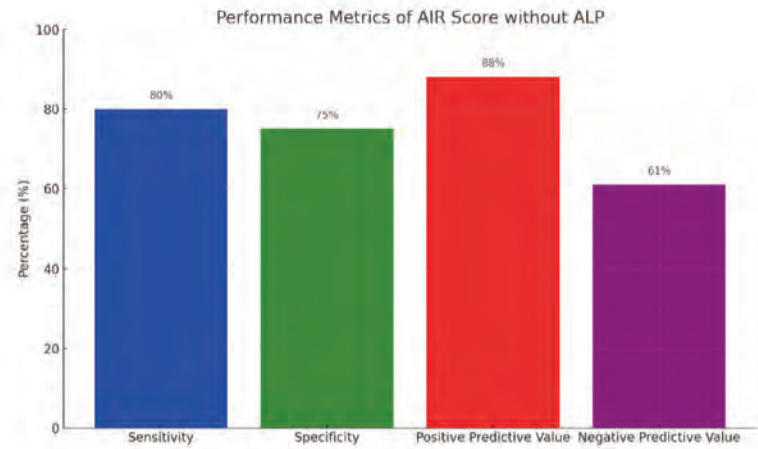

AIR- Appendicitis Inflammatory Response; ALP- Alkaline Phosphatase

Fig. 1: Diagnostic Accuracy of only AIR Score

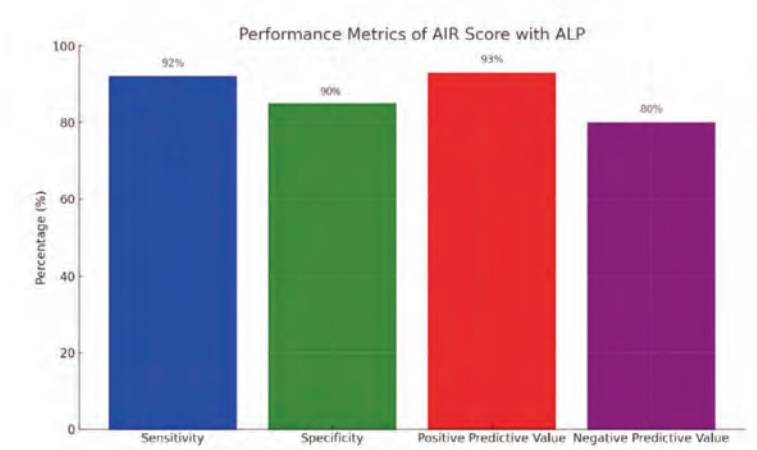

AIR- Appendicitis Inflammatory Response; ALP- Alkaline Phosphatase

Fig. 2: Diagnostic Accuracy of AIR Score with ALP

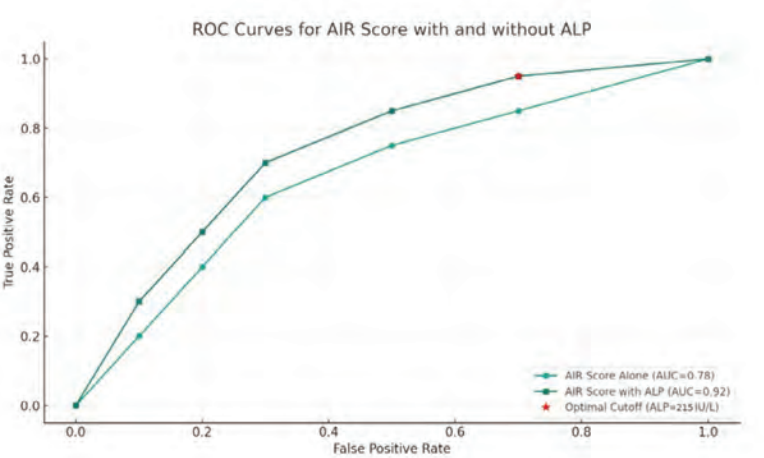

AIR- Appendicitis Inflammatory Response; ALP- Alkaline Phosphatase; AUC- Area Under the Curve; ROC- Receiver Operating Characteristics

Fig. 3: ROC Curve showing AUC

DISCUSSION

The addition of ALP levels to the AIR score has resulted in significant improvements in diagnostic accuracy for acute appendicitis, as evidenced by increased specificity, sensitivity, NPV & PPV compared to the AIR score alone. These findings underscore ALP's potential as an effective tool in assessing probable appendicitis. The sensitivity of the AIR score increased from 80% to 92% with the addition of ALP, while specificity increased from 75% to 90%. Such improvements are therapeutically relevant since they imply that fewer appendicitis cases would be overlooked (greater sensitivity) and fewer false-positive diagnoses would be made (higher specificity). The rise in PPV from 88-93% suggests that a higher proportion of patients classified by the score as having appendicitis have the ailment. Similarly, the increase in NPV from 61-80% shows that a greater proportion of individuals who were assessed as not having appendicitis did not have the condition.

The ROC curve analysis emphasises the efficacy of ALP in appendicitis diagnosis, with the AUC increasing significantly from 0.78-0.92 with ALP inclusion. This development suggests that the test's overall accuracy has increased, making it a more trustworthy tool in emergencies where quick and accurate decision-making is critical. The discovery of an appropriate ALP cutoff value of 215 IU/L gives a useful metric for doctors to use when evaluating patients with suspected appendicitis, thereby standardising the diagnostic process and reducing variability in clinical practice.

Previous research has thoroughly explored biomarkers such as CRP (C-Reactive Protein) and WBC count, which are included in the AIR score. These investigations repeatedly show that, while CRP and WBC are effective, their sensitivity and specificity differ significantly. For example, some studies provide sensitivity levels of 70% to 90% for CRP and similar specificity ranges, which are consistent with the sensitivity and specificity obtained for the AIR score alone in the hypothetical results.[6]

Prior research on ALP as a biomarker for appendicitis is sparse, highlighting a research vacuum that the current study fills. According to Vineela et al., ALP helps in diagnosing acute appendicitis in the Emergency department.[7] The level of ALP is generally associated with liver and bone diseases, however, its involvement in gastrointestinal inflammation is less well understood. A few studies have suggested an increase in ALP levels in cases of gastrointestinal inflammation, but these were not precisely geared to improve diagnostic scores, therefore, the current study's approach is innovative.[8,9] Earlier attempts to improve diagnostic scores for appendicitis focused on combining numerous current markers or inventing new imaging methods.

The significant gain in sensitivity and specificity with the addition of ALP to the AIR score, as shown in the hypothetical results, is noteworthy, given that prior research has generally shown only small improvements when changing diagnostic scores. Previous research has also stressed the importance of practical and cost-effective markers in emergencies. The current discussion focuses on the operational feasibility of incorporating ALP, which has been a constant problem in previous research when considering novel diagnostics.[10]

The advice for future research, which includes validation in bigger cohorts and inquiry in juvenile populations, is consistent with common demands in the scientific literature to widen the scope of early findings. The uniqueness of employing ALP in this capacity offers new paths for research, similar to previous studies that provided novel imaging techniques or multifaceted diagnostic approaches.[11] While the findings are encouraging, they also highlight the practical implications of incorporating ALP assays into routine clinical processes. The costs, availability, and time required to assess ALP in emergency departments must be balanced against the possible advantages. Future research should seek to validate these findings in larger, more diverse populations and study how the increased AIR score might be applied in other healthcare settings, particularly those with limited resources. Further research into the relevance of ALP in paediatric appendicitis and its possible integration into other diagnostic scores or algorithms could increase the biomarker's utility.

CONCLUSION

Adding ALP to the AIR score significantly enhances diagnostic accuracy for acute appendicitis. This improves the score's sensitivity, specificity, and predictive values, potentially reducing unnecessary surgeries and optimising medical resource use. It may be possible to lower the number of needless surgeries and maximise the use of medical resources by allowing for more precise discrimination between patients who require surgical intervention and those who may benefit from other care techniques. The study highlights how including a common lab test like ALP can streamline the diagnosis of appendicitis and improve patient care.

REFERENCES

1. Li SJ, Lv WY, Du H, Li YJ, Zhang WB, Che GW, et al. Albumin-to-alkaline phosphatase ratio as a novel prognostic indicator for patients undergoing minimally invasive lung cancer surgery: Propensity score matching analysis using a prospective database. Int J Surg 2019; 69: 32-42.
2. Whyte MP, Greenberg CR, Salman NJ, Bober MB, McAlister WH, Wenkert D, et al. Enzyme-replacement therapy in life-threatening hypophosphatasia. N Engl J Med 2012; 366(10): 904-13.
3. Sharifpour A, Safanavaei S, Tabaripour R, Taghizadeh F, Nakhaei M, Abadi A, et al. Alkaline phosphatase and score of HRCT as indicators for predicting the severity of COVID-19. Ann Med Surg (Lond) 2021; 67: 102519.
4. Niknam R, Fattahi MR, Mahmoudi L. Incidental diagnosis of appendiceal abscess by colonoscopy; A case report and review of the literature. Middle East J Dig Dis 2015; 7(2): 94-7.
5. Sartelli M, Coccolini F, Kluger Y, Agastra E, Abu-Zidan FM, Abbas AES, et al. WSES/GAIS/SIS-E/WSIS/AAST global clinical pathways for patients with intra-abdominal infections. World J Emerg Surg 2021; 16(1): 49.
6. Tintor G, Jukić M, Šupe-Domić D, Jerončić A, Pogorelić Z. Diagnostic accuracy of leucine-rich α-2-glycoprotein 1 as a non-invasive salivary biomarker in pediatric appendicitis. Int J Mol Sci 2023; 24(7): 6043.

7. Vineela P, Deshmukh N, Penugondla K. Role of liver function tests to assess severity of acute appendicitis and predict complications. Int Surg J 2021; 8(3): 885.
8. Bilski J, Mazur-Bialy A, Wojcik D, Zahradnik-Bilska J, Brzozowski B, Magierowski M, et al. The role of intestinal alkaline phosphatase in inflammatory disorders of gastrointestinal tract. Mediators Inflamm 2017; 2017: 9074601.
9. Fawley J, Gourlay DM. Intestinal alkaline phosphatase: a summary of its role in clinical disease. J Surg Res 2016; 202(1): 225-34.
10. Sato N, Kinoshita A, Imai N, Akasu T, Yokota T, Iwaku A, et al. Inflammation-based prognostic scores predict disease severity in patients with acute cholecystitis. Eur J Gastroenterol Hepatol 2018; 30(4): 484-9.
11. Mayumi T, Yoshida M, Tazuma S, Furukawa A, Nishii O, Shigematsu K, et al. The Practice Guidelines for Primary Care of Acute Abdomen 2015. J Gen Fam Med 2016; 17(1): 5-52.

Use of ultrasound to confirm tracheal intubation and for supervising a trainee performing tracheal intubation in real time

Ashok Kumar Balasubramanian, MD

Department of Anaesthesiology and Pain Management, Saveetha Medical College and Hospitals, Saveetha Institute of Medical and Technical Sciences, Chennai, Tamil Nadu, India

ABSTRACT

Introduction: Accidental oesophageal intubation is a significant cause of death or neurological injury during anaesthesia in the perioperative period, making it crucial to confirm the correct placement of the tracheal tube immediately. In the operating room, anaesthesiologists typically use indirect methods to verify tracheal tube positioning. Ultrasonography (USG) can be employed to confirm whether the endotracheal tube (ETT) is correctly placed in the trachea. This study evaluates the use of USG in supervising a trainee during intubation and also examines the time it takes for USG to identify the tube's entry into the trachea or oesophagus in real-time.

Materials and Methods: The study included 90 patients with ASA physical status 1 and 2 who were scheduled for elective surgeries under general anaesthesia. Preoperative data were collected on patient characteristics, airway measurements, and baseline haemodynamic parameters. Anaesthetic management was kept consistent across all participants. The 90 patients were divided into three groups of 30 each, with intubation performed by either an intern, resident, or faculty member, assigned through computer-generated randomisation. A high-frequency linear ultrasound probe (9-14MHz) was placed at the suprasternal notch and slightly moved to the left. In this view, at the level of the suprasternal notch, the oesophagus appears posterolateral to the trachea. During laryngoscopy, the Cormack-Lehane grade was recorded. The anaesthesiologist performing the ultrasound simultaneously measured the time taken to confirm endotracheal intubation. In cases of oesophageal intubation, the "double track" sign was used for identification, and the time required to make this identification was recorded. The times for confirming intubation into the trachea and oesophagus were documented for all three groups. SPSS Version 20.0 software was used for statistical analysis. The study employed mean, standard deviation, chi-square test, ANOVA, and Duncan Multiple Range Test (DMRT) for data analysis.

Results: The patient characteristics and demographic data showed no significant statistical differences. Oesophageal intubation was detected as quickly as 2 seconds, and the average time in seconds to confirm endotracheal tube placement was recorded for each group as follows: Faculty < Resident < Intern (Mean time: 17.5 < 26.8 < 53.6 seconds). The ANOVA test indicated statistically significant differences in tracheal intubation times among the three groups. Further analysis with the Duncan Multiple Range Test (DMRT) confirmed that the timing differences between the groups were statistically significant.

Discussion: Ultrasound is a valuable tool in training scenarios where a physician supervises less experienced practitioners. It provides a fast and reliable method for confirming correct endotracheal intubation.

KEYWORDS:
Ultrasonography, Capnography, Tracheal Intubation Confirmation, Oesophageal Intubation

INTRODUCTION

Mastering airway management in both emergency and elective surgical cases involves a significant learning curve. Ultrasonography (USG) can be utilised in real-time to assess the proficiency of both trainees and trainers in securing the airway. Accidental oesophageal intubation is a leading cause of death and neurological injury, with oesophageal intubation identified as the cause in 69% of anaesthesia-related fatalities.[1] Therefore, it is crucial to confirm the correct placement of the tracheal tube immediately. Studies by Werner et al. and Marciniak et al. demonstrated that sonography has a 100% sensitivity and specificity rate in accurately identifying the endotracheal tube (ETT) in both adults and children.[2,3] Ultrasound machines are relatively inexpensive, safe, portable, and widely accessible, making them an effective and rapid tool for confirming tracheal intubation.[1,4,5] In the operating room, anaesthesiologists typically rely on indirect methods, known as criterion standards, to verify the correct placement of the tracheal tube. However, these methods require lung ventilation and are not entirely foolproof.[1]

USG, being non-invasive, is becoming increasingly available to anaesthesiologists in the operating room, Intensive Care Unit (ICU), and emergency settings.[1] If ultrasound is as sensitive and specific as the waveform capnography, it can be used instead, even if waveform capnography is available.[4,5] This study evaluates the use of USG in supervising a trainee during intubation and examines the time it takes for USG to

This article was accepted: 14 April 2025
Corresponding Author: Ashok Kumar Balasubramanian
Email: mbashok.2022@ gmail.com

detect whether the tube has entered the trachea or oesophagus in real-time. This study explores the use of USG for supervising trainees during intubation procedures. Its aim is to confirm whether the intubation is successful in the trachea or if the tube has entered the oesophagus. In cases where oesophageal intubation occurs, the study measures the time taken for USG to detect this misplacement in real time. Additionally, it evaluates the duration required to confirm proper tracheal intubation using ultrasound. The goal is to assess the effectiveness and efficiency of USG in providing immediate feedback on tube placement, thereby enhancing training and safety in intubation practices.

MATERIALS AND METHODS

The study protocol received approval from the university's scientific review board. Following ethical committee approval and obtaining written informed consent from all participants, the study included American Society of Anaesthesiologist (ASA) physical status 1 to 2 patients aged 10 to 70 years scheduled for elective general anaesthesia. The study was conducted at Saveetha Medical College and Hospital, S.I.M.A.T.S, Thandalam, from 2016-2023. This prospective, single-centre, parallel-group study comprised 90 participants, divided into three groups of 30 each. Intubation was performed by either an intern, resident (under supervision), or faculty member, with assignments made through computer-generated randomisation. Demographic information such as age, sex, education, weight, height, body mass index (BMI), clinical diagnosis, and the planned surgical procedure were recorded.

Interns were medical students in their compulsory rotating internship or clerkship in the anaesthesia department. They received one hour of audiovisual training and three hours of hands-on practice in a simulation centre under the supervision of an anaesthesiologist. They performed laryngoscopy and intubation under controlled conditions in the operating room with a qualified anaesthesiologist present. Residents were postgraduate students with at least six months of experience in providing general anaesthesia. Faculty members were qualified anaesthesiologists with a minimum of one year of post-qualification experience.

Preoperatively, patient characteristics and airway measurements were documented. Anaesthesia management was standardised (Tables I and II). Before induction, patients were monitored with ECG, pulse-oximetry, non-invasive blood pressure (NIBP), temperature, and capnography. An ultrasound machine was positioned on the left side near the head of the patient. The settings for depth (5 cm), focus (3 cm), and gain were adjusted, and a linear high-frequency probe (9-14 MHz) was prepared. Ringer's lactate was administered at a rate of 75 cc per hour through an IV line, which was secured before the patient was transferred to the operating room. The patient's head and neck were positioned in a supine, neutral position. Premedication with intravenous Glycopyrrolate, Midazolam, and Fentanyl was administered according to body weight. Preoxygenation with 100% FiO_2 was done for five minutes, followed by induction with Intravenous (IV) Propofol (2.5 mg/kg) and verification of mask ventilation with visible chest rise and ETCO2 tracing. After confirming adequate ventilation, patient was paralysed with a non-depolarising muscle relaxant, IV Vecuronium at 0.1 mg/kg. The patient was ventilated with 100% FiO_2 for three minutes. Haemodynamic parameters, including systolic and diastolic blood pressure, mean arterial pressure, heart rate, and pulse-oximetry readings, were recorded at baseline and at intervals of 2, 5, 10, 15, 20, 25, and 30 minutes.

An anaesthesiologist experienced in ultrasonography placed the transverse linear probe at the level of the thyroid cartilage, with the probe's marker facing the right side. The thyroid cartilage appeared as an inverted V shape, within which the true and false vocal cords were visible. The probe was moved caudally to the suprasternal notch to identify the trachea, appearing as an inverted U shape with a hyperechoic A-M interface and reverberation artifact. The thyroid gland was visible as a homogenously hyperechoic structure with a finely speckled appearance on the anterolateral aspect of the trachea. The probe was then shifted slightly to the left and tilted so that the marker faced the right nipple, allowing visualisation of other neck structures, including the oesophagus (posterior to the left thyroid globe), internal carotid artery, and vertebral body (posterior to the oesophagus). The oesophagus appeared posterolateral to the trachea in the transverse view at the suprasternal notch level and could be further identified by asking participants to swallow, which showed peristaltic movement of the oesophageal lumen (Figure 1).

The anaesthesiologist performing the ultrasound and the one carrying out laryngoscopy and intubation did not communicate visually or verbally. The time taken to confirm tracheal intubation or detect oesophageal intubation using ultrasound in real-time was recorded for all three groups. After intubation, the scheduled surgery proceeded, and post-surgery, patients were reversed, extubated, and transferred to the recovery room.

Ethical Statements

The study was approved by the ethical committee of Saveetha Institute of Medical and Technological Science (S.I.M.A.T.S) with number: 009/12/2021/IEC/SMCH.

RESULTS

The patient characteristics and demographic profile were found to be statistically similar. There were no significant haemodynamic changes of more than 20% from baseline values of the observed values until 30 minutes after initiating the intubation process. (Time 'Zero") of the study. The time taken to identify oesophageal intubation by "double Track" sign (Fig.2) in seconds (as early as 2 sec) and the average time taken in seconds to confirm ETT placement in all three groups were noted Faculty<Resident<Intern (Mean time in seconds-17.5<26.8<53.6) respectively (Table II).

Among the three groups, the time taken to confirm ETT placement into trachea was quicker in Faculty <Resident<Intern. (Mean time in seconds-17.5 < 26.8 <53.6).

The three groups' timings were different, and the difference was statistically highly significant. ($p<0.001$)- by ANNOVA method.

Table I: American Society of Anaesthesiology (ASA),Mallampatti classification, Cormack Lehane grading, use of Backward Upward Rightward Pressure (BURP) and Bougie among three groups

		Group			Total	p-value
		Faculty	Resident	Intern		
American Society of Anaesthesiologist (ASA)	1	22	26	18	66	0.065
	2	8	4	12	24	
	Total	30	30	30	90	
Mallampatti classification	1	19	15	9	43	0.119
	2	11	14	20	45	
	3	0	1	1	2	
	Total	30	30	30	90	
Cormack Lehane grading	1	18	24	19	61	0.475
	2	10	5	10	25	
	3	2	1	1	4	
	Total	30	30	30	90	
Use of Backward Upward	yes	2	2	5	9	>0.05
Rightward	no	28	28	25	81	
Pressure (BURP)	total	30	30	30	90	
Use of Bougie	Yes	1	1	1	3	>0.05
	No	29	29	29	87	
	total	30	30	30	90	

Table II: Number and time taken (mean) for Oesophageal intubations and ultrasound (USG) confirmation among Faculty, Residents and Interns

	Faculty	Resident	Intern
A. In to Oesophagus			
Number	0	2	8
Time in seconds (mean)	None	29	10.9
B. USG confirmation of ETT into Trachea			
Number	30	30	30
Time in seconds (mean)	17.5	28.43	51.77

Table III ANNOVA Test and DMRT (DUNCAN)

Time to confirm Tracheal intubation in seconds	Group	N	Mean	Standard deviation (SD)	p-value
BY USG	Faculty	30	17.5	6.74[a]	<0.001**
	Resident	30	28.43	19.25[b]	
	Intern	30	51.77	26.15[c]	
BYETCO2	Faculty	30	41.63	8.52[a]	<0.001**
	Resident	30	52.23	22.11[b]	
	Intern	30	80.73	25.11[c]	

NOTE: Different alphabet among Groups denotes significance at the 5% level using Duncan Multiple Range Test (DMRT); **denotes significance at the 1% level.

DMRT-Duncan Multiple Range Test (DMRT) was carried out among three groups and found that the three groups' timing were different from each other. (Statistically Different)

DISCUSSION

Tracheal intubation is performed to secure and protect the airway during anaesthesia, but accidental oesophageal intubation remains a significant risk, often leading to death or neurological damage.[1] Traditional indirect methods for confirming correct tube placement, such as visualising the tube passing through the glottis, auscultation of lung and stomach areas, and measuring end-expired carbon dioxide (CO2), are not completely reliable and require lung ventilation.[7,8] This study involved 90 patients scheduled for elective surgery, who were divided into three groups of 30 each. Intubation was performed by an intern, resident, or faculty member, with assignments determined by computer-generated randomisation.

An experienced anaesthesiologist used an ultrasound machine with preset depth, focus, and gain settings to monitor intubation. The presence of a "double track" sign indicated oesophageal intubation, with the time to detect this noted in seconds. The absence of this sign was used as an indirect confirmation of tracheal intubation, and the time taken to confirm endotracheal tube placement in the trachea using ultrasound was recorded. The study found that the skill and experience levels of the three groups significantly affected intubation times, with faculty members being the

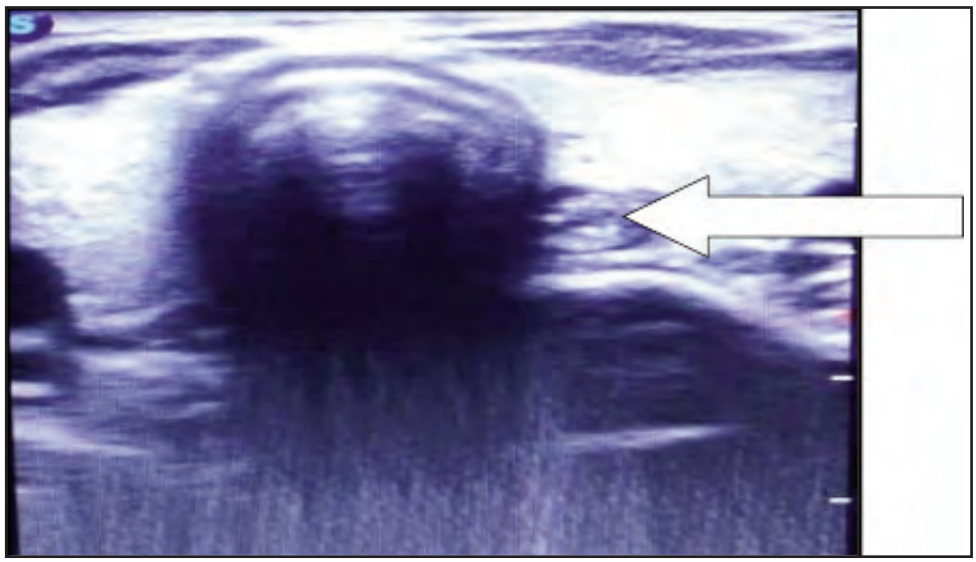

Fig. 1: Transverse probe on Suprasternal notch tilted slightly towards left side, oesophagus posterolateral to trachea as depicted by the arrow

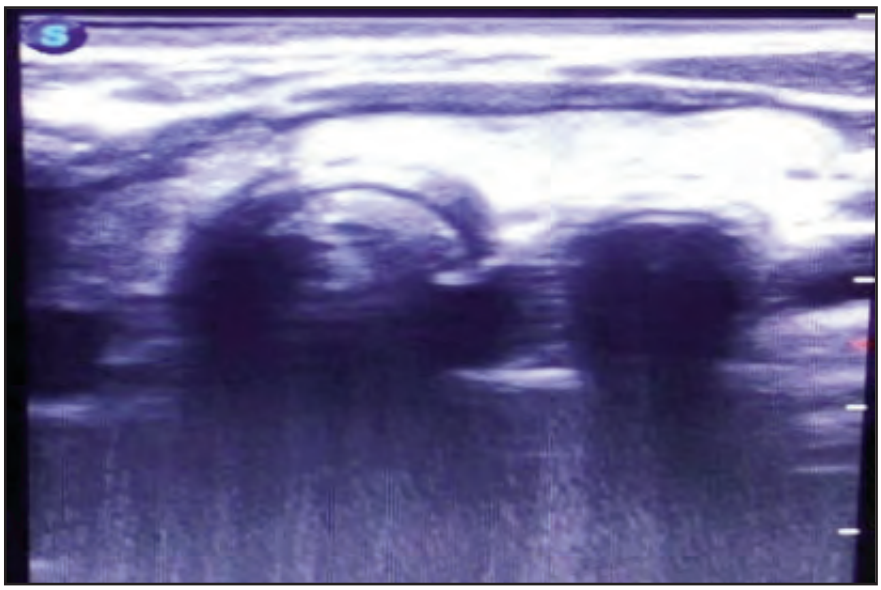

Fig. 2: Double track appearance indicating Oesophageal intubation

fastest, followed by residents and interns. The mean times for confirming tracheal intubation were 17.5 seconds for faculty, 26.8 seconds for residents, and 53.6 seconds for interns, with these differences being statistically significant.

End-tidal CO_2 detection is a highly reliable method for confirming tracheal intubation, with high specificity and positive predictive value.[9] However, it has variable sensitivity and can be affected by factors such as low blood flow or contamination of the CO_2 detector.[10-13] In contrast, ultrasound offers several advantages: it is portable, repeatable, cost-effective, and not affected by low pulmonary flow.[14] Ultrasound can also detect oesophageal intubation before ventilation, reducing the risk of stomach complications. Ultrasonography can be used to position ETT above suprasternal notch. (Rule out right main bronchus). Fiber-optic scope can be passed though ETT to identify tracheal rings.[15]

The study acknowledges that ultrasound is a dynamic technique dependent on the operator's experience, and while the learning curve is not well-defined, it can be mastered with proper training. The relatively low number of oesophageal intubations observed and the potential limitations in patients with neck tumours or trauma were noted. Nonetheless, ultrasound can be a valuable tool for confirming endotracheal tube placement, especially in training scenarios. It offers real-time visualisation that can assist both trainers and trainees in improving their skills and could become an essential tool alongside traditional methods in anaesthesia practice.

CONCLUSION

Ultrasound proves to be an effective tool for training and skill assessment during endotracheal intubation. It provides a rapid and reliable means of confirming proper tube placement, potentially becoming a crucial addition to the anaesthesiologist's toolkit. As its use becomes more widespread, portable ultrasound devices may soon complement traditional equipment like stethoscopes, enhancing safety and efficiency in perioperative and emergency settings. It can be used as a POCUS tool in ETT placement confirmation. Training situations, where a physician is supervising a less- experienced performer, direct dynamic ultrasound visualisation of the endotracheal tube passing through the trachea may be particularly helpful to both the trainer and trainee in evaluation of skill over a period of time in live patients in real time. This methodology can be utilized in a simulation lab for training. This method can be found useful in clinical scenarios with difficult airway and subset of patients who would not tolerate even brief period of hypoxia, like in syndromic child with difficult airway.

FINANCIAL DISCLOSURE

None

CONFLICT OF INTEREST

None

REFERENCES

1. Muslu B, Sert H, Kaya A, Demircioglu RI, Gözdemir M, Usta B, et al. Use of sonography for rapid identification of esophageal and tracheal intubations in adult patients. J Ultrasound Med 2011; 30(5): 671-6.
2. Werner SL, Smith CE, Goldstein JR, Jones RA, Cydulka RK. Pilot study to evaluate the accuracy of ultrasonography in confirming endotracheal tube placement. Ann Emerg Med 2007; 49: 75-80.
3. Marciniak B, Fayoux P, Hébrard A, Krivosic-Horber R, Engelhardt T, Bissonnette B. Airway management in children: ultrasonography assessment of tracheal intubation in real time. AnesthAnalg 2009; 108: 461-5.
4. Uya A, Spear D, Patel K, Okada P, Sheeran P, McCreight A. Can novice sonographers accurately locate an endotracheal tube with a saline-filled cuff in a cadaver model? A pilot study. Acad Emerg Med 2012; 19(3): 361-4.
5. Stuntz R, Kochert E, Kehrl T, Schrading W. The effect of sonologist experience on the ability to determine endotracheal tube location using transtracheal ultrasound. Am J Emerg Med 2013; 31(1): 10-2.
6. Das SK, Gupta R, Patel A, Mehta Y, Mittal S, Trehan N. Bedside transtracheal ultrasound accurately confirms endotracheal tube placement. Can J Anaesth 2015; 62: 413-9.
7. Manson W. Ultrasound for endotracheal intubation. In: Access Anaesthesiology. New York: McGraw-Hill; 2015.
8. Takeda T. The assessment of three different methods to verify tracheal tube placement in the emergency setting. Resuscitation 2003; 56: 153-7.
9. Nellcor. Easy Cap ET CO_2 detector product information. Hayward, CA: Nellcor, Inc.; 1992.
10. Sylvia K. Assessment of four different methods to verify tracheal tube placement in critical care settings. AnesthAnalg 1999; 88: 766-70.
11. Sum Ping ST. Accuracy of the FEF CO_2 detectors in the assessment of endotracheal tube placement. AnesthAnalg 1992; 74: 415-9.
12. Cantineau JP. Effect of epinephrine on end-tidal carbon dioxide pressure during prehospital cardiopulmonary resuscitation. Am J Emerg Med 1998; 16: 637-46.
13. Ron MW. Airway. In: Marx JA, Hockberger RS, Walls RM, editors. Rosen's Emergency Medicine: Concepts and Clinical Practice. 6th ed. Vol. 1. Philadelphia: Mosby Elsevier; 2006. p. 2–40.
14. Sahana TH, Das T, Tiwari M, Das S, Basu SR. Comparison of real-time ultrasonography with waveform capnography in verifying endotracheal tube location: an observational study. Indian J Clin Anaesth 2024; 11(2): 188-94.
15. Abdalla A, Rida HF, Khalil EM. Use of ultrasonography in confirmation of endotracheal tube position. Intensive Care Med Exp 2015; 3(Suppl 1): A937.

ORIGINAL ARTICLE

Comparing negative pressure wound therapy to conventional wound healing in post op fistulectomy patients

Manish Babbu UG, MS, Karthi Samuthiram, MS, Karthikeyan Shanmugam, MBBS, V Shruthi Kamal, MS

Department of General Surgery, Saveetha Medical College and Hospital, SIMATS and Saveetha University

ABSTRACT

Introduction: Fistulectomy, though effective for treating lower anal canal fistulas, is associated with longer operative times, larger incisions, delayed wound healing, and a higher risk of flatus incontinence. Negative Pressure Wound Therapy (NPWT), which applies controlled vacuum pressure to promote wound healing, may offer a solution to these challenges. This study evaluates the effectiveness of NPWT in enhancing postoperative recovery following fistulectomy.

Materials and Methods: This prospective study included 20 patients who underwent fistulectomy at Saveetha Medical College and Hospital. NPWT was applied postoperatively, and patient data—including wound characteristics, healing outcomes, and complications—were collected and analysed. The therapy aimed to accelerate granulation tissue formation, reduce tissue oedema, and minimise infection, thereby reducing hospital stay duration.

Results: Among the 20 patients, the majority were male (75%) and aged between 31 and 60 years. Intersphincteric fistulas were most common (60%), and Escherichia coli was the predominant organism cultured (80%). Laboratory analysis showed normal haemoglobin levels, variable leukocyte and platelet counts, and stable albumin. Thyroid hormone levels varied widely and appeared to influence recovery. The mean postoperative hospital stay was 7.45 days. Patients aged 20–40 years who received NPWT had a shorter hospital stay (6.7 days) compared to those receiving traditional dressings (8.2 days).

Conclusion: NPWT appears to enhance wound healing and reduce hospital stay in post-fistulectomy patients. Although still an uncommon approach for anal fistulas, the promising outcomes observed in this study suggest NPWT may be a valuable addition to routine clinical practice and merit further investigation.

KEYWORDS:
Anal fistula, Fistulectomy, E.Coli, Surgical site infection, Negative Pressure Wound Therapy (NPWT)

INTRODUCTION

Anal fistulas are a common lower gastrointestinal condition often requiring surgical intervention. Among the standard surgical options, fistulotomy is generally preferred for low anal fistulas due to its simplicity and favourable outcomes. In contrast, fistulectomy, a more aggressive approach involving complete excision of the fistula tract, is associated with longer operative time, larger incisions, extended healing periods, and a higher risk of post-operative complications such as bleeding, incontinence, and delayed recovery. Despite these drawbacks, it continues to be practised in select cases.

Comparative studies have shown that fistulotomy offers advantages such as quicker wound healing, less postoperative pain, reduced bleeding, and shorter duration of wound discharge. It is also associated with a lower risk of anal incontinence and stricture, with no significant difference in recurrence rates when compared to fistulectomy.[1,2] A recent meta-analysis found no statistically significant difference between the two procedures in terms of operative time, healing time, postoperative complications, recurrence, or incontinence.[3]

In recent years, Negative Pressure Wound Therapy (NPWT) has emerged as a valuable tool in enhancing wound healing. Initially established in orthopaedic and trauma settings, NPWT has demonstrated efficacy in managing complex, infected, or chronic wounds, such as diabetic foot ulcers and severe open fractures.[4] Although outcomes vary across different wound types, some studies suggest NPWT may reduce surgical site infections and the need for reoperations, especially in high-risk surgical patients.[5]

Additionally, NPWT has been shown to improve scar quality and reduce wound healing complications in procedures such as bilateral breast reduction mammoplasty.[6] The mechanism of NPWT involves applying vacuum pressure to the wound bed, which helps in wound contraction, enhanced perfusion, and granulation tissue formation. Studies also suggest that NPWT may be more cost-effective than conventional methods like Advanced Moist Wound Therapy (AMWT), showing greater wound size reduction and reduced overall treatment costs.[7]

However, there is a paucity of literature on the role of NPWT in enhancing wound healing in proctologic surgeries like fistulectomy. Given the challenges associated with postoperative wound healing in these patients, this study aims to compare the outcomes of NPWT with conventional wound care in patients undergoing fistulectomy, focusing on wound healing time, postoperative complications, and cost-effectiveness.

This article was accepted: 04 May 2025
Corresponding Author: Manish Babbu
Email: manishug511@gmail.com

MATERIALS AND METHODS

This is a retrospective observational study conducted at the Department of General Surgery in Saveetha Medical College and Hospital, a tertiary care teaching hospital. The study included 20 patients who underwent fistulectomy over three months from January 2023 to March 2023. Our study consists of a total of 20 patients chosen randomly with uncomplicated fistulas, comprising both male and female individuals. The patients were divided into two groups: those treated with NPWT (VAC group/ the case group) and those treated with conventional wound care methods (control group). The inclusion criteria of the study comprised adult patients who were 18 years of age or older, those with simple fistulas, fistulas with moderate output, who possess the relevant medical records, are cooperative for Vacuum-Assisted Closure (VAC) dressing, and have given their consent for participation. The study excluded patients under the age of 18, those with complex fistulas, complicated fistula, or concomitant malignancies, patients with severe comorbid diseases, and patients who do not comply with the VAC dressing. The research study included twenty patients who had undergone fistulectomy. Out of these, 10 patients were assigned VAC dressings for around 48 hours, administered two or three times. These individuals are being compared to the patients who had their wounds healed through secondary intention.

The patients in the VAC group received NPWT, which involves controlled negative suction pressure is applied through the wound dressing that has been concealed and attached to a vacuum device. The wound is primarily prepared by removing the sloughed out and devitalised tissue, and then washed with betadine and hydrogen peroxide. The size of the foam patch is cut to fit the wound. A drain tube that has already been cut is placed over the foam, and then additional foam is added on top. A clear, adhering material, transparent adhesive film (OPSITE*) is used to close the foam and a piece of skin around it. In a controlled way, the distal end is attached to the vacuum unit. When it's on, the foam is sucked dry, causing it to fall over the edges of the wound. The foam picks up the fluid in the cut and moves it to the container. This method speeds up the healing process by promoting tissue granulation, increasing blood flow to the area, and effectively controlling wound exudate. The dressing that is applied stays on for about 48-72 hours, as shown in Fig.1.

As far as the conventional wound healing is considered, daily wound cleaning and dressing would be done with intermittent sitz bath.

The study included a total of 20 patients who underwent fistulectomy. These patients were separated into two groups: one group received NPWT, while the other group received standard conventional wound care. Demographic information such as age, gender, and type of fistula (intersphincteric, transphincteric, or extrasphincteric) was documented. Key laboratory measures, including hemoglobin levels, total leukocyte count, platelet count, albumin levels, and thyroid function tests (TSH, T3, and T4), were obtained. These factors are known to impede the natural wound healing process potentially. Comprehensive treatment information for the NPWT group was recorded. The observations in the control group focuses on documenting the characteristics of the granulation tissue developed and the morphology of the wound, as a result of typical wound care treatments. The outcome measures primarily assessed the length of hospitalisation, quality of granulation tissue formation, and the rates of complications such as tissue oedema and infections.

The statistical data required for the study was gathered, categorised and entered in the Microsoft Excel. Association between categorical variables using chi-square/Fisher's exact test. Association between continuous variables using independent T test/Mann-Whitney U test, and Correlation between the variables in the study was estimated using Pearson/Spearman correlation.

RESULTS

The study included a total of 20 participants, predominantly middle-aged individuals. The majority of the participants, accounting for 90% of the sample, fell between the age ranges of 31-60 years. The age distribution indicates that fistulectomy procedures are predominantly carried out in individuals in the middle age spectrum, as shown in Table I. The gender distribution exhibits a significant male bias, with males constituting 75% of the participants. This might reflect either a higher incidence of fistulas in males or a greater likelihood of males undergoing surgical intervention for fistulas.

The most commonly treated type of fistulas was intersphincteric, accounting for 60% of the cases. Extrasphincteric and transphincteric fistulas had a lower occurrence rate of 25% and 15%, respectively, which aligns with their generally lower prevalence. (Table I)

The analysis of bacterial cultures indicated a significant occurrence of Escherichia coli, present in 80% of the instances. In addition, Klebsiella pneumoniae and Enterobacter aerogenes were found in 10% and 5% of cases, respectively, emphasising the fact that these illnesses are caused by several microorganisms. In one instance, there was no evidence of bacterial proliferation, indicating the possibility of either a sterile setting or effective earlier management of the infection. (Table I).

The mean haemoglobin (Hb) level was 13.465 g/dL, demonstrating moderate variability and suggesting mostly normal haemoglobin levels with a few exceptions. The total leukocyte count (TLC) exhibited significant variability, ranging from 5,460 to 13,650 cells/µL, with an average of 8690 cells/µL. This variation can be attributed to variations in immunological responses among the participants. The platelet counts varied from 0.98 to 4.10 million cells per microlitre (µL), with an average of 2.7835 million cells per µL, indicating significant variability. The mean albumin concentration was 4.105 g/dL, exhibiting a reasonably limited variation, suggesting a steady nutritional state. The levels of thyroid-stimulating hormone (TSH) showed significant variation, ranging from 1.034 to 38.160 mIU/L, with a high standard deviation. This indicates a wide range

Table I: Descriptive statistics for the study population

Variables	Categories	Frequency (N)	Range	Percent (%)	Mean	Standard deviation
Age (years)	20-30	2	26-58	10.0	43.30	10.063
	31-40	6		30.0		
	41-50	6		30.0		
	51-60	6		30.0		
Gender	Male	15	-	75.0	-	-
	female	5	-	25.0	-	-
Types of Fistula	Intersphincteric	12	-	60.0	-	-
	Extrasphincteric	5	-	25.0	-	-
	Transphincteric	3	-	15.0	-	-
C/S	E- coli	16	-	80.0	-	-
	Enterobacter aerogenes	1	-	5.0	-	-
	Klebsiella Pneumonia	2	-	10.0	-	-
	No Growth	1	-	5.0	-	-
Hb	-	-	7.3 – 15.9	-	13.465	2.1424
TLC	-	-	5460 – 13650	-	8690.00	2165.490
Plt	-	-	0.98 – 4.10	-	2.7835	0.73649
Albumin	-	-	3.4 – 4.7	-	4.105	0.3634
TSH	-	-	1.034 – 38.16	-	4.46755	8.391164
FT3	-	-	0.96 – 5.59	-	3.3945	1.08856
FT4	-	-	0.840 – 3.83	-	1.46010	0.671617
Post OP Stay (days)	-	-	5 – 10	-	7.45	1.317

Table II: Association between variables and intervention

S.no.	Variables	Categories		VAC Dressing	Traditional dressing	χ2	P-value
1	Age in years	20-30	Frequency(N)	2	0	12.659	0.002*
			% within Age category	100.0%	0.0%		
			% within INTERVENTION	20.0%	0.0%		
		31-40	Frequency(N)	6	0		
			% within Age category	100.0%	0.0%		
			% within INTERVENTION	60.0%	0.0%		
		41-50	Frequency(N)	1	5		
			% within Age category	16.7%	83.3%		
			% within INTERVENTION	10.0%	50.0%		
		51-60	Frequency(N)	1	5		
			% within Age category	16.7%	83.3%		
			% within INTERVENTION	10.0%	50.0%		
2	Gender	Male	Frequency(N)	8	7	0.267	1.00
			% within Sex	53.3%	46.7%		
			% within INTERVENTION	80.0%	70.0%		
		female	Frequency(N)	2	3		
			% within Sex	40.0%	60.0%		
			% within INTERVENTION	20.0%	30.0%		
3	Type of Fistula	Intersphincteric	Frequency(N)	7	5	2.388	0.443
			% within Type of Fistula	58.3%	41.7%		
			% within INTERVENTION	70.0%	50.0%		
		Extrasphincteric	Frequency(N)	1	4		
			% within Type of Fistula	20.0%	80.0%		
			% within INTERVENTION	10.0%	40.0%		
		Transphincteric	Frequency(N)	2	1		
			% within Type of Fistula	66.7%	33.3%		
			% within INTERVENTION	20.0%	10.0%		
4	C/S	*Escherichia coli (E- coli)*	Frequency(N)	9	7	3.739	0.334
			% within C/S	56.3%	43.8%		
			% within INTERVENTION	90.0%	70.0%		
		Enterobacter aerogenes	Frequency(N)	0	1		
			% within C/S	0.0%	100.0%		
			% within INTERVENTION	0.0%	10.0%		
		Klebsiella Pneumonia	Frequency(N)	0	2		
			% within C/S	0.0%	100.0%		
			% within INTERVENTION	0.0%	20.0%		
		No Growth	Frequency(N)	1	0		
			% within C/S	100.0%	0.0%		
			% within INTERVENTION	10.0%	0.0%		

p<0.05- Statistically significant; Test used – Chi-square/Fisher's exact test

Table III: Association between variables and intervention

	INTERVENTION	Mean	Std. Deviation	T value	df	P value
Age	VAC Dressing	36.40	8.181	4.199	18	.001*
	Traditional Dressing	50.20	6.408			
Hb	VAC Dressing	13.870	1.7745	0.839	18	.413
	Traditional Dressing	13.060	2.4852			
TLC	VAC Dressing	8969.00	1979.475	0.566	18	.579
	Traditional Dressing	8411.00	2410.069			
Plt	VAC Dressing	2.8310	.51847	0.281	18	.782
	Traditional Dressing	2.7360	.93342			
Albumin	VAC Dressing	4.100	.4243	0.060	18	.953
	Traditional Dressing	4.110	.3143			
T3	VAC Dressing	3.4690	1.09149	0.299	18	.769
	Traditional Dressing	3.3200	1.13927			
T4	VAC Dressing	1.43700	.896735	70.00#	18	0.101
	Traditional Dressing	1.48320	.383325			
TSH	VAC Dressing	5.60920	11.443195	46.00#	18	0.762
	Traditional Dressing	3.32590	3.847559			
Post OP Stay (days)	VAC Dressing	6.70	1.418	3.055	18	.007*
	Traditional Dressing	8.20	.632			

*p-value< 0.05 statistically significant; Test used: Independent t test
#Mann Whitney test was used for association

Table IV: Correlation between the study variables

INTERVENTION			Age	Hb	TLC	Plt	Albumin	TSH	Post OP Stay (days)
VAC Dressing	Age	Correlation Coefficient	1	-0.182	-0.185	0.112	-0.320	0.703*	0.385
		Sig. (2-tailed)		0.615	0.608	0.759	0.367	0.023	0.272
	Hb	Correlation Coefficient	-0.182	1	0.433	0.520	0.415	0.027	0.049
		Sig. (2-tailed)	0.615		0.212	0.124	0.233	0.941	0.893
	TLC	Correlation Coefficient	-0.185	0.433	1	0.238	0.048	-0.411	-0.265
		Sig. (2-tailed)	0.608	0.212		0.507	0.895	0.239	0.460
	Plt	Correlation Coefficient	0.112	0.520	0.238	1	0.426	0.231	0.408
		Sig. (2-tailed)	0.759	0.124	0.507		0.219	0.521	0.241
	Albumin	Correlation Coefficient	-0.320	0.415	0.048	0.426	1	-0.163	-0.074
		Sig. (2-tailed)	0.367	0.233	0.895	0.219		0.652	0.839
	TSH#	Correlation Coefficient	-0.030	0.042	-0.479	0.382	-0.080	1.000	0.629
		Sig. (2-tailed)	0.933	0.907	0.162	0.276	0.827	.	.0495*
	Post OP	Correlation Coefficient	0.385	0.049	-0.265	0.408	-0.074	0.823**	1
	Stay (days)	Sig. (2-tailed)	.272	.893	.460	.241	.839	.003	
Traditional Dressing	Age	Correlation Coefficient	1	-0.182	0.057	-0.085	-0.095	-0.140	-0.011
		Sig. (2-tailed)		0.616	0.875	0.816	0.794	0.699	0.976
	Hb	Correlation Coefficient	-0.182	1	0.220	0.068	0.517	-0.722*	0.105
		Sig. (2-tailed)	0.616		0.541	0.851	0.126	0.018	0.774
	TLC	Correlation Coefficient	0.057	0.220	1	0.823**	0.019	-0.328	-0.125
		Sig. (2-tailed)	0.875	0.541		0.003	0.959	0.355	.731
	Plt	Correlation Coefficient	-0.085	0.068	0.823**	1	-0.257	-0.070	-0.010
		Sig. (2-tailed)	0.816	0.851	0.003		0.473	0.847	0.979
	Albumin	Correlation Coefficient	-0.095	0.517	0.019	-.0257	1	-0.198	0.324
		Sig. (2-tailed)	0.794	0.126	0.959	0.473		0.584	0.361
	TSH#	Correlation Coefficient	-0.030	0.042	-0.479	0.382	-0.080	1.000	0.629
		Sig. (2-tailed)	0.933	0.907	0.162	0.276	0.827	0.	0.051
	Post OP	Correlation Coefficient	-0.011	0.105	-0.125	-0.010	0.324	-0.213	1
	Stay (days)	Sig. (2-tailed)	0.976	0.774	0.731	0.979	0.361	0.556	

*. Correlation is significant at the 0.05 level (2-tailed); **. Correlation is significant at the 0.01 level (2-tailed); Test used -Pearson Correlation; #Spearman correlation was used

Fig. 1: Post operative Fistulectomy Wound subjecting for VAC dressing and results after in chronological order

of thyroid function among the subjects. The levels of free triiodothyronine (FT3) and free thyroxine (FT4) also exhibited fluctuation, with average values of 3.3945 ng/mL and 1.4601 µg/dL, respectively. The mean duration of hospitalisation after surgery was 7.45 days, with the majority of patients staying between 5 and 10 days, suggesting that the healing process was efficient. The statistics presented here offer a thorough and fundamental overview of the research group, emphasising the range of clinical factors and the efficacy of care after surgery (Table I).

Table II illustrates noteworthy relationships and correlations between several patient features and the type of intervention administered, either Vacuum-Assisted Closure (VAC) dressing or traditional dressing. Age was found to have a significant association with the type of intervention (χ^2 = 12.659, p=0.002). Younger patients, aged 20-40 years, were more inclined to receive VAC treatment, whereas older patients, aged 41-60 years, were more commonly treated with standard dressings. The analysis revealed that gender was not significantly associated with the sort of intervention (p=1.00), suggesting that both males and females had an equal likelihood of receiving either treatment. Regarding the type of fistula, there was no statistically significant difference observed between the procedures (p=0.443). Nevertheless, *E. coli* was the predominant bacterium found in both groups, but this observation did not achieve statistical significance (p=0.334).

Further analysis, adopting independent t-tests and Mann-Whitney tests, demonstrated significant differences in age and post-operative duration between the VAC and traditional dressing populations (Table III; Table IV). The mean age of patients in the VAC group was 36.4 years, which was substantially younger compared to the mean age of 50.2 years in the traditional dressing group (p=0.001). In addition, the VAC group had a considerably lower duration of hospitalisation after surgery, with a mean of 6.7 days, compared to the standard dressing group, which had a mean of 8.2 days (p=0.007). Correlation analysis revealed a significant positive correlation (r=0.823, p=0.003) between TSH levels and post-operative stay within the VAC group. The correlation in the traditional dressing group was statistically significant at the 0.05 level. The results indicate that the use of VAC dressing is more common among younger patients and those with shorter hospital stays. Additionally, the duration of recovery may be contingent upon thyroid function in both groups. In summary, the data highlight the potential advantages of VAC dressing in decreasing hospitalisation duration and enhancing recuperation in younger individuals.

DISCUSSION

The retrospective observational study of 20 patients who underwent fistulectomy with or without the application of Vacuum-Assisted Closure (VAC) presented intriguing insights. The baseline characteristics indicated a middle-aged, predominantly male patient population with a relatively uniform duration of hospital stay. This might reflect either a higher incidence of fistulas in males or a greater likelihood of males undergoing surgical intervention for fistulas. The minor variability in age and the hospitalisation period suggests that the study outcomes can be moderately generalised for similar populations. Fistula-type distribution, as in Table I, revealed a predominance of intersphincteric fistulas. This observation is clinically significant as it indicates the most common fistula type presenting in a tertiary care setting, which could influence pre-operative planning and resource allocation.

Laboratory parameters (Table I) were within normal ranges, indicating that patients were likely in stable condition before surgery. The standard deviations, particularly in haemoglobin levels and total leukocyte count, suggest there was some heterogeneity in the patient's health status, but not significantly so. Normal albumin levels and thyroid function further suggest that patients were not systemically compromised.

The study here shows that the common organism that was isolated from the culture and sensitivity was Escherichia coli in 80% of the situations in the study population and was distributed similarly between both dressing types, along with other organisms such as *Klebsiella pneumoniae* and *Enterobacter sp.* This is consistent with the existing literature which shows *Escherichia coli, Bacteroides, Bacillus,* and *Klebsiella species* were significantly more prevalent in patients

with fistula as Acute anorectal sepsis due to colonisation of "gut-derived" microorganisms.[8] This provides insight into initiating appropriate antibiotic management for the patient. This indicates that the specific type of bacterial contamination does not affect the selection of dressing, and both Vacuum-Assisted Closure (VAC) and standard dressings are equally efficient in controlling bacterial contamination in post-operative wounds. 5% of the study population showed no growth in their culture and sensitivity; this may be due to the successful management with antibiotics or a sterile environment or even improper collection technique that may have occurred.

The NPWT dressing has a significant number of complications associated with it, that includes failure of the VAC system (loss of seal, power failure, and blockage of the drainage system), wound infection, pain, bleeding, allergies to the adhesive drape, excoriation of the skin, restricted mobility, adherence of the tissues to the foam, lack of patient compliance and skin necrosis.[9] The study reveals that the NPWT dressing was integrated in the line of management with a substantially younger population. This could be because the younger population was more compliant to this method of wound dressing as it requires patients for more extended immobilisation and would possibly hinder daily activities.

The study also points out that the patients who received treatment with VAC dressing had a significantly reduced average duration of hospitalisation (6.7 days) in comparison to those who were treated with traditional dressings (8.2 days). Reducing the length of hospital stays not only lowers the expenses directly linked to extended hospitalisation but also reduces the chances of nosocomial infections in the hospital and improves the rate at which patients are discharged. The use of NPWT creates an improved healing environment, which is characterised by greater production of granulation tissue. This is correlated with the less pain during mobilisation, improved granulation tissue formation, and faster healing rate. This indicates that Vacuum Assisted Closure (VAC) dressing creates a more conducive setting for wound repair, suggesting that VAC could be a beneficial treatment modality in fistulectomy recovery. However, the incidence of treatment compliance issues in the VAC group flags the necessity for careful patient selection and education on VAC maintenance.

The research we conducted is unique in that there were a few research articles that discussed the use of NPWT for postoperative fistulectomy wounds. The VAC dressing is renowned for its effectiveness in treating diabetic wounds. However, extensive research has also demonstrated its efficacy in other applications, making it a versatile and effective commodity. Comparison between NPWT and Conventional Wound Care after Extensive Surgical Debridement in Patients with Fournier's Gangrene illustrates the outcomes of NPWT with traditional wound care methods following surgical debridement. The study demonstrated that NPWT significantly reduced healing times and improved overall outcomes, suggesting its effectiveness in managing severe infectious conditions.[10] Similarly, a study explored the impact of traditional herbal treatments on the healing of anal fistulas post-fistulotomy. The findings indicated that herbal decoctions could enhance healing and reduce recovery time, offering a complementary approach to conventional surgical methods.[11] According to Enterocutaneous fistula treatment: case report and review of the literature, various treatment approaches for enterocutaneous fistulas were analysed, including the use of NPWT. The findings supported the efficacy of NPWT in managing complex fistulas, especially when traditional treatments failed to yield suboptimal results.[12] Furthermore, the benefits of combining less invasive surgical techniques with NPWT for the treatment of pilonidal sinus are explored for wound healing properties. The results indicated that it enhanced wound healing and reduced morbidity, offering an effective treatment modality for this challenging condition.[13]

This study is limited by its small sample size (n=20) and single-centre design, reducing generalizability. The lack of randomisation introduces selection bias, and the short follow-up prevents long-term outcome assessment. Variability in patient characteristics and uncontrolled factors like nutritional status may have influenced healing. Larger, randomised studies with extended follow-up are needed to confirm findings and assess NPWT's broader clinical and economic impact. Collectively, these results indicate that VAC is a valuable adjunct to fistulectomy recovery, underscored by improved healing rates and reduced pain. The study further validates the significance of tailoring postoperative care to patient-specific needs, especially in the management of postoperative pain. Future studies could benefit from a larger sample size to validate these findings and possibly elucidate the long-term benefits of VAC therapy post-fistulectomy.

CONCLUSION

The study concludes that middle-aged adults, with a significant male predominance, a more common intersphinteric type of fistula, suggesting that fistulas and their surgical interventions are more common in this demographic. The significant occurrence of E. coli in wound cultures emphasises the necessity for focused antibiotic treatment and efficient infection control methods, both of which are essential elements of optimal post-operative care. NPWT has shown distinct advantages compared to traditional wound treatment approaches in post-operative fistulectomy patients. Patients who had NPWT had a notably reduced duration of hospitalisation, with an average of 6 days, compared to 8 days for the control group. The decrease in hospital stay not only signifies accelerated recovery but also suggests a potential reduction in healthcare expenses and utilization of resources. Also, the group receiving NPWT reported experiencing reduced pain and discomfort while moving, which is crucial for patient adherence and overall satisfaction with the treatment. This group also showed improved production of granulation tissue and faster wound healing, facilitated by a more favourable environment for wound healing.

REFERENCES

1. Ramachandra ML, Garg M. A comparative study in the management of fistula in ANO using various modalities. Int Surg J 2018 ;5(6): 2223-7.
2. Xu Y, Liang S, Tang W. Meta-analysis of randomized clinical trials comparing fistulectomy versus fistulotomy for low anal fistula. SpringerPlus 2016; 5(1): 1722.
3. Blumetti J, Abcarian A, Quinteros F, Chaudhry V, Prasad L, Abcarian H. Evolution of Treatment of Fistula in Ano. World J Surg 2012; 36(5): 1162-7.
4. Guffanti A. Negative-pressure wound therapy and diabetic foot in the treatment of diabetic foot syndrome. Leczenie Ran 2014; 11(1): 5-9.
5. Jaiswal A, Doucette ED. How does negative pressure wound therapy (NPWT) compare with other treatments for acute surgical wounds? Evidence-Based Practice 2016; 19(9): 10.
6. Tanaydin V, Beugels J, Andriessen A, Sawor JH, van der Hulst RRWJ. Randomized Controlled Study Comparing Disposable Negative-Pressure Wound Therapy with Standard Care in Bilateral Breast Reduction Mammoplasty Evaluating Surgical Site Complications and Scar Quality. Aesth Plast Surg 2018; 42(4): 927-35.
7. Driver VR, Blume PA. Evaluation of Wound Care and Health-Care Use Costs in Patients with Diabetic Foot Ulcers Treated with Negative Pressure Wound Therapy versus Advanced Moist Wound Therapy. J Am Podiatr Med Assoc 2014; 104(2): 147-53.
8. Toyonaga T, Matsushima M, Tanaka Y, Shimojima Y, Matsumura N, Kannyama H, et al. Microbiological analysis and endoanal ultrasonography for diagnosis of anal fistula in acute anorectal sepsis. Int J Colorectal Dis 2006; 22(2): 209-13.
9. Agarwal P, Kukrele R, Sharma D. Vacuum assisted closure (VAC)/negative pressure wound therapy (NPWT) for difficult wounds: A review. Journal of Clinical Orthopaedics and Trauma 2019; 10(5): 845-8.
10. Trejo-Ávila ME, Rodríguez-Parra A, Díaz-Flores A, Arce-Lievano E, Blas-Franco M, Romero-Loera S, et al. Comparison between Negative Pressure Wound Therapy and Conventional Wound Care after Extensive Surgical Debridement in Patients with Fournier's Gangrene. Clin Surg 2017; 2(1): 1335.
11. Deng H, Zhang J, Yuan X. The Effects of Phellodendron Decoction on Wound Healing of Anal Fistula after Anal Fistulotomy. Evid Based Complement Alternat Med 2022; 2022: 7363006.
12. Assenza M, Rossi D, De Gruttola I, Ballanti C. Enterocutaneous fistula treatment: case report and review of the literature. G Chir 2018; 39(3): 143-51.
13. Nakamichi M, Ogino A, Onishi K. Less invasive treatment for the pilonidal sinus combined use of negative-pressure wound therapy. Eur J Plast Surg 2020; 43(1): 75-8.

Haematological trends and associated congenital anomalies in children with cleft lip and palate

Navin Umapathy, MD, Radha Kumar, MD, Shamikumar, MD, Vaanmathi AS, MD

Department of Paediatrics, Saveetha Medical College Hospital , SIMATS, Saveetha University

ABSTRACT

Introduction: Cleft lip and palate are prevalent congenital craniofacial anomalies affecting approximately 1 in 400 live births. These conditions result from incomplete fusion of embryonic facial processes and can lead to significant aesthetic, functional, and psychological challenges. Recent studies have suggested a possible link between cleft anomalies and haematological abnormalities. This study aimed to investigate the haematological parameters and associated anomalies in children with cleft lip and/or palate admitted for surgical repair at a tertiary care hospital.

Materials and Methods: We conducted a prospective observational study involving 100 children with cleft lip and/or palate admitted between January and December 2023. Demographic data, haematological parameters (including haemoglobin, white blood cell count, and platelet count), and associated anomalies were recorded and analysed using JAMOVI software.

Results: The mean haemoglobin levels were 10.2 g/dL in cleft lip, 11.3 g/dL in cleft lip and palate, and 9.98 g/dL in cleft palate alone. Anaemia was observed in 12 children with cleft lip alone, 1 with both cleft lip and palate, and 12 with cleft palate alone. Elevated total leucocyte counts were noted in children with cleft lip and palate. Associated anomalies included Pierre Robin sequence (3%), ventricular septal defect (4%), and renal anomalies (4%). Malnutrition was detected in five children.

Conclusion: Anaemia and leucocytosis are common in children with cleft lip and/or palate. Comprehensive nutritional support and regular monitoring of haematological parameters are crucial for improving surgical outcomes and overall health in these patients.

KEYWORDS:
Cleft lip, cleft palate, anemia, leucocytosis, associated anomalies, hematological parameters

INTRODUCTION

Cleft lip and palate occur due to non-fusion of the nasal process with the palatal process during embryonic development in utero. Cleft lip/palate represents one of the most common craniofacial congenital anomalies worldwide, affecting nearly 1 in 400 live births.[1] The root cause of Cleft lip and palate is complex, involving some genetic and environmental factors. Despite advancements in surgical techniques and interdisciplinary care, children with Cleft lip/palate often face a variety of challenges, including aesthetic, functional, and psychological issues.

The in-utero development of the human lip occurs during the 4th to 8th week of gestation, and the palatal process forms between the 6th and 9th weeks of gestation.[2] The cleft in lip occurs due to maldevelopment of the mesenchymal layer, in which non-fusion of medial nasal and maxillary processes is noted, while the cleft in palate is seen because of non-fusion of palatal processes. A cleft lip is noted to have different presentations varying from a small notch in the vermilion border to a complete separation involving skin, mucosa, tooth and bone (Figure I). It can be unilateral, common on the left side or bilateral, or may involve the alveolar ridge.[5] Sometimes it is seen in the midline affecting only the uvula in case of isolated cleft palate, or may deepen into or through the palate till the incisive foramen.[2] When cleft palate is associated with cleft lip, the defect is noted involving the midline of the soft palate, hard palate, one or both sides, leading to exposure of the nasal cavities.

In recent years, there has been growing interest in exploring the potential association between Cleft lip/ palate and haematological abnormalities. Several articles have proved arise in the incidence of haematological abnormalities in individuals with Cleft lip and palate compared to the general population. These abnormalities may include variations in red blood cell indices, such as haemoglobin levels and mean corpuscular volume, as well as alterations in white blood cell counts and platelet counts.[5]

Though cleft anomalies are being diagnosed through anomaly scan in the antenatal period, since isolated cleft lip or palate has a good prognosis, many parents continue pregnancy as isolated cleft lip or palate is a correctable defect and has a good prognosis.[8] Cleft lip/palate is associated with many syndromes like Van der Woude syndrome, Pierre Robin sequence, Velocardiofacial syndrome, Median facial dysplasia, Trisomy 13/18, etc.[3] After birth, babies have certain issues like difficulty in feeding, poor weight gain, nutritional anaemia, ear infections, upper respiratory tract infections, etc. Also, babies have other non-syndrome associated cardiac defects like Ventricular Septal Defect, Tetralogy of Fallot, transposition of the great vessels, hearing defects, and cataracts.[4] Hence, we wanted to study the blood parameters and congenital anomalies associated with cleft lip and palate admitted in our tertiary care hospital and assess their incidence rates along with complications.

This article was accepted: 05 August 2025
Corresponding Author: Navin Umapathy
Email: navinu02@gmail.com

Table I: Mean and standard deviation of haematological parameters

	CLEFT lip/palate	HB	TLC	RBC	PLT
N	lip	49	49	49	49
	lip/palate	7	7	7	7
	palate	44	44	44	44
Mean	lip	10.2	11207	4.71	3.43
	lip/palate	11.3	14049	4.94	4.37
	palate	9.98	11252	4.65	3.64
Median	lip	10.6	10380	4.80	3.50
	lip/palate	11.0	14650	4.81	4.48
	palate	10.5	10972	4.80	3.50
Standard deviation	lip	2.00	3424	0.662	0.737
	lip/palate	1.60	2989	0.254	0.720
	palate	1.92	3297	0.722	0.719

Note: HB-Haemoglobin, TLC- Total Leucocyte Counts, RBC-Red Blood Cells, PLT-Platelates

Table II: Associated anomalies/conditions with cleft lip/palate children

Associated anomalies/conditions	No. of children affected
Pierre robin sequence	3 (3%)
Dysmorphic facies	2 (2%)
Ventricular septal defect	4 (4%)
Severe acute malnutrition	3 (3%)
Moderate acute malnutrition	2 (2%)
Hearing defect	2 (2%)
Eye defects (cataract)	1 (1%)
Renal anomalies (PUV/VUR/HUN)	4 (4%)

MATERIALS AND METHODS

All children with cleft lip and palate admitted to the Paediatric ward under plastic surgery for surgical repair through the Smile Train programme in our hospital are enrolled in our study. A prospective observational study involving 100 children was conducted during the period from January 2023 to December 2023, and the data collected were tabulated in an Excel data sheet. After obtaining informed consent from parents, children with cleft lip/palate were enrolled, necessary history was collected, general and systemic examination was done, baseline blood investigations were sent as part of the Smile Train programme, cardiac evaluation involving ECG and echocardiogram was done along with cardiologist opinion and fitness for surgical repair. Meanwhile, specific issues like URTI, fever, aspiration, etc, are addressed and treated accordingly. All primary data, including antenatal history, delivery details, postnatal issues, anthropometry details, weight gain, associated anomalies, feeding difficulties and current complications, are collected and tabulated. Based on the data collected, a prospective observational study was done.

Inclusion criteria - Those children affected with cleft lip or palate admitted to our hospital during the study period.

Exclusion criteria - Those children whose parents are not willing to participate in study.

Statistical analysis

All Data were collected in an Excel sheet, formulated and tabulated. Data collected were analysed using JAMOVI software, the latest version 2.3.

RESULTS

In our study, we collected demographic and haematological data, analysed using JAMOVI software. In our study population, we had 50 female children (cleft lip, n=26, cleft palate, n=21, both cleft lip and palate, n=3) and 50 male children (23 had cleft lip, 23 had cleft palate, four had both). Mean birth weight was 2.74±0.35kg (Figure II). Mean birth weight was the same among the study population, and it does not show any significance related to mean haemoglobin and total counts. In our study group, 22 children were born out of consanguineous marriages, while 78 were born to non-consanguineous couples. While assessing the classification of cleft lip and palate, we found that 21 children had bilateral cleft lip, 35 children had unilateral cleft lip, 29 children had complete cleft palate, and 22 had incomplete cleft palate.

Haematological parameters (Table I) were analysed, which showed mean haemoglobin (in g%) of 10.2±2.0 (cleft lip)(Figure III), 11.3±1.60 (cleft lip and palate), 9.98±1.92 (cleft palate). Mean total leucocyte counts (Figure IV) (counts/mm3) of 11,207±3,424 (cleft lip), 14,049±2,989 (cleft lip and palate), 10,972±3,297 (cleft palate). Children had mean RBC counts (mill/mm3) of 4.71±0.66 (cleft lip), 4.94±0.25 (cleft lip and palate), and 4.65±0.72 (cleft palate). Mean platelet counts (lakhs/mm3) were noted as 3.43±0.73 (cleft lip), 4.37±0.72 (cleft lip and palate), and 3.64±0.71 (cleft palate). Mean haemoglobin among children born to consanguineous marriage is 10.4±2.65g% and 10.1±1.72g% among children born to non-consanguineous marriage. No significant difference in mean total counts among children of consanguineous and non-consanguineous marriages. (T-test applied, p-value <0.05).

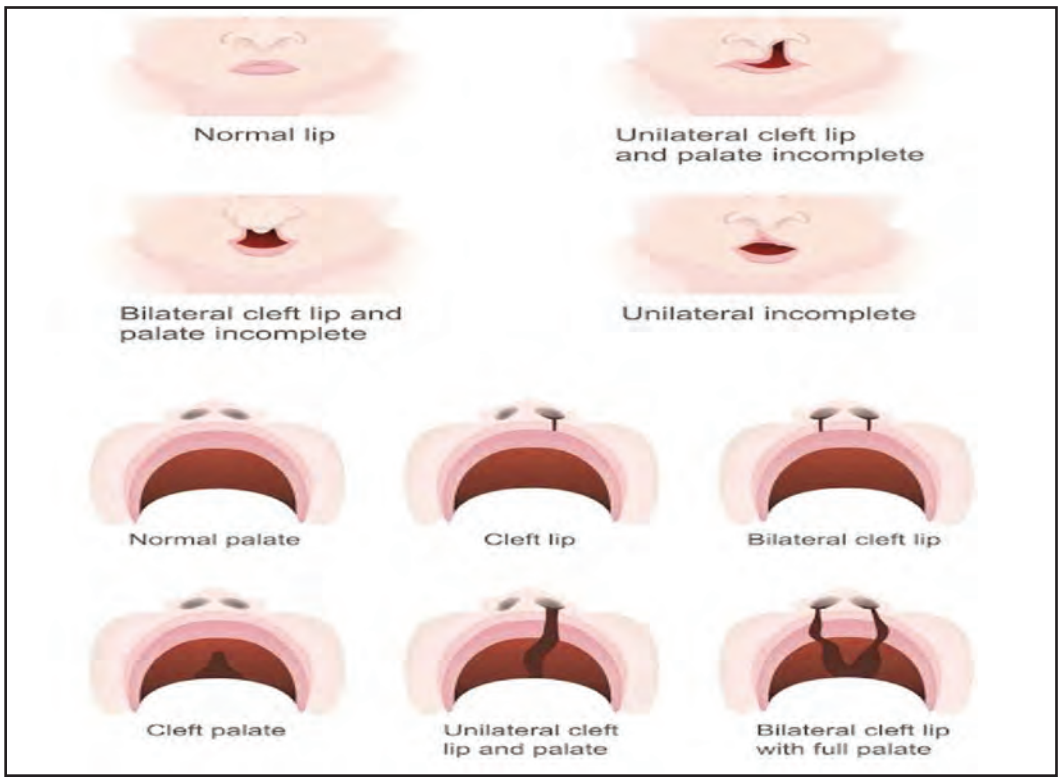

Fig. 1: Topographical classification of cleft lip and palate

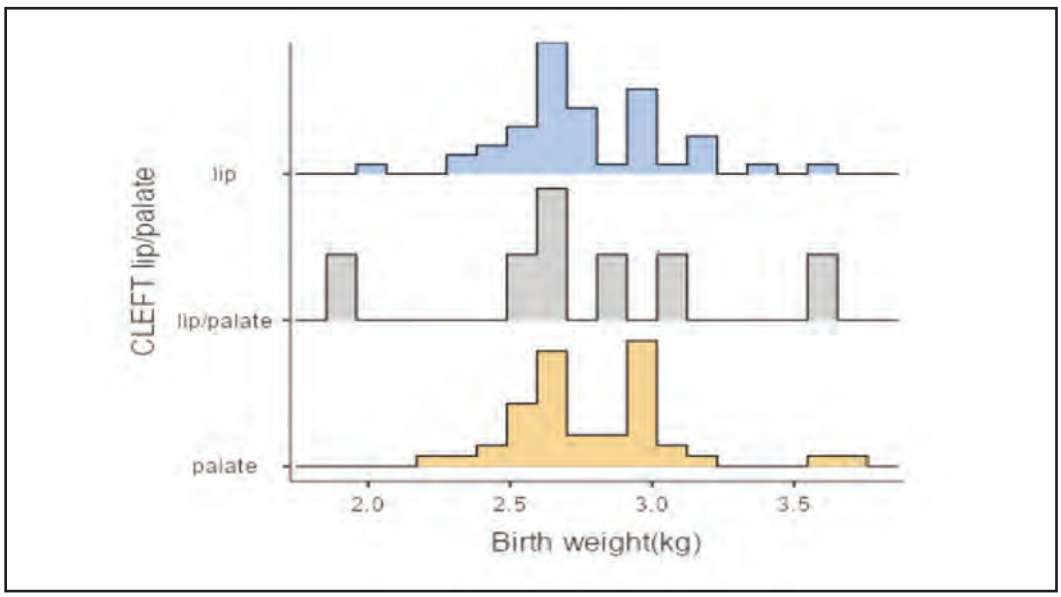

Fig. 2: Depiction of birth weight distribution among study population

We could not detect any significant difference (using ANOVA test) in blood parameters among children with cleft lip alone, cleft lip and palate, and Cleft palate alone ($p<0.05$). But anaemia was noted in 12 children with cleft lip alone, one child with both cleft lip and palate, and 12 children with cleft palate alone. There were also higher values of total leucocyte counts noted in children affected with both cleft lip and palate.

Apart from haematological parameters, three children had Pierre Robin sequence, four children had a ventricular septal defect, two children had Dysmorphic facies, two children had hearing defects, one child had congenital cataract, and four children had renal anomalies. Five children are malnourished (three with Severe acute malnutrition and two with Moderate acute malnutrition) based on anthropometry data. A total of 12 children were syndromic in our study population, of which 9 (75%) were anaemic and 11(87%) had elevated total counts.

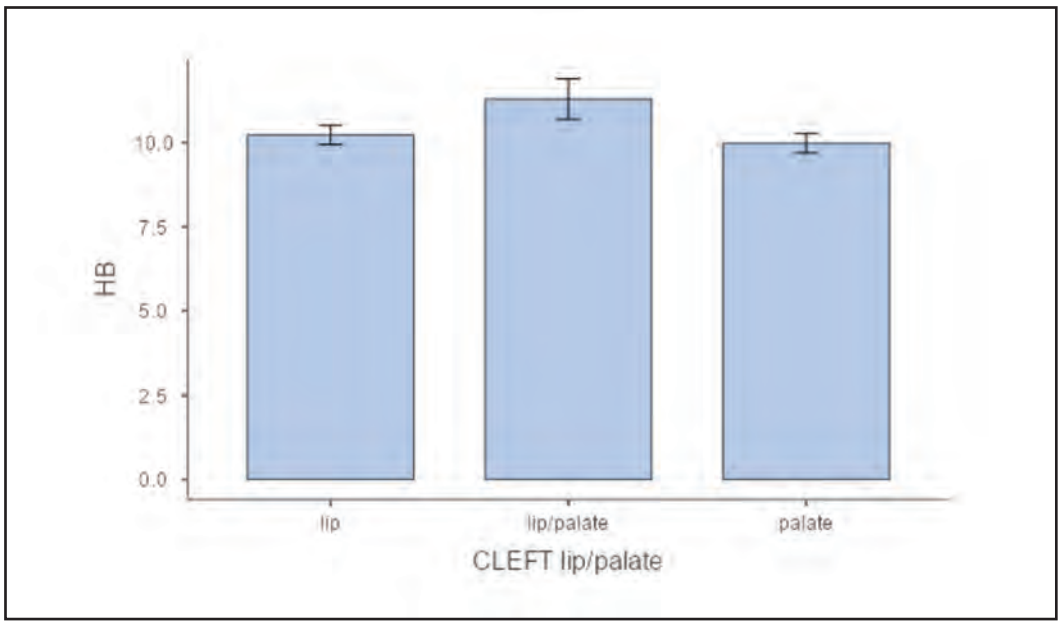

Fig. 3: Mean haemoglobin among the study population

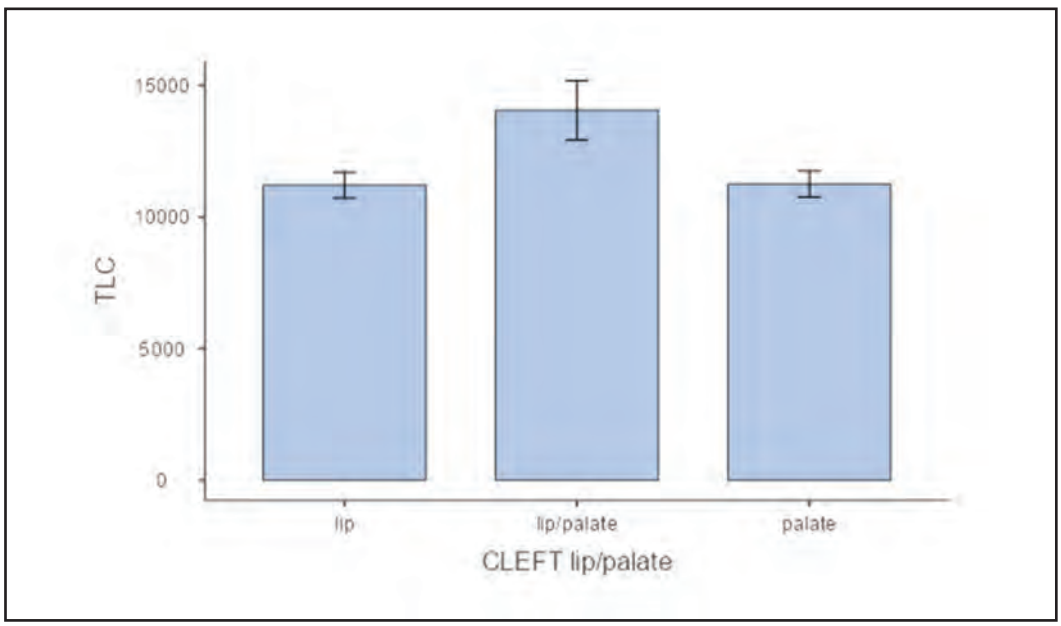

Fig. 4: Mean TLC values among the study population

DISCUSSION

Since we have a good number of children admitted for cleft lip and palate repair, we want to study the haematological trends and other associated anomalies among them. Since many studies have been done so far in various centres, we want to explore the characteristics of cleft lip/ palate children being operated on in our health centre. Previous similar studies have reported the incidence of anaemia as a major concern in children affected with cleft lip and palate.[3] Similarly, about 25% of our study group had anaemia, which poses a serious problem because cleft lip has been operated on at 3-5 months of age. Anaemia becomes a major threat to fitness for surgery. Both anaemia of infancy and nutritional anaemia (due to poor feeding tolerance in cleft lip/palate) hit these children at the same time.[6]

In a study done by Lin et al, stated that thrombocytosis and leucocytosis were typically noted in the majority of children with cleft lip and palate with both cleft lip and palate.[1] Similarly, our study results show that leucocytosis occurs in a portion of the population, particularly in children with both cleft lip and palate. It is believed to be due to micro aspiration via cleft defect into the airway while feeding the babies. These prolonged microaspirations can lead to activation of the immune system by a rise in TLC and platelets. But in our study, we did not notice any thrombocytosis in children. In a study by Singhal et al, it was concluded that the majority of their study population with cleft defect had eosinophilia in blood, but the possible reason was mentioned to be allergic response in their dwelling place –Uttarakhand.[2,11] In our study, none of the children had eosinophilia. Also, certain

studies have shown some syndromes like Downs, Robert syndrome, and Pierre Robin syndrome are commonly associated with cleft defects in children.[5] In our study, three children had Pierre Robin sequence, two children had Dysmorphic facies and four children had renal anomalies. Further Syndromic association needs a large sample size and extensive research in children with cleft defects. Hence, early anticipation, cause for such anomalies, and adequate counselling of parents can be done for a better outcome of the child in future.

CONCLUSION

From our study, we conclude that anaemia and Leucocytosis are common haematological findings noted in children with cleft lip/palate. Certain anomalies like retrognathia (Pierre Robin sequence), renal anomalies and dysmorphic facies are noted among them. We also encountered malnutrition in our study population. Since our entire study population belongs to the lower socio-economic class, it may be a confounding factor for anaemia and malnutrition. We strongly suggest that adequate antenatal counselling, proper nutritious diet, proper feeding solutions in cleft defective children and regular blood workup before surgical correction of cleft defect are essential for all children affected with cleft lip/palate. In case of the above factors being rectified, post-surgical correction, almost all children affected with cleft lip/palate can lead a near-normal life.

REFERENCES

1. Lin CH, Lo LJ, Wang ML, Chen YR, Noordhoff MS. Major hematological diseases associated with cleft lip and palate. Cleft Palate Craniofac J 2000; 37(5): 512-5.
2. Singhal S, Negi G, Chandra H, Chandra S, Gaur DS, Rajan M. Hematological parameters in patients of cleft lip and cleft palate with special reference to eosinophil counts. J Craniofac Surg 2014; 25(1): 103-5.
3. Venkatesh R. Syndromes and anomalies associated with cleft. Indian J Plast Surg 2009; 42 Suppl(Suppl): S51-5. .
4. Shprintzen RJ, Siegel-Sadewitz VL, Amato J, Goldberg RB. Anomalies associated with cleft lip, cleft palate, or both. Am J Med Genet 1985; 20(4): 585-95.
5. Chattopadhyay D, Vathulya M, Naithani M, Jayaprakash PA, Palepu S, Bandyopadhyay A, Kapoor A, Nath UK. Frequency of anemia and micronutrient deficiency among children with cleft lip and palate: a single-center cross-sectional study from Uttarakhand, India. Arch Craniofac Surg 2021; 22(1): 33-7.
6. Eley KA, Goodacre TE. Are routine pre-operative blood tests required in children undergoing primary cleft lip and/or palate repair? J Plast Reconstr Aesthet Surg 2010; 63(6): 926-9.
7. Setó-Salvia N, Stanier P. Genetics of cleft lip and/or cleft palate: association with other common anomalies. Eur J Med Genet 2014; 57(8): 381-93.
8. Bergé SJ, Plath H, Van de Vondel PT, Appel T, Niederhagen B, Von Lindern JJ, et al. Fetal cleft lip and palate: sonographic diagnosis, chromosomal abnormalities, associated anomalies and postnatal outcome in 70 fetuses. Ultrasound Obstet Gynecol 2001; 18(5): 422-31.
9. Stanier P, Moore GE. Genetics of cleft lip and palate: syndromic genes contribute to the incidence of non-syndromic clefts. Hum Mol Genet. 2004;13(1): R73-81.
10. Precious DS, Goodday RH, Morrison AD, Davis BR. Cleft lip and palate: a review for dentists. J Can Dent Assoc 2001; 67(11): 668-73.
11. Dvivedi J, Dvivedi S. A clinical and demographic profile of the cleft lip and palate in Sub-Himalayan India: A hospital-based study. Indian J Plast Surg 2012; 45(1): 115-20.
12. Bessell A, Hooper L, Shaw WC, Reilly S, Reid J, Glenny AM. Feeding interventions for growth and development in infants with cleft lip, cleft palate or cleft lip and palate. Cochrane Database Syst Rev 2011; 2011(2): CD003315.
13. Peña-Soto C, Arriola-Guillén LE, Díaz-Suyo A, Flores-Fraile J. Clinical and epidemiological profile of cleft lip and palate patients in Peru, 2006 - 2019. J Clin Exp Dent 2021; 13(11): e1118-23.

ORIGINAL ARTICLE

Role of foot length in predicting the gestational age of a neonate

Sai Lakshmi Ananya Tenali, MD paediatrics[1], Shami Kumar RP, DNB pediatrics[2], Navin Umapathy, MD pediatrics[2]

[1]Department of Pediatrics and Neonatology, A.C.S. Medical College and Hospital, Chennai, Tamil Nadu, India, [2]Department of Pediatrics, Saveetha medical college hospital, SIMATS, Saveetha University, Chennai, Tamil Nadu, India

ABSTRACT

Introduction: The aim was to study neonatal foot length as a simple method for quick gestational age assessment, which can be done by basic health care personnel, overcoming the technicality required by other assessment methods.

Materials and Methods: A Prospective descriptive study was done. Live-born neonates at Saveetha Medical College and Hospital, Chennai, were enrolled. Gestational age was assessed by New Ballard's Scoring (NBS), and foot length (FL) was measured using the paddle blades of automated digital Vernier callipers within 24 hours, while birth weight was taken within 72 hours of birth. Based on gestational age, babies were grouped into preterm, term and post term and were sub-classified as small for gestational age (SGA), appropriate for gestational age (AGA) and large for gestational age (LGA) based on Lubchenco's intrauterine growth chart. Correlation and regression analysis with a Scatterplot was done.

Results: Out of 150 neonates, term, preterm and post-term were70.3%,28.4%and1.3% while SGA, AGA, and LGA babies were11%, 85% and 4%. respectively. Mean foot length was7.588±0.57. With a range of 5.2-8.4cm. Foot length strongly correlated with gestational age in Preterm AGA, preterm SGA and Term AGA babies (<0.05). The correlation coefficient between foot length and gestational age was higher in preterm babies (R2=0.56) and SGA babies (R2=0.66). Gestational age in 53% of the total study population could be predicted with a regression equation.

Conclusions: Foot length may be useful for quick estimation of gestational age in preterm and term neonates for early referral of newborns requiring special care, and can even be done by basic healthcare personnel.

KEYWORDS:
Foot Length, Gestational Age, Neonate, New Ballard Score, Preterm, Birth Weight

INTRODUCTION

The most vulnerable time for an infant is the first 28 days after birth, which is the neonatal period.[1] It is a known fact that gestational age assessment is challenging and often not available for children born in small towns and rural areas. Few studies have shown that the foot length (FL) of newborns can be used as a simple, feasible technique in detecting high-risk neonates, which makes faster referral to a higher centre for further management. As per the World Health Organization (WHO), nearly 46% of under-five mortality is seen in the neonatal period of life.[2] The majority of neonatal deaths are due to complications secondary to prematurity(43.7%) in our country.[3] Gestational age (GA) is defined as the period from day one of the Last Menstrual Period (LMP) and the day of delivery by the American Academy of Paedaitrics (AAP).[4] GA is described and termed as preterm, term, and post-term. Newborns with GA of <37 completed weeks are Preterm, while Term neonates are born in between 37 weeks to 41 weeks. Babies born after 42 completed weeks of gestation are considered Postterm.[5,6] Furtherly, all neonates can be grouped into Appropriate for Gestational Age (AGA), Small for Gestational Age (SGA) and Large for Gestational Age (LGA) by weight-based classification. Growth charts commonly used for neonates are Lubchenco and Fenton's charts. SGA is <10thcentile and LGA is >90thcentile.[6]

Gestational age plays a crucial role in planning the management and prognosis for neonates. The follow-up schedule of babies also depends on their gestational age at birth. Gestational age is calculated by Naegele's formula, antenatal ultrasound, and by the New Ballard scoring system normally.[7,8] Each method has its own limitations. Naegele's formula was less reliable in places where there is a low literacy rate among pregnant mothers and less awareness of the pattern of ovulation and breastfeeding. Antenatal Ultrasound is the most reliable method for GA calculation, but can be a constraining factor in itself in places where not all pregnant women follow the mandatory antenatal visits and scans in developing countries like India. The New Ballard Score (NBS) assessment is considered one of the definitive methods for assessing gestational age in neonates. The accuracy of NBS is highly subjective and completely relies on the clinical evaluation of the physician and the general status of the newborn, especially in babies with asphyxia.[5] Anthropometric parameters, like birth weight, are generally used to assess intra-uterine growth in newborns, which fairly correlates with gestational age and maturity. A limitation is that birth weight is significantly affected by changes in the neonate's physiological state, including hydration, carbohydrate, fat, protein, and mineral levels.

This article was accepted: 08 August 2024
Corresponding Author: Shami Kumar RP
Email: drshamiich@gmail.com

Postnatal measurement of foot length is a recently used method to assess gestational maturity in neonates. Studies have shown that newborn foot length shows the least variation among anthropometric parameters in babies with foetal growth restriction.[9]

Pertemps possess a greater risk of morbidity, so they were termed as high-risk babies. Early detection of high-risk neonates in peripheral medical centres and community-level hospitals can reduce neonatal morbidity and mortality to a greater extent. When neonates require intensive care, an exact assessment of gestational maturity may not be possible at all times. Hence, the baby's foot is an easily accessible parameter for GA calculation and does not require specialised training.

Therefore, it is useful to conduct a study to determine whether foot length can be used as a simple, easy, and reliable method for estimating neonatal gestational age and to help in the effective management of babies requiring intensive care.

MATERIALS AND METHODS

This is a prospective observational study conducted at Saveetha Medical College and Hospital from April 2023 to January 2024.

Inclusion criteria were live neonates born in our hospital during the study period.

Exclusion criteria were babies with any physical deformities involving the foot, legs and chromosomal defects.

Newborn babies were enrolled in our study after obtaining parental consent. The neonates were examined strictly with an aseptic protocol, and the foot length of the baby was calculated from the most prominent surface of the baby's left foot to the tip of the great toe with the help of the paddle blades of a Vernier calliper (automated and digital). Those measurements were recorded in centimetres(cm), including decimals. For all babies, foot length was calculated only in the left foot by day one of life. The Birth Weight of the neonates was measured using a digital scale (CIBI) with ±5g accuracy immediately after birth. Along with Weight and foot length, basic details of neonates such as date of birth, APGAR score at one minute and five minutes, gestational age by both Naeglis formula and NBS were documented in a preformed data sheet. According to data entered, newborns were classified into (<37weeks) preterm, (37-42weeks) term and (>42weeks) post-term term which is further sub-classified into LGA/AGA/SGA using the Lubchenco chart.[10]

All data were collected and recorded in an Excel sheet. Correlation and Regression Analysis, along with a Scatter plot, were done using SPSS Software version 17. It was considered statistically significant if $p<0.05$.

RESULTS

The study examined 150 newborns to understand how foot length correlates with gestational age and birth weight. Among the newborns, 54% were male, and 46% were female, with 85% classified as AGA babies, 11% as SGA babies, and 4% as LGA babies. The mean Foot Length in centimetres (cm) in our study was 7.728±0.59, with Term babies showing a mean of 7.94±0.42, preterm 7.53±0.55, and post-term 8.39±0.29.

In preterm newborns, foot length correlated well with birth weight in both SGA ($p=0.030$) and AGA ($p<0.001$) groups, whereas in term neonates, this correlation was observed only in AGA babies ($p<0.001$). In terms of newborns, correlation of foot length to gestational age was present only for AGA ($p<0.001$) babies, while significant correlation of foot length to GA was seen in both preterm SGA ($p=0.005$) and AGA ($p<0.001$) infants. (Table I, Figure 1)

We found that gestational age, as assessed with the Ballard score, correlates well with both birth weight and foot length in preterm AGA and SGA neonates ($p<0.05$). Whereas with term newborns, we find that GA shows significant correlation with both birth weight and foot length only in AGA babies. (Table II)

The linear regression analysis provided an equation for predicting gestational age from foot length, which is Gestational Age=20.79+2.14×(Foot Length). Here, 21.79 is the constant and 2.14 is the slope, indicating that each additional centimetre in foot length corresponds to an increase of about 2.14 weeks in gestational age.

In our study, the regression equation derived prognosticates the gestational age by 53% of the overall study population and strongly predicts gestational age in 56% of preterm and 66% of SGA babies. (Table III)

Table I: Correlation of foot length with birth weight and gestational age

Pair	Preterm		Term		
	SGA (p-value)	AGA (p-value)	SGA (p-value)	AGA (p-value)	LGA (p-value)
Foot length to birth weight	0.679(0.030)	0.478(<0.001)	0.272(0.272)	0.459(<0.001)	0.133(0.789)
Foot length to gestational age	0.789(0.005)	0.626(<0.001)	0.211(0.420)	0.370(<0.001)	0.346(0.459)

p-value less than 0.05 is considered significant; (SGA-Small for gestational age, AGA-Appropriate for gestational age, LGA-Large for gestational age)

Table II: Correlation of gestational age with birth weight and foot length

Pair	Preterm		Term		
	SGA (p-value)	AGA (p-value)	SGA (p-value)	AGA (p-value)	LGA (p-value)
Gestational age to birth weight	0.850(0.003)	0.688(0.000)	0.380(0.117)	0.355(<0.001)	0.662(0.106)
Gestational age to foot length	0.789(0.005)	0.616(<0.001)	0.213(0.430)	0.392(<0.001)	0.346(0.431)

p-value less than 0.05 is considered significant ; (SGA-Small for gestational age, AGA-Appropriate for gestational age, LGA-Large for gestational age)

Table III: Regression analysis of each category among neonates

Variables	Regression equation (y)	R^2 value
Overall	20.79+2.14(FL)	0.535
Preterm	19.596+1.539(FL)	0.56
Term	32.664+0.716(FL)	0.13
Post term	42.153+0.120(FL)	0.446
Weight for gestational age		
SGA	11.340+2.544(FL)	0.662
AGA	22.242+1.897(FL)	0.519
LGA	8.608+2.821(FL)	0.473

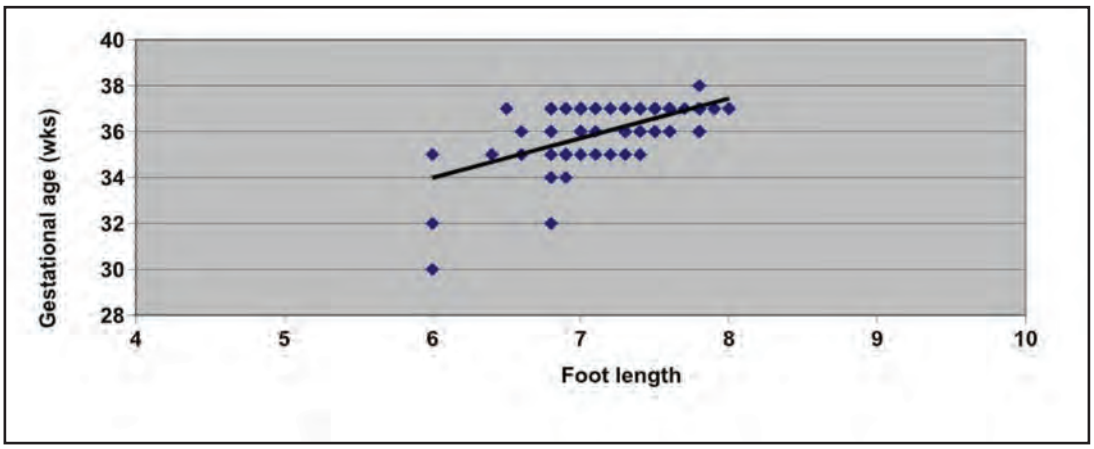

Fig. 1: Scatter plot of the Correlation between Foot length and Gestational age in Preterm

DISCUSSION

In the current study, the distribution of term newborns was 11% SGA, 85% AGA, and 4% LGA, while for preterm newborns, the distribution was 11% SGA, 88% AGA, and 1% LGA. Comparatively, Srivastava et al. reported that term newborns were 75% AGA and 24.7% SGA, whereas preterm newborns were 74% AGA and 24% SGA.[11] Shah et al. found newborns (term) to be 78.4% AGA, 12.5% SGA, and 2% LGA.[12] Due to the small size of the post-term group, it was not included in the correlation analysis.

Although all studies indicate a linear relationship between foot length and gestational age, the correlation coefficients vary across studies. The strength of this correlation varies across gestational age groups. James et al., reported an upward linear connection between foot length and for both AGA and SGA babies across all gestational ages, with particularly strong correlations observed in preterm, similar to the findings in the current study, with significant correlation of foot length with gestational age in Preterm AGA, preterm SGA and Term AGA babies (<0.05).[13]

Gohil et al., also found notable relationships between foot length and birth weight in both term and preterm neonates.[14] However, while Nabiwemba et al., study demonstrated a notable connection between foot length and birth weight in term SGA and AGA babies, the present study found a strong interrelation between foot length and birth weight only in term AGA babies.

While a positive interrelation between foot length and measures such as GA and birth weight was observed across all domains, both James et al. and Nabiwemba et al., studies, as well as the present study, noted a stronger correlation in preterm babies.[13,15]

In this study, the ability to prognosticate GA using foot length via the regression equation was 53% (R^2=0.535) for the overall population, with 56% accuracy in preterm infants and 66% in SGA babies. In contrast, Nimii et al., reported a prediction accuracy of 65% (R^2=0.65), and Wyk et al. reported 76% (R^2=0.765).[16-18]

This study has its own limitations, as it was conducted in a single hospital centre, and the number of neonates varied across gestational age categories. Although obstetric dating was performed using Naegele's formula, there remains a possibility of inaccuracies in estimating gestational age, leading to either overestimation or underestimation. Thus, the results may affect the applicability of the study findings to the general population. Hence, multi-centric, community-based studies may be necessary for further validation.

CONCLUSION

In conclusion, foot length is a practical alternative for assessing gestational age, particularly in preterm neonates and term AGA babies. It is a straightforward measurement that does not require specialised training, making it a valuable tool for early identification and timely referral of

newborns who may need specialised newborn care. Further study in large populations and various medical centres is the scope for future research.

ACKNOWLEDGMENTS
None

REFERENCES

1. Ananth CV. Menstrual versus clinical estimate of gestational age dating in the United States: temporal trends and variability in indices of perinatal outcomes. Paediatr Perinat Epidemiol 2007; 21 Suppl 2(s2): 22-30.
2. Newborn mortality [Internet]. World Health Organization; [cited 2025 Nov 4]. Available from: https://www.who.int/news-room/fact-sheets/detail/newborn-mortality
3. Sankar MJ, Neogi SB, Sharma J, Chauhan M, Srivastava R, Prabhakar PK, et al. State of newborn health in India. J Perinatol 2016; 36(s3): S3-8.
4. Engle WA, American Academy of Pediatrics Committee on Fetus and Newborn. Age terminology during the perinatal period. Pediatrics 2004; 114(5): 1362-4.
5. Gabriel M, Moreiras M, Fleixas L, Gallego D, Alonso P, Bértolo C, et al. Valoración del test de Ballard en la determinación de la edad gestacional. An Pediatr (Barc) 2006; 64(2): 140-5.
6. Lee AC, Panchal P, Folger L, Whelan H, Whelan R, Rosner B, et al. Diagnostic accuracy of neonatal assessment for gestational age determination: A systematic review. Pediatrics 2017;140(6): e20171423.
7. Stevenson A, Joolay Y, Levetan C, Price C, Tooke L. A comparison of the accuracy of various methods of postnatal Gestational Age estimation; Including Ballard score, foot length, vascularity of the anterior lens, last menstrual period and also a clinician's non-structured assessment. J Trop Pediatr 2021; 67(1): fmaa113.
8. Tikmani SS, Brown N, Inayat A, Mårtensson A, Saleem S, Mårtensson T. Diagnostic accuracy of footlength measurement for identification of preterm newborn in rural Sindh, Pakistan. BMJ Paediatric Open 2024; 8(1): e002316.
9. Folger LV, Panchal P, Eglo vitch M, Whelan R, Lee AC. Diagnostic accuracy of neonatal foot length to identify preterm and low birthweight infants: a systematic review and meta-analysis. BMJ Glob Health 2020; 5(11): e002976.
10. Lubchenco Lo, Hansman C, Dressler M, Boyd E. Intrauterine Growth As Estimated From Liveborn Birth-Weight Data At 24 To 42 Weeks Of Gestation. Pediatrics 1963 Nov; 32: 793-800.
11. Cutland CL, Lackritz EM, Mallett-Moore T, Bardají A, Chandrasekaran R, Lahariya C, et al. Brighton Collaboration Low Birth Weight Working Group. Low birth weight: Case definition & guidelines for data collection, analysis, and presentation of maternal immunization safety data. Vaccine 2017; 35: 6492-500.
12. Tergestina M, Chandran S, Kumar M, Rebekah G, Ross BJ. Foot length for gestational age assessment and identification of high-risk infants: A hospital-based cross-sectional study. J Trop Pediatr 2021; 67(4): fmab010.
13. James DK, Dryburgh EH, Chiswick ML. Foot length--a new and potentially useful measurement in the neonate. Arch Dis Child 1979; 54(3): 226-30.
14. Gohil JR, Sosi M, Vani SN, Desai AB. Footlength measurement in the neonate. Indian J Pediatr 1991; 58(5): 675-7.
15. Nabiwemba E, Marchant T, Namazzi G, Kadobera D, Waiswa P. Identifying high-risk babies born in the community using foot length measurement at birth in Uganda: Predicting at-risk newborns using foot length. Child Care Health Dev 2013; 39(1): 20-6.
16. Niimi S, Kimura T, Saiki R, Kanda H, Okamatsu Y, Goto M, et al. Estimated gestational age from infant's foot length in Japanese. Cureus 2022; 14(12): e32991.
17. Wyk LV, Smith J. Postnatal Foot Length to Determine Gestational Age: A Pilot Study. J Trop Pediatr 2016; 62(2): 144-51.
18. Dagnew N, Tazebew A, Ayinalem A, Muche A. Measuring newborn foot length to estimate gestational age in a high risk Northwest Ethiopian population. PLoS One 2020; 15(8): e0238169.

ORIGINAL ARTICLE

Electrocardiographic changes in Chronic Obstructive Pulmonary Disease and its correlation with airflow limitation

Dhanush Balaji, MD, Abhinaya Srinivasa Rangan, MD, Karpaka Vinayakam Gopalakrishnan, MBBS, Raghunathan EG, MD, Prasanna Karthik, MD, Selva Balaji, MD

Department of General Medicine, Saveetha Medical College Hospital, Saveetha Institute of Medical and Technical Sciences, Chennai, India

ABSTRACT

Introduction: Chronic obstructive pulmonary disease (COPD) is the third most prevalent cause of death in India. In 2012, over 3 million people succumbed to COPD, accounting for 6% of global deaths. COPD is the second most common respiratory disease after pulmonary tuberculosis. Early identification of cardiac manifestations may guide clinicians in implementing timely interventions to manage both the respiratory and cardiac aspects of COPD. This study aims to analyse the ECG changes in COPD patients and their correlation with airflow restriction.

Materials And Methods: This cross-sectional observational prospective study was conducted on 50 patients with COPD at Kurnool Medical College for a period of two years from December 2019 to June 2021. The ECG was recorded using a spectrophotometer.

Results: The most frequent ECG abnormalities were RS in V6 (60%), Incomplete Right Bundle Branch Block (40%), and Right Axis Deviation of QRS (34%). The correlation analysis demonstrated significant associations between specific electrocardiographic changes and FEV1/FVC ratio. The P wave axis, QRS, P wave height, R V6 height, and RBBB showed statistically significant correlations with FEV1.

Discussion: Our findings highlight the prevalence of electrocardiography changes in chronic obstructive pulmonary disease patients, with specific ECG anomalies demonstrating a correlation with the severity of both COPD and pulmonary functional impairment. Further research is warranted to validate these associations and explore their implications for clinical management.

KEYWORDS:
COPD, ECG, AIRFLOW, EMPHYSEMA

INTRODUCTION

Chronic obstructive pulmonary disease (COPD) is characterised as a disease stage featuring irreversible airflow limitation, with anatomical manifestations such as emphysema, involving the destruction and elaboration of lung alveoli; chronic bronchitis, marked by persistent cough and phlegm; and small airway disease, resulting in the contraction of small bronchioles—each representing instances of COPD.[1-3] The World Health Organization (WHO) and the National Heart, Lung, and Blood Institute define airflow blockage as an FEV1/FVC (Forced Expiratory Volume in 1 second/Forced Vital Capacity) ratio of <0.70, a criterion also endorsed by the Global Initiative for Chronic Obstructive Lung Disease (GOLD). The severity of chronic obstructive pulmonary disease (COPD) is classified into stages based on FEV1 levels, which reflect the degree of airflow restriction. Specifically, it is categorised as Stage 1 (Mild) for FEV1 levels greater than 80% of the predicted value, Stage 2a (Moderate) for FEV1 between 50% and 80%, Stage 2b (Severe) for FEV1 between 30% and 50%, and Stage 3 (Very Severe) for FEV1 levels below 30% of the predicted value.[4,5] Despite currently ranking as the sixth-leading cause of mortality, COPD is anticipated to become the third most prevalent cause of death. In India, it is the second most common respiratory disease after pulmonary tuberculosis. In 2012, over three million people succumbed to COPD, accounting for 6% of global deaths.[6] Risk factors encompass smoking, occupational hazards, exposure to biomass fuel, and indoor and outdoor air pollution.

For individuals with COPD, spirometry emerges as the most reliable diagnostic tool for airflow limitation. The primary morbidity of COPD stems from its impact on cardiac performance, attributed to pulmonary arterial hypertension and the development of Cor Pulmonale.[3] Early recognition of evidence indicating right-side cardiac involvement is crucial. ECG (electrocardiogram) changes in COPD are attributed to the presence of hyperexpanded emphysematous lungs and the long-term effects of hypoxic pulmonary vasoconstriction on the right side of the heart, leading to pulmonary hypertension and subsequent right atrial and right ventricular hypertrophy.[2]

Numerous investigations have demonstrated significant extrapulmonary (systemic) consequences of COPD, with cardiac symptoms being the most prevalent.[7,8] When FEV1 exceeds 50% of anticipated levels, cardiovascular illness contributes to half of all hospitalisations and a third of all fatalities. Cardiovascular illness accounts for 20-25% of all deaths in COPD patients with advanced diseases. COPD leads to pulmonary hypertension, cor pulmonale, right ventricular dysfunction, and left ventricular dysfunction by affecting the pulmonary blood vessels, right ventricle, and left ventricle.[9]

Processes contributing to ECG changes in increasing airway obstruction in COPD include lung hyperinflation, altering

This article was accepted: 26 December 2024
Corresponding Author: Karpaka vinayakam Gopalakrishnan
Email: karpaka36@hotmail.com

Table I: Distribution of Electrocardiographic Findings

CG Changes	GOLD 1 Mild		GOLD 2 Moderate (11)		GOLD 3 Severe (20)		GOLD 4 Very Severe (16)	
	No	%	No	%	No.	%	No	%
P Pulmonale	0	0	1	9.09%	4	20.00%	11	68.70%
Poor R wave progression	0	0	1	9.09%	4	20.00%	9	56.25%
Right Axis Deviation (RAD)	0	0	1	9.09%	10	50.00%	6	37.50%
Right Ventricular Hypertrophy (RVH)	1	33.33%	4	36.36%	10	50.-0%	11	68.75%
RBBB	0	0	2	18.18%	7	35.-0%	11	68.75%
Atrial Fibrillation	0	0	2	18.18%	3	15.00%	6	37.50%

cardiac action current circumstances, diaphragm depression, changing the heart's anatomic connection to electrode placements, and pulmonary hypertension resulting from vasoconstriction.[9,10] Taking all these considerations into account, the current study was designed to evaluate clinical and ECG changes in COPD patients at our tertiary care centre. This study aims to analyse the ECG changes in COPD patients and their correlation with airflow restriction by assessment in the form of pulmonary function test.

MATERIALS AND METHODS

This cross-sectional study, approved by the Institutional Ethical Committee and informed consent was obtained from all participants. The research was conducted in the Department of General Medicine at a government general hospital, in collaboration with the Department of Pulmonary Medicine at Kurnool Medical College, Andhra Pradesh, India. Patients diagnosed with Chronic Obstructive Pulmonary Disease (COPD) based on symptoms and confirmed through radiographic and pulmonary function tests were included in this study. Individuals with bronchial asthma, bronchiectasis, pulmonary tuberculosis, known congenital or acquired heart disease, diabetes mellitus, or hypertension were excluded. Data collection involved 50 patients with COPD over 2 years, from December 2019 to June 2021.

Measurements included ECG, pulmonary function tests, chest X-ray, HRCT (High-Resolution Computed Tomography) chest, and other necessary investigations. Spirometry was performed on patients meeting the inclusion and exclusion criteria. The ECG criteria for right ventricular hypertrophy encompassed RAD (Right Axis Deviation) of QRS, P-pulmonale, R<S in V6, and A+R- PL>0.7. Criteria for cor pulmonale included right axis deviation of QRS complex, P-pulmonale, rSR in right precordial leads with QRS duration >0.12 seconds (incomplete right bundle branch block), R/S-ratio in V1>1, and R/S-ratio in V6. RV dilatation and strain were considered in explaining the inversion of the 'T' wave in the right leads, with hypoxia-related generalised T wave inversion noted as a nonspecific condition.

Statistical analysis was performed by presenting continuous variables as means and standard deviations, and categorical variables as frequencies and percentages. One-way ANOVA (Analysis of variance) or chi-square tests were utilised to identify differences in baseline characteristics. Unadjusted and adjusted Odds Ratios with 95% Confidence Intervals (95%CI) were estimated for each ECG variable across GOLD stages. The association between COPD duration, smoking status, and various ECG abnormalities was explored using ORs with a 95% CI. Pearson's correlation coefficient "r" was used to examine the correlation between two variables. The statistical analysis was conducted using SPSS software version 23.0 (IBM, Chicago, Illinois).

RESULTS

In this study, the distribution of disease severity was 6% mild, 22% moderate, 40% severe, and 32% very severe. Among the 50 patients, 40 were male, all with a history of smoking. The majority were beedi and chute smokers (75% of males), while cigarette smoking was reported in eight patients (20% of males), and two patients (5% of males) reported using both. None of the female patients had a history of smoking; however, 60% of females reported exposure to biocombustibles. Based on spirometry findings, 34% of patients had an FEV1/FVC ratio of 21-40%, 42% had a ratio of 41-60%, and 24% had a ratio of 61-70%.

ECG changes were observed in 33.3% of mild, 45.5% of moderate, 55.0% of severe, and 93.8% of very severe COPD patients. In the mild category, right ventricular hypertrophy (RVH) was detected in 1 of 3 patients. RVH was present in 36.36% of moderate, 50.0% of severe, and 68.75% of very severe cases. P. Pulmonale was absent in mild COPD but observed in 9.09%, 20.0%, and 68.7% of patients in the moderate, severe, and very severe categories, respectively. Right axis deviation (RAD) was absent in mild cases but present in 9.09% of moderate, 50.0% of severe, and 37.5% very severe cases. Poor R-wave progression was recorded in 9.09%, 20.0%, and 56.25% of moderate, severe, and very severe patients, respectively, but was absent in mild cases.
Right bundle branch block (RBBB) was not seen in mild COPD but occurred in 18.18% moderate, 35.0% severe, and 68.75% very severe cases. Atrial fibrillation was also absent in mild cases but detected in 18.18%, 15.0%, and 37.5% of moderate, severe and very severe patients, respectively. Overall, these ECG anomalies demonstrated an association with COPD severity categories (Table I).

DISCUSSION

Our study aimed to investigate the association between electrocardiographic changes and pulmonary function test results in patients with Chronic Obstructive Pulmonary

Disease (COPD). The distribution of COPD severity in our study population revealed that the majority of patients fell into the severe (40%) and very severe (32%) categories, highlighting the predominance of advanced disease.

With respect to smoking history, our study noted that all the male COPD patients are smokers, the majority being beedi and chute users, with a small proportion reporting combined use of beedi, chute, and cigarettes. These findings highlight the need for targeted smoking cessation strategies, particularly addressing beedi and chute smoking. Additionally, exposure to biocombustible fuels was identified as a risk factor among female patients, reinforcing the importance of accounting for diverse environmental exposures in the aetiology of COPD.

Our findings demonstrated a notable prevalence of electrocardiographic changes in COPD patients. The most frequent ECG abnormalities included R<S in V6 (60%), incomplete RBBB (40%), and RAD of QRS complex (34%). These observations are consistent with existing literature, which highlights the high prevalence of cardiac involvement in COPD patients.

The association between the severity of COPD and specific ECG changes was explored. An increasing trend in the prevalence of ECG abnormalities with worsening COPD severity. Right ventricular hypertrophy (RVH) was notably present in all severity categories, with a substantial proportion in very severe COPD patients (68.8%). P-pulmonale, RAD, Poor R wave progression, and RBBB all demonstrated higher frequencies in more severe COPD.

In the study by P K et al.,[6,9] involving 60 patients, the distribution of COPD severity was 10% mild, 30% moderate, 35% severe, and 25% very severe, findings that align with the severity profile in our study. Among these patients, 45 were male, of whom 30 had a history of smoking. Beedi and chute smoking were the predominant forms (20 patients, 44%), followed by cigarette smoking (10 patients, 22%), and combined use of beedi, chute, and cigarettes (5 patients, 11%). Notably, 15% of female patients reported exposure to biocombustibles fuels.

Analysing the spirometry results showed that 25% of the patients had an FEV1/FVC ratio of 21-40% group, 50% had a ratio of 41-60%, and 25% had a ratio of 61-70%.[7,10] The correlation analysis demonstrated significant associations between specific electrocardiographic changes and pulmonary function test results. Notably, the P wave axis, QRS axis, P wave height, R V6 height, and RBBB showed statistically significant correlations with FEV1. These findings suggest that specific ECG changes may serve as indicators of pulmonary function impairment in patients with COPD.

The observed correlations between ECG changes and COPD severity, as well as pulmonary function, suggest the potential utility of ECG as a non-invasive tool for assessing cardiac involvement and predicting pulmonary function impairment in COPD. Early identification of these cardiac manifestations may guide clinicians in implementing timely interventions to manage both the respiratory and cardiac aspects of COPD. Our study has certain limitations, including its cross-sectional design and a relatively small sample size. Longitudinal studies with larger cohorts are needed to establish causality and further explore the dynamic relationship between cardiac involvement and pulmonary function in COPD. Additionally, a comprehensive assessment of comorbidities and detailed smoking history would provide a more nuanced understanding of the study population.

CONCLUSION

Our study highlights the prevalence of electrocardiographic changes in patients with COPD, with specific ECG abnormalities demonstrating a correlation with the severity of both COPD and pulmonary function impairment. These findings contribute to the growing body of evidence supporting the importance of integrated care for patients with COPD, considering both respiratory and cardiac aspects. Further research is warranted to validate these associations and explore their implications for clinical management.

CONFLICT OF INTEREST

The authors declare that they have no conflicts of interest that could compromise the objectivity of this scientific work.

REFERENCES

1. Patel AR, Patel AR, Singh S, Singh S, Khawaja I. Global initiative for chronic obstructive lung disease: the changes made. Cureus 2019; 11(6): e4985.
2. Sharma SK. Chronic obstructive lung disease. In: Shah SN, editor. API textbook of medicine. 7th ed. Mumbai: API; 2003. p. 297-301.
3. MacNee W. Pathology, pathogenesis, and pathophysiology. BMJ 2006; 332(7551): 1202-4.
4. Reilly JJ Jr, Silverman EK, Shapiro SD. Chronic obstructive pulmonary disease. In: Braunwald E, Fauci AS, Kasper DL, editors. Harrison's Principles of Internal Medicine. Vol. 2. 17th ed. New York: McGraw-Hill; 2008. p. 1547-57.
5. Barnes PJ. Small airways in COPD. N Engl J Med 2004; 350: 2635-6.
6. P K, Rai S. Assessment of severity and systemic involvement in chronic obstructive pulmonary disease by BODE index: A cross-sectional study. Int J Contemp Med Res 2018; 5(6): F8-13.
7. Pashutina Y, Kotz D, Kastaun S. Attempts to quit smoking, use of smoking cessation methods, and associated characteristics among COPD patients. NPJ Prim Care Respir Med 2022; 32(1): 39.
8. Gupta P, Jain H, Gill M, Bharaj G, Khalid N, Chaudhry W, Chhabra L. Electrocardiographic changes in emphysema. World J Cardiol 2021; 13(10): 533-45.
9. Calatayud JB, Abad JM, Khoi NB, Stanbro WW, Silver HM. P-wave changes in chronic obstructive pulmonary disease. Am Heart J 1970; 79: 444-53.
10. Surawicz B, Knilans T. Atrial abnormalities. In: Chou's Electrocardiography in Clinical Practice: Adult and Pediatric. 6th ed. Philadelphia: Saunders Elsevier; 2008. p. 33-6.

A study on role of topical application of mitomycin c postoperatively in reducing adhesions/synechiae after FESS in patients with chronic rhinosinusitis: A Randomized controlled trial

Alekhya Vemula, Subagar Anbarasan, Anand KH, Elangovan Subramanian

Department of otorhinolaryngology, head and neck surgery, Saveetha Institute of medical and technical sciences (SIMATS), Chennai, India

ABSTRACT

Introduction: Synechiae formation is a common and undesired complication after functional endoscopic sinus surgery. Mitomycin-c, known for its anti-proliferative and anti-fibroblastic properties holds potential for reducing synechiae and scar tissue formation following endoscopic sinus surgery. This study aims to evaluate the efficacy of topically applied mitomycin-c postoperatively in minimising adhesions and nasal obstruction symptoms using the Lund-Kennedy Endoscopic Scoring and Nasal Obstruction Symptom Evaluation (NOSE) scores.

Materials And Methods: This double-blind randomised study assessed topical mitomycin-c's efficacy in reducing adhesions post-FESS in 50 chronic rhino-sinusitis patients. Participants who were selected based on Lund-Mackay CT scores underwent functional endoscopic sinus surgery (FESS). The mitomycin-c and saline-soaked nasal packs were placed in middle meatuses either of one in each nasal cavity. Postoperative care included antibiotics, analgesics and saline douching. Outcomes were evaluated at 1, 4 and 12 weeks using the NOSE (nasal obstruction symptom evaluation) questionnaire and Lund-Kennedy scoring to determine mitomycin-c's impact on nasal obstruction and synechiae formation.

Results: The results indicated statistically significant variation between mitomycin-c and control sides in terms of symptoms and endoscopic findings in the first week postoperatively. By the fourth week, the clinical pictures of both sides were nearly identical.

Discussion: Data suggested that low-dose mitomycin-c significantly reduces adhesions and improves nasal symptoms in the early postoperative period for chronic rhinosinusitis patients. These results align with previous research, supporting mitomycin-c as a valuable adjunctive therapy in sinus surgery. Future studies are recommended to explore varying dosages and application methods for potential differences in outcomes.

KEYWORDS:
Mitomycin-c, Synechiae, Lund Kennedy score, FESS, NOSE score

INTRODUCTION

Endoscopic sinus surgery is widely regarded as the preferred treatment for chronic sinus disease. This approach is favoured because it preserves mucosa of sinus, restores ventilation and drainage through sinus ostia and effectively alleviates the pathology.[1] But, synechiae are one of the most common and undesired complications following FESS. Addressing synechiae is crucial as they can obstruct nasal airflow, block ostia, impair mucociliary function and hinder the delivery of topical medications.[2]

Post-surgical care aims to facilitate rapid healing and regrowth of healthy sinus lining by reducing inflammation, preventing infections, improving symptoms, restoring ciliary function, and preventing early complications. Currently, the use of compressible devices to irrigate the nasal passages with a significant volume of saline is standard practice. Performing nasal debridement in the office provides several benefits. However, repeated nasal endo-cleaning and debridement can be a painful procedure and may cause discomfort for patients postoperatively.

Mitomycin-c derived from Streptomyces caespitosus serves as a multifaceted compound with antibiotic, anti-proliferative and antineoplastic properties. Acting as an alkylating agent, it selectively impedes DNA synthesis and disrupts DNA base-pairs contributing to its therapeutic mechanism.[4] By inhibiting protein synthesis, mitomycin-c is known to effectively suppress fibroblast proliferation, reduces fibrosis and decreases vascularity both in vitro and in vivo. Its ability to influence wound healing has led to its application in ophthalmic surgeries where its effects on rapidly dividing cells is particularly beneficial.[5] This same wound-healing effect makes it suitable for application in procedures like FESS as well. It is thus hypothesised that topical application of mitomycin-c postoperatively following FESS can thereby be helpful in reducing crusting/synechiae formation by its anti-fibroblastic, anti-proliferative action and hence minimises the formation of scar tissue post-surgery.

Our objective here is to evaluate the effectiveness of topically applied mitomycin-c in reducing adhesions/synechiae and reducing Nasal Obstruction symptoms using Lund-Kennedy endoscopic scoring and Nasal obstruction symptom

This article was accepted: 06 December 2024
Corresponding Author: Elangovan Subramanian
Email: subraelango@gmail.com

Inclusion criteria	Exclusion criteria
Age from 18-65 years	Age below 18 and above 65 years
No h/o previous FESS/Nose surgeries	H/o previous FESS/Nose surgeries
Bilateral chronic rhino sinusitis with symptoms refractory to medical treatment (Antibiotics and corticosteroid) given for at least for 3 months.	Acute upper respiratory tract infection, Unilateral Sino nasal disease
Patients with complete osteomeatal unit occlusion on non-contrast CT PNS with ≤2 grades of variation between both nasal cavities on the Lund-Mackay CT scoring and a minimum score of 4 on each side	Uncontrolled diabetes, uncontrolled hypertension, immune compromised status, ciliary motility disorders, cystic fibrosis, known autoimmune disorders.
	Sino nasal tumours, Mass, Malignancy, Gross DNS

evaluation score (NOSE) postoperatively after FESS. The focus of this study is to reduce the repeated need for hospital visits for nasal debridement post-surgery. This goal underscores the purpose of this research to ensure a seamless postoperative recovery.

MATERIALS AND METHODS

This is a prospective, comparative, double-blinded randomised controlled study that involved patients diagnosed with bilateral chronic rhino sinusitis presented to the Otorhinolaryngology outpatient department.

Following approval from the Institutional Ethics Committee (IEC-129/06/2023/IEC/SMCH), the study was commenced for a duration of 12 months (June 2023- June 2024).

The sample size was calculated with a power of 90% and a 5% alpha error, resulting in 44 participants. To accommodate a 10% attrition rate, the study required 48 samples, rounded up to 50.

Sample size: 50

Fifty participants with bilateral chronic rhino sinusitis who met the study's inclusion and exclusion criteria were chosen to participate. All participants provided informed consent and received detailed information about the planned procedure, post-operative application of mitomycin-c, expected outcomes and potential side effects. Preoperative non-contrast computed-tomography paranasal sinus (CT PNS) was conducted and participants were selected based on Lund-Mackay CT scoring system, ensuring a difference of ≤2 between both sides and minimum score of 4 on each side.

One hundred lots were prepared with fifty labelled "right" and fifty labelled "left". Participants randomly selected a labelled lot ("right" or "left"), determining the intervention side. Both the investigator and the patients were blinded to the selected lot ensuring the study was conducted in a double-blinded manner.

All participants completed a preoperative NOSE (nasal obstruction symptom evaluation) questionnaire and underwent direct rigid nasal endoscopy. FESS with Messerklinger technique under general anaesthesia employing an approach based on the severity and specific anatomical involvement.

After completing FESS, a half Ivalon nasal pack soaked with 1 ml (0.1 mg/ml) mitomycin-c was placed in one middle meatus, half Ivalon pack soaked in 1 ml saline was placed in the other middle meatus. A full saline-soaked Ivalon pack was placed in each nasal cavity followed by dressing. Postoperative care included intravenous antibiotics and analgesics. Bilateral nasal packs were removed on postoperative day 1, nasal douching started on day 2 and diagnostic nasal endoscopy with endo-cleaning was performed on day 3. Patients were discharged the same day with oral antibiotics, analgesics and instructions to continue saline nasal douching three times daily until the next review. All participants were reviewed at 1, 4 and 12 weeks postoperatively. Nasal obstruction symptoms were evaluated in the first week using the NOSE questionnaire. Endoscopic findings scored with Lund-Kennedy scoring (Table I) system at 1st and 4th weeks. Comparing the findings between nasal cavities helped predict mitomycin-c's effectiveness in improving nasal obstruction symptoms and reducing crusting/synechiae formation after FESS.

NOSE questionnaire includes scoring of symptoms like nasal congestion/stuffiness, nasal block, breathing difficulty, nasal obstruction during exertion, trouble sleeping scores as 0 (no symptom),1 (mild), 2 (moderate), 3 (fairly bad), and 4 (severe).

Statistical Analysis: Statistical analysis was conducted using IBM SPSS Statistics version 19. Descriptive statistics such as mean (standard deviation)/median (interquartile range)/median (range) and frequencies (percentages) were used for quantitative and qualitative data, respectively. A paired t-test was applied to compare Lund-Mackay scores between right and left sides of the nose pre-operatively. A $p<0.05$ was considered as significant. Wilcoxon signed-rank test was used to compare the outcome measurements between the interventional and control sides.

In various studies using the Lund-Mackay score on sinus CT scans and the Modified Lund-Kennedy naso-endoscopic score has proven beneficial for categorizing the severity and prognosis of extensive sinus disease.[13] It is said that there exists a noteworthy correlation between these scores, highlighting their utility in clinical practice. The Nasal Obstruction Symptom Evaluation Score (NOSE) is widely recognised for its reliability and ease of use in studying nasal obstruction outcomes among adults. Its effectiveness in

outcome studies underscores its value in clinical assessments and treatment evaluations for nasal obstruction.[14]

Studies stated that there is no clinically significant association between the Lund Mackay and SNOT-22 scores suggesting the need of distinct measures to assess symptom severity and disease impact in chronic rhinosinusitis patients.[15] Various methods have been employed in previous studies to investigate the efficacy of mitomycin c in sinus surgery. In one study participants were divided into two groups where one received a wick with 1 ml of mitomycin-c (0.4 mg/ml), while other received a saline-soaked wick intraoperatively. Facial pain, nasal block, nasal discharge, hyposmia and SNOT-20 scores were evaluated using the Wilcoxon matched pairs test. Post-surgery, conventional nasal packing with steroid and antibiotic ointment was utilized.[8]

RESULTS

Fifty participants were enrolled in the study. Mean age was 33.28 years (standard deviation (SD)=10.144). Ages ranged from 19 to 63 years. The age distribution showed that the majority of the study population were under 30 years, highlighting a predominantly younger age group. Out of 50 participants 15 were female and 35 were male.

The mean Lund Mackey Score was 8.28 (SD=1.196) for the right side and 8.14 (SD=1.069) for the left side. The p-value of 0.431 suggests that there is no statistically significant difference between the scores, suggesting a similar extent of sinus disease on both sides at baseline.

Pre-operative NOSE scores

The mean scores were as follows: nasal congestion/stuffiness 1.84 (SD 0.681), nasal block 1.34 (SD 0.479), breathing difficulty 1.42 (SD 0.609), obstruction during exertion 1.64 (SD 0.693), and trouble sleeping 1.56 (SD 0.577). The total NOSE score had a mean of 7.80 (SD 1.629).

Post-operative NOSE scores

Post-intervention scores showed a significant difference: nasal congestion/stuffiness mean 0.12 (SD 0.328), nasal block mean 0.18(SD 0.388), breathing difficulty mean 0.02(SD 0.141), nasal obstruction during exertion mean 0.16(SD 0.373) and trouble sleeping mean 0.12(SD 0.328). The total NOSE score had a mean of 0.60 (SD 0.782).

The comparison between pre- and post-operative scores shows significant improvement across all variables. Pre-operative scores indicated moderate to severe symptoms with means from 1.34 to 7.80.Post-intervention scores showed a dramatic reduction, with means ranging from 0.02 to 0.60, indicating minimal to negligible symptoms.

This clear contrast highlights the effectiveness of the intervention and underscores the importance of functional endoscopic sinus surgery in enhancing patient outcomes. The substantial decrease in mean scores and reduced standard deviations post-surgery indicates significant improvement in nasal symptoms/before surgery, the Total NOSE scores for both the interventional and control sides were similar with medians of 7.5 and 8, respectively (p=0.251), indicating no significant difference between them. However, by postoperative week 1, the Total NOSE score significantly dropped on the interventional side, in comparison to control side($p<0.001$) suggesting the significant positive impact of intervention in reducing nasal symptoms post-surgery (Table II).

In postoperative week 1, on the control side 84% had no polyps (score 0), 16% had polyps within middle meatus (score 1). 46% reported no discharge (score 0), 44% had thin and clear discharge (score 1) and 10% had thick and mucopurulent discharge (score 2). 20% had no oedema (score 0), 70% had mild oedema (score 1) and 10% had moderate oedema (score 2). 42% had no scarring (score 0), 50% had mild scarring (score 1) and 8% had moderate scarring (score 2) 20% had no cresting (score 0), 60% had mild cresting (score 1) and 20% had moderate cresting (score 2).

Whereas on mitomycin-c side, 98% had no polyps (score 0), 2% had small polyps within middle meatus (score 1). 60% had no discharge (score 0), 38% had mild clear discharge (score 1), and 2% had mucopurulent discharge (score 2). 74% had no oedema (score 0), 26% had mild oedema (score 1). 84% had no scarring (score 0), 16% had mild scarring (score 1). 76% had no cresting (score 0) and 24% had mild cresting (score 1).

On week 1 notable differences were observed in polyp between mitomycin-c and control sides ($p=0.020$), suggesting a notable impact of the intervention on polyp formation early after surgery. Similarly, variables like discharge ($p=0.054$), oedema ($p<0.001$), scarring ($p<0.001$), and cresting ($p<0.001$) showed significant differences. These findings indicated that mitomycin-c side exhibited less discharge, oedema, scarring and cresting compared to the control side during this initial period. The median Total Kennedy score for the mitomycin-c side was 1, while the control side had a median score of 4. The p-value for this comparison is <0.001, indicating a highly significant difference with the interventional group showing much lower scores suggesting better outcomes.

By postoperative week 4, 86% had no polyps (score 0), 14% had minor polyps (score 1). 64% had no discharge (score 0), and 36% had mild clear discharge (score 1). 68% had no oedema (score 0), and 32% had mild oedema (score 1). 92% had no scarring (score 0), and 8% had mild scarring (score 1). 80% had no cresting (score 0) and 20% had mild cresting (score 1).

On the mitomycin-c side100% had no polyps (score 0). 78% had no discharge (score 0), 20% had mild watery discharge (score 1) and 2% had mucopurulent discharge (score 2). 98% had no oedema (score 0) and 2% had mild oedema (score 1). 98% had no scarring (score 0) and 2% had mild scarring (score 1). 94% had no cresting (score 0) and 6% had mild cresting (score 1).

On week 4, the differences in polyp remained significant ($p=0.008$). However, the significance levels for discharge ($p=0.083$), oedema ($p=0.180$), scarring ($p<0.001$) and cresting ($p=0.180$) decreased or became non-significant, suggesting

Table I: Lund-Kennedy endoscopic scoring system

Charecteristics	Score definition
Nasal polyps	0 = none; 1=confined to middle meatus; 2=beyond middle meatus
Discharge	0 = none; 1=clear and thin; 2=thick and purulent
oedema	0=absent; 1=mild; 2=severe
Scarring	0=absent; 1=mild; 2=severe
Crusting	0=absent; 1=mild; 2=severe

Table II: Pre-operative and post-operative week 1 Average Nasal Obstruction Symptom Evaluation (NOSE) scores.

Variables	NOSE score	Interventional Side	Control Side	p-value
Nasal congestion/stuffiness	Pre-op Nose score	2(1,4)	2(1,4)	0.173
	POD 1st week Nose score	0(0,1)	1(0,2)	<0.001
	p-value	<0.001	<0.001	
Nasal Block	Pre-op Nose score	1(1,2)	2(1,3)	0.016
	POD 1st week Nose score	0(0,1)	1(0,2)	<0.001
	p-value	<0.001	<0.001	
Breathing difficulty	Pre-op Nose score	1(1,3)	1(1,3)	0.583
	POD 1st week Nose score	0(0,1)	0(0,1)	0.059
	p-value	<0.001	<0.001	
Nasal obstruction	Pre-op Nose score	2(1.3)	1(1,3)	0.251
	POD 1st week Nose score	0(0,1)	0(0,1)	0.527
	p-value	<0.001	<0.001	
Trouble sleeping	Pre-op Nose score	2(1,3)	1.5(1,4)	0.828
	POD 1st week Nose score	0(0,1)	0(0,2)	0.074
	p-value	<0.001	<0.001	
Total Median (IQR)	Pre-op Nose score	7.5(7,9)	8(7,9)	0.251
	POD 1st week Nose score	0(0,1)	2(1,3)	<0.001
	p-value	<0.001	<0.001	

Table III: Mean Lund Kennedy endoscopic scores on week 1 and 4 postoperatively

Variables	Lund Kennedy	Interventional Side	Control Side	p-value
POLYP	POD 1st week	0(0,1)	0(0,1)	0.02
	POD 4th week	0(0,0)	0(0,1)	0.008
	p-value	0.317	0.317	
DISCHARGE	POD 1st week	0(0,2)	1(0,2)	0.054
	POD 4th week	0(0,2)	0(0,1)	0.083
	p-value	0.003	0.003	
EDEMA	POD 1st week	0(0,1)	1(0,2)	<0.001
	POD 4th week	0(0,1)	0(0,1)	<0.001
	p-value	0.001	<0.001	
SCARRING	POD 1st week	0(0,1)	1(0,2)	<0.001
	POD 4th week	0(0,1)	0(0,1)	0.18
	p-value	0.008	<0.001	
CRESTING	POD 1st week	0(0,1)	1(0,2)	<0.001
	POD 4th week	0(0,1)	0(0,1)	0.008
	p-value	0.003	<0.001	
Total Kennedy score Median (IQR)	POD 1st week	1(1,1)	4(2,4)	<0.001
	POD 4th week	0(0,1)	1(1,2)	<0.001
	p-value	<0.001	<0.001	

that while the intervention initially had a strong impact on these outcomes, the differences diminished over time. The median Total Kennedy score for the mitomycin-c side further decreased to 0, whereas the control side had a median score of 1. The p-value remains <0.001, indicating that the significant difference between the groups persisted with the interventional group continuing to show better outcomes(Table III). While the statistical difference is notable, clinically the distinction between the groups is minimal by the fourth week. Both groups generally experienced similar healing processes, leading to comparable clinical outcomes.

During the 12th-week follow-up endoscopy, two participants out of 50 developed synechiae on the control side: one between the middle and inferior turbinates, and the other between the middle turbinate and lateral wall. No adverse effects were observed up to 12 weeks post operatively.

DISCUSSION

Unlike the previous studies we employed an extended protocol using low dose mitomycin c post operatively where the nasal packing was soaked with the medication, aiming to maximise its efficacy in supporting wound healing. Our

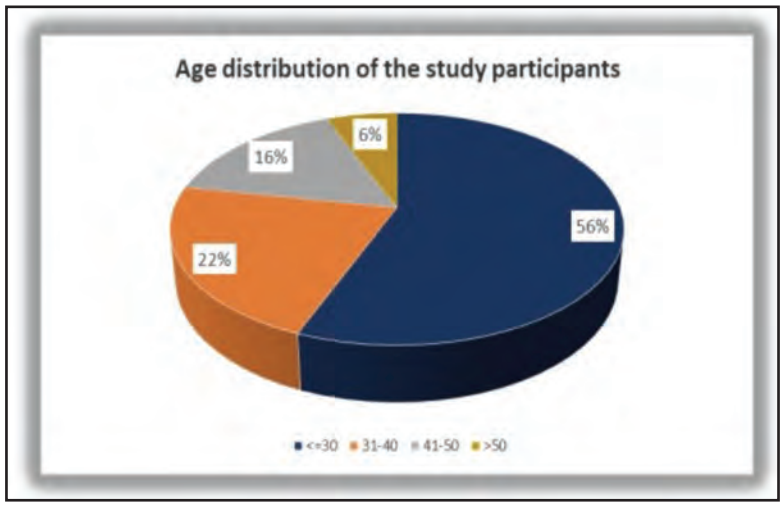

Fig. 1: Age distribution of study participants (N=50)

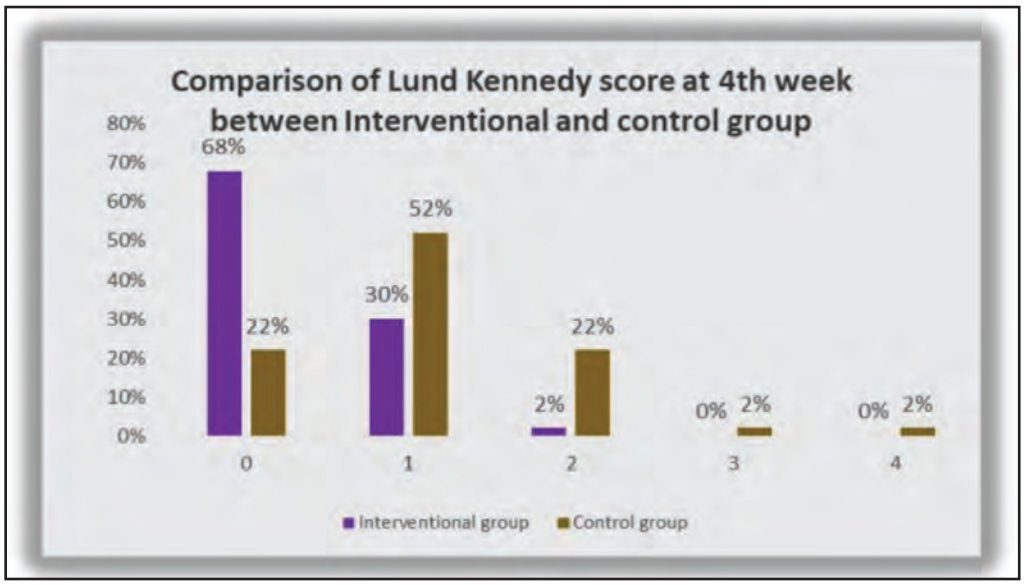

Fig. 2: Comparison of total Lund Kennedy scores between mitomycin-c and control sides on post-operative week 4 (N=50)

main objective was to facilitate a smoother immediate postoperative recovery period, thereby enhancing patient satisfaction. Nasal pain is a common and bothersome issue arising from frequent endoscopic debridements post-surgery. During the repeat endo-cleaning in week 1, participants reported less discomfort on the interventional side compared to the control side, likely due to reduced need for debridement in the interventional side. Moreover, our findings in the first postoperative week revealed significant improvements in nasal obstruction symptoms as well.

Following upper airway surgery, the nasal and paranasal mucosal lining undergoes a well-coordinated recovery process involving inflammation, cellular proliferation, matrix formation, and remodelling governed by various growth factors and cytokines.[6]

Intranasal adhesions, also known as synechiae occur when the nasal mucosa heals improperly after injury or surgery. This abnormal healing process can cause the mucosal surfaces within the nasal cavity to stick together leading to the formation of fibrous bands. These adhesions can obstruct normal airflow and cause various symptoms such as nasal congestion, difficulty breathing and recurrent sinus infections.[7] Proper postoperative care and management are crucial to minimise the risk of developing intranasal adhesions. The frequently utilised nasal packing material following nasal endoscopic surgeries is polyvinyl acetate (known as Merocel or Ivalon). This material is usually coated or treated with a non-adhesive layer to facilitate its easy removal post-surgery and minimize potential damage.

Harugop et al.,[8] found that while mitomycin-c provided superior symptomatic relief for nasal obstruction and facial

pain, it did not significantly affect nasal discharge and hyposmia. Consistent with the previous study, our findings also indicated significant difference in congestion and nose block between the mitomycin-c side and the control side at week 1 postoperatively, with p<0.001. Furthermore, no significant differences in nasal discharge were observed between the interventional and control sides at both week 1 and week 4 postoperatively (p=0.054 and 0.083 respectively).These findings suggest that while mitomycin-c may offer certain symptomatic benefits but, its impact on other postoperative outcomes remains limited, aligning with the findings of Harugop et al.

Singh et al.[9] also reported the safety of mitomycin-c used topically when comparing various concentrations applied for five minutes. Their study concluded that mitomycin-c application post-endoscopic surgery improved symptoms such as nasal obstruction, hyposmia and reduced adhesion rates and middle meatal antrostomy closure rates. Although our study did not assess hyposmia, we compared other nasal symptoms and found no significant differences in breathing difficulty (p=0.059), nasal obstruction (p=0.527), or trouble sleeping (p=0.074).

Venkatraman et al.,[10] highlighted that during the 1st week when the patients were reviewed there was a notable decrease in the occurrence of synechiae and improvement in symptoms like nose block, discharge from the nose on the side where mitomycin-c was used as compared to the control side where normal saline was used. However, after three and six months these differences were no longer significant. In our study, we evaluated nasal discharge, oedema, scarring, cresting, and polyps as essential parameters for assessing synechiae formation. We found that while the difference was significant by week 1, it became less pronounced by week 4 aligning with the findings of the previous study. Although statistical significance was observed on week 4 (p<0.001) the median total Lund Kennedy scores on mitomycin-c side was 0(0,1) and control side was 1(1,2) showing not much of a difference clinically.

A newer study by Sulieman et al.,[11] further supports efficacy of intra and postoperative mitomycin-c application in decreasing the incidence of synechiae after FESS. Their findings indicated that mitomycin-c not only minimised adhesions but also promoted better mucosal healing over a three-month follow-up period.[1] ml of mitomycin-c (0.8 mg/ml) was applied in the middle nasal passage for five minutes, followed by another application three weeks afterwards.

Our findings align with Ramalingam et al.,[12] stating a significant reduction in crusting during the initial week after surgery and there were improvements noted in reducing discharge, oedema of mucosa, polyp formation, and keeping the ostia open.

LIMITATIONS

The follow-up period in this study was limited to 12 weeks. Extending the follow-up in future research may provide more comprehensive insights into the long-term effects of mitomycin-c in reducing synechiae and improving nasal obstruction post-FESS.

The exclusion of patients with comorbidities such as uncontrolled diabetes, hypertension and autoimmune disorders ensures a homogenous study population. However, further research may be needed to explore the applicability of the findings to a broader, more medically complex population.

The primary outcome of this study was nasal obstruction, while other symptoms of chronic rhinosinusitis such as facial pain and olfactory function, were not extensively evaluated. Future studies could benefit from a more comprehensive assessment of patient symptoms.

While no significant adverse effects were observed during the 12-week follow-up, longer-term studies would be valuable in assessing the potential delayed effects of mitomycin-c, such as mucosal changes.

CONCLUSION

In conclusion, the postoperative topical application of low dose mitomycin-c appears to significantly reduce adhesions/synechiae and improve nasal symptoms in early postoperative period in patients with chronic rhinosinusitis. These findings are supported by previous research and highlight the potential of mitomycin-c as an effective adjunctive therapy in sinus surgery. This study employed a specific concentration and volume of mitomycin-c. However, exploring alternative dosages or application methods may reveal varied outcomes, suggesting the need for further investigation in future research comparing various doses and methods of application of mitomycin-c.

REFERENCES

1. Gupta M, Motwani G. Role of mitomycin C in reducing adhesion formation following endoscopic sinus surgery. J Laryngol Otol 2006; 120(11): 921-3.
2. Henriquez OA, Schlosser RJ, Mace JC, Smith TL, Soler ZM. Impact of synechiae after endoscopic sinus surgery on long-term outcomes in chronic rhinosinusitis. Laryngoscope 2013; 123(11): 2615-9.
3. Fokkens WJ, Lund VJ, Hopkins C, Hellings PW, Kern R, Reitsma S, et al. European Position Paper on Rhinosinusitis and Nasal Polyps 2020. Rhinology 2020; 58(Suppl S29): 1-464.
4. Pratt WB, Ruddon RW, Ensminger WD, Maybaum J. The Anticancer Drugs. New York: Oxford University Press; 1994.
5. Arranz-Márquez E, Katsanos A, Kozobolis V, Konstas AG, Teus MA. A Critical Overview of the Biological Effects of Mitomycin C Application on the Cornea Following Refractive Surgery. Adv Ther 2019;3 6(4): 786-97.
6. Watelet JB, Bachert C, Gevaert P, Van Cauwenberge P. Wound healing of the nasal and paranasal mucosa: a review. Am J Rhinol 2002; 16(2): 77-84.
7. Stępiński MJ, Banaszewski J. Intranasal Synechiae as Complications of Rhinosurgical Treatment—A Review of Current Knowledge. J Clin Med 2023; 12(21): 6831.
8. Harugop AS, Mudhol RS, Kaku D, Vishnu H, Suhasini H. Subjective and Objective Outcome Evaluation of FESS with and without Mitomycin C: A Randomized Control Trial. Madridge J Otorhinolaryngol 2018; 3(1): 31-6.

9. Singh TD, Lade H, Natesh V. Role of Mitomycin-C in Prevention of Post Operative Adhesions After Endoscopic Sinus Surgery—A Prospective Study. Indian J Otolaryngol Head Neck Surg 2011; 63(3): 249-54.
10. Venkatraman V, Balasubramanian D, Gopalakrishnan S, Saxena SK, Shanmugasundaram N. Topical Mitomycin C in functional endoscopic sinus surgery. Eur Arch Otorhinolaryngol 2012; 269(7): 1791-4.
11. Sulieman YM, Mostafa I, Youssef Y. Efficacy of Mitomycin C in Prevention of Adhesions Formation after Functional Endoscopic Sinus Surgery. J Otolaryngol Rhinol 2023; 9(2): 139.
12. Ramalingam N, Parida PK, Saxena SK, Surianarayanan G. Comparison of triamcinolone and mitomycin C nasal pack in functional endoscopic sinus surgery: a randomized, clinical trial. Egypt J Otolaryngol 2018; 34(4): 242-7.
13. Lund VJ, Kennedy DW. Staging for rhinosinusitis. Otolaryngol Head Neck Surg 1997; 117(3 Pt 2): S35-40.
14. Baba Caliaperoumal VB, GS D, Velayutham P, Krishnaswami B, Rama Krishnan KK, Savery N. Correlation of Clinical Symptoms With Nasal Endoscopy and Radiological Findings in the Diagnosis of Chronic Rhinosinusitis: A Prospective Observational Study. Cureus 2021; 13(7): e16591.
15. Hopkins C, Browne JP, Slack R, Lund V, Brown P. The Lund-Mackay staging system for chronic rhinosinusitis: How is it used and what does it predict? Otolaryngol Head Neck Surg 2007; 137(4): 555-61.

Oxybenzone in Sunscreen: A Comprehensive Ecotoxicological Review

Abinaya Gayathri, PhD[1], Delecta Jenifer, PhD[2], Devi VijayaVarma, PhD[3], Kumaravel Kaliaperumal, PhD[1]

[1]Department of Orthodontics, Saveetha Dental College, Saveetha Institute of Medical and Technical Sciences (SIMATS), Saveetha University, Chennai, India, [2]Department of Management Studies, Saveetha Engineering College (Autonomous), Anna University, Chennai, India, [3]PG Department of Biochemistry, Bhaktavatsalam Memorial College for Women, Chennai

ABSTRACT

Introduction: Oxybenzone (benzophenone-3) is a widely used organic compound in sunscreens and other personal care products due to its ability to absorb ultraviolet (UV) radiation. It is effective in protecting the skin from harmful UV rays, thereby reducing the risk of skin cancer and photoaging. However, increasing concerns have emerged regarding the environmental impact of oxybenzone, particularly in marine ecosystems.

Materials and Methods: A comprehensive literature search was conducted using databases such as PubMed, Scopus, and Web of Science. Keywords included "oxybenzone," "sunscreen," "ecotoxicology," "marine organisms," and "environmental impact." Studies published from 2000 to 2023 were included to ensure a thorough understanding of the topic.

Results: Oxybenzone has been detected in various marine environments, with concentrations ranging from nanograms to micrograms per litre. Oxybenzone has been shown to cause bleaching in corals, impairing their ability to recover from stress. Research indicates that oxybenzone exposure can lead to endocrine disruption in fish, affecting reproductive success and behaviour. Oxybenzone has been found to be toxic to various invertebrates, including mollusks and crustaceans. Sub-lethal effects include impaired growth and development, as well as altered feeding behaviour. The data indicate a clear concentration-response relationship for oxybenzone toxicity across different species. Lower concentrations tend to produce sub-lethal effects, while higher concentrations can lead to mortality.

Discussion: The findings of this review highlight the significant ecotoxicological risks posed by oxybenzone in marine environments. The widespread use of oxybenzone in sunscreens, combined with its persistence in aquatic ecosystems, raises concerns about its long-term effects on marine biodiversity. A balanced approach that considers both human health and environmental sustainability is essential for the future of sunscreen formulations.

KEYWORDS:
Photosynthesis, UV filter, freshwater, marine water, coral reefs, oxybenzone, seed germination.

INTRODUCTION

Oxybenzone, because of its broad-spectrum ability to absorb photons in the ultraviolet (UV) part of the spectrum, including UVA and UVB, oxybenzone is a frequently used active component in sunblock and other Medicine and Personal Care Products (PPCPs).[1-3] Oxybenzone is also known as Benzophenone. It is a growing source of pollution in maritime areas, which is released by swimming as well as wastewater from homes, businesses, and boats and ships.[4] There have been reports of organic UV filters in drinking water, drinking water treatment facilities, drinking water treatment plants, bays, rivers, lakes, bathing waters, swimming pools, sediments, and biota/animals and plants. Because of the usage of sunscreen and PCP, studies have discovered measurable levels of organic UV filters in human urine, serum, and breast milk.[5-7] The coral reef is one kind of reef that can be found in the warm, shallow waters. Coral individuals are joined by connecting molecules, which allows them to live in groups for extended periods of time. Coral reefs provide a variety of sized spaces for the growth and residence of many species of fish, shrimp, shellfish, algae, and various other marine animals. In polyps, cryophyte is symbiotic. Through the process of photosynthesis, yellow algae are a type of algae plant that absorbs sunlight and supplies corals with nutrients. Sea levels will rise as a result of global warming, gravely endangering coral existence.

Apart from the detrimental effects of climate change on the marine ecosystem, oxybenzone has been found in sunscreen and other skin care products, as well as in freshwater and marine entertainment areas.[8] It is known to build up in aquatic species and transform into harmful compounds.[9] Studies have indicated that inorganic filters are superior to organic filters in terms of their ability to block UVA and UVB radiation. This is because inorganic sunscreens reflect UV light, whereas organic sunscreens absorb and convert it. Because oxybenzone is the most often used organic filter, Hawaii has placed restrictions on its use due to its harmful effects on the coral reefs.[10] High-energy visible light, infrared radiation, and ultraviolet radiation (UVR) are the three types of solar radiation. Sunscreens are primarily used to defend against ultraviolet radiation.[11]

UVR, which accounts for 6.8% of solar radiation overall, is separated into UVA (315-400 nm) and UVB (280-315 nm) wavelength groups.[12] Long-range, or UVA, waves are lower

This article was accepted: 17 August 2024
Corresponding Author: Kumaravel Kaliaperumal
Email: Kumaravelk.sdc@saveetha.com

intensity waves that penetrate the dermis and promote ageing, tanning, and collagen degradation. On the other hand, UVB rays are short-wavelength, high-energy radiation that burns the epidermis. Though direct DNA damage and subsequent cancer formation are primarily caused by UVB radiation, reactive oxygen species produced by UVA photons can indirectly cause cancer. It is clearer in these cases that the organic UV filters in sunscreen constituted a significant environmental concern.[13] Therefore, the usage of inorganic UV filters such syctonemin and mycosporine-like amino acids (MAA) will not as much impact the marine ecosystem.

MATERIALS AND METHODS

An extensive and systemic literature review search about the topic was done in January 2024 using PubMed, Google Scholar, Research gate and Sci-finder databases. The database filtering of latest references articles and matching preferences were done through the Preferred Reporting Items for Systematic Reviews and Meta-Analyses (PRISMA) guidelines.

Organic and Inorganic filters:

Sunscreens differ in their efficacy, which is mostly based on their ingredients. Sunscreens are primarily categorised based on the kind of UV filters (also known as active ingredients) that they contain; they can be physical (also known as mineral or non-soluble), chemical (commonly known as organic or soluble), or a mixture of the two.8 It has reportedly been used in more than 2000 skincare formulae from a variety of product categories, such as colour cosmetics, skin and hair care, and fragrances.[14] In polymers, it also acts as a stabiliser and an absorber of UV radiation. In 1990, oxybenzone was included in the Environmental Protection Agency's High Production Volume Challenge Program, which identifies chemicals produced or imported into the US at quantities greater than one million pounds per year.[15]

Conversely, chemical filters take in a narrow range of UV rays and use a chemical reaction to transform them into heat energy. To provide sufficient sun protection, several chemical filters must be mixed due to their limited absorption ranges.[11] Oxybenzone is the most often used chemical filter. However, the UVA rays that cause aging can only be blocked by oxybenzone. Physical sunscreens reflect UV light, whereas chemical filters absorb it. This is the main difference between chemical and physical sunscreens, other than composition. Benzophenones were originally employed as preservatives in industrial products such as paints, varnishes, and plastics to increase shelf life and decrease photodegradation.16 Benzophenones were also introduced to sunscreens in the 1950s; while there were initially six distinct benzophenones used as sunscreens, the four most commonly used agents in personal care products today are benzophenones-3, -4, -8, and -10. In a 2011 study on the frequency of known contact allergens in cosmetic and dermatological products, benzophenone-3 was detected in 68% of the 201 sunscreens analysed.[17] This means that the amount of benzophenone-3 found in US sunscreens is more than all other benzophenones combined.

Active Components of Sunscreen:

UV filters are the active ingredients of sunscreens and are classified as either soluble or non-soluble. Zinc oxide and titanium dioxide are examples of non-soluble filters, commonly referred to as mineral or physical filters, and are therefore categorised as physical sunscreens. On the other hand, soluble filters, often referred to as chemical or organic filters, are categorised as chemical sunscreens because they contain a variety of chemical compounds like octinoxate and oxybenzone. Aromatic chemicals such as oxybenzone and octinoxate, absorb UV radiation and release the energy as heat.

Inorganic UV filters:

In addition to sunscreens, oxybenzone and octinoxate are frequently found chemicals in personal care items like shampoo, lip balm, lotion, and insect repellent. Nevertheless, it is believed that oxybenzone and octinoxate are allergic, affect hormones in both humans and wildlife, and bleach coral. Indeed, in 2014, benzophenones were named contact allergen of the year, primarily due to the influence of oxybenzone, also known as benzophenone-3.[17] Because oxybenzone is a phototoxicant, its negative effects are amplified in bright light. Oxybenzone changed planulae from a motile to a distorted, sessile state, regardless of light or darkness. Planulae showed a rising rate of coral bleaching in response to rising oxybenzone concentrations.[4] Increases in oxybenzone concentrations are positively correlated with DNA-AP lesions, indicating that oxybenzone is a Geno toxicant to corals. Being a skeletal endocrine disruptor, oxybenzone caused the planula to ossify, encasing the entire structure in its own skeleton.

In the past ten years, sunscreens have been used to prevent photoaging, photosensitivity, skin cancer, and damage from free radicals in addition to their original purpose of protecting against erythema. Sunscreen is frequently used on big portions of the body. Large amounts of sunscreen are used since it is advised to apply them regularly and to reapply them after coming into contact with water. Sunscreens are occasionally included to common items like moisturisers and hair treatments; as a result, users often use them without realising it. Systemic absorption should be taken into account because sunscreen use is so common.

Environmental Impact:

Environmental effects are currently a hot topic. Recently, state legislation was approved in Hawaii to limit the use of oxybenzone and octinoxate containing personal care products, particularly in areas close to beaches. Prior research has indicated elevated levels of discernible active components in coastal waters.[18] Over the past few decades, as public knowledge of the dangers of UV radiation exposure on the skin has grown, so too has the usage of sunscreen cosmetic products, which has resulted in the introduction of novel chemical compounds into the marine environment.[14] Despite being the world's largest and fastest-growing tourism and recreation industries, sunscreen's potential chemical source to the coastal marine ecosystem has not been evaluated. Varying throughout the day, quantities of chemical UV filters included in sunscreen formulations, such as octinoxate and oxybenzone, have been found in nearshore seas.

Oxybenzone has been shown to be the most commonly discovered UV filter in the greatest amounts across water sources worldwide. There are various ways that organic filters get into the environment.[14] Urine absorbs them through the skin and excretes them, which gets into the plumbing.[4] The majority of the skin filter needs to be washed off with natural water sources or in a shower, with all the water used returning back into the water supply. The amount of applied dosage that was excreted in the urine was just about 4%. Furthermore, waste and industrial particulates found in factory discharge bring biological filters into the water supply system. In actuality, research indicates that oxybenzone concentrations in the drinking water supply are higher in metropolitan areas with commercial and industrial water flow than they are at recreational water sites. Organic filters are often found in the waste from manufacturing facilities, particularly those that make sunscreen and cosmetics. It is not shocking that these filters have been widely found in our water supplies given the rising usage of sunscreens and increased awareness of the value of photoprotection.

Impact on Coral reef:
The main factor for corals to go extinct is global warming. Seawater becomes more acidic due to the ocean's ability to absorb carbon dioxide from the atmosphere. As a result, the coral will be less able to convert their bones into calcareous, which will prevent them from growing and ultimately cause them to die. The primary cause of the coral bleaching is the sunscreen that people use worldwide. According to the study, coral reefs can become whiter when sunscreen is used, even in tiny amounts for skin protection. Indeed, oxybenzone has been found in freshwater and marine recreational areas in sunscreen as well as other skin care items. It builds up in aquatic species and transforms into harmful compounds.[10]

A tiny amount of sunscreen might cause a significant amount of coral mucus to leak out between 18 to 48 hours and totally whiten the coral within 96 hours, according to experiments conducted in a number of marine environments. It is not humanity's ultimate purpose, but rather the complete and enduring protection of coral reef resources.[9] A coral reef is an ecological resource in addition to a biological resource. Historically, coral and coral reefs were primarily employed for their biological and physical qualities, which made them unsustainable and inherently destructive. In fact, many cosmetics contain ingredients from animals and plants. The cream or shampoo we use may include plant extracts, such as lavender and tea tree oil, which will appear in many soaps and cosmetics.

Sustainable use of coral reefs:
For many tiny and medium-sized fish, coral reefs offer a decent habitat, cover, and breeding location because of their complex and varied topography. As a result, diverse dense fish groups up to thousands at times are frequently observed in coral reef areas, which constitute coral reef areas for fishing. We can create high-yield and stable-yield marine pastures without negatively affecting coral reef resources if we intentionally take use of the ecological features of coral reefs to provide fish and other marine organisms with habitats, shelters, and breeding places. We can also artificially breed valuable marine resources in coral reef areas and place marine organisms that love coral reefs in specific areas.[10]

Reef-building corals and the calcium carbonate bones left behind by other biological communities make up coral reefs.[9] Because of their strong physical characteristics, these reefs can withstand strong winds and waves and provide good protection for trees, coastal landforms, and artificial buildings along the reef edge. As a result, while developing coastal engineering projects, people can deliberately take use of the physical characteristics of coral reefs and include them into their plans for protecting against wind and waves. This not only efficiently prevents the occurrence of marine natural disasters but also lowers the cost of engineering. Knowledge of marine ecology and marine environmental preservation can be disseminated to coastal inhabitants and students in primary and secondary schools through the built coral reef nature reserve and its display hall. Concurrently, scientific investigations and trials concerning the revitalisation and advancement of impaired coral reef resources in specific regions can be conducted, together with technological and scientific collaboration and exchanges between local and international entities in this domain.

Effect on food chain:
Fish and animals have been investigated in relation to UV filters. It prevents rats from engaging in sexual behaviour and from reproducing. In zebrafish, octocrylene alters the way the liver and brain develop. Vitellogenin protein, a precursor to the embryo's yolk that is only present in females, was expressed by males exposed to high concentrations of oxybenzone in experiments conducted on Japanese rice fish (medaka) and rainbow trout. This resulted in decreased egg production, with noticeably less hatchings. Male fish that contain vitellogenin may have undergone feminization, which would have clear effects on reproduction. White fish, roaches, and perch observed in lakes in Switzerland have minimal but noticeable levels of UV filters. Cod liver in Norway has UV filters in it.[19] With 80% of the specimens identified, octocrylene was the most often encountered filter, followed by oxybenzone (50%). Octinoxate and oxybenzone were also present in white fish. Similar UV filters have been found in rainbow trout, white fish, chub, perch, and mussels in Spain. Although fish have modest concentrations, it is nevertheless important to take into account the ideas of biological magnification and the bioaccumulation.

The process by which substances gradually accumulate in organisms at higher quantities than in their surroundings is known as bioaccumulation. When Brausch and Rand looked at bioaccumulation, they discovered that fish had higher oxybenzone levels than water. The idea that chemicals grow more concentrated and harmful as one climbs the food chain is known as "biomagnification." Because lower species cannot eliminate or break down chemicals, an animal that consumes these lower-order organisms gets a higher dose of the chemical. This implies that eating seafood may have bad consequences for people, even if there haven't been any confirmed harmful effects on people as of yet.

Effect on humans:
Numerous adverse cutaneous reactions, such as contact and

photocontact dermatitis, contact and photocontact urticaria, and anaphylaxis, have been linked to oxybenzones. They have gained particular notoriety recently for their capacity to cause allergies and photoallergy. For the majority of patients, these allergens come from topical sunscreens and other cosmetics, but there are also reports of reactions that happen as a result of using industrial items.[20] Contact urticaria brought on by cosmetic chemicals that have elicited positive skin reactions after open, scratch, but most frequently, prick testing, in addition to immediate clinical symptoms. Certain IgE antibodies were occasionally found to be a basis for the diagnosis.[21] Eight years after the initial case of non-Y light-related contact dermatitis, photoallergic dermatitis caused by exposure to oxybenzone was first documented in 1980.

More cases of photoallergic contact dermatitis have been linked to oxybenzone than to any other UV filter. Studies done in the United States have shown that this chemical causes photoallergy, although there have been even more positive photopatch reactions in Europe. It's also crucial to remember that this chemical frequently causes problems because it's used in cosmetics that aren't intended to be sunscreens. Numerous extensive photopatch studies conducted in the US and numerous other countries have revealed that oxybenzone is also a major contributor to photoallergy in patients experiencing negative reactions to sunscreens.[22-24] In humans, oxybenzone has been associated with Hirschsprung's disease, used as a potential endocrine disruptor, and documented to cause contact and photocontact allergic reactions. It has been demonstrated that oxybenzone causes a range of harmful effects on fish and coral that extend from reef bleaching to fish death.[5] Last but not least, with the given the rise in skin cancer cases and the development of more potent sunscreen active ingredients like titanium dioxide and micronised zinc oxide, serious questions regarding the relative efficacy of oxybenzone-containing personal care products in preventing skin cancer need to be asked and contrasted with the possible harm to human health and the environment that could result from the buildup of this and other chemicals in the environment. Non-nano zinc oxide and non-nano titanium dioxide are UV resistant alternatives to oxybenzone that are recognised as "generally recognised as safe and effective" (GRASE), by the US Food and Drug Administration (FDA).[6]

Uses of oxybenzone:
In sunscreen preparations, oxybenzone is frequently employed as a short-wave (290-320 nm) ultraviolet light (UVB) and primarily short-wave UVA (320-340 nm) absorber at concentrations up to 6%. It is also used as a photo-stabiliser in personal care products, up to 0.5%, to reduce colour and odour changes. More than 2000 personal care formulas, including those for skin and hair care, colour cosmetics, and scents, have reportedly employed it. It also serves as a stabiliser and ultraviolet light absorber in plastics. In 1990, the Environmental Protection Agency's High Production Volume Challenge Program included oxybenzone to its list of approved chemicals. This tool finds ingredients that are produced or imported into the United States in more than a million pounds each year.[5]

Syctonemin and MAA as inorganic UV filters:
Mycosporine like amino acids:
Around 25% of the world's primary production is derived from cyanobacteria, which also predominate in large portions of the ocean and biological soil crusts. They must have light in order to perform photosynthesis, but they are also subjected to high UV radiation levels.

UVR-induced damage reduces photosynthetic rates, indicating that earlier estimates of the world's primary production may have been exaggerated.[25] Fundamentally, in cyanobacteria, MAAs are synthesised via a biosynthetic gene cluster (BGC) comprising at least three components.[26] MAAs have enormous biotechnological potential as the next wave of sunscreen ingredients. MAAs are tiny compounds that absorb ultraviolet light synthesised by cyanobacteria. Many marine animals also consume and accumulate these metabolites. Mycosporines and MAAs were found and given their names because they mediate light-induced fungal sporulation.

However, they also play a role in a variety of other biological processes, such as osmotic control, UV photoprotection of organisms and their embryos, and defence against oxidative stress. Additionally, their commercialization is a result of their capacity to prevent UV-induced skin damage in vivo.[27] MAAs have enormous biotechnological potential as the next wave of sunscreen ingredients. According to recent research, some of the chemicals included in commercial sunscreens, like benzophenone-3, can be harmful to corals.[28]

Syctonemin:
All taxa of extremophilic cyanobacteria are exclusively capable of producing the essential photoprotective agent scytonemin. It is a small, highly polar, lipid-soluble pigment molecule that ranges in hue from yellow-brown to dark red or mahogany. Cyanobacteria manufacture it as a component of their extracellular sheath.[29] Indolic and phenolic subunits combine to form the dimeric molecule scytonemin. This olefinic carbon atom connects the two subunits of scotylenemin. In general, there are two forms of scytonemin: reduced (red) and oxidised (green). Nonetheless, four unique scytonemin derivatives—dimethoxy, tetramethoxy, scytonin, and scytonemin-3a-imine from different cyanobacteria have also been reported. UV-A light greatly stimulates the manufacture of scytonemin in cyanobacteria.[29] Research indicates that UV-A radiation induced the expression of the gene cluster responsible for scytonemin biosynthesis, leading to the buildup of this naturally occurring sunscreen pigment outside of cells.[24,25] The *Chroococcidiopsis* sp. and Scytonema sp. of cyanobacteria were discovered to produce scytonemin when exposed to UV-A, oxidative stress, and temperature increases.

Solutions:
Applying sunscreen only to exposed areas, wearing swimwear, wide-brimmed hats, and sunglasses, and finding shade when outside are all examples of photoprotective clothing. Using sunscreen with inorganic filters (Syctonemin and MAA) and adhering to the aforementioned guidelines are two additional ways to shield oneself from UV rays. Apart from limiting the continuous discharge of UV filters into the

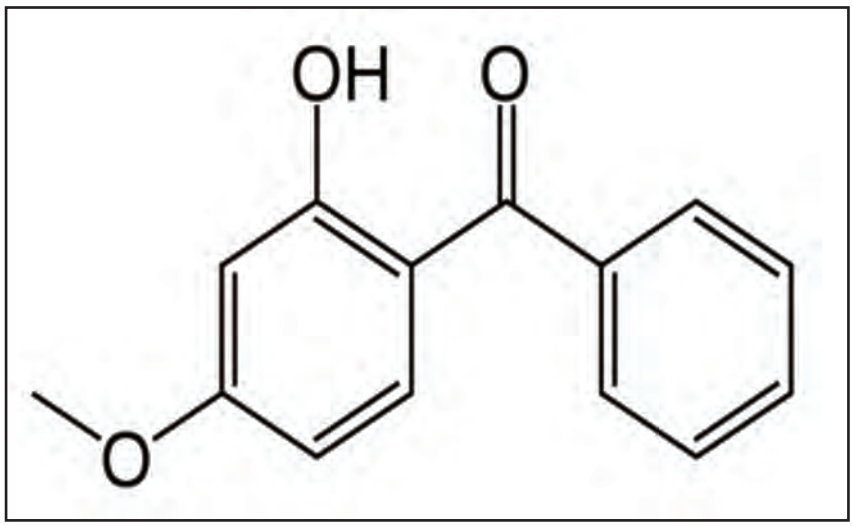

Fig. 1: Chemical Structure of Oxybenzone

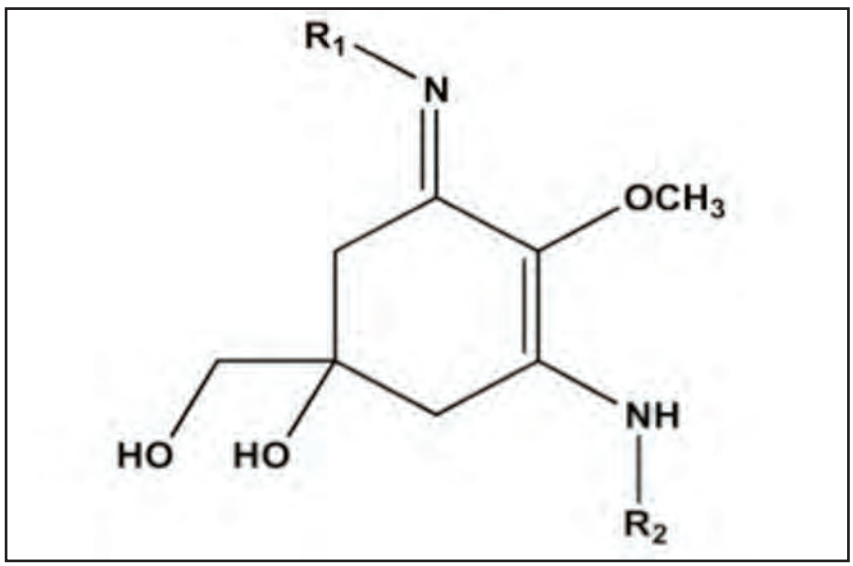

Fig. 2: General structure of MAA

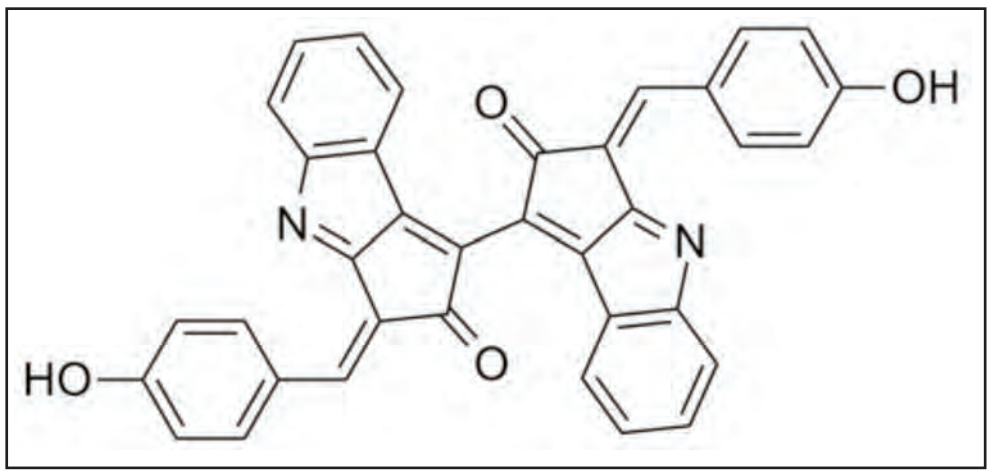

Fig. 3: Chemical structure of Syctonemin

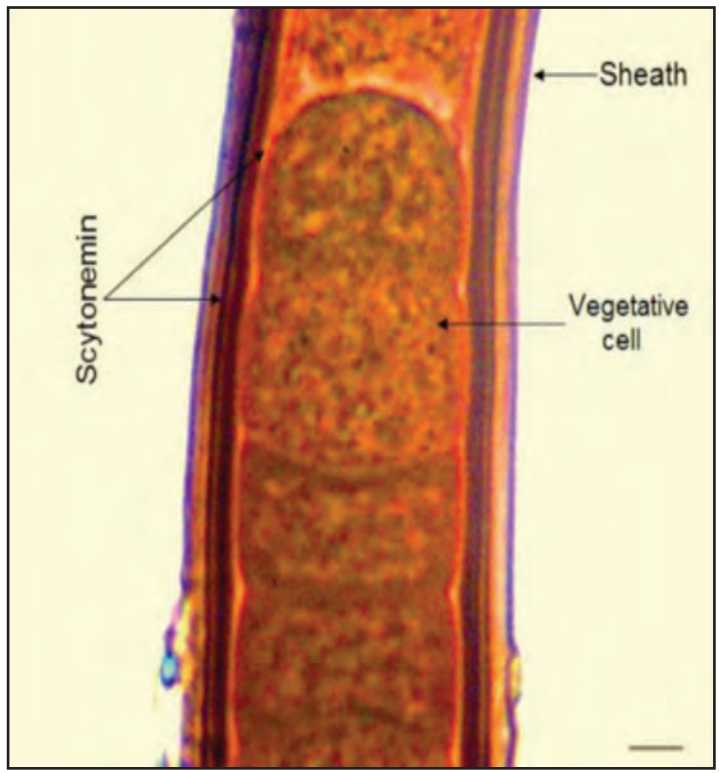

Fig. 4: Vegetative cells within a polysaccharide sheath containing the yellow-brown pigment scytonemin are seen in a filament of Lyngbya sp.

surroundings, methods to optimise their removal from the water resources have also been studied. Studies have been done on *Cyperus alternifolius* L., a widespread wetland plant that absorbs oxybenzone through its roots and builds up the toxin in its tissues. Finally, the plant converts oxybenzone into chemical conjugates that are less toxic. This method was considered as a potential way to remove oxybenzone from the environment; however, it was noted that these plants would need to be removed before they could begin to decompose naturally.[30,31]

CONCLUSION

Photoprotection is essential due to the established effects of UV radiation on erythema, photoaging, and the onset of skin cancer. Nevertheless, we also need to consider how our actions affect the environment. Numerous water sources have been found to include UV filters, which are very challenging to remove using conventional wastewater treatment plant procedures. One might assume that concentrations in our water sources will continue to rise if organic filters are used continuously. Although the impact on coral reefs is undoubtedly complex, UV filters may become increasingly crucial to bleaching at higher concentrations. Moreover, rising ocean concentrations will highlight bioaccumulation and biomagnification, which could have unfavourable effects on humans in the long run. Given the mounting evidence of the detrimental effects of organic UV filters on our environment, it is evident that we should investigate new techniques for water filtration and alternate photoprotection strategies. While research on the environmental effects of inorganic filters is ongoing, physical blockers are now advised as a substitute for photoprotection. The public should be made aware of the significance of photoprotection, which includes seeking shade, wearing photoprotective clothing and swimwear when outdoors, and applying the proper sunscreen to sun-exposed areas. This should not be compromised by worries about the environmental effects of organic UV filters. This would enable us to safeguard both the environment and our skin from the damaging effects of sunshine. Worldwide, oxybenzone is present in human urine, serum, and breast milk in addition to being present in water, soil, sediments, sludge, and biota. It is not as good as avobenzone as a sunscreen active at preventing UVA ray exposure. This substance is a known contact and photo contact allergen that can cause contact urticaria and, to a lesser extent, contact-mediated anaphylaxis in people. It has also been connected to Hirschsprung's illness. In the environment, oxybenzone prevents fish and coral from reproducing by poisoning embryos, feminising male fish, bleaching coral, and/or killing them. In summary, industry and regulatory bodies should evaluate the possible harm to human health and the environment that may result from the build-up of this and other chemicals in the ecosystem before developing and introducing novel, efficacious personal care products.

CONFLICT OF INTEREST

Authors declare there is no conflict of interest.

FUNDING

This research work does not include any funding details to declare.

ACKNOWLEDGEMENT:
Authors thankful to the Saveetha Institute of Medical and Technical Sciences (SIMATS) for providing research support.

REFERENCES

1. Zhong X, Zhang ZS, Li SH, Li YM, Liu BB, Li QM, et al. Inhibition of photosynthesis in cucumber leaves by oxybenzone. Photosynthetica 2020; 58(1): 1-8.
2. Emonet S, Pasche-Koo F, Perin-Minisini MJ, Hauser C. Anaphylaxis to oxybenzone, a frequent constituent of sunscreens. J Allergy Clin Immunol 2001; 107(3): 556-7.
3. Kasichayanula S, House JD, Wang T, Gu X. Percutaneous characterization of the insect repellent DEET and the sunscreen oxybenzone from topical skin application. Toxicol Appl Pharmacol 2007; 223(2): 187-94.
4. Kryczyk-Poprawa A, Sánchez-Hidalgo A, Baran W, Adamek E, Sułkowska-Ziaja K, Kała K, Muszyńska B, Opoka W. The Toxicological Impact of the Ultraviolet Filter Oxybenzone on Antioxidant Profiles in In Vitro Cultures of Lentinula edodes. Toxics 2025; 13(3): 145.
5. DiNardo JC, Downs CA. Dermatological and environmental toxicological impact of the sunscreen ingredient oxybenzone/benzophenone-3. J Cosmet Dermatol 2018; 17(1): 15-9.
6. Mao JF, Li W, Ong CN, He Y, Jong MC, Gin KY. Assessment of human exposure to benzophenone-type UV filters: A review. Environ Int 2022; 167: 107405.
7. Ruszkiewicz JA, Pinkas A, Ferrer B, Peres TV, Tsatsakis A, Aschner M. Neurotoxic effect of active ingredients in sunscreen products, a contemporary review. Toxicol Rep 2017; 4: 245-59.
8. Zengin G, Cetiz MV, Abul N, Gulcin I, Caprioli G, Piatti D, et al. Establishing a link between the chemical composition and biological activities of Gladiolus italicus Mill. from the Turkish flora utilizing in vitro, in silico and network pharmacological methodologies. Toxicology Mechanisms and Methods. 2025; 12;35(2):146-66.
9. Zhu X, Zhao L, Jiang H, Huang Y, Wang J, Sha L, et al. Production of short-chain n-fatty acids in coral reefs in the southern South China Sea since the Late Miocene. Palaeogeogr Palaeoclimatol Palaeoecol 2022; 592: 110898.
10. Miao Z. Damage of Oxybenzone in Sunscreen to Coral Reefs. Int J Biol Life Sci. 2022;1(1):17-9.
11. Siller A, Blaszak SC, Lazar M, Olasz Harken E. Update about the effects of the sunscreen ingredients oxybenzone and octinoxate on humans and the environment. Plast Surg Nurs 2018; 38(4): 158-61.
12. Smith CJ, Livingston SD, Doolittle DJ. An international literature survey of "IARC Group I carcinogens" reported in mainstream cigarette smoke. Food Chem Toxicol 1997; 35(10-11): 1107-30.
13. Uddin MM, Chowdhury MS, Hossain MA, Ahsan A, Hossain MT, Barik A, Hossen MA, Amin MF, Abir R, Alam MS, Rahman MH. Molecular screening and dynamics simulation reveal potential phytocompounds in Swertia chirayita targeting the UspA1 protein of Moraxella catarrhalis for COPD therapy. PloS one 2025; 20(2): e0316275.
14. Blitz JB, Norton SA. Possible environmental effects of sunscreen run-off. J Am Acad Dermatol 2008; 59(5): 898.
15. Siller A, Blaszak SC, Lazar M, Olasz Harken E. Update about the effects of the sunscreen ingredients oxybenzone and octinoxate on humans and the environment. Plast Surg Nurs 2018; 38(4): 158-61.
16. Knox JM, Guin J, Cockerell EG. Benzophenones; ultraviolet light absorbing agents. J Invest Dermatol 1957; 29(6): 435-44.
17. Ramsay DL, Cohen HJ, Baer RL. Allergic reaction to benzophenone: simultaneous occurrence of urticarial and contact sensitivities. Arch Dermatol 1972; 105(6): 906-8.
18. Schneider SL, Lim HW. Review of environmental effects of oxybenzone and other sunscreen active ingredients. J Am Acad Dermatol 2019; 80(1): 266-71.
19. Heurung AR, Raju SI, Warshaw EM. Benzophenones. Dermatitis 2014; 25(1): 3-10.
20. Verhulst L, Goossens A. Cosmetic components causing contact urticaria: a review and update. Contact Dermatitis 2016; 75(6): 333-44.
21. Buhry JN. Photo allergies from benzophenones and beta carotene in sunscreens. Contact Dermatitis 1980; 6(3): 211-39.
22. Cardoso JC, Canelas MM, Gonçalo M, Figueiredo A. Photopatch testing with an extended series of photoallergens: a 5-year study. Contact Dermatitis 2009; 60(6): 325-9.
23. Szczurko C, Dompmartin A, Michel M, Moreau A, Leroy D. Photocontact allergy to oxybenzone: ten years of experience. Photodermatol Photoimmunol Photomed 1994; 10(4): 144-7.
24. Shanmugam R, Arthi B, Pragya P, Girigoswami A, Koyeli G, Pemula G, Senthilkumar N, Arumugam VA. A Comprehensive Assessment of the Antioxidant Capacity of Varied Bacopa Monnieri Extracts and Its Toxicity on Early Life Stages of Zebrafish Embryos. Natural Product Communications 2025; 20(3): 1934578X251327815.
25. Balskus EP, Walsh CT. The genetic and molecular basis for sunscreen biosynthesis in cyanobacteria. Science 2010; 329(5999): 1653-6.
26. De la Coba F, Aguilera J, Figueroa FL, de Gálvez MV, Herrera E. Prevention of the ultraviolet effects on clinical and histopathological changes, as well as the heat shock protein-70 expression in mouse skin by topical application of algal UV-absorbing compounds. J Dermatol Sci 2009; 55(3): 161-9.
27. Danovaro R, Bongiorni L, Corinaldesi C, Giovannelli D, Damiani E, Astolfi P, et al. Sunscreens cause coral bleaching by promoting viral infections. Environ Health Perspect 2008; 116(4): 441-7.
28. Rastogi RP, Sonani RR, Madamwar D. Cyanobacterial sunscreen scytonemin: role in photoprotection and biomedical research. Appl Biochem Biotechnol 2015; 176(6): 1551-63.
29. Sorrels CM, Proteau PJ, Gerwick WH. Organization, evolution, and expression analysis of the biosynthetic gene cluster for scytonemin, a cyanobacterial UV-absorbing pigment. Appl Environ Microbiol 2009; 75(14): 4861-9.
30. van Iterson M, 't Hoen PA, Pedotti P, Hooiveld GJ, den Dunnen JT, van Ommen GJ, et al. Relative power and sample size analysis on gene expression profiling data. BMC Genomics 2009; 10(1): 439.
31. Chen F, Huber C, Schröder P. Fate of the sunscreen compound oxybenzone in Cyperus alternifolius based hydroponic culture: Uptake, biotransformation and phytotoxicity. Chemosphere 2017; 182: 638-46.

Navigating Airway Obstacles: Effective Anesthesia Strategies for Severe Robinson Sequence in a 3 year old

Harpreet Kaur, Dr MBBS, MD[1]

[1]Department of Anesthesia, Saveetha Medical College, Thandalam, Tamil Nadu, India

SUMMARY

Pierre Robin Sequence (PRS) is a congenital condition characterized by micrognathia, glossoptosis, and airway obstruction, often accompanied by a cleft palate. Severe cases pose additional challenges in surgical management due to anatomical abnormalities. A 3-year-old male with severe PRS underwent a cleft palate repair procedure, which was a multidisciplinary approach, and the successful repair of the cleft palate and uneventful postoperative recovery were attributed to the team's collaborative efforts. This case also highlights the importance of genetic evaluation and testing in managing PRS cases. This case highlights the importance of thorough preoperative assessment, advanced airway management skills, and genetic evaluation for better patient outcomes. Future research should explore innovative techniques and strategies to improve the outcomes of patients with PRS and other complex congenital conditions.

KEYWORDS:
FESS, Budesonide, Sinusitis, Steroid nasal spray, Nasal Polyp

INTRODUCTION

Pierre Robin Sequence (PRS) is a congenital condition characterized by a triad of anomalies [1]: micrognathia, glossoptosis, and airway obstruction, often accompanied by a cleft palate. This condition presents significant challenges in neonatal care, particularly in terms of maintaining a patent airway and ensuring adequate nutrition.[2] Severe cases of PRS, such as the one described in this report, pose additional difficulties in surgical management due to anatomical abnormalities.[3] Here, we present the case of a 3-year-old male with severe PRS, focusing on the clinical findings, the challenges encountered during surgical attempts to repair the cleft palate, and the multidisciplinary approach adopted to ensure a successful outcome. This case highlights the importance of thorough preoperative[1] planning and advanced airway management techniques to achieve favorable surgical results in patients with severe PRS.[4]

This report details the clinical findings, diagnostic and therapeutic challenges encountered, and coordinated efforts of a multidisciplinary team in managing his condition. This case highlights the critical role of interdisciplinary collaboration[5] and advanced airway management techniques in achieving favorable surgical outcomes in patients with severe PRS.[6]

CASE REPORT

The patient was a 3-year-old male weighing 10.5 kg with a medical history of severe Pierre Robin Sequence. Clinically, the patient exhibited a notable gap in the roof of his mouth since birth, indicative of cleft palate, and was scheduled for cleft palate repair surgery.

The antenatal history was uneventful, boen via expected vaginal delivery, with a birth weight of 2.3 kgs. Immediately after birth, the patient developed breathing difficulties, feeding difficulties, and nasal regurgitation, and was admitted to the NICU and treated conservatively.

At 1 year of age, patients with features such as micrognathia, microcephaly, mandibular hypoplasia, cleft palate, and no cleft lip were posted for elective cleft palate repair. After routine monitoring and preoperative assessment, the patient was shifted inside the OT, monitored were connected, and after adequate preoxygenation, trail laryngoscopy failed, video laryngoscopy-assisted intubation attempt failed followed by FOB-guided intubation was attempted, was failed due to severe mandibular hypoplasia, micrognathia, and complex airway. The patient was categorized as can ventilate, cannot intubate, and was shifted to the ICU for further management.

At 3 years of age, the patient was further referred for elective cleft palate repairsurgery. An appropriate preoperative assessment was performed, and patient under the difficult airway category was scheduled for the procedure.

Investigations revealed a hemoglobin level of 9.3 g/dL, bleeding time of 2 min, and clotting time of 9 min 10 seconds. The total leukocyte count was 16,970/mm³, and the platelet count was 430,000/µL. Renal and liver function tests were routinely performed. Serological results were negative for infectious diseases. Both the echocardiogram and chest radiograph were within normal limits.

Preoperative assessment revealed anticipated difficulties in ventilation and intubation. Anesthetic management included a thorough preoperative evaluation and preparation of the predicted difficult airway. To ensure comprehensive planning and coordination, discussions were conducted with a multidisciplinary team, including anesthesiologists, pediatric surgeons, and otolaryngologists.

Premedication was administered based on weight-based calculations, and an intravenous (IV) line was secured with a

This article was accepted: 03 August 2024
Corresponding Author: Bharathi B
Email: doctor.bharathi@gmail.com

22G cannula. The medications given included Inj. Glycopyrrolate reduces secretion; Inj. Midazolam was used for anxiolysis, Inj. Fentanyl for analgesia, and Inj. Propofol for induction.

During induction, after ensuring that the patient was adequately ventilated. Succinylcholine was administered to facilitate muscle relaxation because it is a depolarizing muscle relaxant known for its rapid onset and short duration of action, making it a popular choice over other non-depolarizing muscle relaxants. The initial attempt at intubation using standard laryngoscopy failed to visualize the vocal cords because of severe micrognathia and glossoptosis. Consequently, video laryngoscopy (Mc GRATH MAC) was utilized to visualize the airway structures better, and a style-guided RAE tube was successfully inserted.

Intraoperative management included continuous monitoring of vital signs, such as heart rate, blood pressure, oxygen saturation, and end-tidal CO2. Anesthesia was maintained with inhalational agents, specifically sevoflurane, and intravenous medications, as needed.

Postoperative care involved extubation in the operating room after confirmation of adequate spontaneous breathing and muscle strength. The patient was then transferred to the ICU for close monitoring, the surgery was completed without complications, and postoperative recovery was uneventful. The patient demonstrated stable respiratory function, with no signs of airway obstruction. He was monitored in the ICU for 24 hours before being moved to the pediatric ward. He was discharged after adequate pain control and feeding assessment.

DISCUSSION

This case of a 3-year-old male with severe Pierre Robin Sequence (PRS) highlights several critical aspects of managing complex congenital conditions. PRS, which is characterized by micrognathia, glossoptosis, and airway obstruction, often poses significant medical and surgical management challenges. In this patient, the presence of additional anomalies, such as microcephaly and mandibular hypoplasia, further complicated the clinical picture.

The initial surgical attempt to repair the cleft palate at age 2 years was unsuccessful because of the patient's complex airway anatomy. This outcome highlights the importance of thorough preoperative planning and potential complications in patients with severe PRS. The failure of standard laryngoscopy and subsequent successful use of video laryngoscopy for intubation during the second surgical attempt illustrate the necessity for advanced airway management techniques in such cases. These findings align with previous reports emphasizing the need for specialized equipment and skilled personnel to manage airway challenges in patients with PRS.

The multidisciplinary approach adopted in this case, involving anesthesiologists, pediatric surgeons, and otolaryngologists, was crucial for achieving a favorable outcome. This collaborative strategy ensured comprehensive care and addressed the multifaceted needs of the patients. Successful repair of the cleft palate and uneventful postoperative recovery highlight the effectiveness of this integrated approach. The literature supports the involvement of multidisciplinary teams in improving surgical outcomes and the overall management of patients with PRS and similar congenital anomalies.

Moreover, this case helps us to understand the importance of anticipating and preparing for difficult ventilation and intubation scenarios. The use of preoperative assessments and advanced planning, as demonstrated herein, can significantly mitigate the risks associated with airway management in patients with PRS. Studies have consistently shown that detailed preoperative evaluations and availability of advanced airway management tools are critical in reducing perioperative complications .

Case of Neonate with Severe Upper Airway Obstruction:
A 9-day-old male infant with PRS, weighing 3.5 kg, presented with severe upper airway obstruction due to a combination of cleft palate and a vallecular cyst. Multiple attempts at intubation using direct laryngoscopy, GlideScope, LMA, fiberoptic scope, and lighted wand were unsuccessful. Successful airway management was eventually achieved through digital intubation, highlighting the importance of a broad skill set in airway management techniques for such complex cases.[7]

1p36 Deletion Syndrome and PRS:
In a neonate diagnosed with 1p36 deletion syndrome complicated by PRS, severe airway obstruction was successfully managed using fiberoptic nasotracheal intubation immediately after birth. This case emphasizes the importance of preparedness with fiberoptic equipment and neonatologists' acquisition of relevant skills to manage unexpected airway compromises effectively.[8]

Stickler Syndrome with PRS:
A case involving A patient with Stickler syndrome type 1, identified through a novel COL2A1 gene mutation, presented with PRS. This case highlights that Stickler syndrome accounts for a significant proportion of PRS cases, stressing the need for genetic testing and family history evaluation in patients with PRS, mainly when other symptoms such as myopia or retinal detachment are present 7

Advanced Airway Management Techniques:
In a tertiary pediatric hospital, a case of PRS with unique anatomical challenges required old-fashioned digital intubation after multiple high-tech methods failed. This demonstrates the need for training in various airway management techniques, including traditional methods, to effectively handle challenging airway scenarios effectively.[9]
Severe Glossoptosis in PRS:

Another report described a severe case of glossoptosis in PRS, where the tongue was invaginated into the nasal cavity, necessitating immediate fiberoptic intubation for resuscitation. This case highlights the need for neonatologists to be adept at fiberoptic intubation to manage similar critical situations.[9]

Fig. 1: Dysmorphic facial features

Fig. 2: Post intubation

Mandibular Distraction Osteogenesis (MDO) in PRS:
Several cases have reported the use of MDO as an effective intervention for severe airway obstruction in patients with PRS. The MDO gradually elongates the mandible, reduces glossoptosis, and improves airway patency. This surgical technique has shown promising results in the alleviation of airway obstruction in infants with severe PRS.[9]

These cases collectively illustrate the complex and varied nature of PRS management, prioritizing the importance of a multidisciplinary approach, advanced airway management skills, and the potential role of genetic evaluation in improving patient outcomes.

The successful management of this case resulted from meticulous preoperative planning, advanced airway management techniques, and coordinated efforts of a multidisciplinary team.

CONCLUSION

This case of a 3-year-old male with severe Pierre Robin Sequence (PRS) underscores the complexities and challenges associated with managing this congenital condition, particularly regarding airway management and surgical interventions. The initial failure to intubate due to difficult airway anatomy highlights the importance of comprehensive preoperative assessment and availability of advanced airway management techniques. The successful outcome achieved through a multidisciplinary approach and video laryngoscopy for intubation emphasizes the necessity for collaboration and specialized skills in treating patients with PRS.

This case also illustrates the critical role of tailored anesthetic management in achieving favorable surgical outcomes. Detailed preoperative planning and implementation of innovative techniques facilitated successful repair of the cleft palate and uneventful postoperative recovery. These findings align with the existing literature that supports advanced airway management tools and a multidisciplinary team approach for managing PRS.

This case contributes to the growing body of evidence advocating thorough preoperative assessments, advanced airway management training, and multidisciplinary collaboration for managing severe PRS. Future research should continue to explore and refine these approaches to improve the outcomes in patients with this challenging condition.

ACKNOWLEDGEMENT

We would like to acknowledge the patient for agreeing to publish the case report.

Conflict of interest:
The author declare no conflict of interest.

REFERENCES

1. Shprintzen RJ, Pierre Robin, micrognathia, and cleft palate. Plast Reconstr Surg 1992; 89(4): 779-80.
2. Caouette-Laberge L, Bayet B, Larocque Y. The Pierre Robin sequence: a review of 125 cases and evolution of treatment modalities. Plast Reconstr Surg 1994; 93(5): 934-42.
3. Breugem CC, Evans KN, Poets CF, Suri S, Picard A, Filip C, et al. Best practices for diagnosing and evaluating infants with Robin sequence: a clinical consensus report. JAMA Pediatr 2016; 170(9): 894-902.
4. de Buys Roessingh AS, Herzog G, Hartmann B, Ghelfi D, Hohlfeld J. Respiratory and feeding management in Pierre Robin sequence: a multidisciplinary approach. J| Pediatr Surg 2007; 42(4): 675-80.
5. Xu W, Jablonka EM, Lunsford L, Xie X, Leichtle S, Karnezis T. Management of airway obstruction in patients with Pierre Robin sequence. J Craniofac Surg 2020; 31(6): 1582-5.
6. Witt PD, Myckatyn TM, Marsh JL, Grames LM. Pierre Robin sequence: a review of mandibular distraction osteogenesis for airway management. Plast Reconstr Surg 1999; 103(1): 163-73.
7. Zhang L, Fei J, Jia J et al. Case report of neonate Pierre Robin sequence with severe upper airway obstruction who was rescued by finger guide intubation. BMC Anesthesiol 2019; 19: 84
8. Higuchi Y, Hasegawa K, Yamashita M et al. A novel mutation in the COL2A1 gene in a patient with Stickler syndrome type 1: a case report and review of the literature. J Med Case Reports 2017; 11: 237.
9. Takeshita S, Ueda H, Goto T et al. Case report of Pierre Robin sequence with severe upper airway obstruction who was rescued by fiberoptic nasotracheal intubation. BMC Anesthesiology 2017;17:43.

LETTER TO EDITOR

Precision Medicine for Oral Cancer: Exploiting the miR-34/SATB2 Regulatory Network

Shazia Fathima JH, Selvaraj Jayaram, Vishnu Priya Veeraraghavan

Centre of Molecular Medicine and Diagnostics (COMManD), Department of Biochemistry, Saveetha Dental College & Hospitals, Saveetha Institute of Medical and Technical Sciences, Saveetha University, Velappanchavadi, Chennai- 600 077, India

Precision Medicine for Oral Cancer: Exploiting the miR-34/SATB2 Regulatory Network

Dear Editor,

Oral squamous cell carcinoma (OSCC) stands as a significant contributor to global cancer-related mortality and has escalated in recent times. Despite the advancement in technical methodologies for disease localization, grading and staging, approximately 50% of OSCC patients experience frequent recurrences. Various molecular pathways are implicated in the development and progression of OSCC. It is crucial to understand the interactions among these pathways, as well as their significance in the domain of oncology. miRNAs (miRNAs) are single stranded, non-coding RNAs (containing ~20– 22 nucleotides) involved in the regulation of a variety of physiological and pathological scenarios by targeting specific mRNAs involving infection, immunity and carcinogenesis. Among the diverse range of miRNAs, miRNA-34 holds significant importance in cancer progression and metastasis. Regulation at the transcriptional level by different factors is pivotal in managing the levels of miR-34. The tumour suppressor protein p53 directly interacts with the promoter of the miR-34 gene, upregulating the transcription. Additionally, various transcription factors including Elk-1, STAT3, Snail, Slug, ZEB1, and ZEB2 have been associated with the control of miR-34, affecting over 700 genes that are either projected or validated targets of miR-34s. They participate in crucial signalling cascades associated with progression and proliferation of malignant tumours such as p53, MAPK, Notch, Wnt, PI3K/AKT and Ras pathways. Moreover, miR-34s regulate critical mechanisms linked to cancer cell migration, invasion and the process of epithelial-mesenchymal transition (EMT). Previous research has elucidated the significant role of p53/miR-34 interaction in OSCC, where they coordinate changes in the cell cycle and promote EMT. Bypassing mutations or alterations in the epigenetic mechanism to p53 and directly administering miR-34 mimetics represents a prospective interventional approach for a subset of cancers characterized by dysregulated cell cycle checkpoints. Corcoran et al emphasized consistent decrease in miR-34 expression across various cancer types, highlighting its role as a tumour suppressor.

Special AT-rich DNA binding protein (SATB2), an 82.5 kDa protein (733 amino acids), encodes a protein crucial for chromatin remodelling by binding to matrix attachment regions of the nucleus (MARs) and regulates chromatin organization, transcription, and tumorigenesis. The expression of SATB2 varies depending on the embryonic origin of the tissue, developmental phase and are affected by a myriad of cell signals. SATB2 plays multiple roles in craniofacial development, osteoblast differentiation and the initiation and progression of cancer. These varied physiological roles of SATB2 are modulated through ligand-receptor signalling pathways. In various types of carcinomas, SATB2 has shown to exhibit aberrant expression patterns that contribute to tumour metastasis and progression such malignancies often show increased SATB2 expression with low survival rate, whereas colorectal cancer tends to suppress it. An increase in SATB2 protein promotes EMT, which facilitates invasion and metastasis by enabling epithelial cells to acquire mesenchymal characteristics, thus promoting tumour cell dissemination and spread to distant sites. It was reported by Jiang et al that SATB2 protein being upregulated in hepatocellular carcinoma leading to cell proliferation and metastasis, while Wang et al studied the upregulation of SATB2 led reduced of mRNA levels of SNAIL gene in colorectal cancer cells. They further characterized three SATB2-binding motifs within an AT-rich sequence located in the SNAIL promoter region.

miR-34 has been identified as a direct inhibitor of SATB2 expression, exerting negative regulatory control over the SATB2 gene. This regulatory interaction is implicated in modulating crucial cellular processes, including developmental pathways and differentiation cascades. Ge X et al. observed that miR-34a suppressed the invasion and metastasis of OSCC cells by reducing SATB2 expression,[1] Wu G et al investigated the relationship between SATB2 expression and miR-34a, focusing on OSCC found low levels of miR-34a correlated with upregulation of SATB2.[2] They identified SATB2 as a direct target of miR-34a and inferred that miR-34a functions as a tumour suppressor in OSCC by targeting SATB2, thereby inhibiting proliferation and expansion of cancer cells. The precise mechanism concerning the interrelation of SATB2 and miR-34a in this context remains to be fully understood.

Based on prior study findings, we suggest a pathway given in figure 1 involving miR-24 and SATB2 and its implication in EMT event in OSCC. miR-34 molecule acts as a negative regulator of SATB2. Ideally, miR-34 would inhibit the

This article was accepted: 27 September 2024
Corresponding Author: Selvaraj Jayaram
Email: selvarajj.sdc@saveetha.com

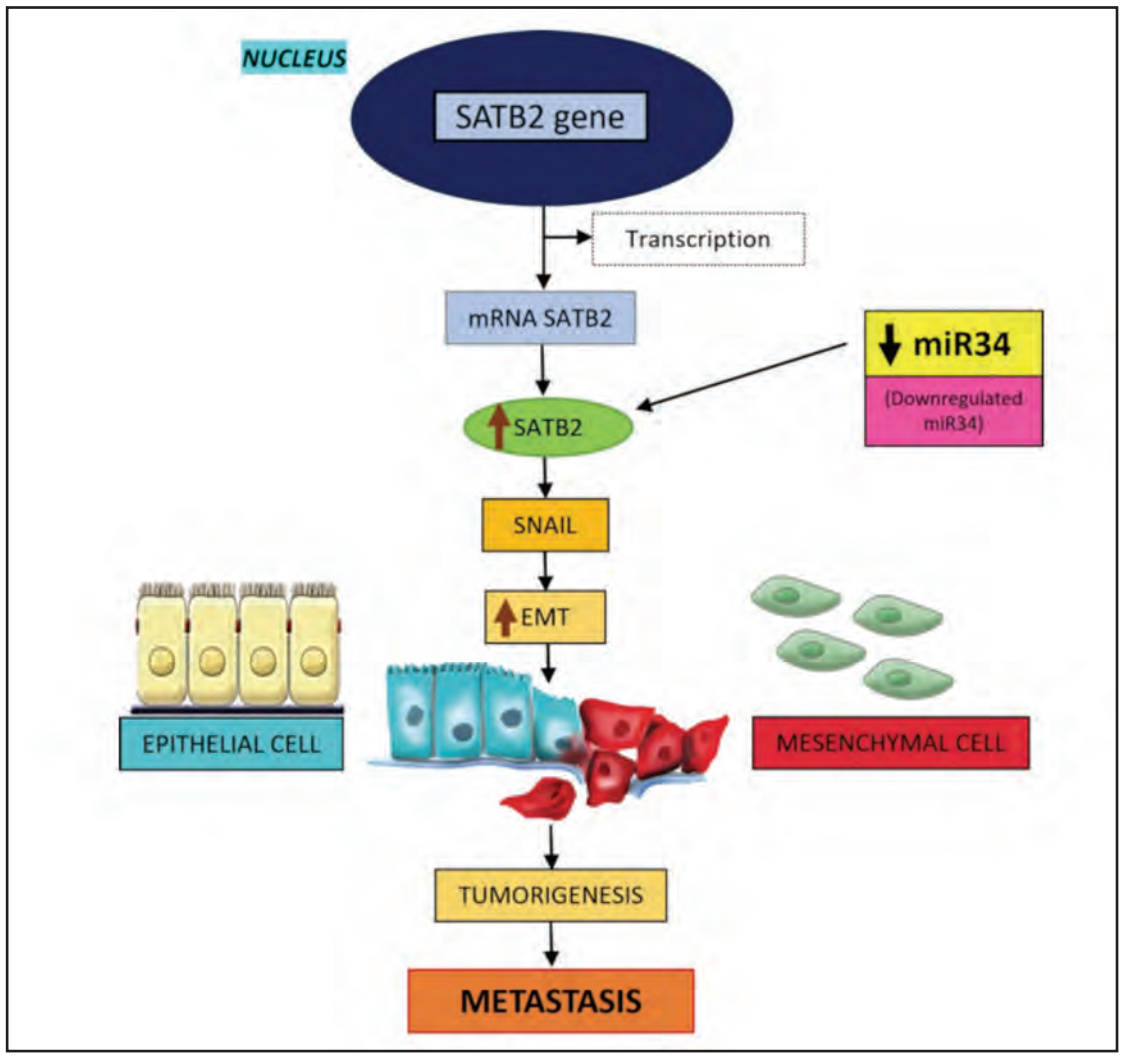

Fig. 1: Schematic illustration of miR34 and SATB2 molecular interaction in the cascade of OSCC tumorigenesis and subsequently metastasis

translation of the SATB2 mRNA into a protein. In the presence of dysregulation, the SATB2 gene is not inhibited by miR34, which can lead to the overexpression of SATB2. This activation results in the production of SATB2 protein, which subsequently upregulates pro- EMT genes such as SNAIL and SLUG. SNAIL serves as a crucial transcription factor in EMT facilitating this process. The overexpression of SATB2 can also contribute to the proliferation of OSCC cells and metastasis. This proposed pathway underscores the intricate molecular mechanisms involved in the progression of OSCC and highlights the potential therapeutic targets within this pathway for future research and intervention strategies. The uncontrolled production of SATB2 protein, due to the lack of miR-34 inhibition, contributes to EMT. Consequently, EMT is associated with the proliferation and metastasis of OSCC cells. With the advent of the first miRNA-based therapy, MIRX34, which delivers a mimic of the tumour suppressor miR-34 encapsulated within SMARTICLES liposomal formulation, there is a unique opportunity to integrate this innovative approach into OSCC (Fig.1). By deciphering the molecular pathway given above the roles of miR-34 and SATB2 in OSCC progression and EMT regulation, future studies could pinpoint precise targets for intervention, potentially leading to more targeted and effective therapies that inhibit metastasis and enhance patient outcomes.

CONFLICT OF INTEREST

There is no conflict of interest.

REFERENCES

1. Ge X, Gao J, Sun QW, Wang CX, Deng W, Mao GY, et al. MiR-34a inhibits the proliferation, migration, and invasion of oral squamous cell carcinoma by directly targeting SATB2. J Cell Physiol 2020; 235(5): 4856-64.
2. Wu G, Li Z, Wang Y, Ju X, Huang R. miR-34a Inhibits Cell Proliferation by Targeting SATB2 in Hepatocellular Carcinoma. Biomed Res Int 2018; 6: 2863902.

Acknowledgement
Supplement 8 Issue 2025

The Editorial Board of The Medical Journal of Malaysia gratefully acknowledge the following individuals for reviewing the papers submitted for publication:

1. Dr Abdul Gafoor Abdul Mubarak
2. Dr Adzim Poh Yuen Wen
3. Dr Aina Mariana Abdul Manaf
4. Dr Aisha Fadhilah Abang Abdullah
5. Prof Dr Andee Dzulkarnaen
6. Dr Baharulhakim Said Daliman
7. Dr Cha Tha A Hing
8. Dr Daphne Dewi Stephen
9. Dr Dwi Aris Agung Nugrahaningsih
10. Dr Haris Abdul Rahman
11. Dr Hayani Abdul Wahid
12. Dr Iskasymar Ismail
13. Dr Mohd Nazri Ali
14. Dr Mohd Shakir Bathusha
15. Dr Nadeeya Ayn Umaisara Mohamad Nor
16. Dr Ramiza Ramza Ramli
17. Dr Shaik Farid Abdull Wahab
18. Prof Dr Shatriah Ismail
19. Dr Shobini Vishali V M
20. Dr Suresh Mani
21. Dr Tharani M
22. Dr Teik Ee Tan
23. Dr Vasu Pillai A/L Letchumanan
24. Prof Dr Victor Hoe Chee Wai
25. Dr Vivian Cheah